

**Total Maximum Daily Loads for Dioxins
in the Houston Ship Channel**

**Contract No. 582-6-70860
Work Order No. 582-6-70860-18**

Quarterly Report No. 3

MODELING REPORT – Revision 2

Prepared by
*University of Houston
Parsons Water & Infrastructure*

Principal Investigator
Hanadi Rifai

PREPARED IN COOPERATION WITH THE
TEXAS COMMISSION ON ENVIRONMENTAL QUALITY AND
U.S. ENVIRONMENTAL PROTECTION AGENCY

The preparation of this report was financed through grants from the U.S. Environmental Protection Agency through the Texas Commission on Environmental Quality

TCEQ Contact:
Larry Koenig
TMDL Team
P.O. Box 13087, MC - 203
Austin, Texas 78711-3087
lkoenig@tceq.state.tx.us

November 2008

TABLE OF CONTENTS

TABLE OF CONTENTS	ii
LIST OF TABLES	IV
LIST OF FIGURES	V
UNIT SYMBOLS, ABBREVIATIONS, AND CONVERSIONS	VII
ACRONYMS AND ABBREVIATIONS	VIII
CHAPTER 1 INTRODUCTION.....	1
1.1 OVERALL DESCRIPTION OF THE DIOXIN PROJECT	2
1.2 DESCRIPTION OF THE REPORT	2
1.3 MODEL DEVELOPMENT	2
CHAPTER 2 HYDRODYNAMIC MODEL OF THE HOUSTON SHIP CHANNEL AND UPPER GALVESTON BAY USING RMA2	5
2.1 GENERAL WATERSHED CHARACTERISTICS	5
2.1.1 Climatology	5
2.1.2 Hydrology	6
2.2 HYDRODYNAMIC MODEL ISSUES	7
2.3 RMA2 MODEL SEGMENTATION AND TIME STEP	9
2.4 DATA FOR MODEL INPUT	11
2.4.1 Geometry and Bottom Elevation Data	11
2.4.2 Tide Data	18
2.4.3 Freshwater Inflow Data	19
2.4.4 Meteorology	23
2.5 SPIN-UP TIME DETERMINATION.....	23
2.6 MODEL CALIBRATION	25
2.6.1 Water Surface Elevation	25
2.6.2 Velocity and Flow	29
2.7 LONG-TERM RUNS	51
2.8 HSCREAD INTERFACE.....	54
CHAPTER 3 IN-STREAM WATER QUALITY MODEL OF THE HOUSTON SHIP CHANNEL AND UPPER GALVESTON BAY USING WASP7.....	58
3.1 WASP SEGMENTATION AND TIME STEP	62
3.2 MODEL INPUT.....	63
3.2.1 Hydrodynamics	63
3.2.2 Boundary Concentrations.....	63
3.2.3 Loads	70
3.2.4 Initial Concentrations	80
3.2.5 Solid Transport Parameters	83
3.2.6 Pore Water Diffusion	85
3.3 SPIN-UP TIME DETERMINATION.....	85
3.4 SALINITY MODEL.....	86
3.5 DIOXIN MODEL CALIBRATION.....	90

3.6 SENSITIVITY ANALYSIS	111
3.6.1 Effect of Diffusion Coefficient	112
3.6.2 Effect of Dispersion	112
3.6.3 Effect of Partition Coefficient.....	116
3.6.4 Effect of Settling	117
3.6.5 Effect of Scour	120
3.6.6 Effect of Benthic Concentration.....	120
3.6.7 Effect of Benthic Layer Depth	124
3.6.8 Effect of Runoff Load	124
3.6.9 Effect of Point Source Load.....	127
3.6.10 Effect of Deposition Load.....	127
3.6.11 Summary of Sensitivity Analysis.....	130
3.7 LOAD SCENARIOS	137
CHAPTER 4 SPREADSHEET APPROACH TO SUMMARIZE WASP RESULTS AND OBTAIN LOADS ACROSS WATER QUALITY SEGMENTS.....	144
4.1 SPREADSHEET CONCEPTUAL MODEL	146
4.2 SOURCE LOADS BY WATER QUALITY SEGMENT	153
4.2.1 Point Source Loads	153
4.2.2 Runoff Loads.....	154
4.2.3 Upstream Loads.....	155
4.2.4 Direct Deposition Loads	156
4.3 LOADS ACROSS SEGMENT BOUNDARIES	157
4.4 CONVERTING DIOXIN FLUXES INTO LOAD ALLOCATION EQUATIONS	169
REFERENCES.....	170

APPENDICES

APPENDIX A - CROSS-SECTIONS FROM BEAMS USED TO SET UP THE 1-D PORTION OF THE MAIN CHANNEL

APPENDIX B – INPUT TIME SERIES

APPENDIX C - MODEL INPUT AND OUTPUT FILES

APPENDIX D – MASS-BALANCE SPREADSHEETS

LIST OF TABLES

<u>TABLE #</u>	<u>TITLE</u>	<u>PAGE #</u>
Table 2.1	Major Tributaries and USGS Gages	7
Table 2.2	Dimensions of Cross-Sectional Areas for Tributaries in the Model.....	18
Table 2.3	Tide Gages in the Modeled Area	19
Table 2.4	Upstream Boundary Conditions for the RMA Model	21
Table 2.5	Flow from Point Sources in the RMA2 Model.....	22
Table 2.6	Model Summary Statistics for Water Elevations.....	29
Table 2.7	Difference between Measured and Predicted Cross-sectional Areas	31
Table 2.8	Model Summary Statistics for Water Flows.....	51
Table 3.1	TOXI5 Systems and Levels of Complexity	59
Table 3.2	Data Requirements for the Dioxin WASP Model for the HSC	61
Table 3.3	Physical Characteristics of WASP Segments	65
Table 3.4a	Average 2378-TCDD Loads and Concentrations at Upstream Boundaries ...	67
Table 3.4b	Average 12378-PeCDD Loads and Concentrations at Upstream Boundaries	67
Table 3.4c	Average 123678-HxCDD Loads and Concentrations at Upstream Boundaries	68
Table 3.4d	Average 2378-TCDF Loads and Concentrations at Upstream Boundaries	68
Table 3.4e	Average 23478-PeCDF Loads and Concentrations at Upstream Boundaries	69
Table 3.4f	Average 123678-HxCDF Loads and Concentrations at Upstream Boundaries	69
Table 3.5	Summary of Point Source Loads in the WASP Model.....	72
Table 3.6	Runoff Curve Numbers for the HSC Watershed	77
Table 3.7	Storm Water Runoff Loads to the WASP Model	78
Table 3.8	Direct Deposition in the WASP Model	81
Table 3.9	Model Summary Statistics for Salinity	90
Table 3.10	Model Summary Statistics for WASP Models	104
Table 3.11	Summary of Sensitivity Analysis Scenarios	112
Table 4.1	Estimated Loads from Point Sources.....	153
Table 4.2	Estimated Dioxin Runoff Loads by Subwatershed.....	155
Table 4.3	Estimated Dioxin Loads from Upstream Tributaries.....	156
Table 4.4	Dioxin Loads from Direct Deposition	157
Table 4.5	Mass-balance Spreadsheet for 2378-TCDD	161
Table 4.6	Mass-balance Spreadsheet for 12378-PeCDD.....	162
Table 4.7	Mass-balance Spreadsheet for 123678-HxCDD	163
Table 4.8	Mass-balance Spreadsheet for 2378-TCDF	164
Table 4.9	Mass-balance Spreadsheet for 23478-PeCDF	165
Table 4.10	Mass-balance Spreadsheet for 123678-HxCDF	166
Table 4.11	Mass-balance Spreadsheet for Σ TEQ _{major congeners}	168
Table 4.12	Daily Fluxes from Galveston Bay to Lower Bay System and Clear Lake ...	169

LIST OF FIGURES

<u>FIGURE #</u>	<u>TITLE</u>	<u>PAGE #</u>
Figure 1.1	RMA2-WASP7 Modeling Process	4
Figure 2.1	RMA2 Model Segmentation	10
Figure 2.2	Bottom Elevations for the Houston Ship Channel (upstream San Jacinto River)	12
Figure 2.3	Bottom Elevations for the Tidal Portions of Major Tributaries to the HSC... ..	13
Figure 2.4	Tide and Flow Gages in the Model Domain	20
Figure 2.5	Verification of Spin-up Time for the Hydrodynamic Model.....	24
Figure 2.6	Observed and Simulated Water Surface Elevations in the HSC	26
Figure 2.7	Scatterplots of Observed and Modeled Water Surface Elevations in the HSC	27
Figure 2.8	Velocity and Flow Calibration Locations	30
Figure 2.9	Modeled and Measured Water Velocities.....	33
Figure 2.10	Modeled and Measured Water Flows	34
Figure 2.11	Scatterplots of Observed and Modeled Water Velocities using Discrete Values	35
Figure 2.12	Scatterplots of Observed and Modeled Water Flows using Discrete Values ..	36
Figure 2.13a	Goodness of Fit for HSC @ Morgan’s Point using Flow Regression	38
Figure 2.13b	Goodness of Fit for HSC @ Lynchburg using Flow Regression.....	39
Figure 2.13c	Goodness of Fit for HSC @ Battleship using Flow Regression.....	40
Figure 2.13d	Goodness of Fit for HSC @ Greens using Flow Regression.....	41
Figure 2.13e	Goodness of Fit for HSC @ I-610 using Flow Regression	42
Figure 2.13f	Goodness of Fit for Buffalo Bayou using Flow Regression.....	43
Figure 2.13g	Goodness of Fit for Brays Bayou using Flow Regression.....	44
Figure 2.13h	Goodness of Fit for Sims Bayou using Flow Regression	45
Figure 2.13i	Goodness of Fit for Vince Bayou using Flow Regression.....	46
Figure 2.13j	Goodness of Fit for Hunting Bayou using Flow Regression	47
Figure 2.13k	Goodness of Fit for Greens Bayou using Flow Regression.....	48
Figure 2.13l	Goodness of Fit for Carpenters Bayou using Flow Regression.....	49
Figure 2.13m	Goodness of Fit for San Jacinto River @ I-10 using Flow Regression	50
Figure 2.14	Observed and Simulated Water Surface Elevations in the HSC	52
Figure 2.15	Long-term Modeled Flow Rates	53
Figure 3.1	WASP Model Segmentation	64
Figure 3.2	Point Sources in WASP	71
Figure 3.3	Determination of Spin-up Time for the WASP Model.....	86
Figure 3.4	Salinity Calibration Locations	88
Figure 3.5	Modeled and Measured Salinity Concentrations	89
Figure 3.6a	Modeled and Observed 2378-TCDD Concentrations (Averages).....	92
Figure 3.6b	Modeled and Observed 12378-PeCDD Concentrations (Averages)	93
Figure 3.6c	Modeled and Observed 123678-HxCDD Concentrations (Averages)	94
Figure 3.6d	Modeled and Observed 2378-TCDF Concentrations (Averages).....	95

Figure 3.6e	Modeled and Observed 23478-PeCDF Concentrations (Averages).....	96
Figure 3.6f	Modeled and Observed 123678-HxCDF Concentrations (Averages).....	97
Figure 3.7a	Modeled and Observed 2378-TCDD Concentrations (Medians).....	98
Figure 3.7b	Modeled and Observed 12378-PeCDD Concentrations (Medians).....	99
Figure 3.7c	Modeled and Observed 123678-HxCDD Concentrations (Medians).....	100
Figure 3.7d	Modeled and Observed 2378-TCDF Concentrations (Medians).....	101
Figure 3.7e	Modeled and Observed 23478-PeCDF Concentrations (Medians).....	102
Figure 3.7f	Modeled and Observed 123678-HxCDF Concentrations (Medians).....	103
Figure 3.8a	Observed versus Modeled Average 2378-TCDD Concentrations.....	105
Figure 3.8b	Observed versus Modeled Average 12378-PeCDD Concentrations.....	106
Figure 3.8c	Observed versus Modeled Average 123678-HxCDD Concentrations.....	107
Figure 3.8d	Observed versus Modeled Average 2378-TCDF Concentrations.....	108
Figure 3.8e	Observed versus Modeled Average 23478-PeCDF Concentrations.....	109
Figure 3.8f	Observed versus Modeled Average 123678-HxCDF Concentrations.....	110
Figure 3.9	Diffusion Coefficient Scenarios.....	114
Figure 3.10	Dispersion Scenarios.....	115
Figure 3.11	Partition Coefficient Scenarios.....	118
Figure 3.12	Settling Scenarios.....	119
Figure 3.13	Scour Scenarios.....	122
Figure 3.14	Benthic Concentration Scenarios.....	123
Figure 3.15	Benthic Layer Depth Scenarios.....	125
Figure 3.16	Runoff Load Scenarios.....	126
Figure 3.17	Point Source Load Scenarios.....	128
Figure 3.18	Deposition Load Scenarios.....	129
Figure 3.19	Sensitivity Summary for 2378-TCDD.....	131
Figure 3.20	Sensitivity Summary for 12378-PeCDD.....	132
Figure 3.21	Sensitivity Summary for 123678-HxCDD.....	133
Figure 3.22	Sensitivity Summary for 2378-TCDF.....	134
Figure 3.23	Sensitivity Summary for 23478-PeCDF.....	135
Figure 3.24	Sensitivity Summary for 123678-HxCDF.....	136
Figure 3.25a	2378-TCDD Load Scenarios.....	138
Figure 3.25b	12378-PeCDD Load Scenarios.....	139
Figure 3.25c	123678-HxCDD Load Scenarios.....	140
Figure 3.25d	2378-TCDF Load Scenarios.....	141
Figure 3.25e	23478-PeCDF Load Scenarios.....	142
Figure 3.25f	123678-HxCDF Load Scenarios.....	143
Figure 4.1	Distribution of Initial Dioxin Concentrations in Sediment in the WASP Models.....	145
Figure 4.2	Conceptual Model for Mass-Balance Spreadsheet.....	146
Figure 4.3	Spreadsheet Segmentation.....	148
Figure 4.4	Schematic of Mass-balance Spreadsheet for the Houston Ship Channel.....	149
Figure 4.5	Example Spreadsheet Format.....	159
Figure 4.6	Average Sediment Contribution (dS) by Segment.....	167

UNIT SYMBOLS, ABBREVIATIONS, AND CONVERSIONS

Symbol or abbreviation	Text	Unit Equivalence	Unit Type
°C	degrees Celcius		temperature
kg	kilograms	10 ³ grams	mass
g	grams	454 grams ~ 1 pound	mass
mg	milligrams	10 ⁻³ grams	mass
µg	micrograms	10 ⁻⁶ grams	mass
ng	nanograms	10 ⁻⁹ grams	mass
pg	picograms	10 ⁻¹² grams	mass
fg	femtograms	10 ⁻¹⁵ grams	mass
L	liter	3.78 liters ~ 1 gallon	volume
mL	milliliter	10 ⁻³ liters	volume
µg/L	micrograms per liter	~10 ⁻⁹ , or 1 ppb	mass/volume concentration
ng/L	nanograms per liter	~10 ⁻¹² , or 1 ppt	mass/volume concentration
pg/L	picograms per liter	~10 ⁻¹⁵ , or 1 ppq	mass/volume concentration
ng/kg	nanograms per kilogram	=10 ⁻¹² , or 1 ppt	mass/mass concentration
mg/g	milligrams per gram	10 ⁻³	mass/mass concentrations
g/cm ²	gram per square centimeter		cumulative mass
ppm	parts per million	10 ⁻⁶	unitless concentration
ppb	parts per billion	10 ⁻⁹	unitless concentration
ppt	parts per trillion	10 ⁻¹²	unitless concentration
ppq	parts per quadrillion	10 ⁻¹⁵	unitless concentration

ACRONYMS AND ABBREVIATIONS

CN	curve number
ERDC	US Army, Engineer Research and Development Center
HCOEM	Harris County Homeland Security and Emergency Management
H-GAC	Houston-Galveston Area Council
HSC	Houston Ship Channel
msl	mean sea level
NOAA	National Oceanic and Atmospheric Administration
NRCS	Natural Resources Conservation Service
OCS	off-channel storage
PCB	polychlorinated biphenyl
PCDD	Polychlorinated dibenzo- <i>p</i> -dioxin
PCDF	dibenzofuran
PCS	Permit Compliance System
PS	point source
SJR	San Jacinto River
TCEQ	Texas Commission on Environmental Quality
TEF	toxicity equivalent factor
TEQ	toxicity equivalent concentration
TMDL	total maximum daily load
TSARP	Tropical Storm Allison Recovery Project
TSS	total suspended solids
USEPA	U.S. Environmental Protection Agency
USGS	U.S. Geological Survey
WASP	Water Quality Analysis Simulation Program
WQ	water quality

CHAPTER 1

INTRODUCTION

Polychlorinated dibenzo-*p*-dioxins (PCDD) and dibenzofurans (PCDF) and polychlorinated biphenyls (PCB) are halogenated aromatic compounds that have been widely found in the environment. The PCDDs include 75 congeners, and PCDFs include 135 different congeners. Only seven of the 75 PCDD congeners and 10 of the 135 PCDF congeners have been identified as having dioxin-like toxicity. There are 209 PCB congeners, of which 12 are identified as having dioxin-like toxicity. These dioxin-like compounds are highly toxic and persistent environmental contaminants and, consequently, have received a great deal of attention by environmental regulators and researchers.

Dioxin (the term used to refer to dioxin-like compounds) presents a likely cancer hazard to humans¹ (U.S. Environmental Protection Agency [USEPA], 2000a) and can cause health problems even at extremely low doses. Reproductive problems, behavioral abnormalities, and alterations in immune functions are among the health effects caused by exposure to dioxin. Because dioxin-like compounds have been proven to bioaccumulate in biological tissues, particularly in animals, the major route of human exposure is through the food chain. Thus, several food advisories have been issued across the United States to prevent people from consuming unhealthy doses of these compounds.

¹ U.S. Environmental Protection Agency (2000a). “Dioxin: Scientific Highlights from Draft Reassessment.” *Information Sheet 2*, National Center for Environmental Assessment, Office of Research and Development, Washington, DC.

1.1 OVERALL DESCRIPTION OF THE DIOXIN PROJECT

The overall purpose of this project is to develop a Total Maximum Daily Load (TMDL) allocation for dioxin in the Houston Ship Channel System, including upper Galveston Bay, and a plan for managing dioxins to correct existing water quality impairments and to maintain good water quality in the future.

The dioxin TMDL study has been divided into various phases. Phase I of the TMDL was focused on assessing current conditions and knowledge about dioxins. Phase II was focused on gathering data in all media to quantify dioxin levels in the channel and their sources. Phase III is focused on model development and load allocation.

This Work Order (582-6-70860-08) is part of Phase III and includes the following tasks:

1. Project administration
2. Continuing development and refinement of TMDL models
3. Participating in stakeholder involvement with the dioxin TMDL project
4. TMDL allocations

1.2 DESCRIPTION OF THE REPORT

This document constitutes the third quarterly report for Work Order No. 582-6-70860-18 (Contract No. 582-6-70860) of the Dioxin TMDL Project. The document contains a comprehensive summary of the modeling activities conducted for the project.

1.3 MODEL DEVELOPMENT

The goal of the modeling task is to use models to elucidate the sources and major processes controlling observed levels of dioxins in the Houston Ship Channel (HSC) and to

identify the maximum permissible loading that would not impair water quality. Development of a preliminary mass-balance of dioxins in the HSC was completed during WO7 using the MEGA-TX model (a modification of the QUAL-TX model completed for this project) to ensure that all the sources and processes had been identified. In addition, a steady-state WASP model of the HSC was developed as well as a one-month transient WASP simulation.

The modeling effort for this Work Order consisted of the coupling of a hydrodynamic model (RMA2) to the in-stream water quality model (WASP7) for the HSC and its major tributaries, for use in developing total maximum daily loads (TMDL) for dioxin. The models are being used for several purposes:

- to aid in understanding the processes affecting the fate of dioxins in the HSC system,
- to quantify pollutant loadings to the various water quality segments and allocate them among sources, and
- to quantify the loading reductions required to achieve water quality standards.

Because the output from the hydrodynamic model (RMA2) cannot directly be read by the in-stream water quality model (WASP7) and because segmentation for WASP7 is much coarser than that for RMA2, an interface (HSCREAD) has been written as part of this project. Figure 1.1 shows a schematic of the modeling approach for this project.

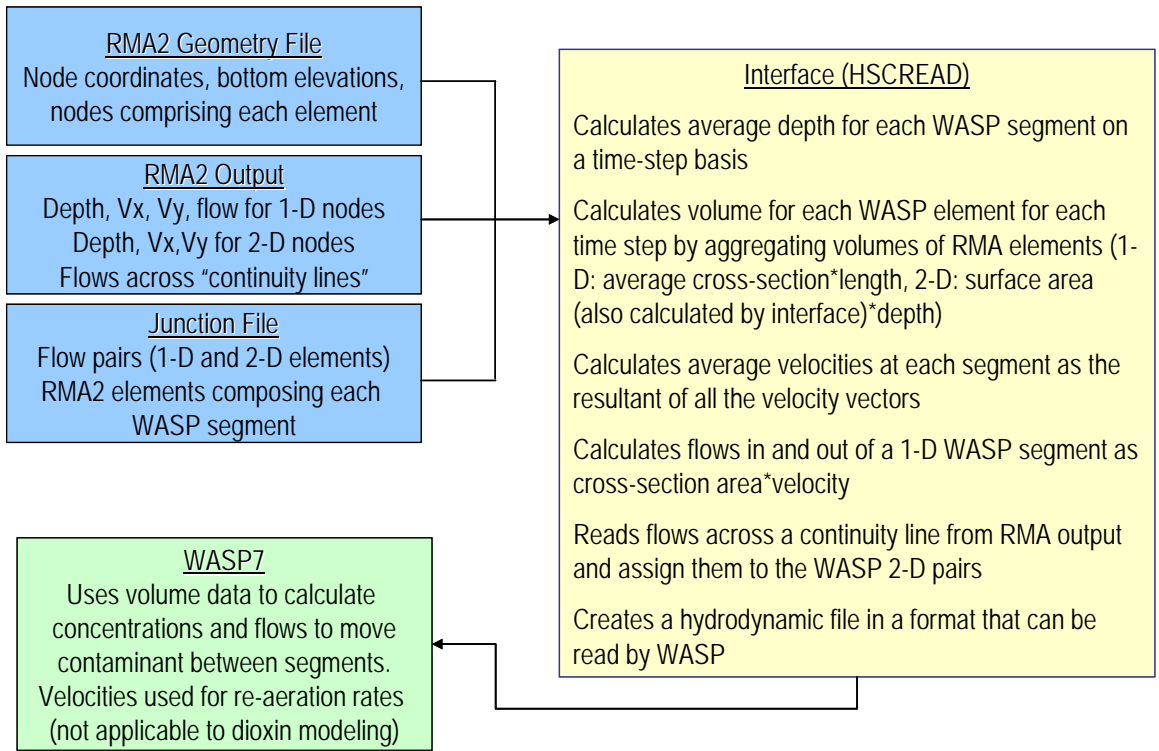


Figure 1.1 RMA2-WASP7 Modeling Process

CHAPTER 2

HYDRODYNAMIC MODEL OF THE HOUSTON SHIP CHANNEL AND UPPER GALVESTON BAY USING RMA2

This chapter summarizes the development of a hydrodynamic model of the HSC System (including Upper Galveston Bay and Bayport Channel) using the RMA2 WES 4.5 Program (ERDC, 2005). An initial RMA2 model was developed during the second quarter of 2006. However, due to a number of issues encountered with the initial model, the RMA2 model segmentation was significantly changed during summer and fall 2006. The model details and results presented in this report correspond to the latest model segmentation and are preceded by a summary of the issues that motivated changes to the model.

RMA2 is a two-dimensional depth averaged finite element hydrodynamic numerical model. It computes water surface elevations and horizontal velocity components for subcritical, free-surface two-dimensional flow fields (ERDC, 2005). The RMA2 model is composed of elements and nodes. Elements represent a finite stretch of the channel or tributary, and hold water. Each 1-D element is composed of three nodes, while each 2-D element is composed of either six or eight nodes. Nodes are the points where water surface elevation and velocity calculations are performed, and all linkages between elements occur at nodes.

2.1 GENERAL WATERSHED CHARACTERISTICS

2.1.1 Climatology

The climate throughout the Houston area is predominantly marine due to its proximity to the Gulf of Mexico and Galveston Bay. Prevailing winds are from the south and southeast,

except during winter months when periodic passages of high-pressure cells bring polar air and prevailing northerly winds.

Temperatures are moderated by the influence of the warm Gulf waters, which results in mild winters. Average monthly temperatures range from 29.9°C (85.9°F) in July to 10.9°C (51.7°F) in December.

Another effect of the nearness of the Gulf is abundant rainfall. The peak rainfall period is during the fall months with a secondary peak in the spring. Annual average precipitation is about 137 cm (54 inches). Significant snowfall is rare, but traces of snow are recorded during many winters. The relative humidity in the area is high, with the annual average ranging from 60 percent at 12:00 noon to 87 percent at 6:00 p.m.

2.1.2 Hydrology

The HSC system is an estuarine system that is composed of the tidally influenced HSC and San Jacinto River (SJR) and free-flowing tributaries which become tidal as they approach the HSC. The SJR is tidal from the Lake Houston Dam to the HSC.

The HSC has been dredged at mid-channel to a project depth of 15 m to allow for the passage of ocean-going vessels. In the upper channel from the Turning Basin to the confluence with the SJR, widths range from 100 to 670 m and average depths range from 4.8 to 14.4 m. In the lower channel from the SJR to Morgan's Point, widths range from 450 to 790 m and average depths range from 3.6 to 15.5 m. During low-flow conditions on the SJR, widths range from 70 to 1,020 m and the average depths range from 5.5 to 13 m.

The tributaries of the HSC are characterized by moderately low flows dominated by domestic wastewater effluents except during periods of intense rainfall when the flows can rise

dramatically. The United States Geological Survey maintains continuous flow recording gages on most of the tributaries as indicated in Table 2.1.

Table 2.1 Major Tributaries and USGS Gages

Tributary	Station Description	USGS gage	Watershed Area (km²)	Long-term median flow (m³/s)
San Jacinto River	San Jacinto River at Sheldon	08072050 ^a	7,370	NA
Lake Houston	Lake Houston near Sheldon	08072000 ^a	7,240	NA
Buffalo Bayou	Buffalo Bayou at Shepherd	08074000	916	3.3
Whiteoak Bayou	Whiteoak Bayou at Heights	08074500	221	1.1
Greens Bayou	Greens Bayou at Ley Rd	08076700 ^b	466	38.7 ^b
Greens Bayou	Greens Bayou at Houston	08076000	176	0.7
Halls Bayou	Halls Bayou at Houston	08076500	73	0.3
Garners Bayou	Garners Bayou near Humble	08076180	79	0.4
Brays Bayou	Brays Bayou at Houston	08075000	243	2.9
Sims Bayou	Sims Bayou at Houston	08075500	161	1.2
Vince Bayou	Vince Bayou at Pasadena	08075730	21	0.1
Patrick Bayou	None	None	11	NA
Carpenters Bayou	None	None	66	NA
Hunting Bayou	Hunting Bayou at IH-610	08075770	41	0.3
Goose Creek	Goose Creek at Baytown	08067525 ^a	40	NA
Cedar Bayou	Cedar Bayou near Baytown	08067510	433	NA
Clear Creek	Clear Creek at Friendswood	08077540 ^c	255	NA

^a Only water elevation data are available for the simulation period

^b Flow data for this gage appear too high so data from upstream gage is to be used in the model

^c Recent data for this gage are not available

NA – not available

2.2 HYDRODYNAMIC MODEL ISSUES

The initial version of the HSC RMA2 model presented a number of problems listed below:

- The net flow out of the side bays was high, even though most of the bays do not have any freshwater inflow. Flow in and out of side bays is the result of tidal elevation and, thus, net flow should be near zero,
- Mass-balance was not preserved for individual RMA2 elements. The RMA2 model globally

maintains mass-conservation in a weighted residual manner; however, checks on an element-basis should be done separately by using continuity lines or by calculating volumes as a function of flows in and out of elements. Large mass conservation discrepancies indicate possible oscillations and a need to improve model resolution and/or correct large boundary break angles (ERDC, 2005),

- The model output flows for continuity lines with only one element at the interface (two nodes) were found to be inaccurate,
- There were flow losses between some of the 1-D elements, and
- Wetting/drying of the upstream reaches (Buffalo and Whiteoak Bayou) caused the long-term run to crash.

To address the above mentioned issues the following changes were made to the model:

- The geometry of 1-D elements at some junctions was modified to eliminate water leaks.
- Upstream reaches with bottom elevations above -0.5 m mean sea level (msl) were eliminated and the associated volume replaced using off-channel storage.
- The RMA2 model segmentation was refined (from 1032 to 3356 elements) to minimize mass-balance problems. Segment volumes can be calculated using two different methods:

$$V_t = V_{t-1} + (Q_{in_t} - Q_{out_t}) \cdot dt \quad (2.1)$$

And
$$V_t = \overline{A_{xs_t}} \cdot L \text{ (for 1-D elements)} \quad (2.2a)$$

$$V_t = A_s \cdot \overline{D_t} \text{ (for 2-D elements)} \quad (2.2b)$$

where: V_t is volume at time t , Q_{in} is flow into a WASP segment, Q_{out} is flow out of a WASP segment, dt is time step, $\overline{A_{xs_t}}$ is the average cross-section area of a 1-D WASP segment, L is

the length of a 1-D WASP segment, A_s is the surface area of a 2-D WASP segment, and \overline{D}_l is the average depth of a 2-D WASP segment. The goal of the refinement was that for each of the WASP segments, the difference in volumes calculated using equations 2.1 and 2.2 would not be greater than 3 percent of the volume at any time step (calculated using equation 2.2).

- Continuity lines were specified so that at least two RMA2 elements were on each side of the continuity line.

2.3 RMA2 MODEL SEGMENTATION AND TIME STEP

The conceptual model includes a 1-D section from the Turning Basin until the confluence with the SJR and a 2-D section from the SJR confluence until Eagle Point (boundary of segment 2421). The channel was discretized into 108 linear elements (including the tidal portions of the major tributaries), 3,228 2-D elements, 17 junction elements, and five transition elements. The grid was defined using the SMS 9.0 software (Brigham Young University, 2005). The model grid is shown in Figure 2.1.

Calibration was conducted using six-minute time steps and covered the period March 20 to April 21, 2005. This time period was selected because it corresponded to the period when flow measurements were made in this project. It is noted that a three-week spin-up time was added at the beginning of the simulation to account for the time needed by WASP to equilibrate.

Once calibration was complete, the calibrated RMA2 model was extended to simulate the period 6/17/2002 to 4/30/2005 (the period prior to 7/20/2002 corresponds to the spin-up time). The simulation was split into three runs: 6/17/2002 to 06/30/2003, 7/1/2003 to 6/30/2004, and 7/1/2004 to 4/30/2005. The model was additionally run using 30-minute time steps to shorten the long computational time as well as reduce the size of the output files. This was justified by the

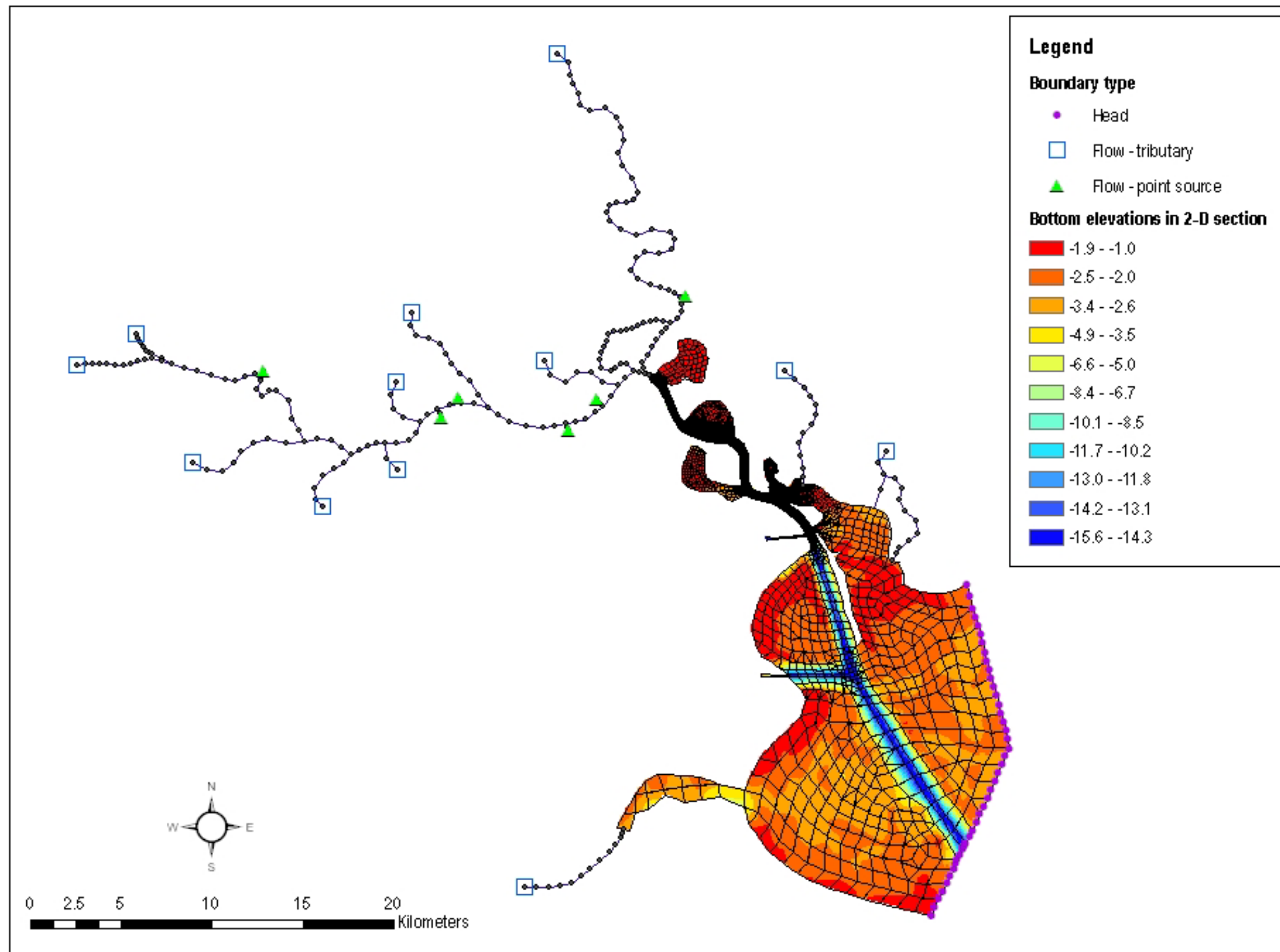


Figure 2.1 RMA2 Model Segmentation

fact that a decrease in time step size (six minutes vs. 30 minutes) did not improve the calibration substantially. However, because the WASP model exhibited numerical dispersion with a 30-minute time step, the 30-minute results from RMA2 were interpolated linearly using the interface (HSCREAD) to obtain six-minute datasets for WASP.

2.4 DATA FOR MODEL INPUT

2.4.1 Geometry and Bottom Elevation Data

For the 1-D section of the model, two sources of data were relied upon: (i) HSC cross-sections from the deep draft channel survey, available on-line at <http://beams.swg.usace.army.mil/surveys.html>, and (ii) cross sections for major tributaries from the Tropical Storm Allison Recovery Project (TSARP). For the 2-D section of the model, bathymetry data were obtained from the Texas General Land Office website <http://www.glo.state.tx.us/> and interpolated for the selected grid (Figure 2.1) to assign bottom elevations.

Data from TSARP were used to assign bottom elevations to the nodes in the main channel and the major tributaries, as shown in Figures 2.2 and 2.3, respectively. The RMA2 model accepts only trapezoidal cross-sections, so the dimensions for the various 1-D elements were determined as follows: (i) for the main channel, the cross-sections for the dredged portions were obtained from the deep channel survey (see Appendix A); (ii) the shallow portions of the main channel were simulated using off-channel storage (OCS)²; to determine the width of the

² “The off-channel assignment should be thought of as the average combined left and right over bank volumetric contributions. The volume of the off-channel storage interacts with the continuity equation, but makes no contribution to the momentum equation.” (ERDC, 2005).

OCS, the total width of the channel at the various nodes was measured using aerial photographs for the project area, for most locations the critical elevation (surface water elevation at which the OCS option is activated) is 2 m below msl; (iii) for the tributaries, constant channel dimensions were assumed so that the average cross-sectional areas (water surface elevation at about 0 m above mean sea level-msl) were within 10 percent of the areas measured during flow sampling in Spring 2005 as summarized in Table 2.2³; and (iv) off-channel storages were assigned to the first node of most of the major tributaries to account for the volume of water between the boundary of the tidal sections and the beginning of the modeled segments as illustrated in Figure 2.3. The slope of the off-channel storage was used as a calibration parameter.

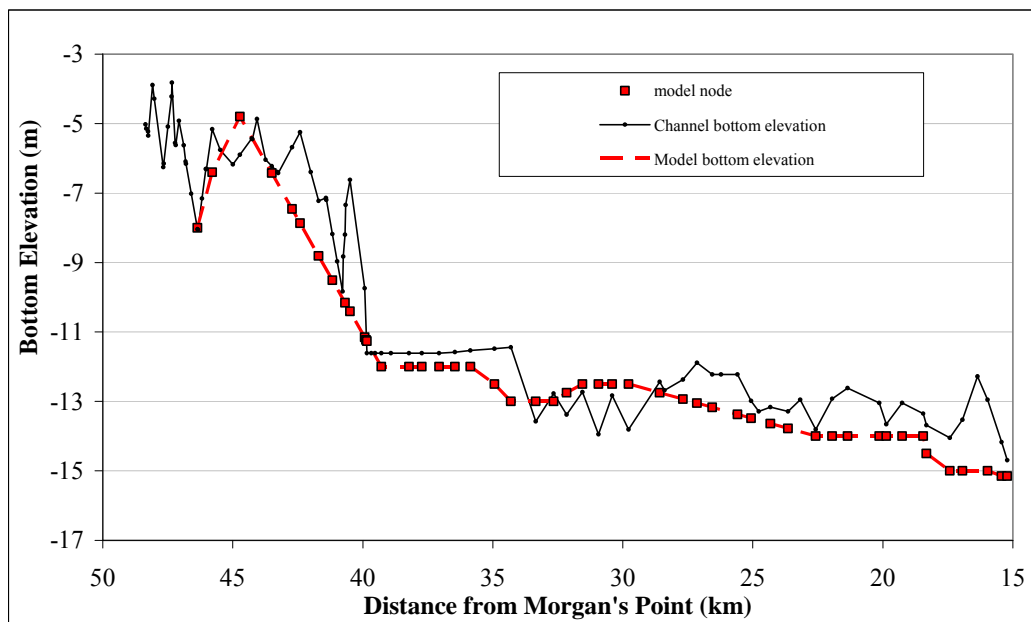
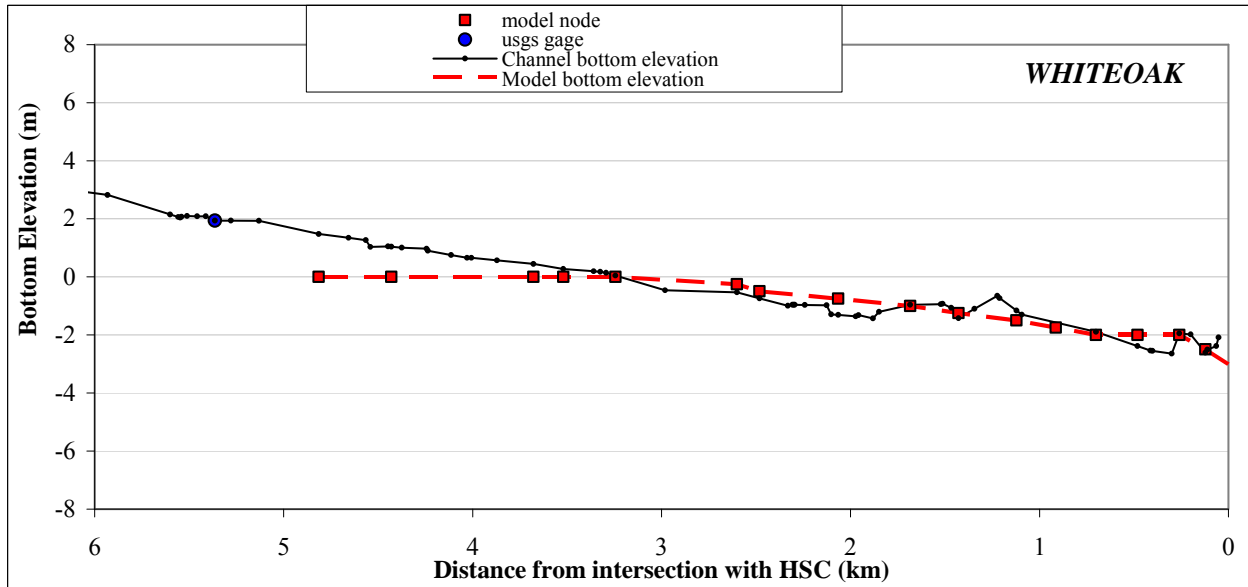
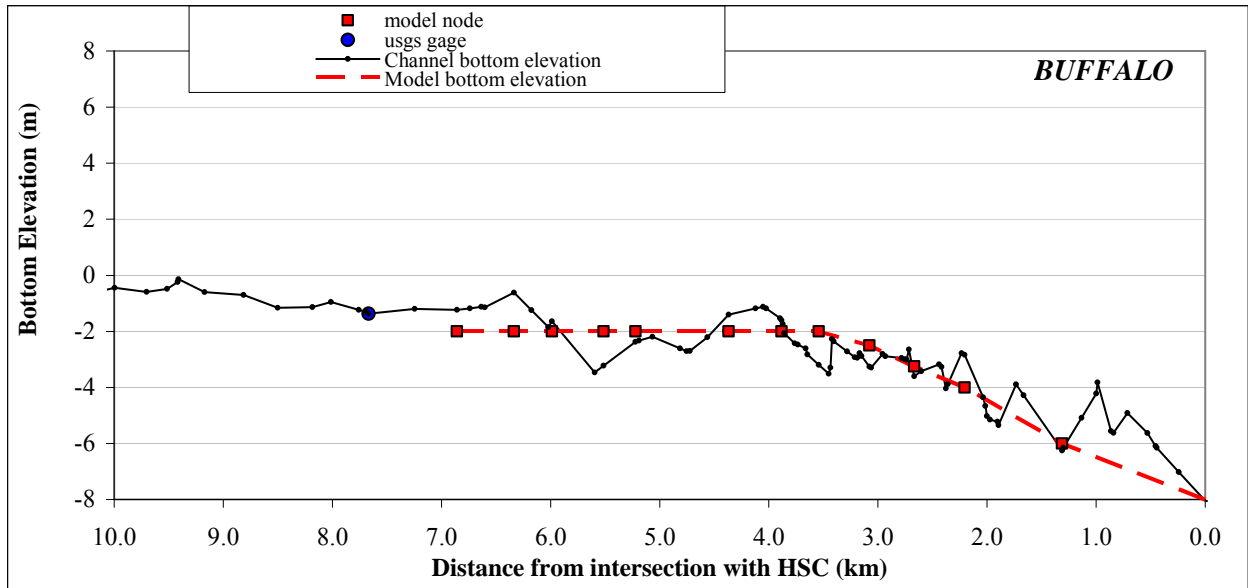


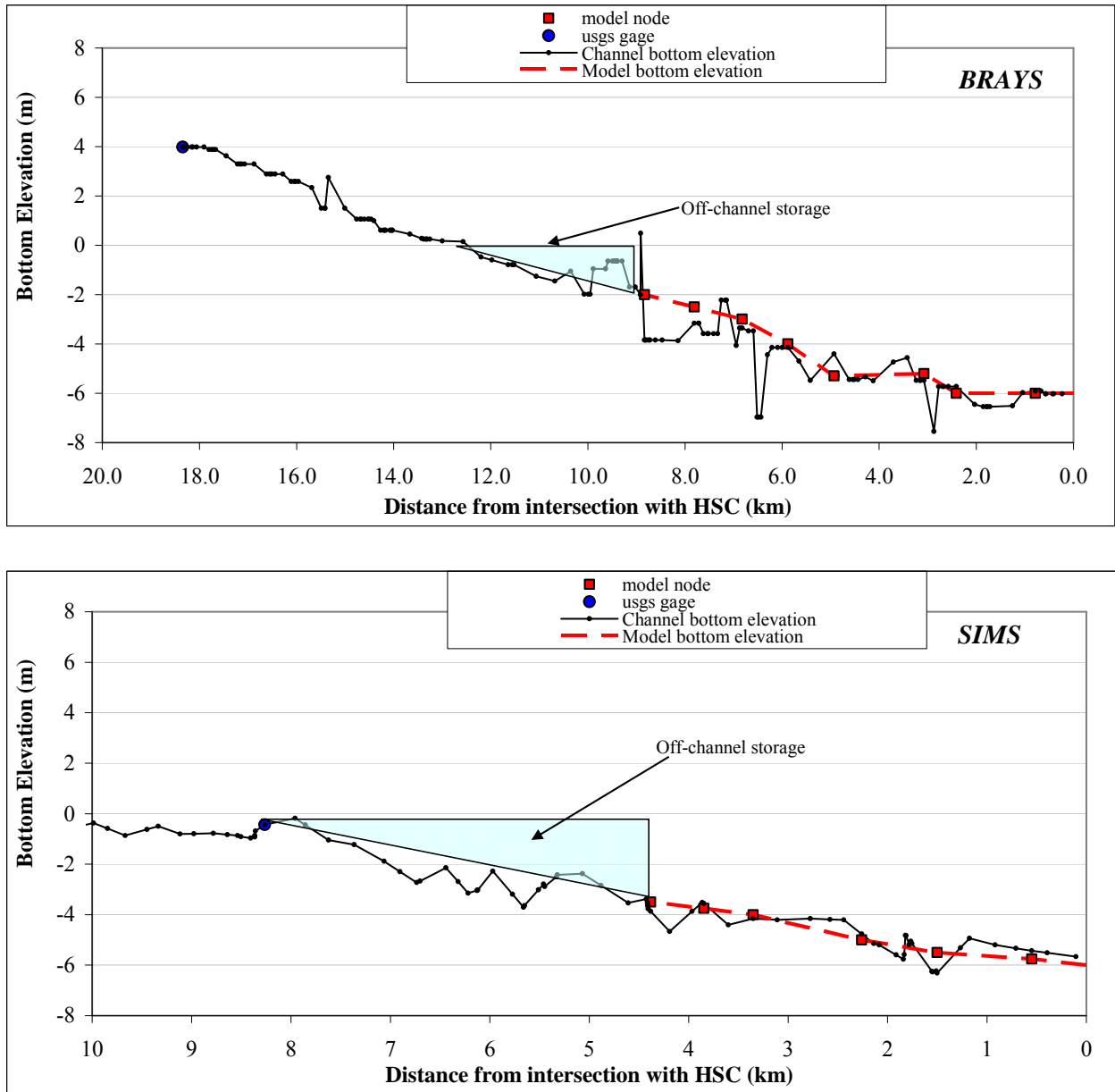
Figure 2.2 Bottom Elevations for the Houston Ship Channel (upstream San Jacinto River)

³ An attempt was made to simulate the tributaries using the cross-sections obtained from TSARP, but the steep side slopes caused the model to crash.



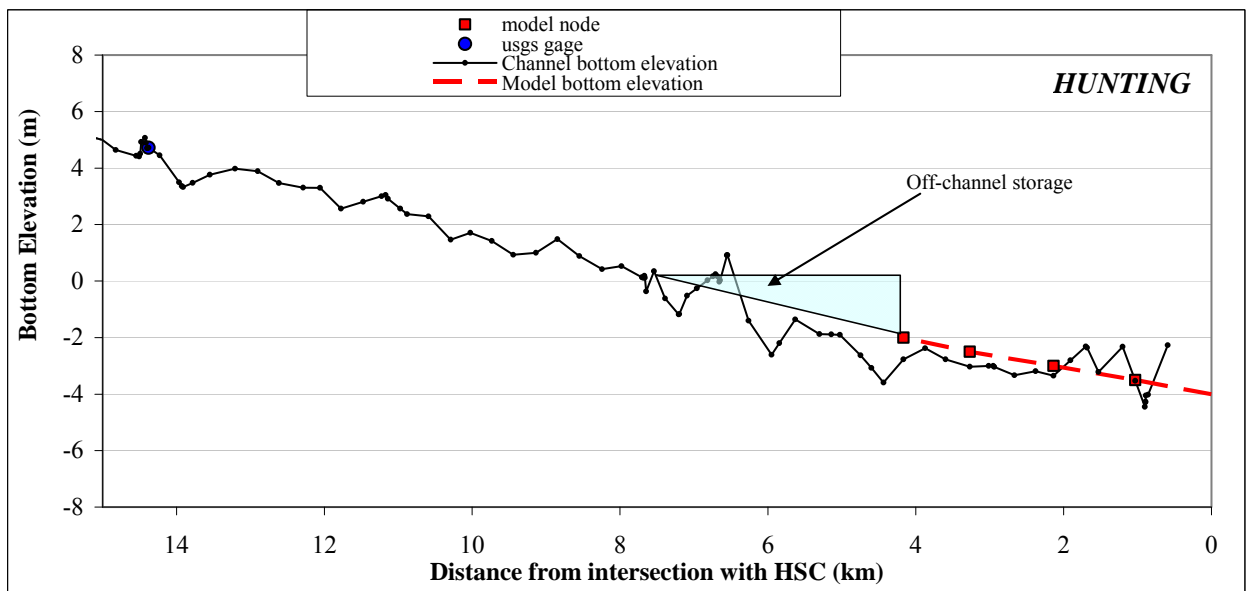
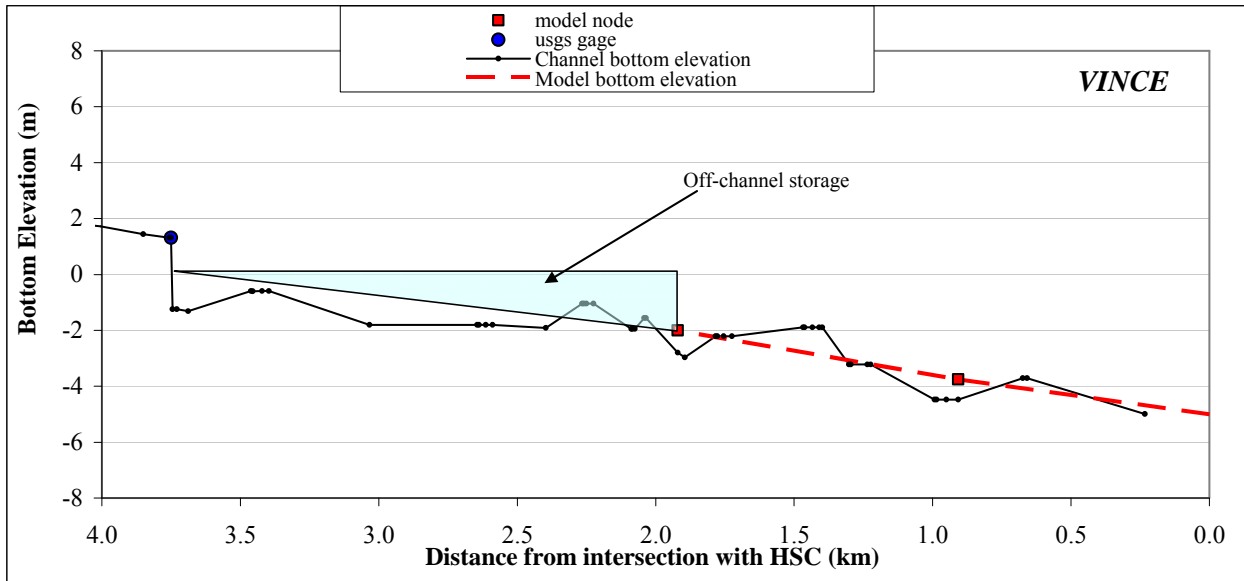
Bottom elevations were obtained from the TSARP cross-sections for the relevant portions of the various tributaries

Figure 2.3 Bottom Elevations for the Tidal Portions of Major Tributaries to the HSC



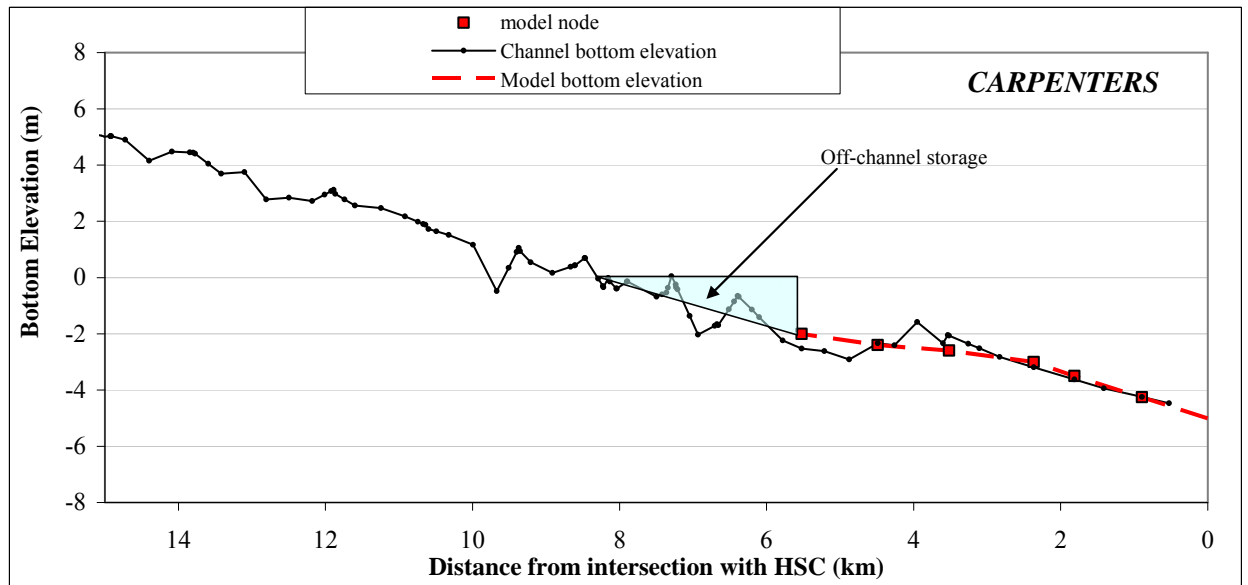
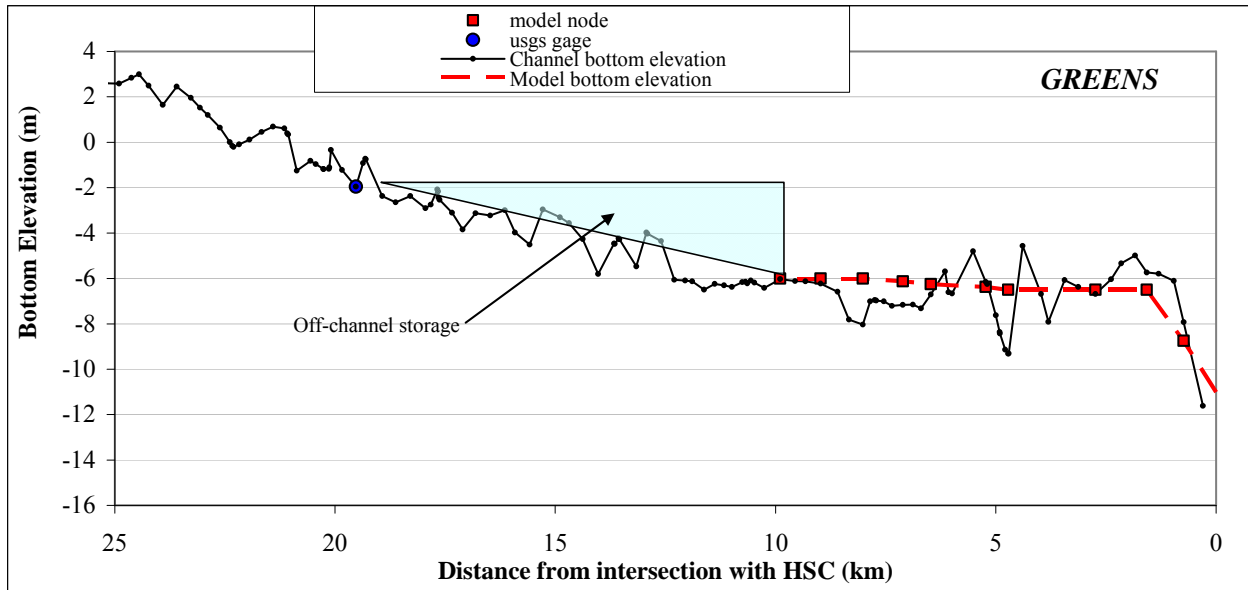
Bottom elevations were obtained from the TSARP cross-sections for the relevant portions of the various tributaries

Figure 2.3 Bottom Elevations for the Tidal Portions of Major Tributaries to the HSC – Cont'd



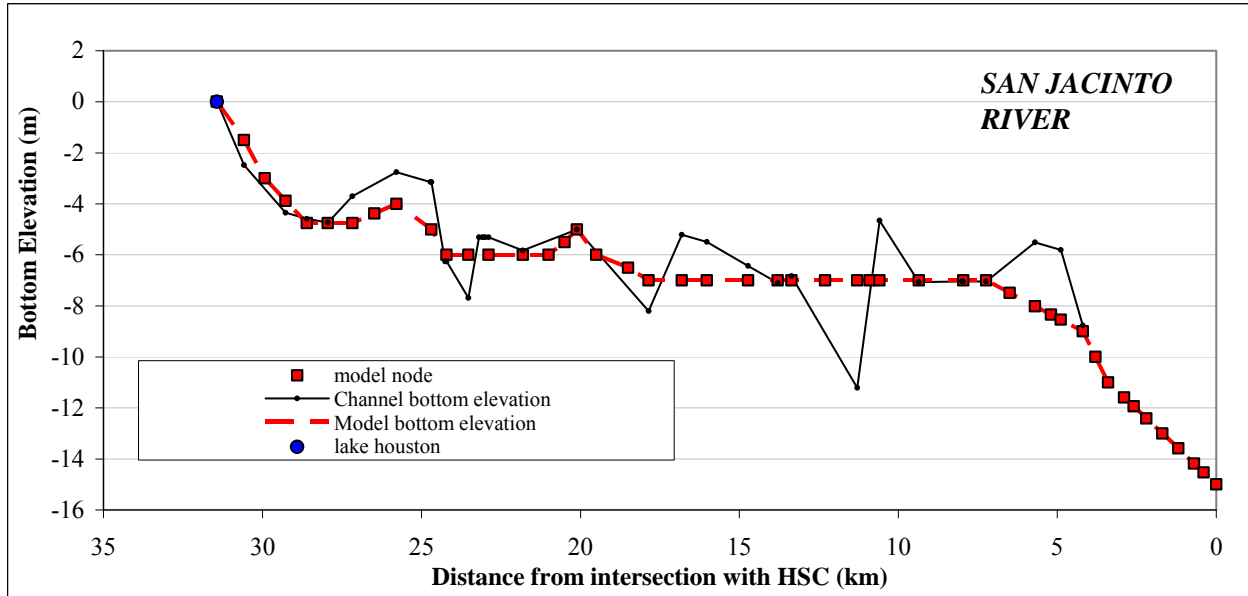
Bottom elevations were obtained from the TSARP cross-sections for the relevant portions of the various tributaries

Figure 2.3 Bottom Elevations for the Tidal Portions of Major Tributaries to the HSC – Cont'd



Bottom elevations were obtained from the TSARP cross-sections for the relevant portions of the various tributaries

Figure 2.3 Bottom Elevations for the Tidal Portions of Major Tributaries to the HSC – Cont'd



Bottom elevations were obtained from the TSARP cross-sections for the relevant portions of the various tributaries

Figure 2.3 Bottom Elevations for the Tidal Portions of Major Tributaries to the HSC – Cont’d

For the entire model grid, the bottom roughness coefficient was assumed to change with depth using an RMA2 model feature that provides for real-time adjustment of the Manning’s n-value of an element depending on the water depth. Generally, the roughness value decreases with higher water depths. The corresponding n-value is calculated in the model using the following equation:

$$n = \frac{n_{nv}}{D_{avg}^{RC}} + 0.036 \cdot e^{\frac{-D_{avg}}{2}} \quad (2.3)$$

where n = Manning’s n-value,

n_{nv} = maximum n-value for non-vegetated water (final calibration value 0.03),

RC = roughness by depth coefficient (final calibration value 0.08), and

D_{avg} = average depth.

Table 2.2 Dimensions of Cross-Sectional Areas for Tributaries in the Model

Tributary	Average Measured Area (m ²)	Bottom Width (m)	Side Slopes	Average Depth (m) ^a	Average Modeled Area (m ²)
Buffalo Bayou at McKee St.	137	12	3.5	4.7	134
Whiteoak Bayou	121 ^b	12	3.5	4.3	116
Brays Bayou at Broadway Blvd.	300	35	3.5	5.4	332
Sims Bayou at Lawndale Ave.	169	10	3.5	5.4	158
Vince Bayou at North Richey St.	132	25	3	3.4	122
Hunting Bayou at Federal Rd.	103	16	3.5	3.4	97
Greens Bayou at I-10 bridge	247	20	3	6.3	246
Carpenters Bayou at South Sheldon Rd.	69	20	3.5	2.5	74
Goose Creek	115 ^b	12	3.5	4.1	108

^a From preliminary model runs

^b Flow was not measured at those tributaries. The cross-sectional area was determined using TSARP cross-sections

2.4.2 Tide Data

There are four NOAA stations and one USGS station in the modeled area (Table 2.3 and Figure 2.4). Six-minute gage data for the simulation period were downloaded from TCOON⁴ <http://lighthouse.tamucc.edu/TCOON/HomePage>. Hourly gage data for the SJR station were obtained from the USGS. Tide data for Eagle Point was input to the model as the downstream boundary condition. Water surface elevations for the other stations were used for calibration purposes. It is noted that because the boundary data had spikes that might cause numerical problems in RMA2 (divergence), the data series was smoothed using a Daniell smoothing

⁴ Texas Coastal Ocean Observation Network

technique⁵ available in the Statistica package.

Table 2.3 Tide Gages in the Modeled Area

Station Description	Gage ID	Gage Maintained By
Eagle Point	87710131	NOAA
Morgan’s Point	87706131	NOAA
Battleship Texas	87707431	NOAA
Manchester	87707771	NOAA
San Jacinto River at Sheldon	08072050	USGS

A database containing the tide data is included in Appendix B.

2.4.3 Freshwater Inflow Data

Hourly flow data for the USGS gages in the modeled area (Figure 2.4) were obtained for the period January 2002 to May 2005. These flow data were used as the upstream boundary condition for the main tributaries in the model. For the tributaries with no available flow data, either a constant flow rate or a flow series from a tributary with a similar drainage area was assumed. Table 2.4 presents a summary of the assumed flow boundary conditions for the various tributaries.

For the SJR, hourly gage height data were obtained for Lake Houston (gage 08072000) and hourly discharges from the Lake were calculated using a rating curve developed by the USGS (see Appendix B).

⁵ This is a simple equal weight smooth where the weight of neighboring observations is divided by two for each time step away from the time step of interest. So for a time series with $t = -3, -2, -1, 0, 1, 2, 3$ the weights of the observations would be $1/8, 1/4, 1/2, 1, 1/2, 1/4, 1/8$.

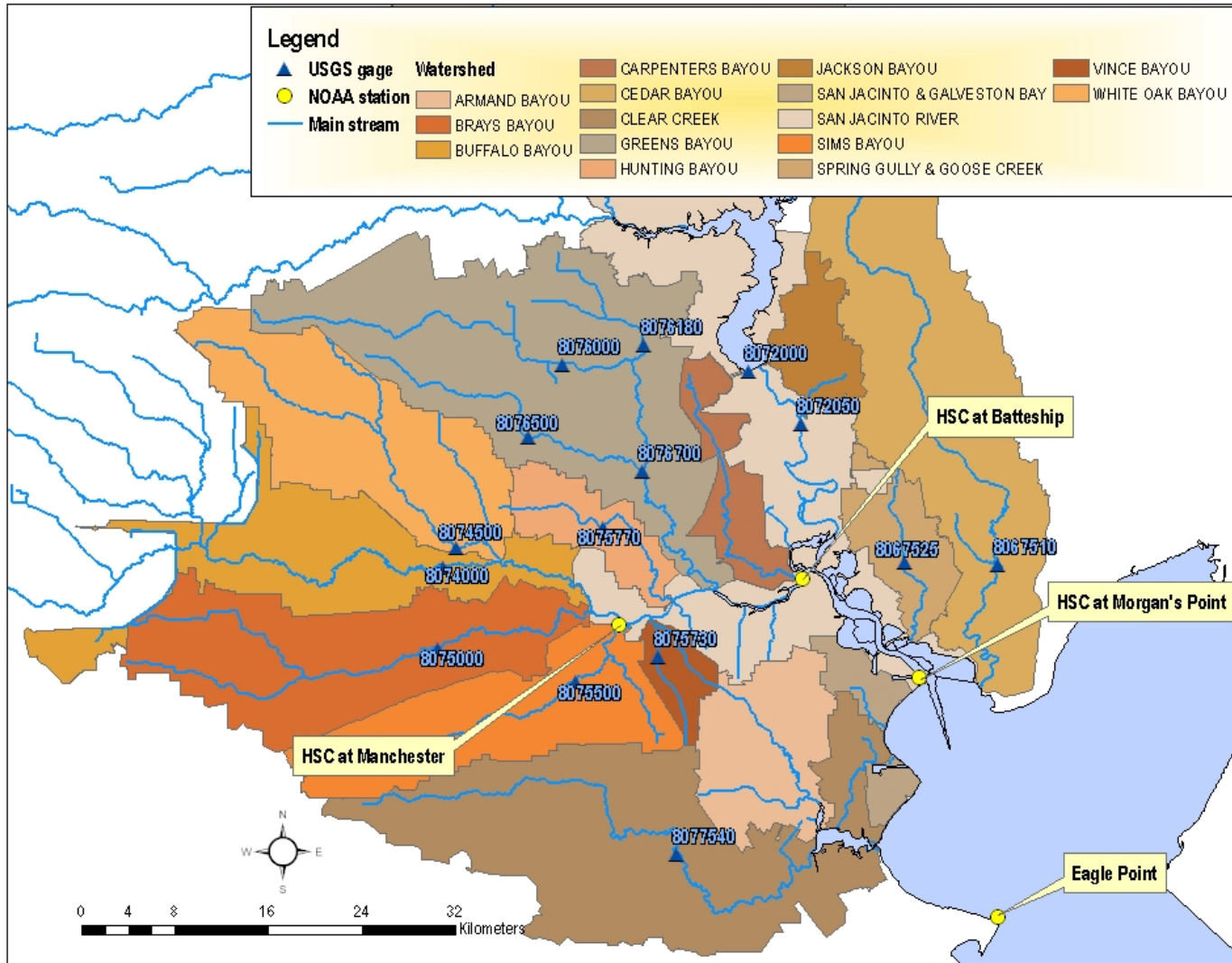


Figure 2.4 Tide and Flow Gages in the Model Domain

Table 2.4 Upstream Boundary Conditions for the RMA Model

Tributary	Boundary Type	Source of data
Buffalo Bayou	Transient unit flow rate	Hourly data for gage 08074000
Whiteoak Bayou	Transient unit flow rate	Hourly data for gage 08074500
Brays Bayou	Transient unit flow rate	Hourly data for gage 08075000
Sims Bayou	Transient unit flow rate	Hourly data for gage 08075500 for the model period are not available. Assumed hourly data for Brays Bayou
Vince Bayou	Transient unit flow rate	Hourly data for gage 08075730
Hunting Bayou	Transient unit flow rate	Hourly data for gage 08075770
Greens Bayou	Transient unit flow rate	Hourly dataset for gage 08076700 for the simulation period is incomplete and flows appear too high. Summation of hourly data for gages 08076000, 08076180, and 08076500
Carpenters Bayou	Transient unit flow rate	No USGS gages are located in this watershed. Assumed hourly data for Hunting Bayou (similar drainage area)
San Jacinto River	Transient unit flow rate	Rating curve for gage 08072000
Goose Creek	Constant unit flow rate (0.5 m ³ /s)	Average flow rate for Hunting Bayou (similar drainage area) for simulation period
Cedar Bayou	Constant unit flow rate (1 m ³ /s)	Assumed
Clear Creek	Constant unit flow rate (2 m ³ /s)	Average flow for period of record for gage 08077540

Flows from point sources discharging to the tributaries downstream of the USGS gages (Table 2.5) were added to the flows reported from USGS. For point sources discharging directly to the main channel, flows were input at five locations (Table 2.5). To include these inflows into the system, model elements (or reaches) were created at the points of discharge and a constant flow rate equal to the sum of the average self-reported flows for years 1997-2002 was used. The only exception was the flow from the City of Houston-69th Street Plant. Self-reported monthly average flows for 2005 for this plant were downloaded from the USEPA Permit Compliance System (PCS) database at www.epa.gov/enviro. The monthly flow rates were then converted to hourly values using conversion factors developed for the Buffalo Bayou and Whiteoak Bacteria

TMDL Project (University of Houston, 2005a). The hourly flow dataset for the 69th Street Plant is included in Appendix B. Finally, there is a facility near Cedar Bayou (Cedar Bayou Power Plant) that pumps water from Cedar Bayou and discharges it to the Trinity River delta. Virtually all the water moves from Tabbs Bay upstream through Cedar Bayou to the pump intake, most of it moving through an artificial channel (the “cut-off channel”) between Tabbs Bay and the bayou, greatly impacting the hydrodynamics in Cedar Bayou and Tabbs Bay. To account for the effects of the pumping at the facility, monthly average flows reported in the USEPA PCS database were subtracted from the upstream inflow in Cedar Bayou. It is noted that although during the calibration period the power plant did not use much water (only 1.9 m³/s on average), there were months for which the average rate of pumped water was greater than 40 m³/s, greatly affecting the long-term runs.

Table 2.5 Flow from Point Sources in the RMA2 Model

Stream	Model node	Total Flow (m³/s)
Brays Bayou	Boundary	0.5
Sims Bayou	Boundary	1.5
Vince Bayou	Boundary	0.7
Greens Bayou	Boundary	0.9
Goose Creek	Boundary	0.2
Cedar Bayou	Boundary	-1.9
Main Channel – 69th St	3106	3.5 ^a
Main Channel	3035	1.4
Main Channel	3021	0.5
Main Channel	2993	1.2
Main Channel	2962	1.7
San Jacinto River	2980	0.5

^a Average self-reported flow. A 1-hr time series was input to the model.

2.4.4 Meteorology

Hourly wind speed and direction data for the NOAA station at Eagle Point was input to the model (Appendix B). Wind data are used in the model to calculate wind friction to obtain proper setup and system circulation of shallow areas with strong wind influences. Wind data were globally applied throughout the model domain.

Rainfall and evaporation were input to the model as a global condition. The data series are included in Appendix B.

Appendix C contains the ASCII input decks (geometry and boundary conditions) for the RMA2 model of the HSC.

2.5 SPIN-UP TIME DETERMINATION

For dynamic runs, the initial conditions can adversely affect the results during the first part of a simulation. This is because the model is “shocked” by the initial conditions if they are not very close to what is expected. To eliminate any adverse effects, the model was initially run starting two days prior to the period of calibration (480 time steps).

To verify if the two-day period was sufficient, the time needed for RMA2 to stabilize was verified by inputting a smooth sinusoidal repetitive water surface elevation boundary condition signal at the downstream boundary together with constant fresh water inflows for the upstream boundaries. The spin-up time was then estimated by determining when the model begun to repeat the solution for both water surface and velocity at two control points: HSC at Morgan’s Point and Buffalo Bayou at McKee as illustrated in Figure 2.5.

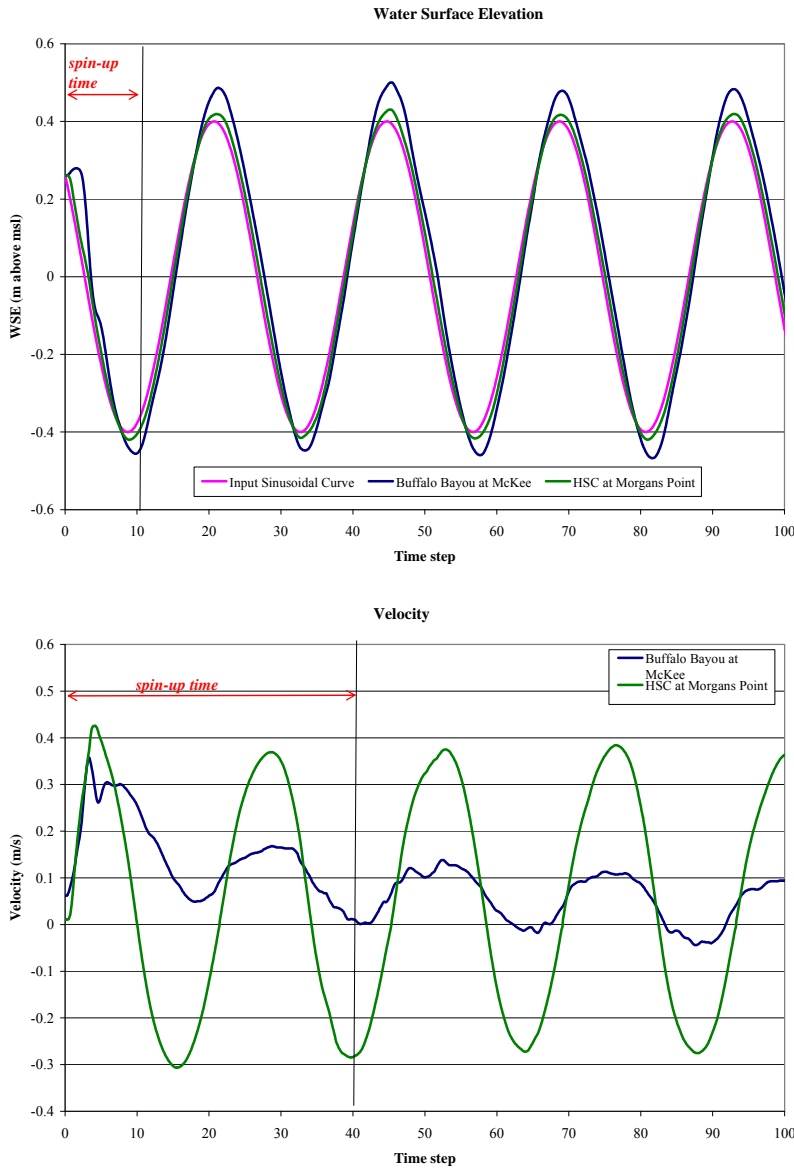


Figure 2.5 Verification of Spin-up Time for the Hydrodynamic Model

As can be observed in Figure 2.5, the HSC RMA2 model required 10 time steps to repeat the water surface elevation solution and 40 time steps to repeat the velocity solution. Therefore, the spin-up time for the model is 40 time steps, which is shorter than the two days (480 time steps) assigned in the model setup. Thus, results for the calibration period were not expected to be affected by the initial conditions. The spin-up time was ultimately set to three weeks to

account for the time needed by WASP to stabilize. A description of how this time period was determined is presented later in the report.

2.6 MODEL CALIBRATION

2.6.1 Water Surface Elevation

The RMA2 model of the HSC system was first calibrated to NOAA and USGS water elevation data for the model period. The main calibration parameter was the Manning’s n-value. Figure 2.6 compares the simulated and observed water surface elevation time series for the various gages. It can be seen that the model accurately reproduces the tide heights observed at Morgan’s Point, Battleship, and Manchester (IH-610), with a slight decrease in accuracy as one moves upstream in the system. However, the water surface elevations for the USGS gage in the SJR could not be matched; the model simulates the general patterns of the data, but the modeled levels are consistently below the observed values. There appears to be a datum problem with the data for this location that results in measured water levels in the SJR that are about 30 cm higher than those measured in the HSC and Galveston Bay.

Plots of modeled versus observed tide data are presented for the three NOAA stations in Figure 2.7. The best-fit line and the 1:1 line are also presented in the plots to aid in determining the goodness-of-fit. It can be seen that the regression lines are very close to the 1:1 line, with slopes around 1 and relatively small intercepts (between 0.7 and 6.6 cm). This observation confirms that the model is simulating the tide data well.

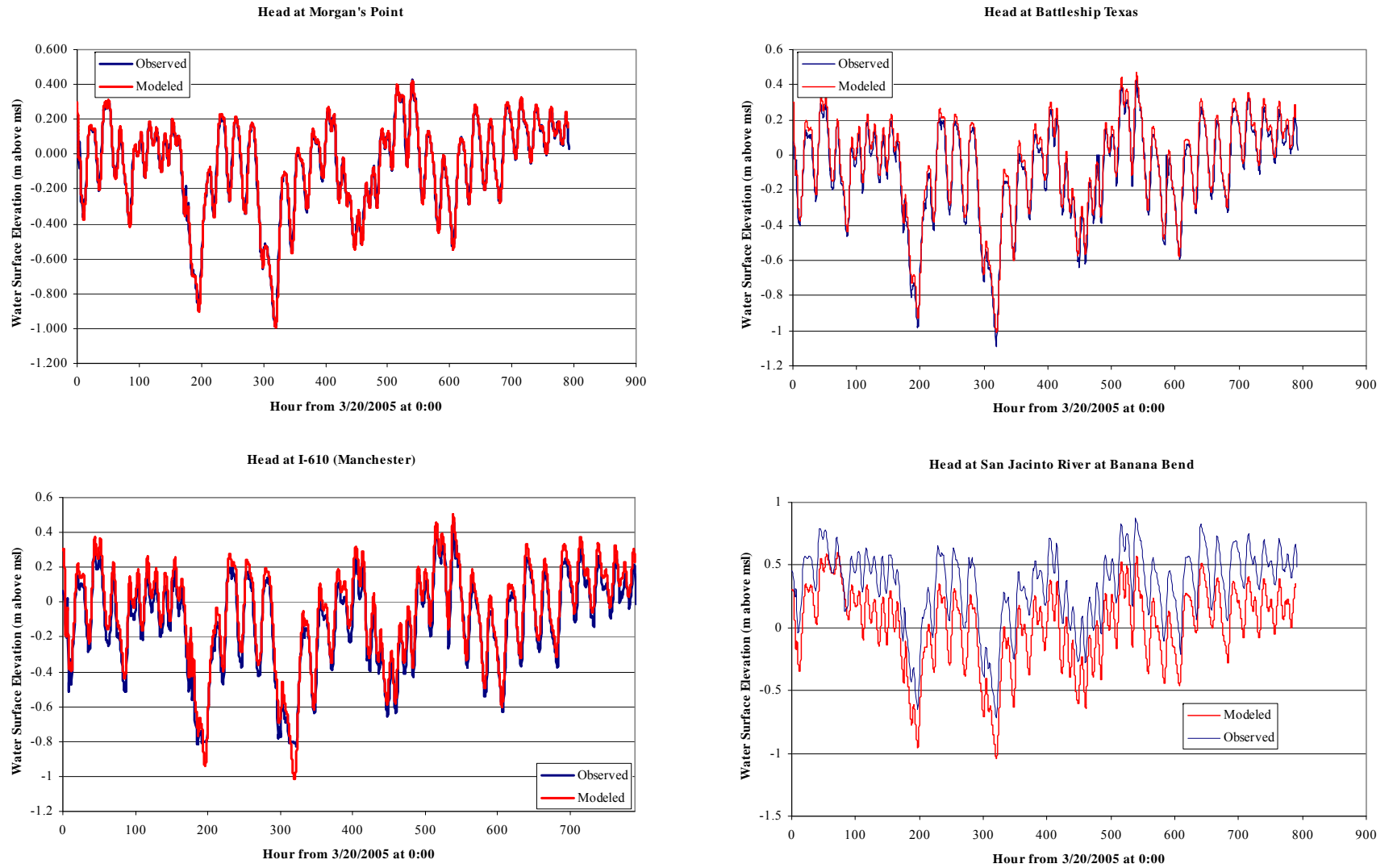


Figure 2.6 Observed and Simulated Water Surface Elevations in the HSC

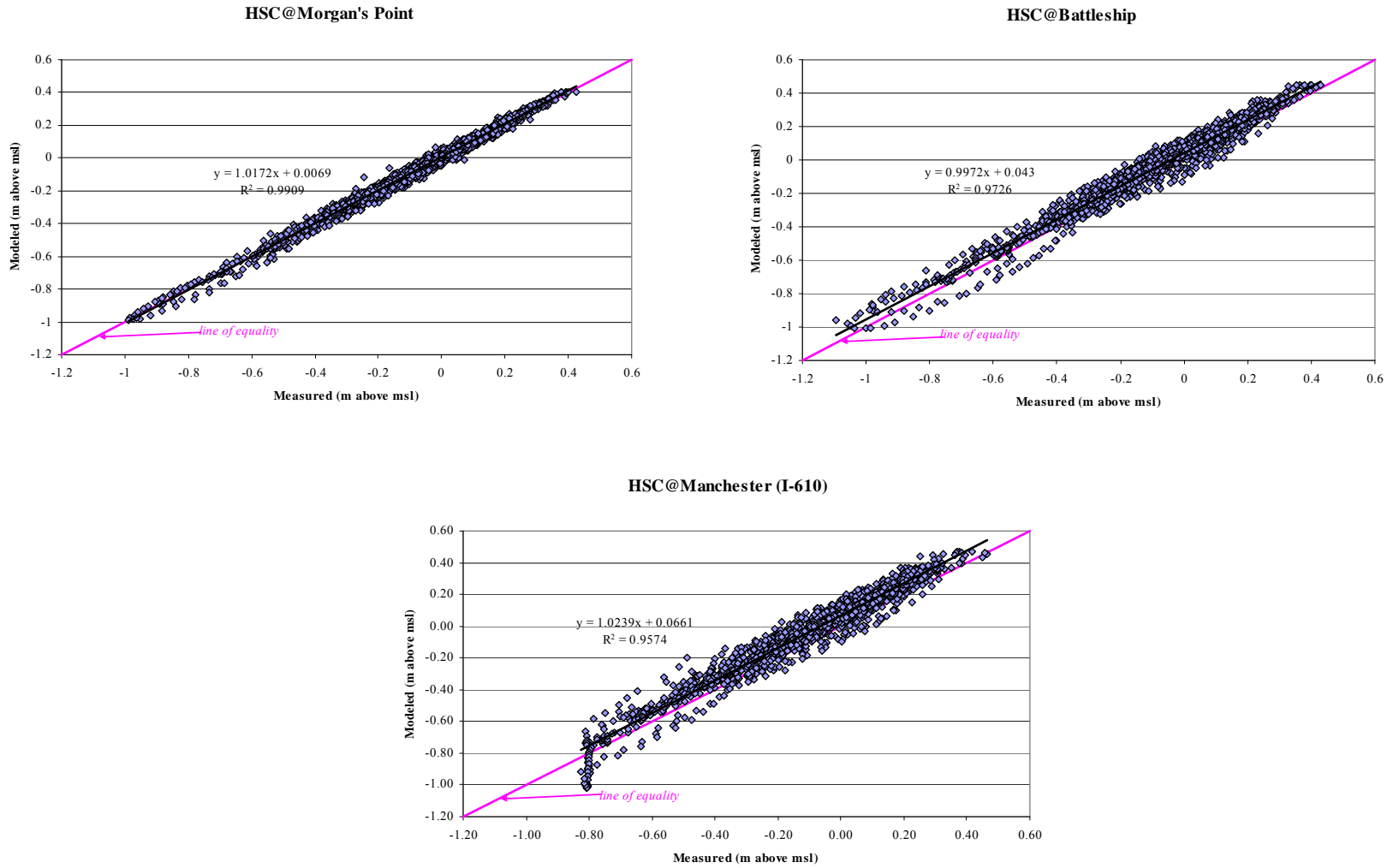


Figure 2.7 Scatterplots of Observed and Modeled Water Surface Elevations in the HSC

In addition to the plots previously presented, a variety of model statistics were calculated to measure model performance. These are discussed in Stow *et al.*, (2003) and Legates and McCabe (1999) and include:

1. the correlation coefficient of model predictions and observations, r :

$$r = \frac{\sum_{i=1}^n (O_i - \bar{O})(P_i - \bar{P})}{\sqrt{\sum_{i=1}^n (O_i - \bar{O})^2 \sum_{i=1}^n (P_i - \bar{P})^2}} \quad (2.4)$$

2. the model efficiency, MEF :

$$MEF = \frac{\sum_{i=1}^n (O_i - \bar{O})^2 - \sum_{i=1}^n (P_i - O_i)^2}{\sum_{i=1}^n (O_i - \bar{O})^2} \quad (2.5)$$

3. the index of agreement, d :

$$d = 1.0 - \frac{\sum_{i=1}^n (P_i - O_i)^2}{\sum_{i=1}^n (|P_i - \bar{O}| + |O_i - \bar{O}|)^2} \quad (2.6)$$

4. the root mean squared error, $RMSE$:

$$RMSE = \frac{\sqrt{\sum_{i=1}^n (P_i - O_i)^2}}{n} \quad (2.7)$$

where n =number of observations, O_i = i th of n observations, P_i = i th of n predictions, and \bar{O} and \bar{P} =observation and prediction averages, respectively.

The correlation coefficient, r , ranges from -1 to 1 and measures the tendency of the predicted and observed values to vary together linearly⁶. The model efficiency, MEF , measures how well a model predicts relative to the average of observations; a value close to 1 indicates a good match between observations and model predictions. The index of agreement, d , varies from 0 to 1 , with higher values indicating better agreement between the model and observations. Finally, the root mean squared error, $RMSE$, measures the magnitude of the discrepancies between predicted and observed values, with values close to zero indicating a good match. A summary of the different statistics calculated for water surface elevations at the various gages is presented in Table 2.6. Results presented in Table 2.6 indicate an excellent level of agreement between predicted and observed values.

Table 2.6 Model Summary Statistics for Water Elevations

Statistic	HSC@Morgan’s	HSC@Battleship	HSC@I-610
r	0.996	0.992	0.986
MEF	0.991	0.960	0.915
d	0.998	0.990	0.987
$RMSE(m)$	0.001	0.001	0.002

2.6.2 Velocity and Flow

The model was calibrated to the velocities and flows measured in the channel during Spring 2005. The locations of the observation points are shown in Figure 2.8. The calibration

⁶ This parameter is equivalent to the square root of the coefficient of determination (r^2) of the best-fit line presented in Figure 2.7.

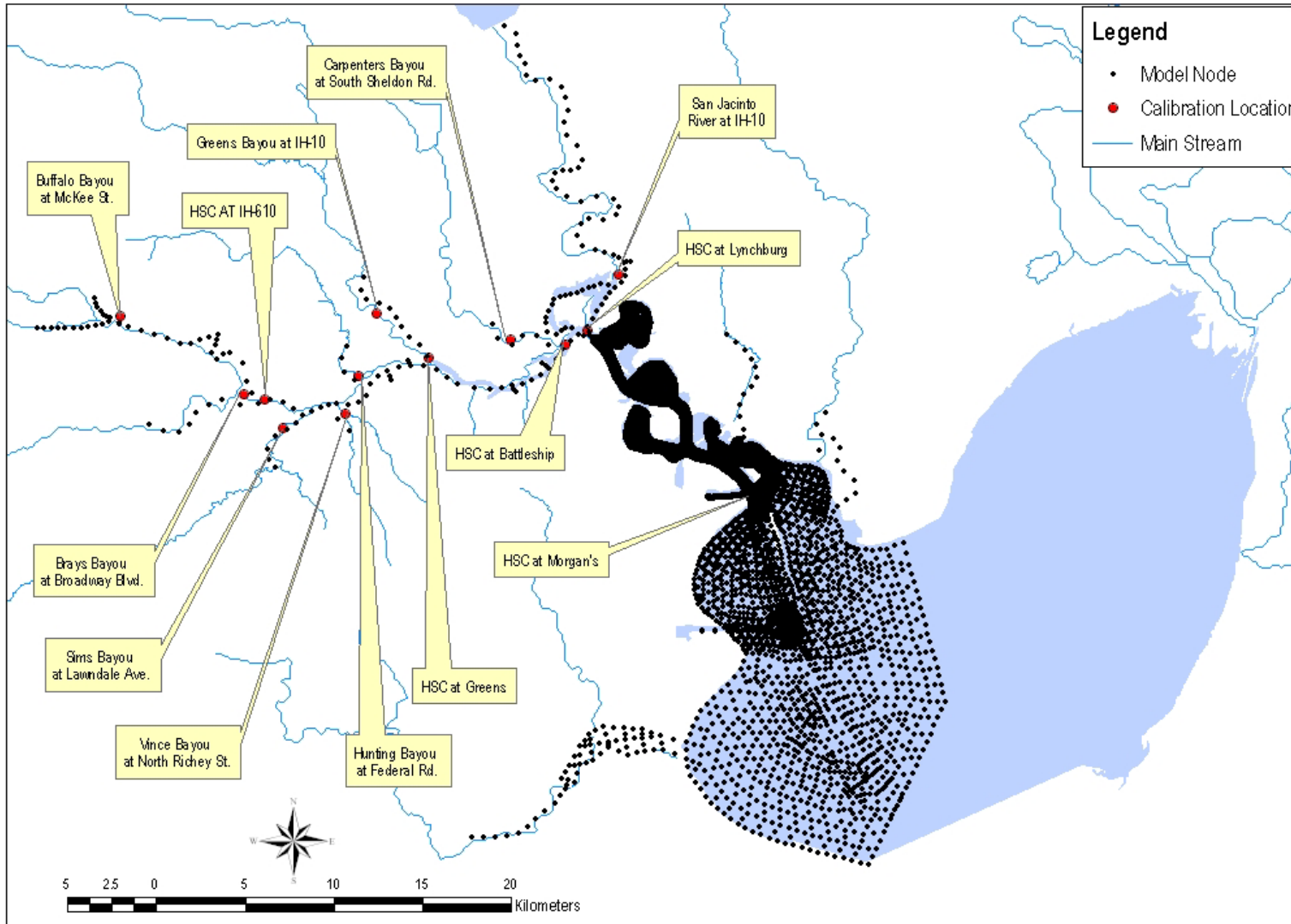


Figure 2.8 Velocity and Flow Calibration Locations

procedure was as follows: first, the average cross-section areas for the entire simulation period were calculated for each location to verify that they were within acceptable criteria ($\pm 10\%$ of the measured areas); second, the velocity time-series were compared to the measured data, model parameters (Manning’s n and off-channel storage slope) were adjusted until the velocity series matched the ranges of measured values; and, finally, once cross-sectional areas and velocities were calibrated, output flow time-series were compared to measured flows to verify the model results. Table 2.7 summarizes the percent error in average cross-sectional areas predicted by the model.

Table 2.7 Difference between Measured and Predicted Cross-sectional Areas

Location	Model node	Average Measured Area (m ²)	Average Modeled Area (m ²)	Error ^b
HSC@Morgan's Point	NA ^a	3853	4023	4%
HSC@Lynchburg Ferry	2753	4330	3955	-9%
HSC@Battleship	2951	3824	3835	0%
Carpenters Bayou@Sheldon Rd	2963	69	74	7%
San Jacinto River@I-10	2957	1438	1312	-9%
HSC@Greens Bayou	3015	2250	2101	-7%
Greens Bayou&I-10	3031	247	246	0%
Hunting Bayou@Federal Rd	3055	103	97	-6%
Vince Bayou@North Richey St	3071	132	122	-8%
Sims Bayou@Lawndale Ave	3085	169	158	-7%
HSC@I-610	3087	1542	1492	-3%
Brays Bayou@Broadway Blvd	3097	300	332	11%
Buffalo Bayou@McKee St	3118	137	150	9%

^a This observation location is in the 2-D section of the model, so parameters were calculated for a continuity line rather than at a single node

^b Error was calculated as $\frac{(A_{\text{mod}} - A_{\text{obs}})}{A_{\text{obs}}} \cdot 100\%$

Figure 2.9 displays the time series of observed and predicted water velocities for the thirteen sampled locations. While there is some deviation between observed and modeled velocities (especially for some of the tributaries), the ranges of predicted values correspond to

those measured in the field. It should be recognized that there is substantial error or uncertainty in the flow measurement data, and in regression-based flow predictions based on those measurements. This error is due both to measurement problems, as well as temporal error and the fact that the flows are constantly changing with tide while flow measurements take several minutes. Thus, when looking at calibration results for an individual site, the measurement may be as much or more responsible than the model for the calibration error.

Similarly, Figure 2.10 provides a graphic comparison of predicted to measured flows at the 13 observation locations in the HSC system. As expected from the calibration of cross-sectional areas and water velocities, the model predicts reasonably well the magnitude and direction of the flows.

To measure model performance, scatterplots of modeled versus observed data were prepared and compared to 1:1 lines for all the observation locations (Figures 2.11 and 2.12). When one-to-one comparisons are made, the model performance is rather poor. The best results were obtained for HSC@Lynchburg, HSC@Greens, SJR, Greens Bayou, Sims Bayou, and Brays Bayou. One-to-one calibration at HSC@Battleship showed the worst results, with a best-fit-line slope near zero. It is noted, however, that a comparison between the time series produced by the model and a few observations available for each location is, by itself, not an indication of overall model performance. Furthermore, in most of the tributaries several measurements that varied within a relatively wide range were made within a period of an hour or shorter. The model is not expected to simulate these sudden changes in velocity and flow. This caused the slopes of the best-fit lines to be significantly different from 1.

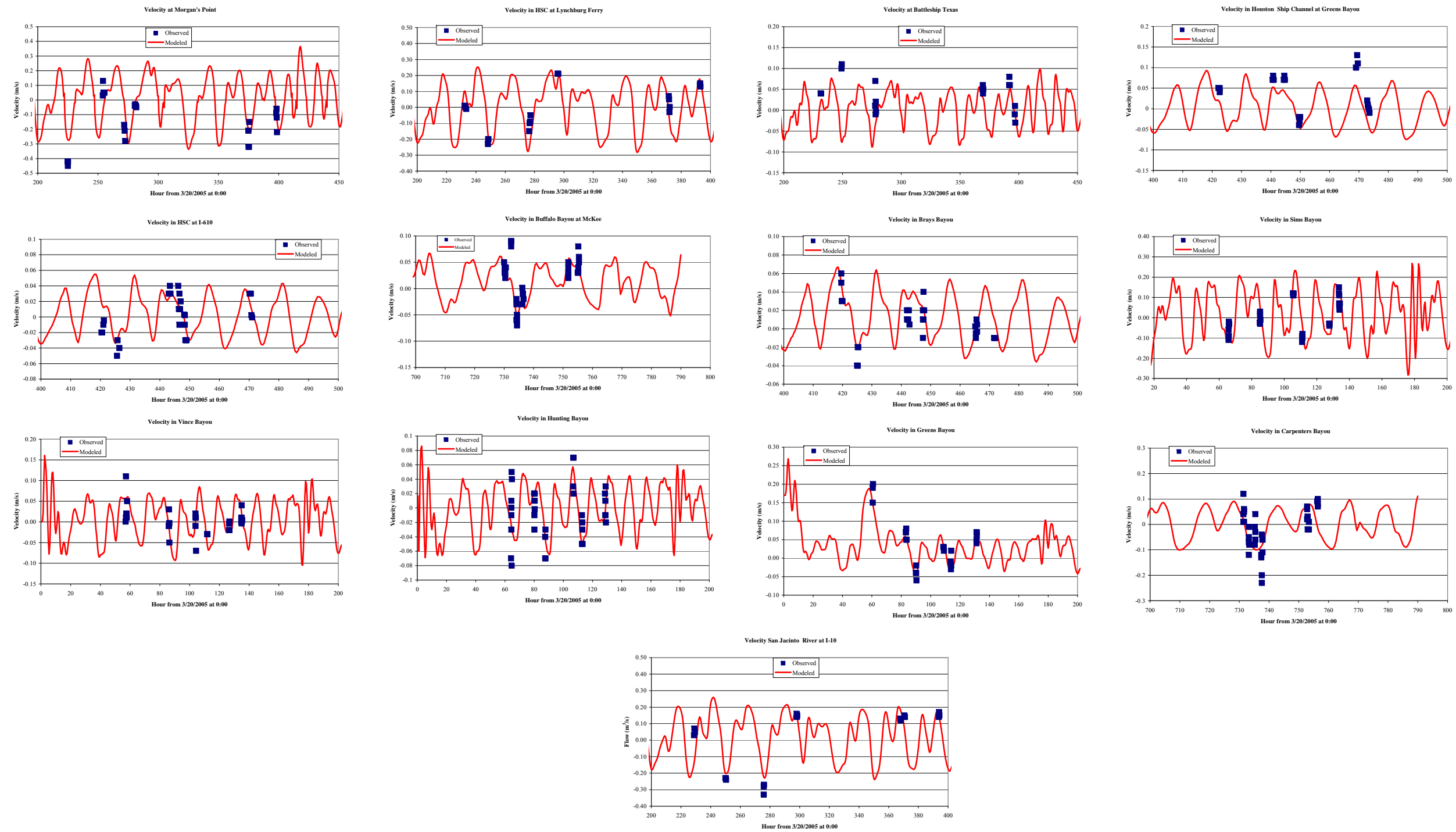


Figure 2.9 Modeled and Measured Water Velocities

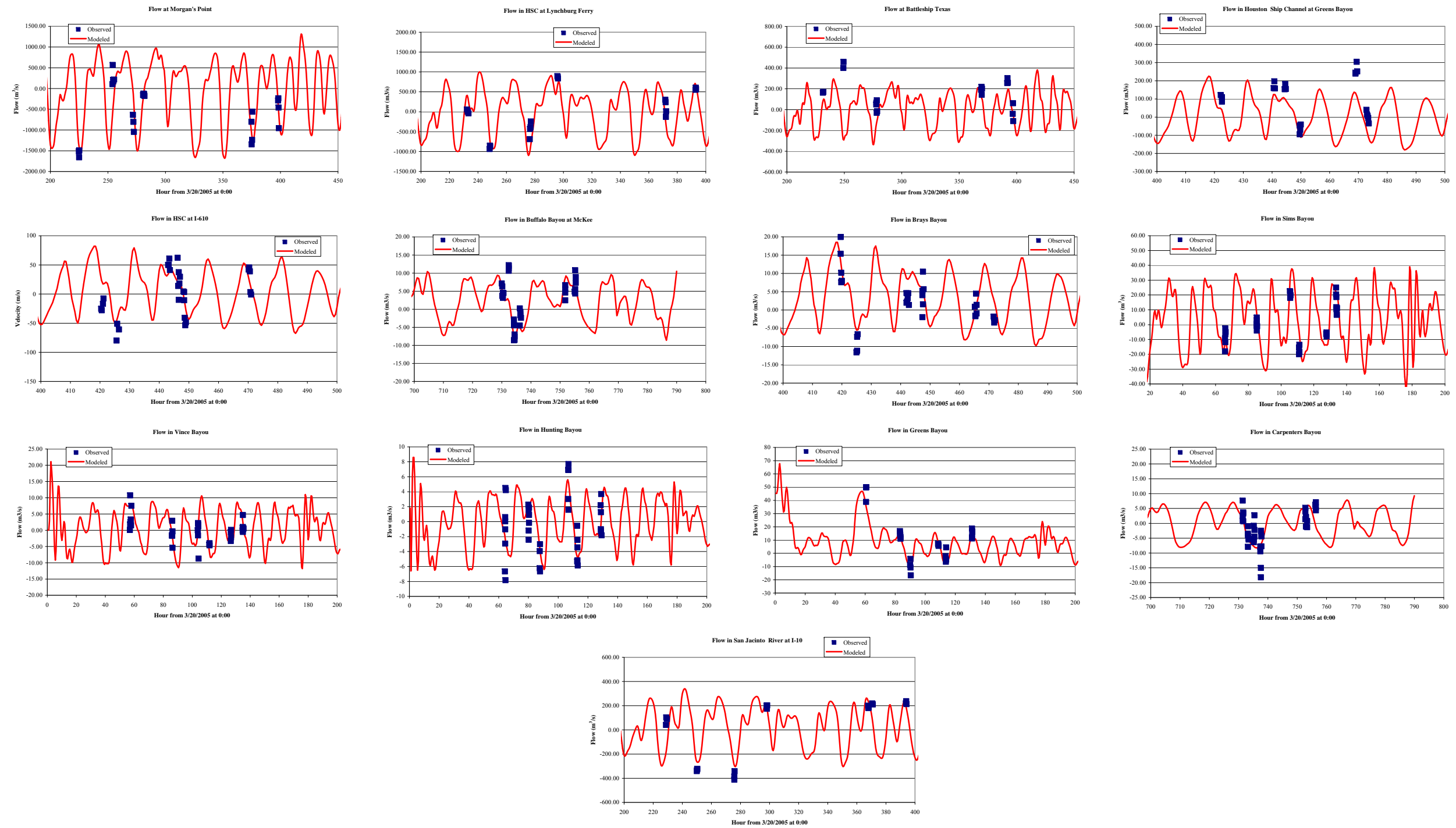


Figure 2.10 Modeled and Measured Water Flows

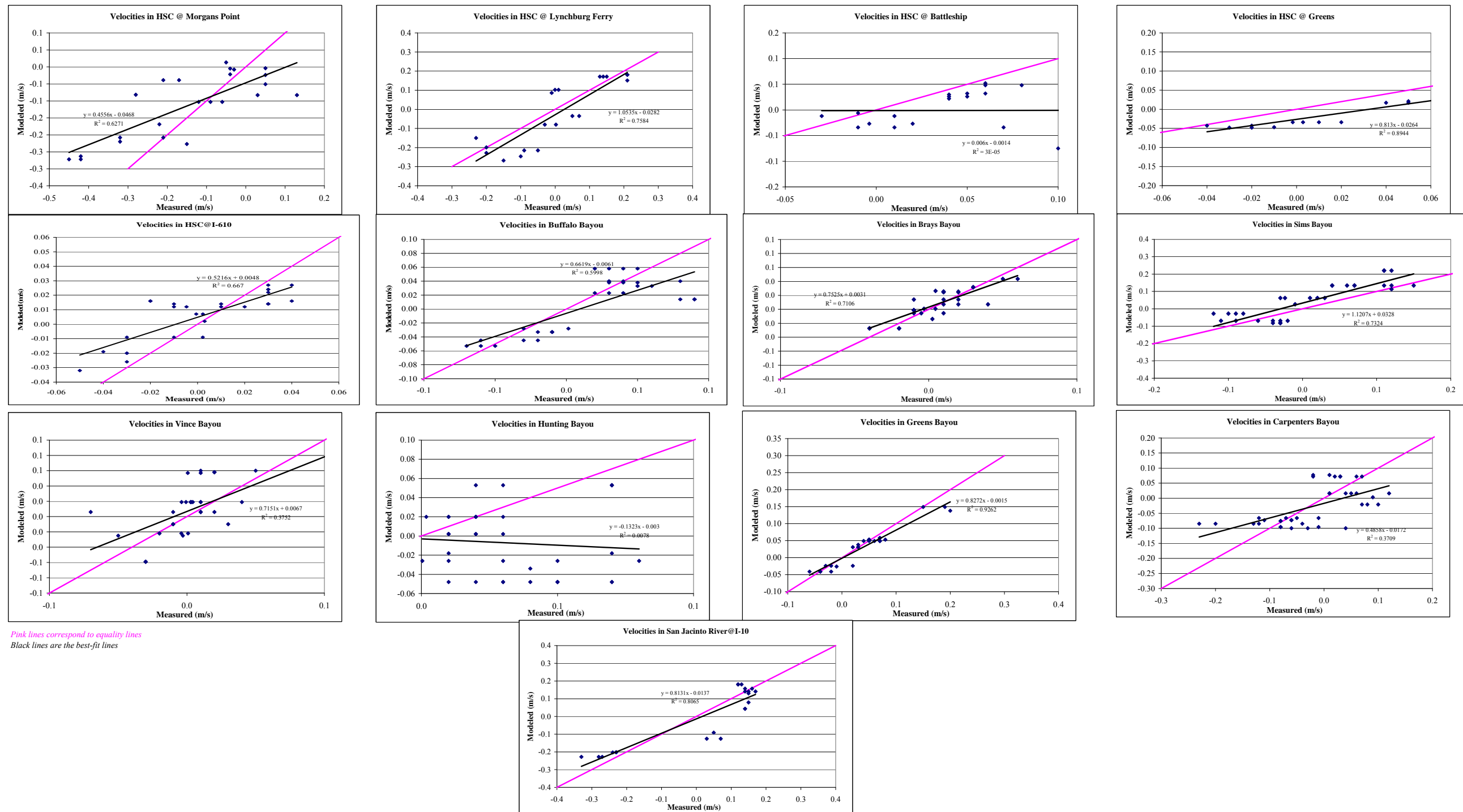


Figure 2.11 Scatterplots of Observed and Modeled Water Velocities using Discrete Values

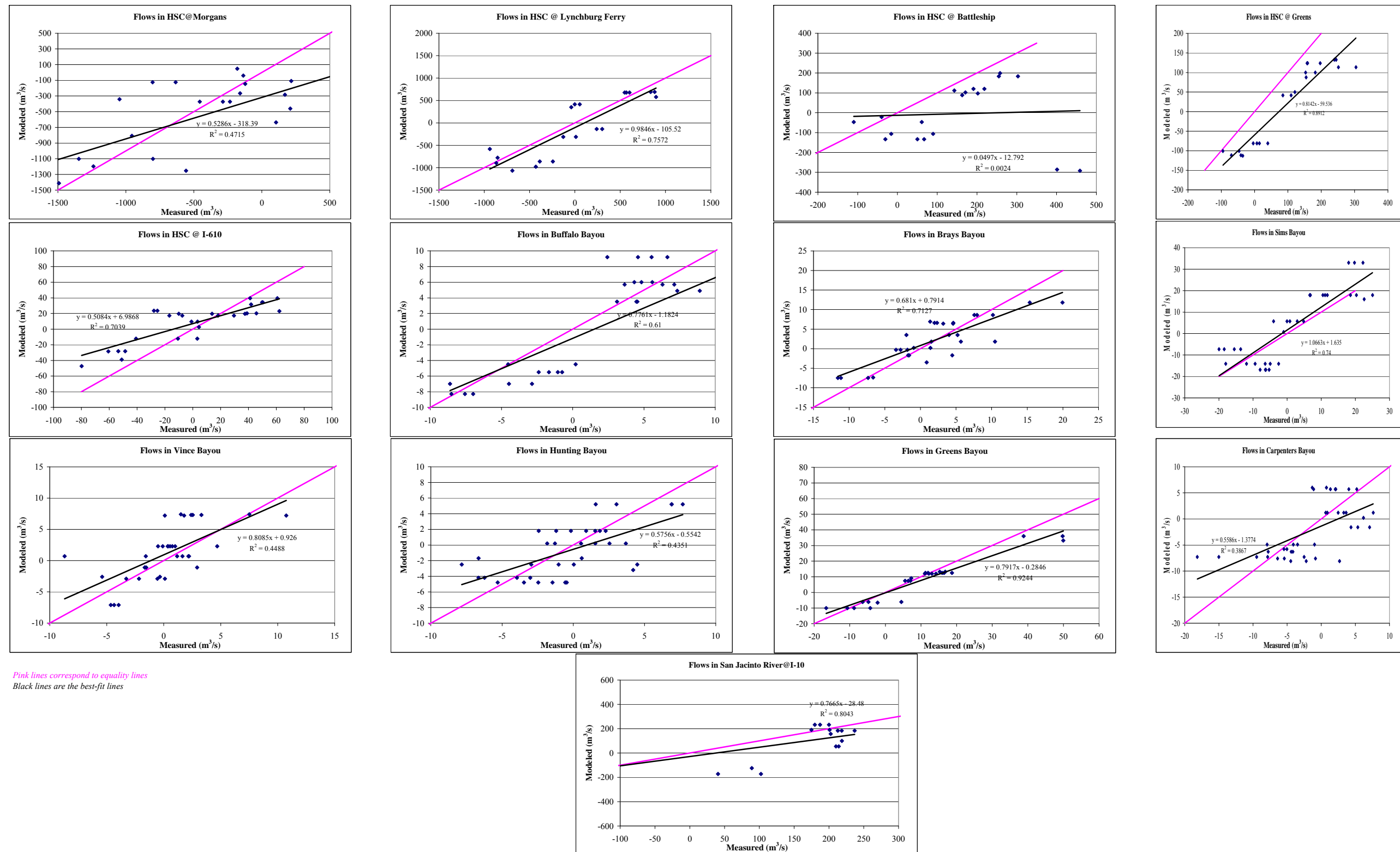


Figure 2.12 Scatterplots of Observed and Modeled Water Flows using Discrete Values

To get a reflection of how well the model reproduces the overall patterns, a second criterion was applied, as shown in Figures 2.13a through m. The criterion used in the figures consists of comparing the model flow output (blue line) to continuous time-series developed by the project team using linear regressions (green line) between the measured flows and the change in tide height for the various locations (University of Houston, 2005b)⁷. For this criterion, the calibration targets included the coefficient of determination (r^2) and the flow duration curve. The top plots, comparisons of model results with the flows from regressions, clearly show that the model output reflects the magnitude and pattern of the observed data for most locations. For the main channel (Figures 2.13a to 2.13e), the model performance is good based on r^2 values varying between 0.61 and 0.92. In addition, the simulation agrees well with the observed flow duration curves across all flow conditions, with the exception of the location in Greens Bayou where positive flows are being underpredicted while negative flows are slightly overpredicted. For the tributaries, the best results were obtained for Carpenters Bayou and the SJR. While the model is overpredicting the negative flows for Buffalo, Vince, Sims, and Hunting Bayous, and is overpredicting most of the flows for Brays Bayou, results are within reasonable ranges and the model was considered calibrated.

⁷ The green line shown corresponds to a smoothing of the regression presented in the Final Report for WO7. In addition, the regression for San Jacinto River presented in the Final Report for WO No. 582-0-80121-07 was modified to include the impact of freshwater inflows. The updated regression statistics are included in Appendix C.

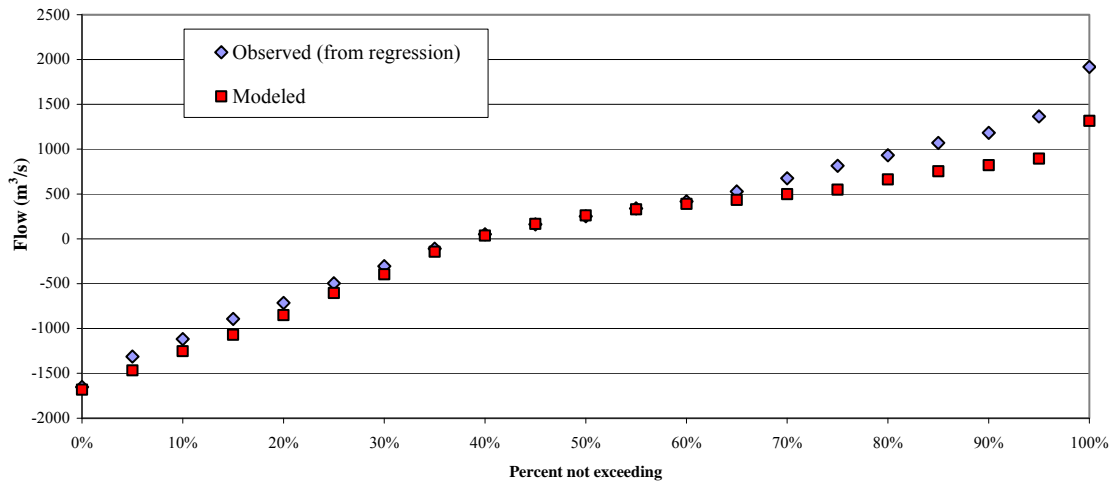
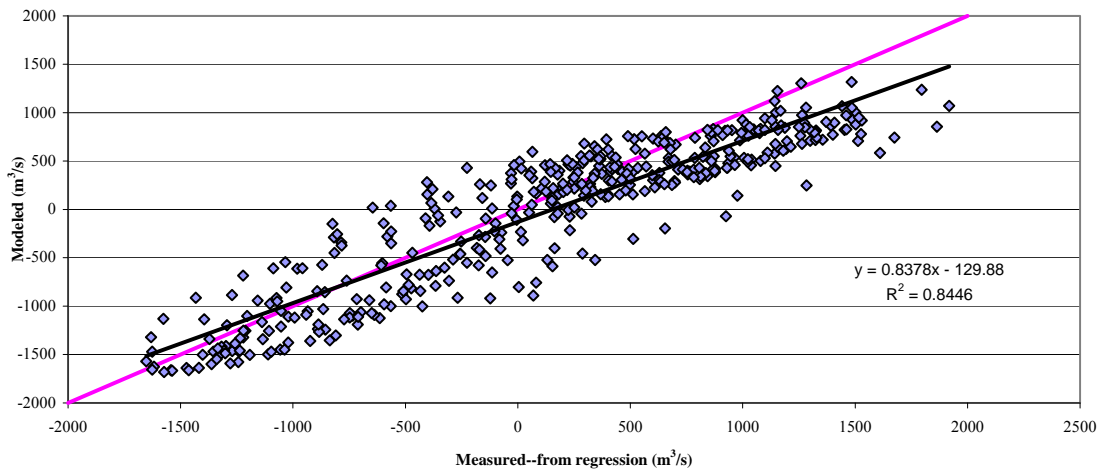
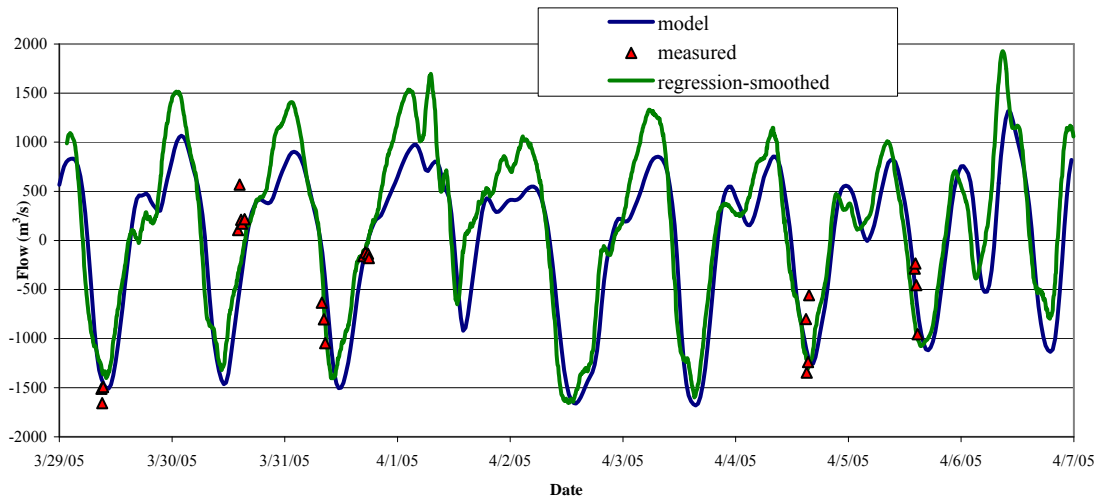


Figure 2.13a Goodness of Fit for HSC @ Morgan’s Point using Flow Regression

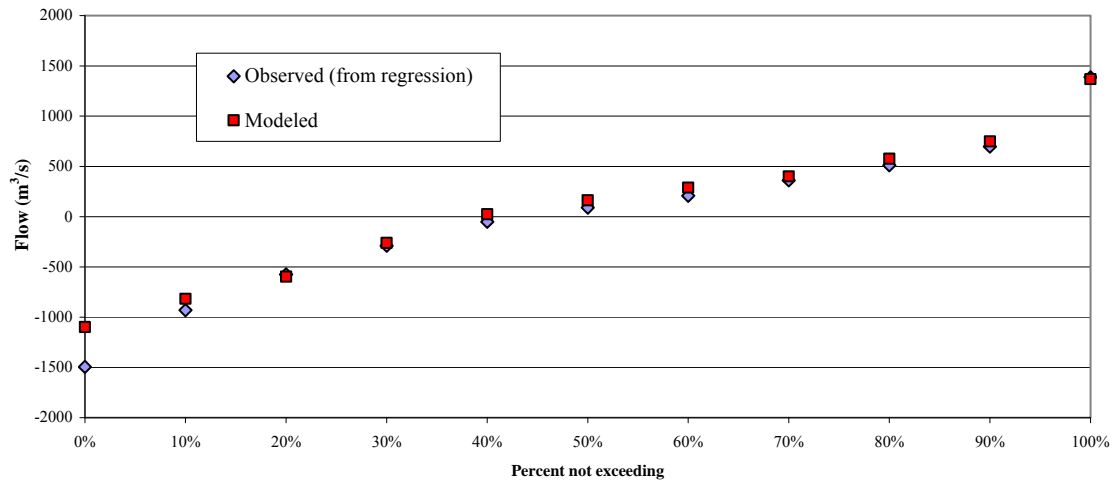
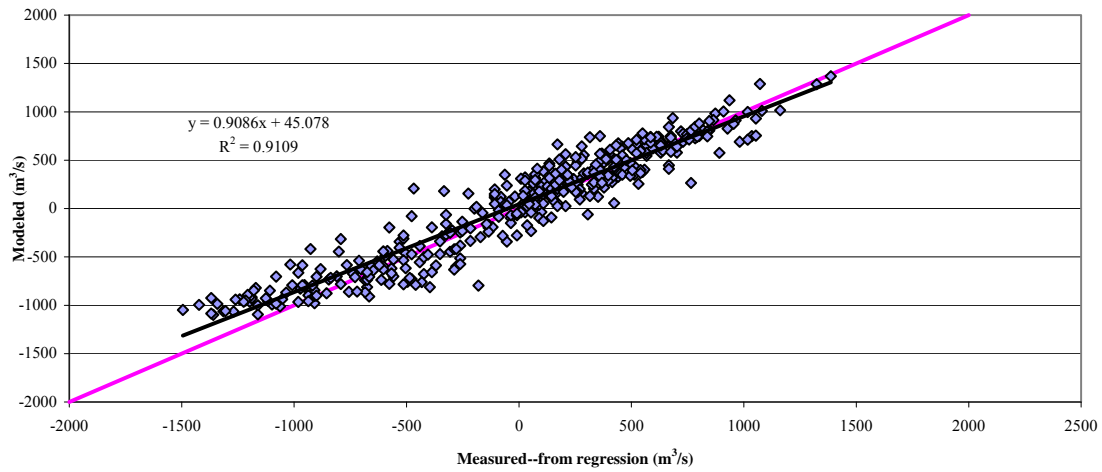
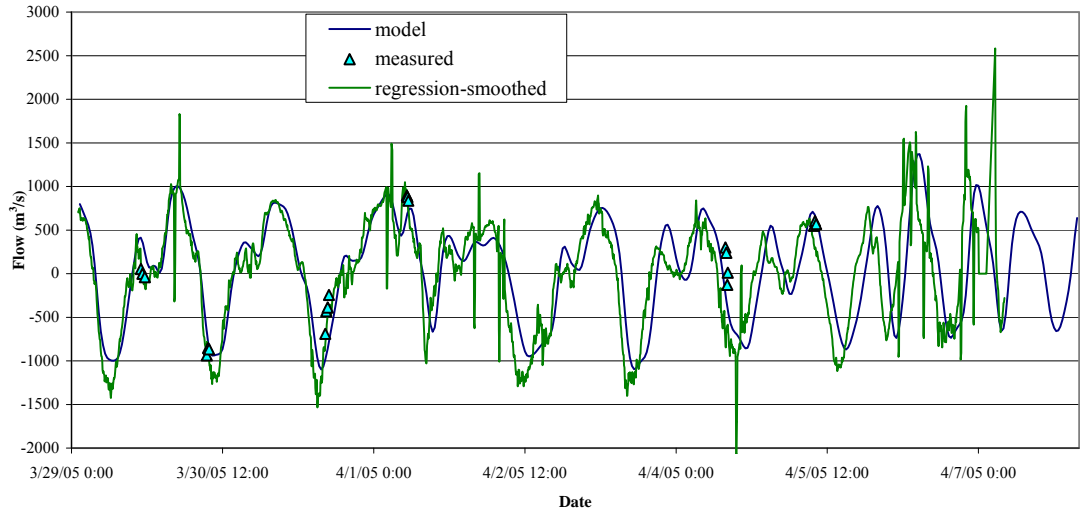


Figure 2.13b Goodness of Fit for HSC @ Lynchburg using Flow Regression

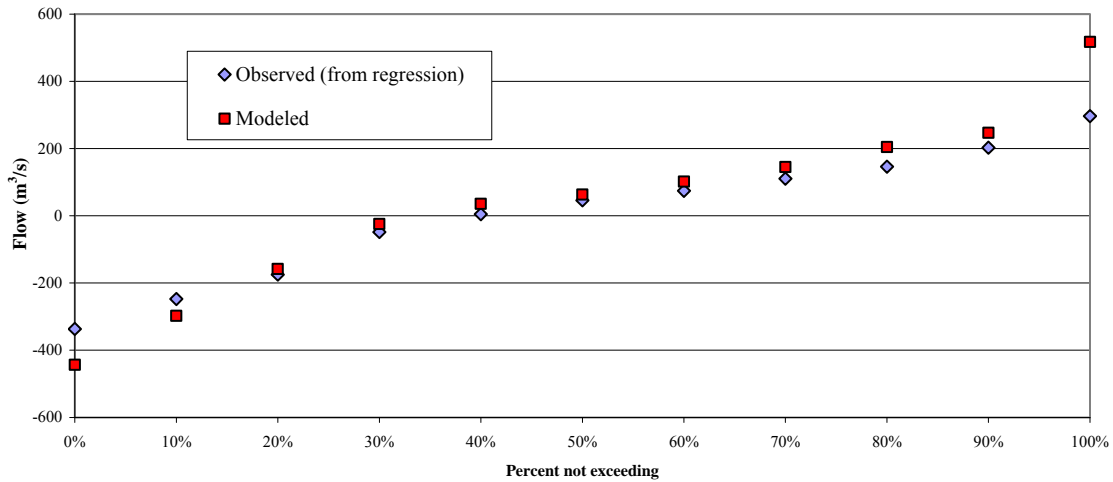
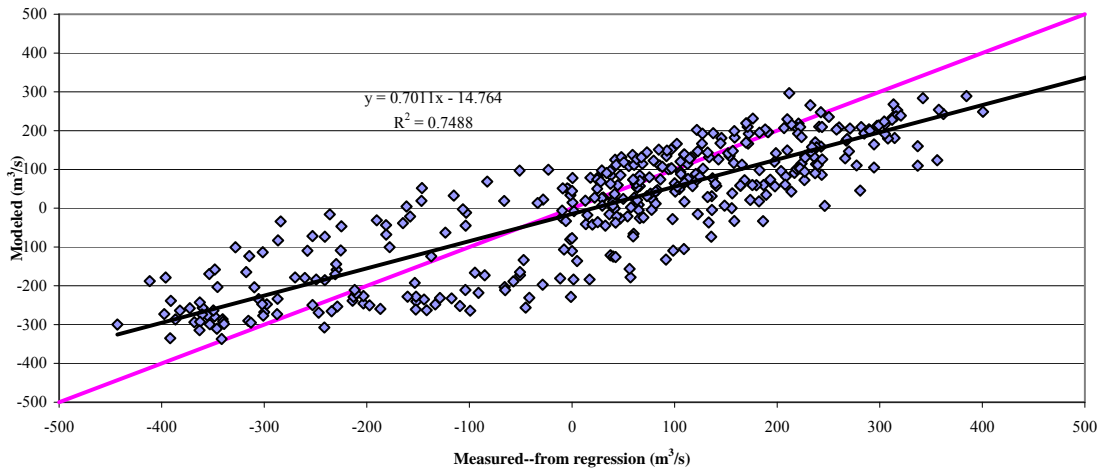
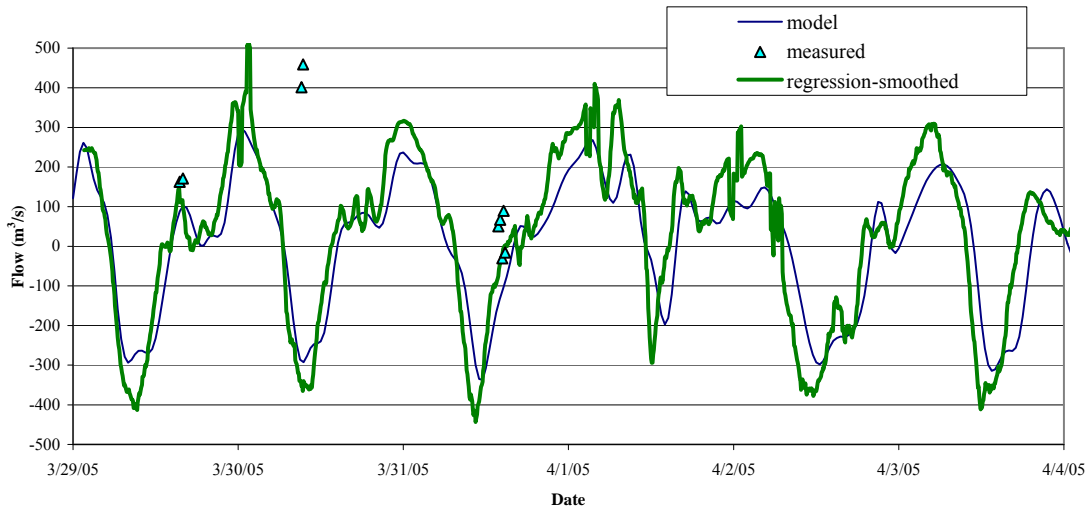


Figure 2.13c Goodness of Fit for HSC @ Battleship using Flow Regression

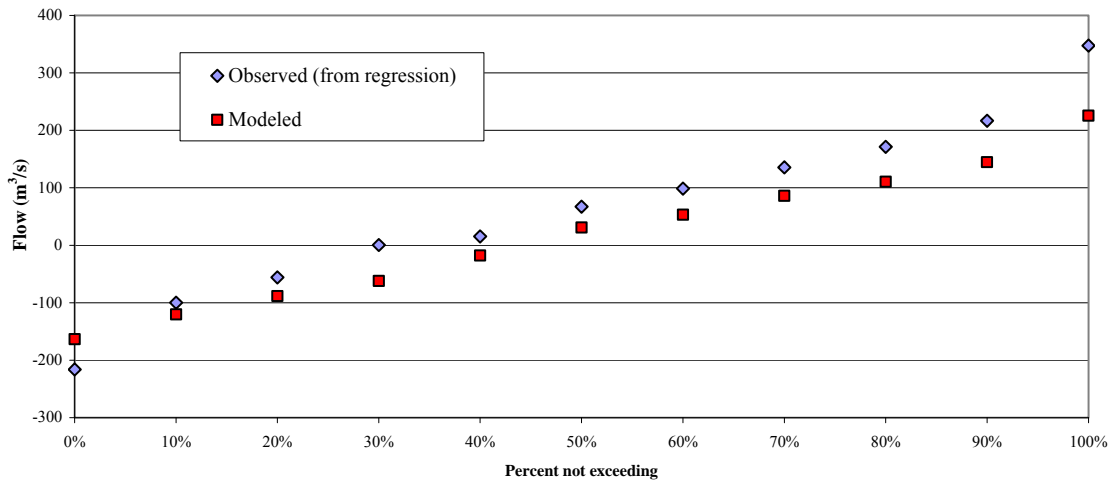
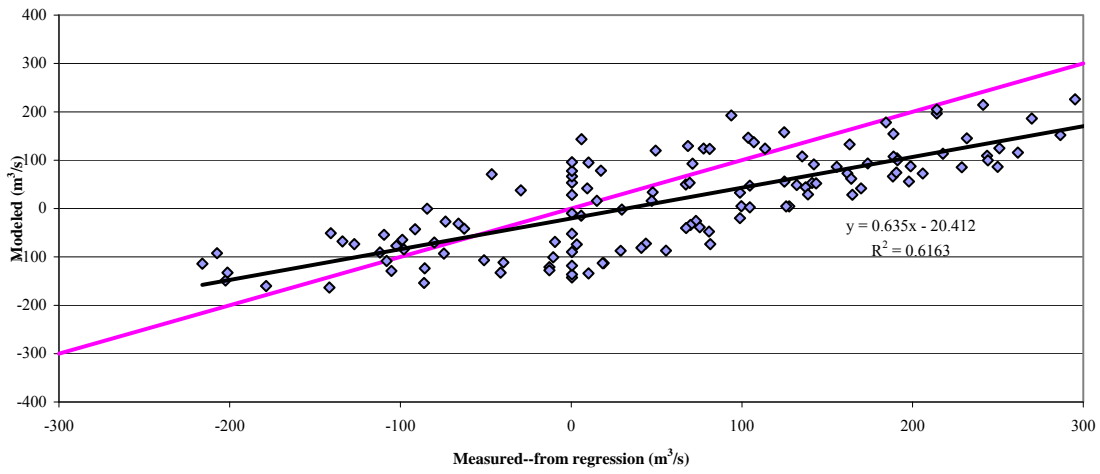
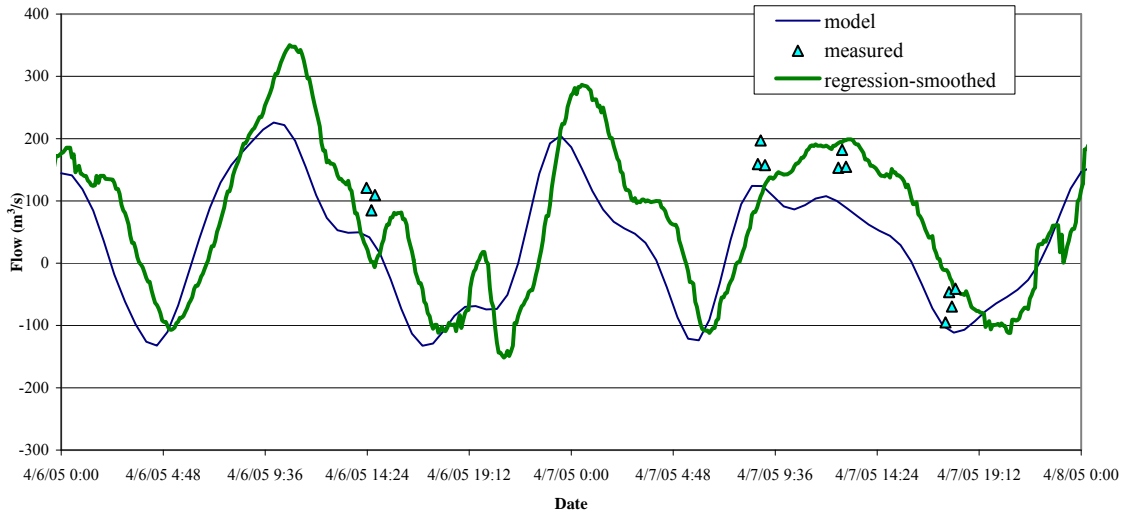


Figure 2.13d Goodness of Fit for HSC @ Greens using Flow Regression

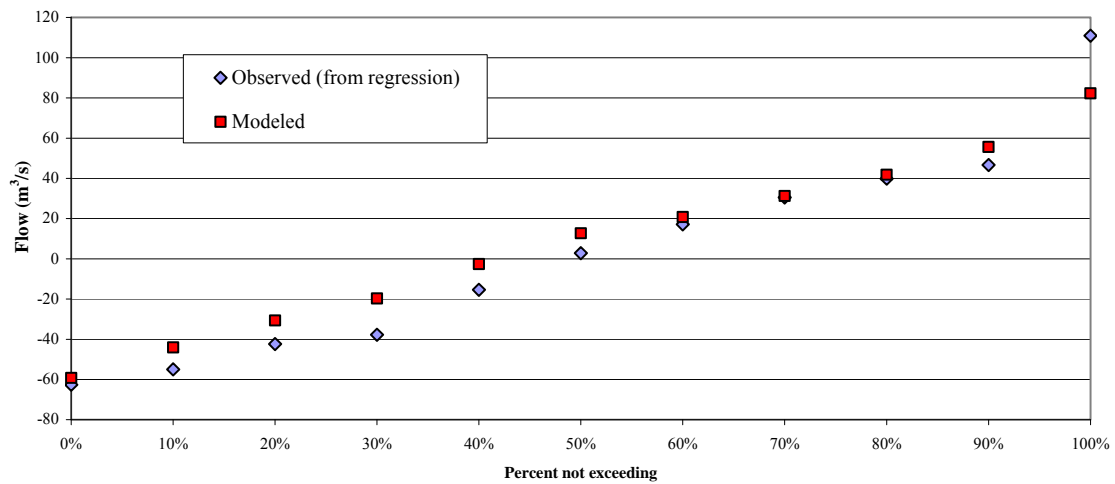
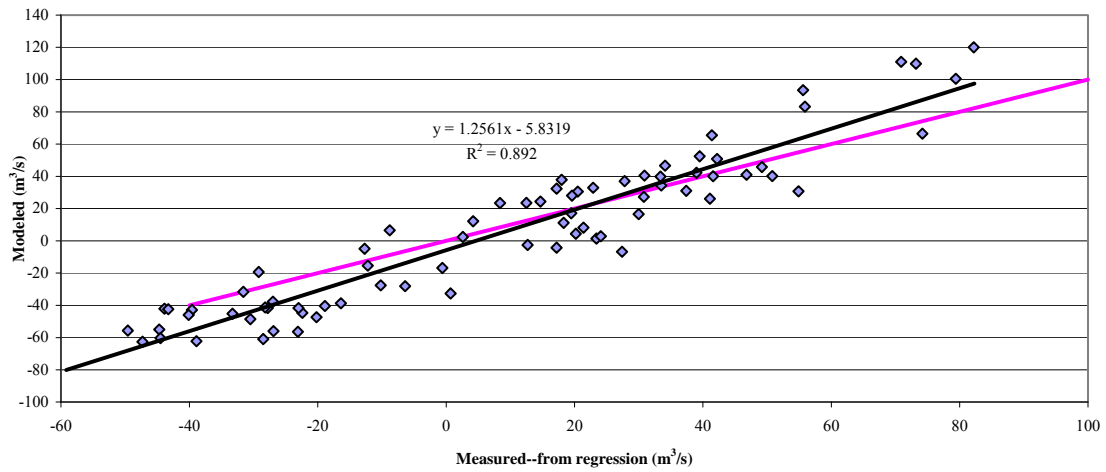
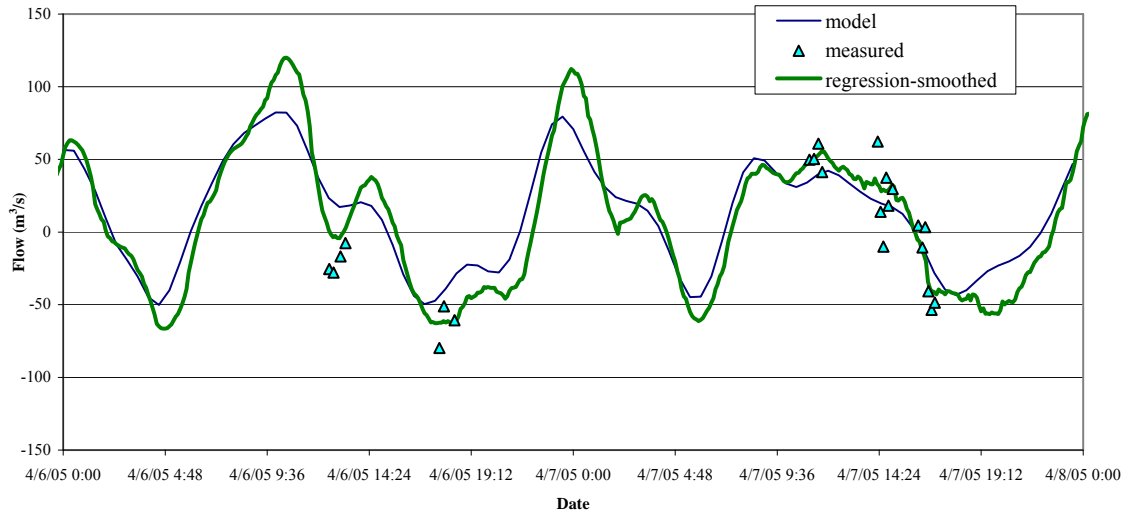


Figure 2.13e Goodness of Fit for HSC @ I-610 using Flow Regression

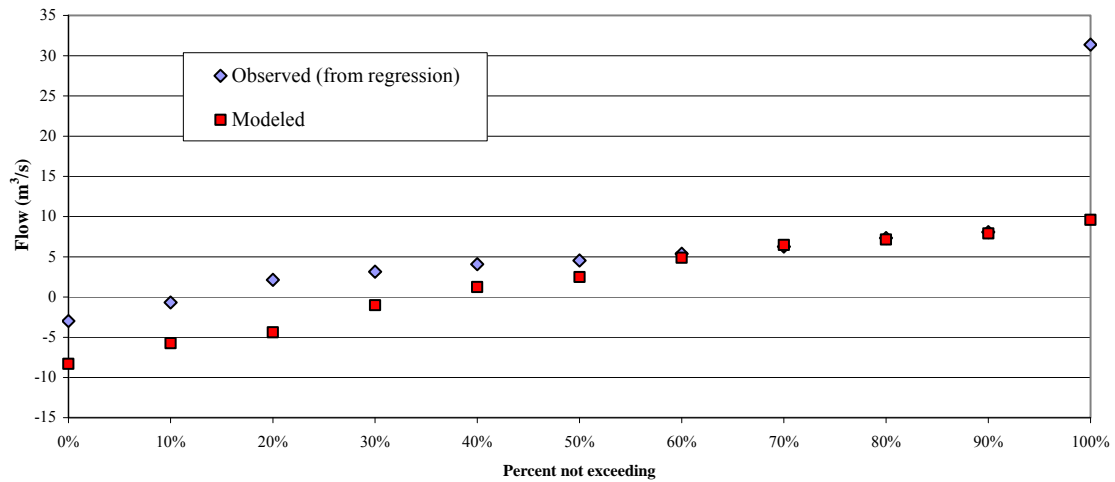
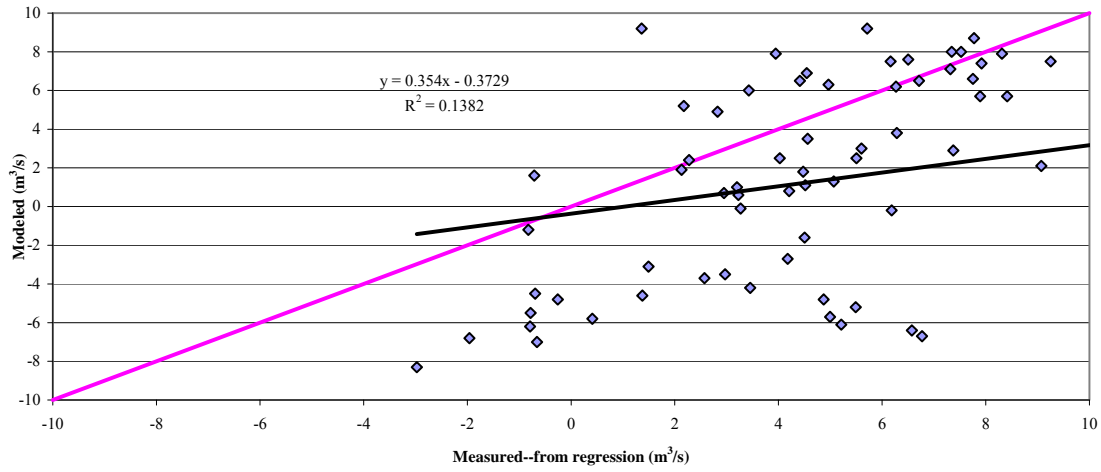
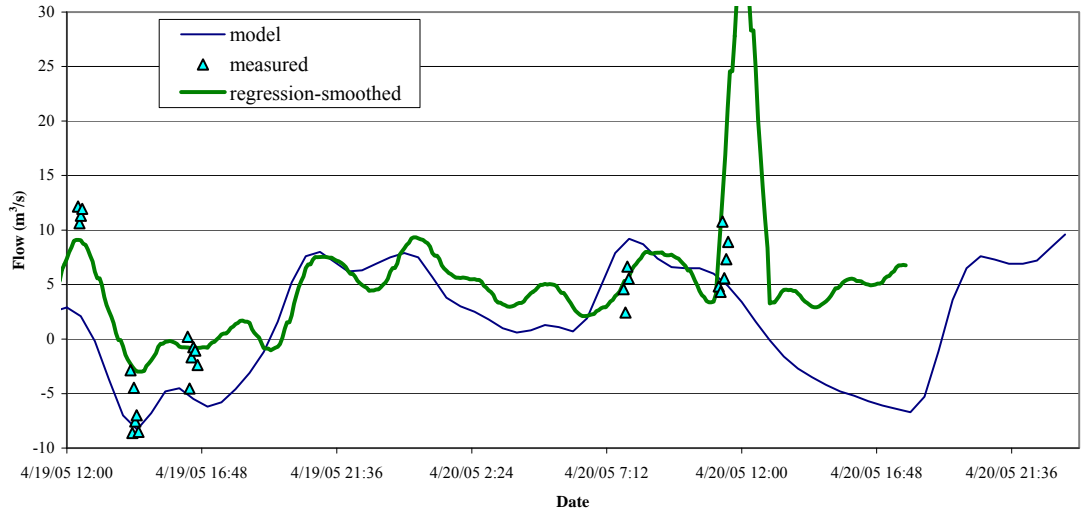


Figure 2.13f Goodness of Fit for Buffalo Bayou using Flow Regression

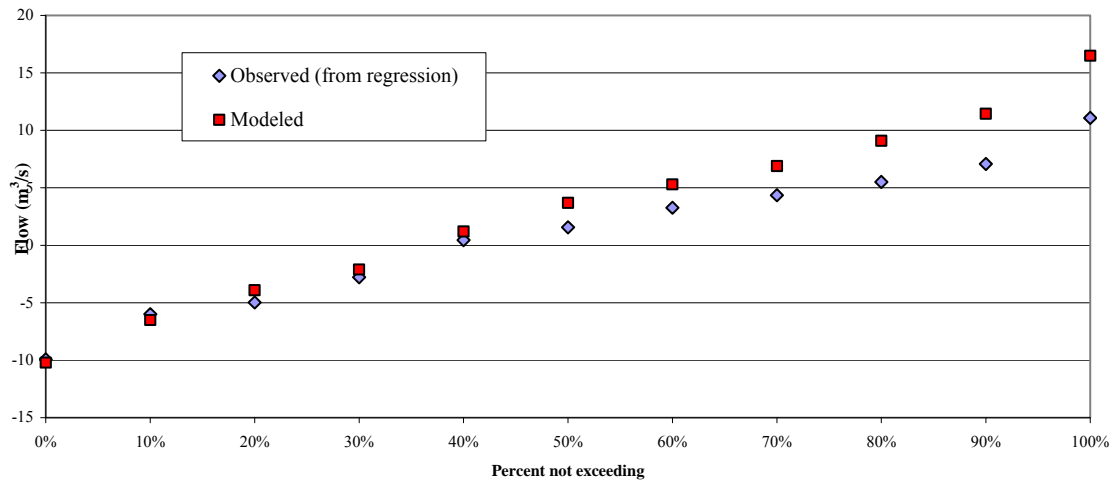
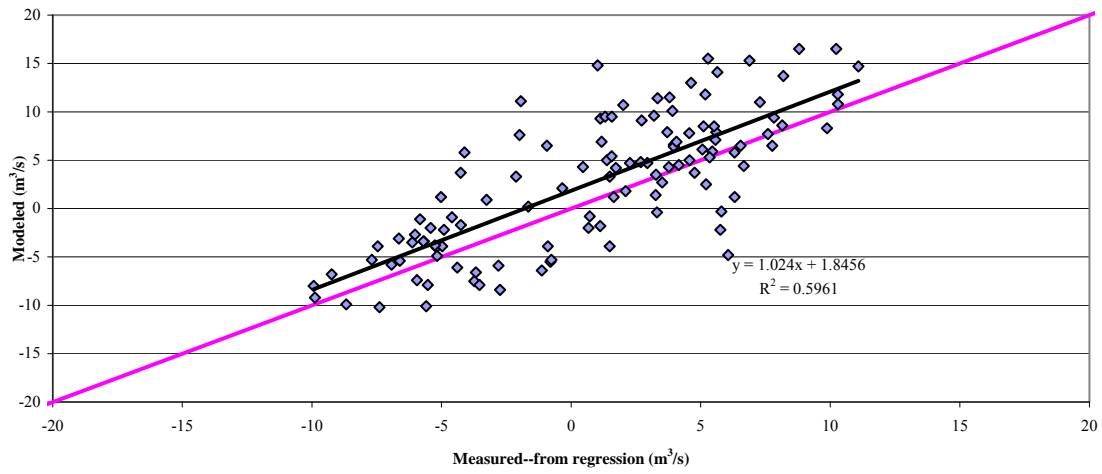
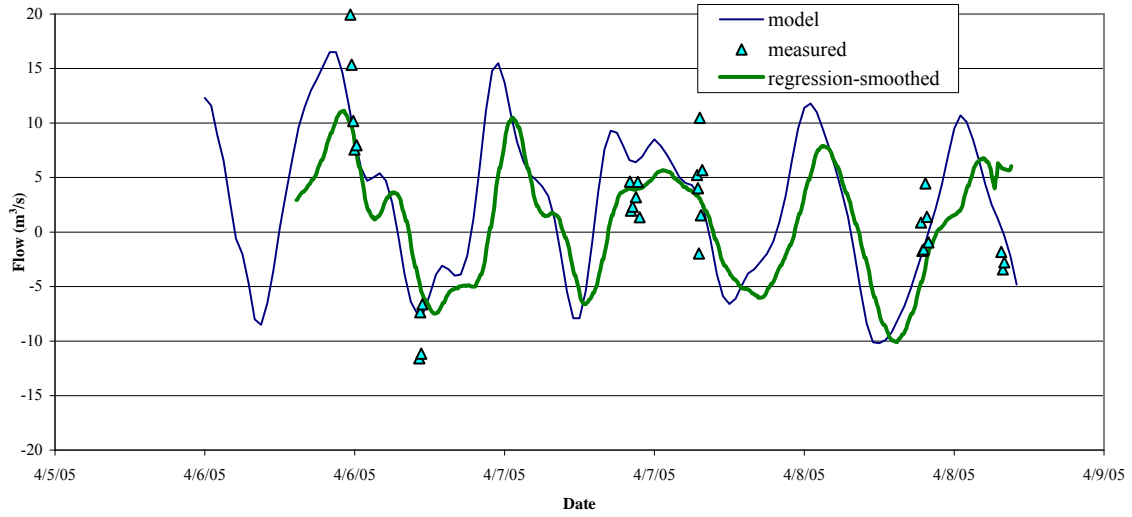


Figure 2.13g Goodness of Fit for Brays Bayou using Flow Regression

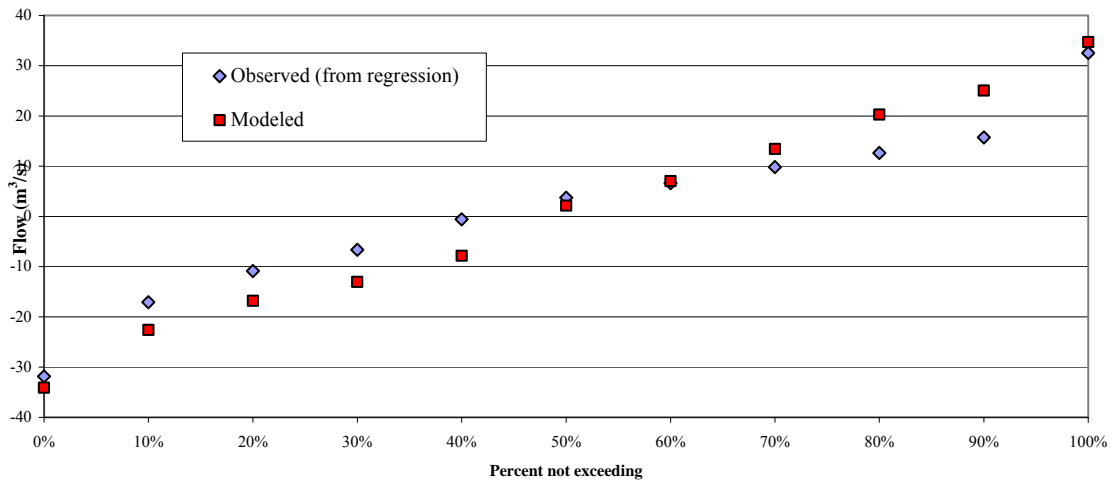
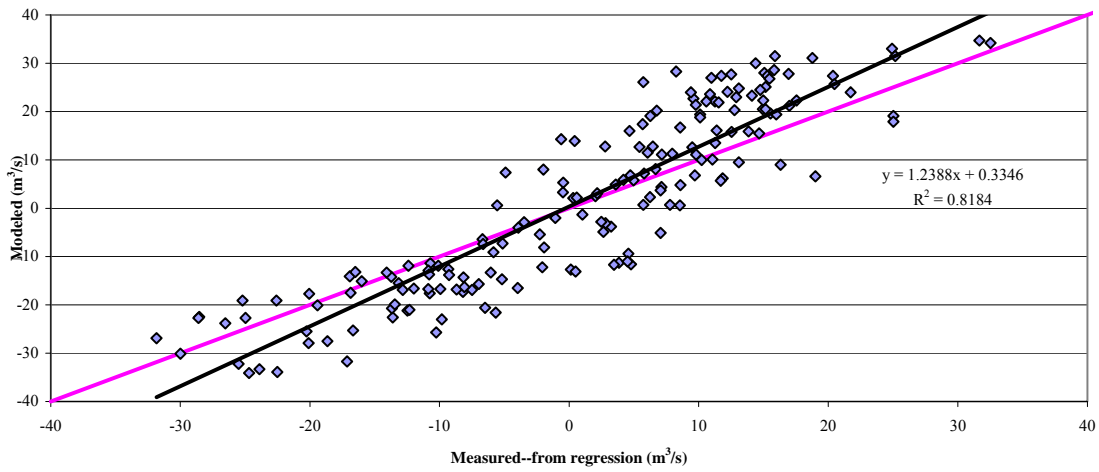
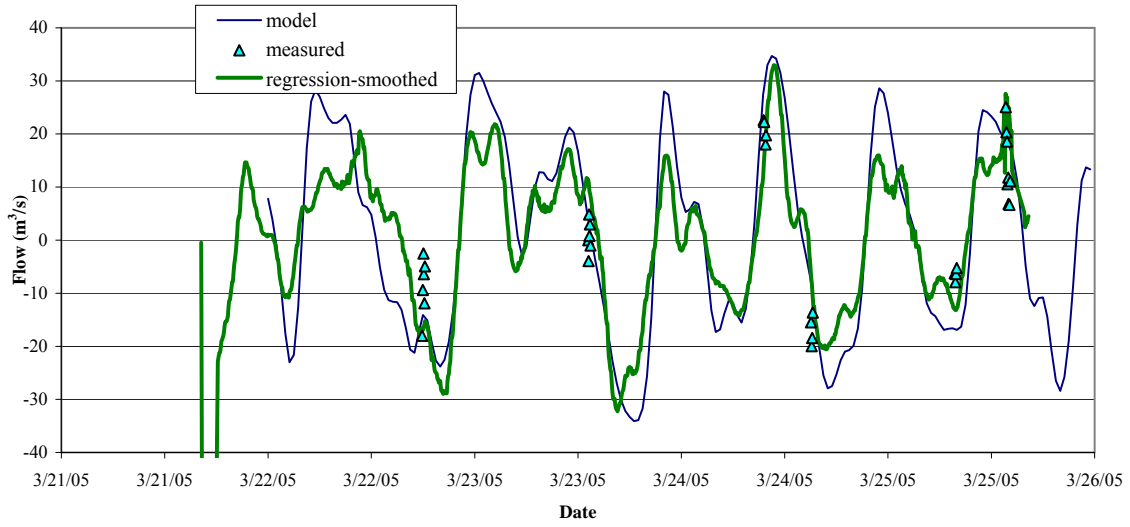


Figure 2.13h Goodness of Fit for Simsbayou using Flow Regression

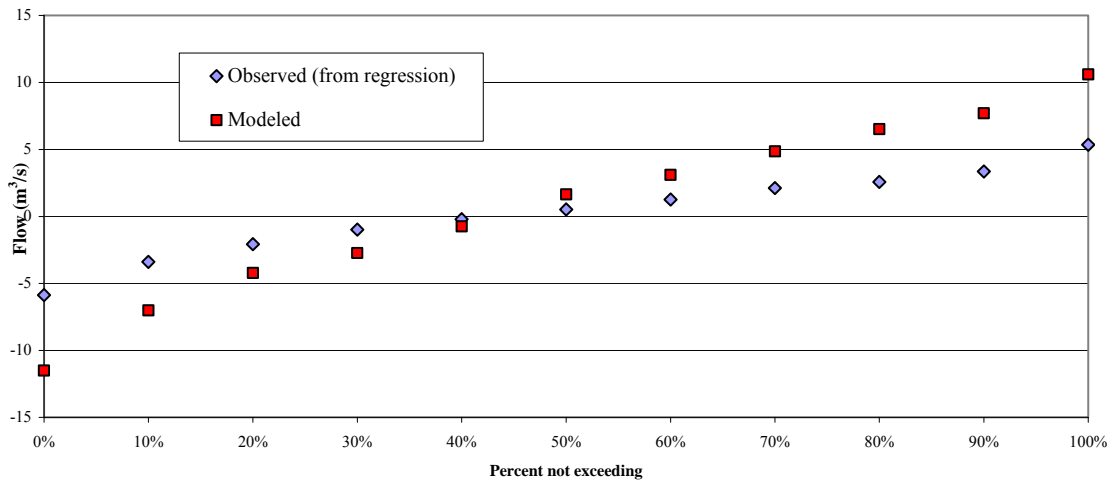
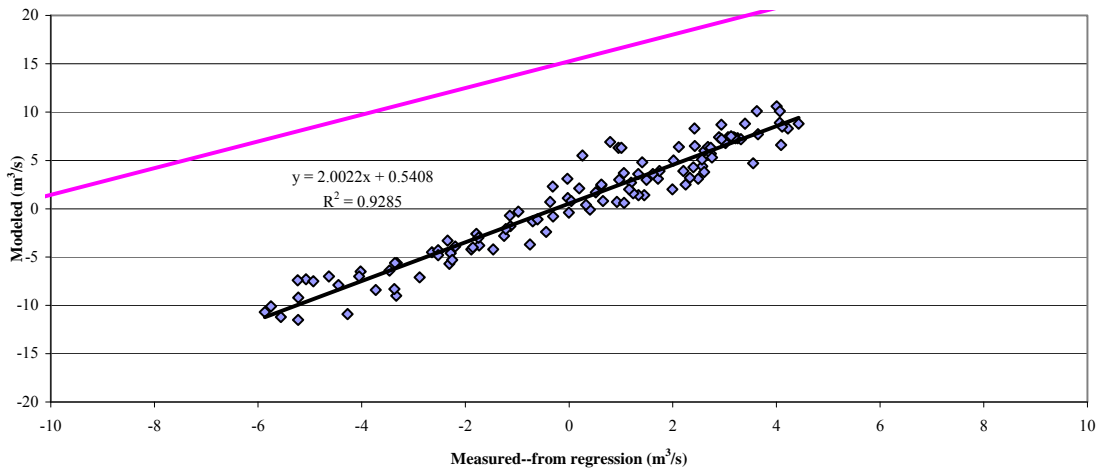
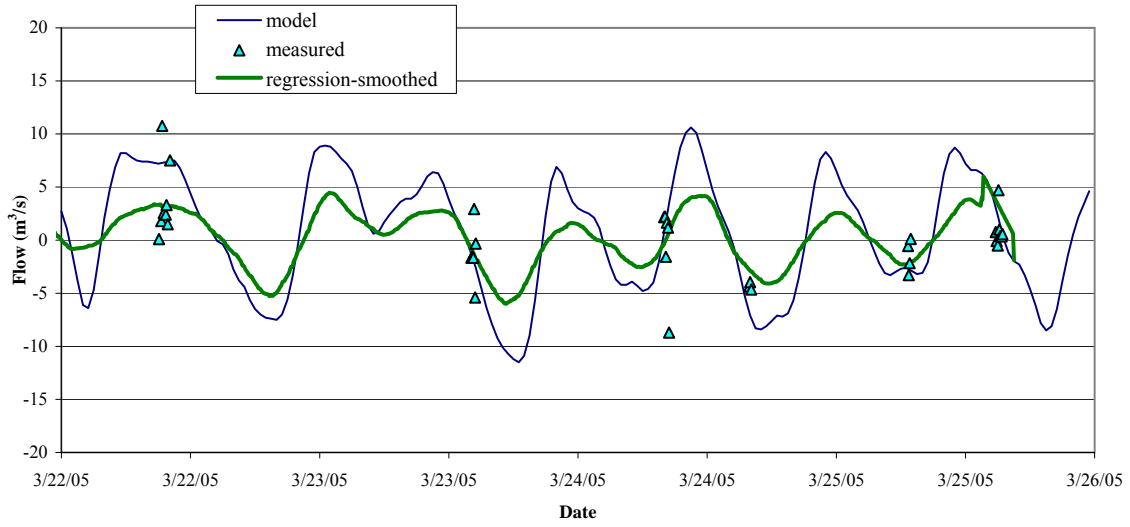


Figure 2.13i Goodness of Fit for Vince Bayou using Flow Regression

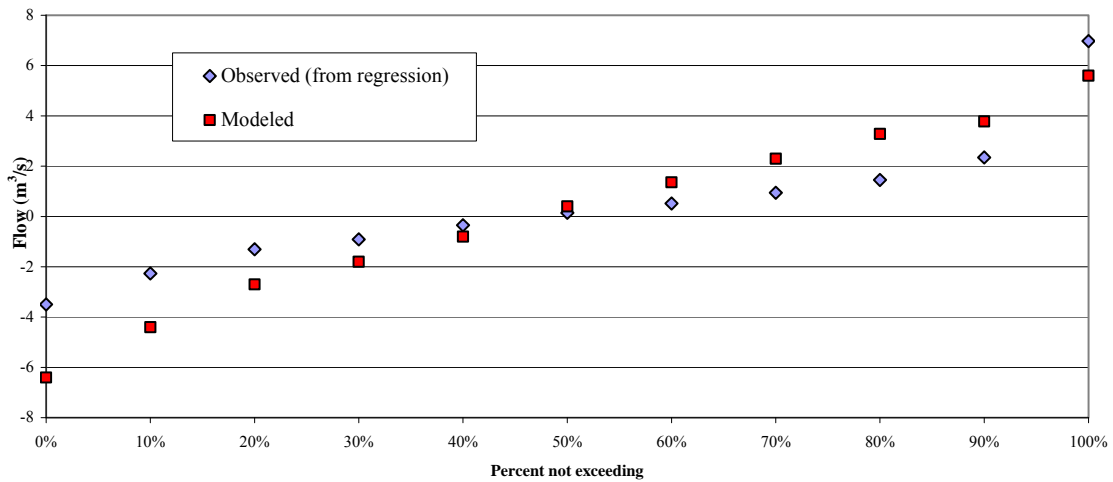
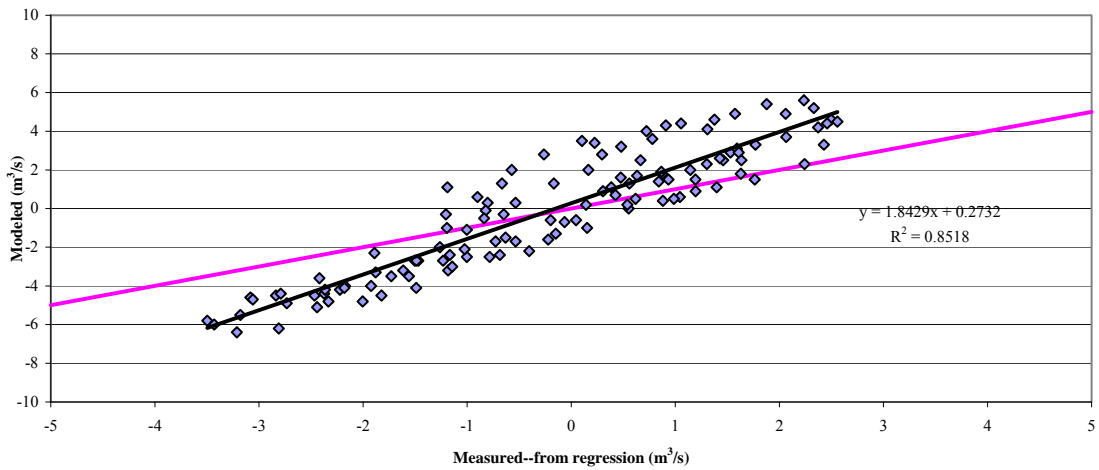
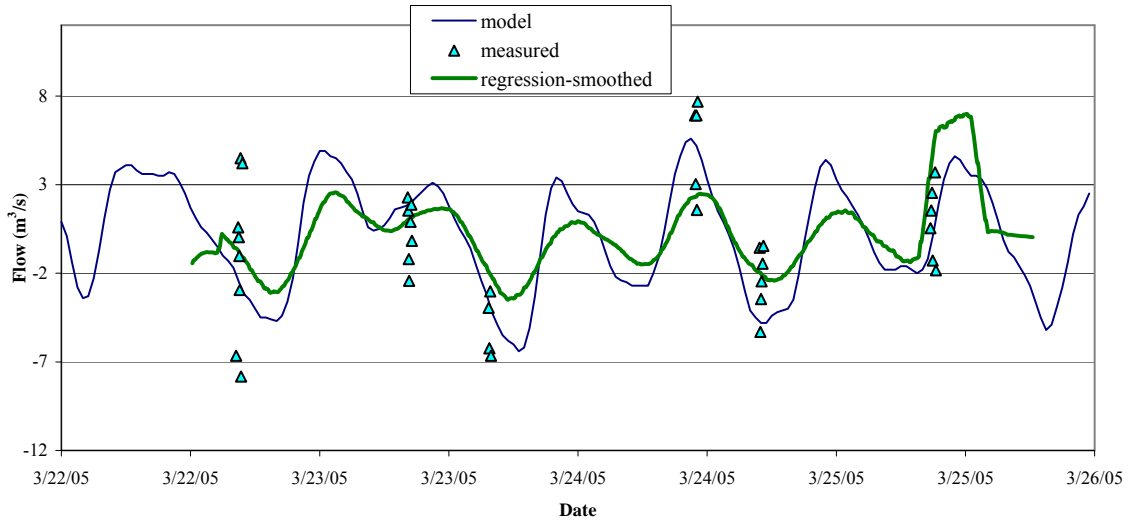


Figure 2.13j Goodness of Fit for Hunting Bayou using Flow Regression

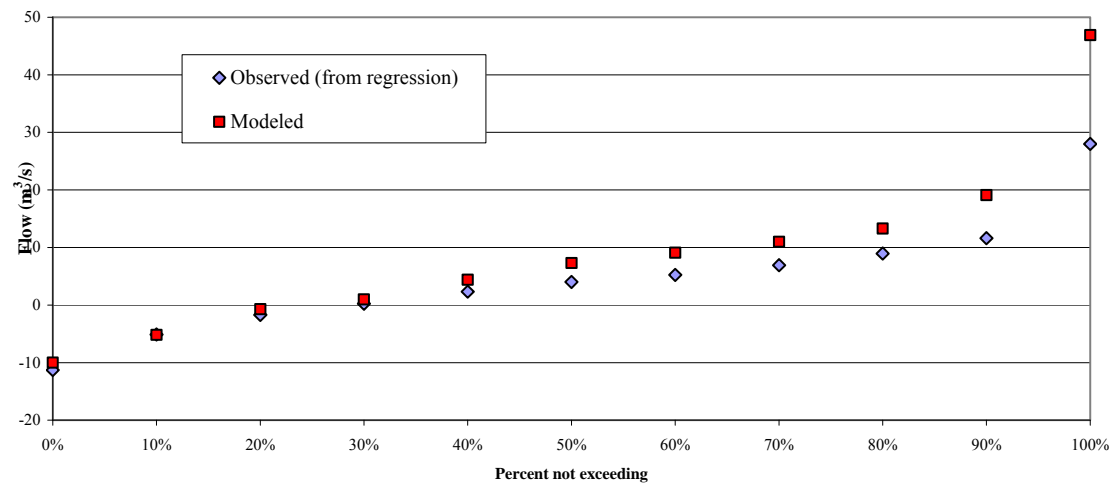
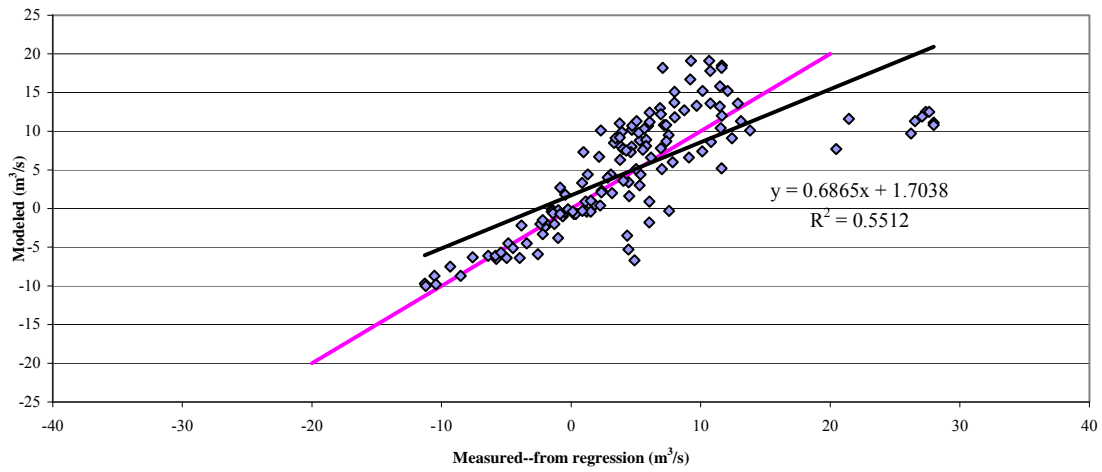
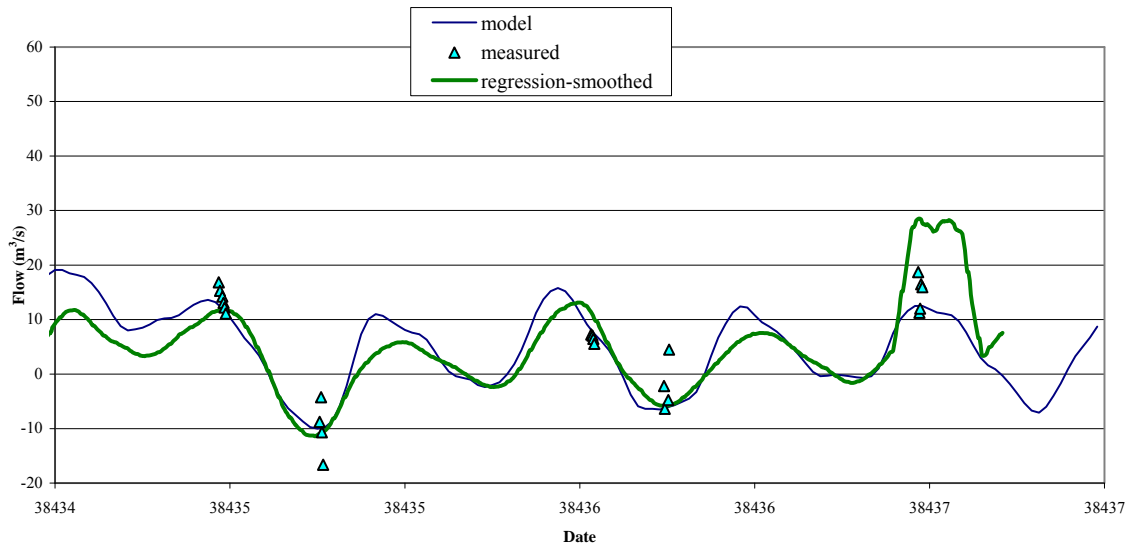


Figure 2.13k Goodness of Fit for Greens Bayou using Flow Regression

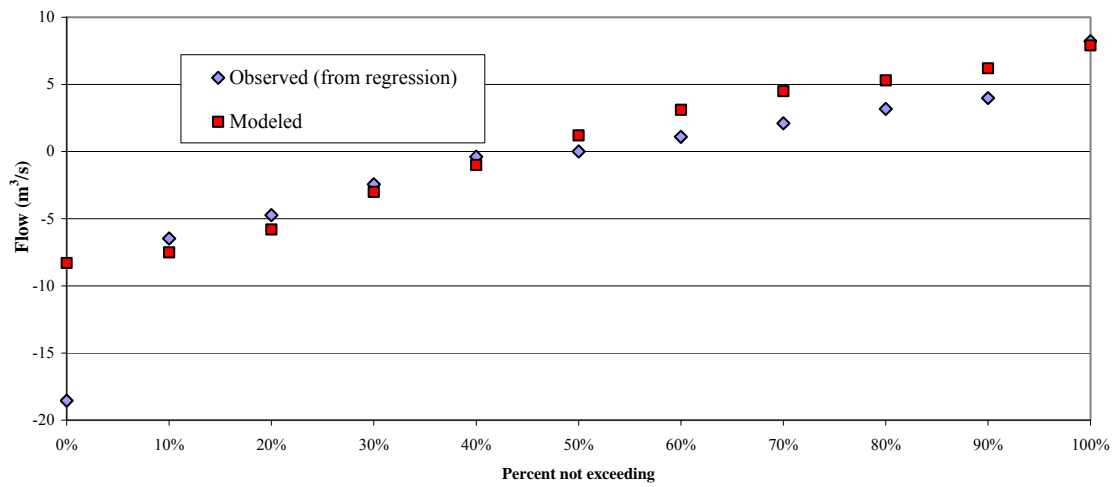
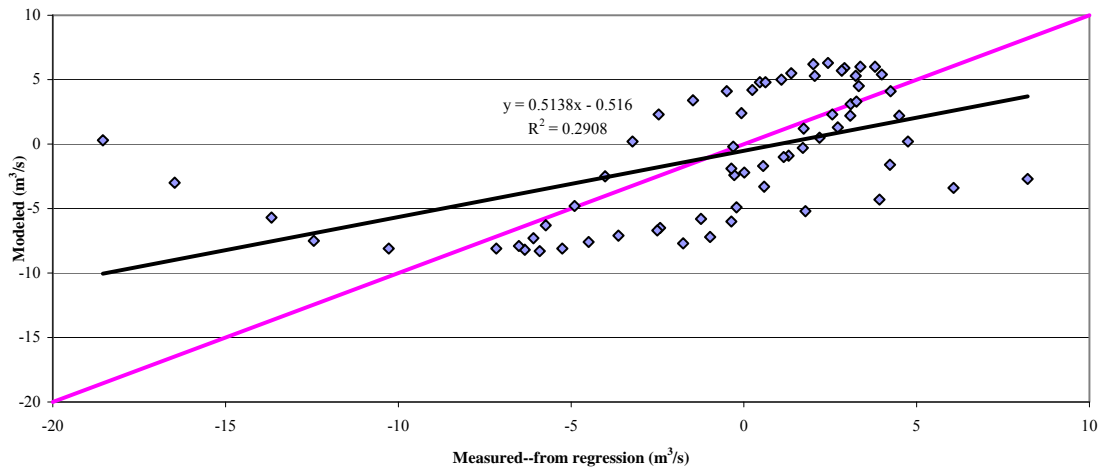
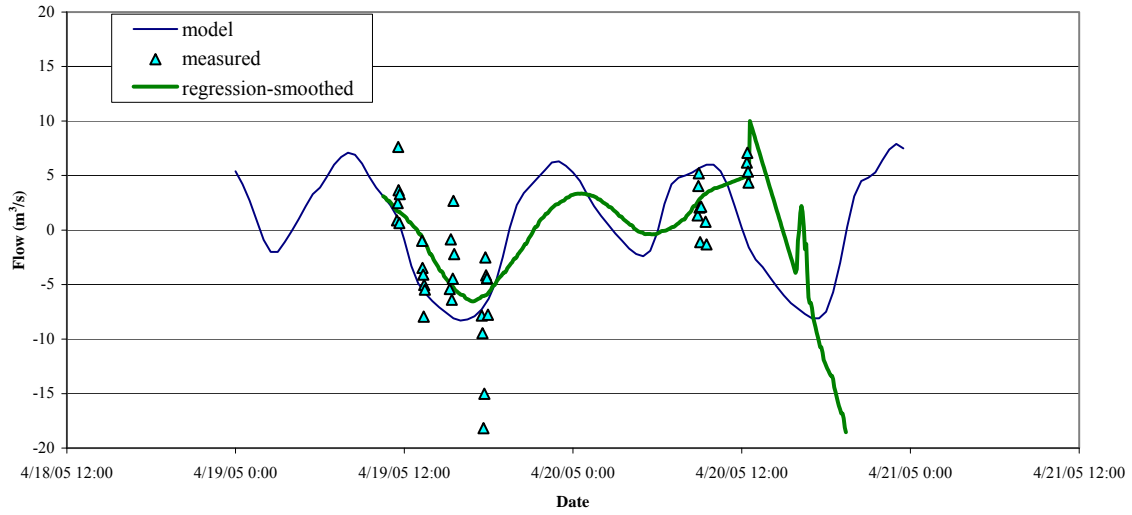


Figure 2.13I Goodness of Fit for Carpenter's Bayou using Flow Regression

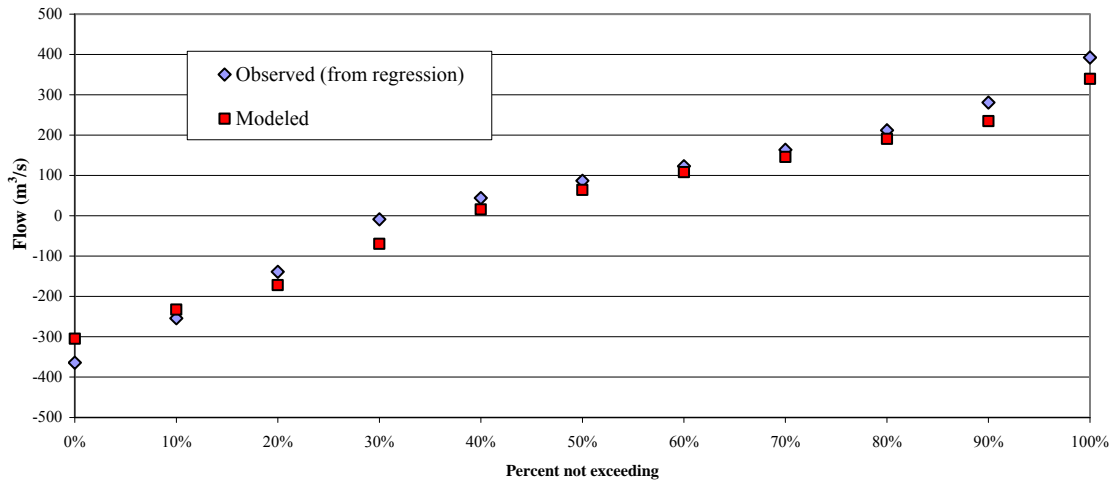
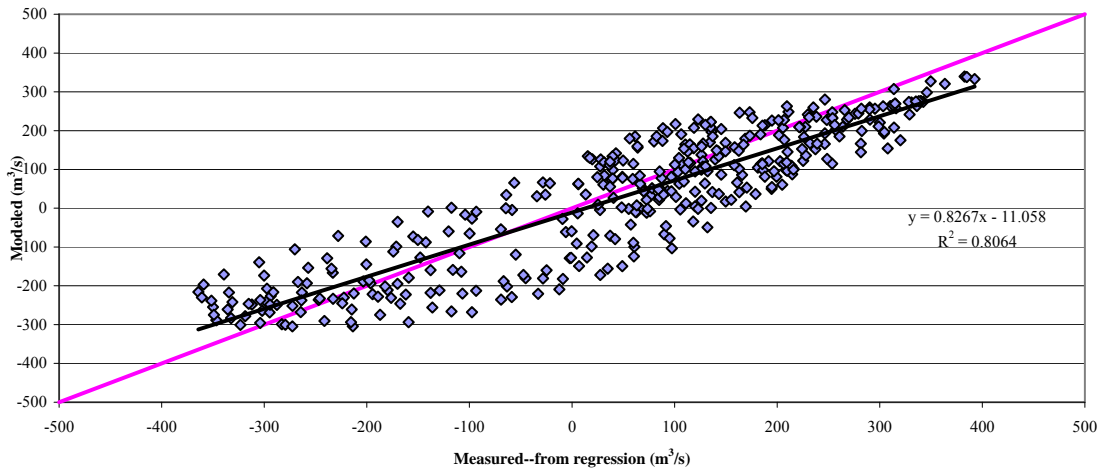
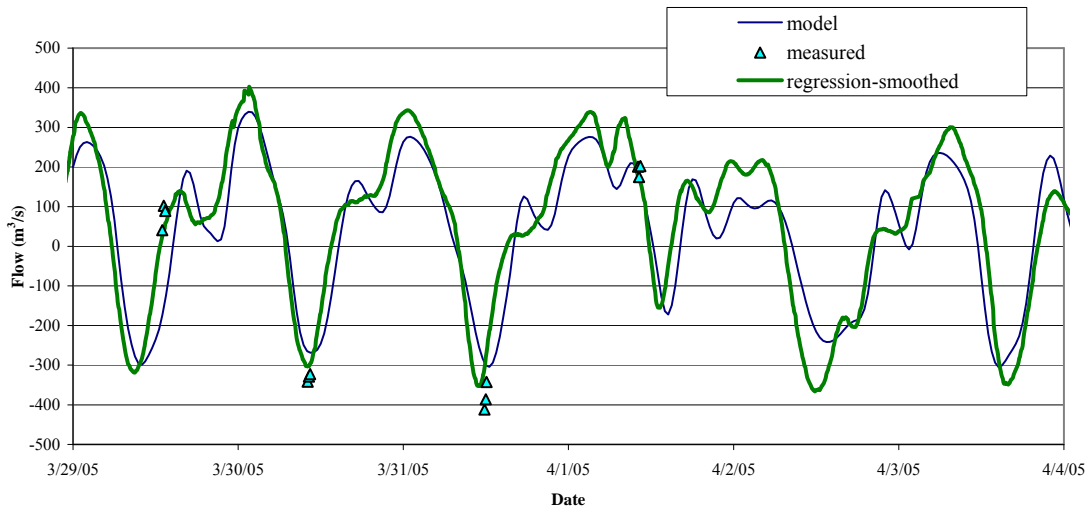


Figure 2.13m Goodness of Fit for San Jacinto River @ I-10 using Flow Regression

Finally, the statistics described in Equations 2.4 through 2.7 were computed to quantify model performance and compare the goodness-of-fit for the different locations. The summary statistics are presented in Table 2.8.

Table 2.8 Model Summary Statistics for Water Flows

Observation Point	r^a	MEF^b	d^c	$RMSE$ (m³/s)
HSC@Morgan's	0.919	0.811	0.947	17.7
HSC@Lynchburg	0.932	0.857	0.962	10.7
HSC@Battleship	0.865	0.731	0.914	5.2
HSC@Greens	0.780	0.487	0.837	7.6
HSC@I-610	0.938	0.840	0.948	2.0
Buffalo Bayou	0.366	-0.672	0.525	0.8
Brays Bayou	0.771	0.161	0.939	0.4
Sims Bayou	0.904	0.601	0.926	0.6
Vince Bayou	0.933	-0.647	0.830	0.3
Hunting Bayou	0.791	0.191	0.852	0.1
Greens Bayou	0.563	0.006	0.732	0.6
Carpenters Bayou	0.509	0.102	0.717	0.6
San Jacinto River	0.898	0.795	0.942	4.3

^a A negative value indicates that the observed and predicted values are inversely correlated

^b A value near 1 indicates a close match, a value near zero indicates that the model predicts individual observations no better than the average of observations, a negative value indicates that the observation average would be a better predictor than the model results (Stow *et al.*, 2003)

^c Higher values indicate higher agreement between the model and observations

The RMA2 output file for the calibrated model is included in Appendix C.

2.7 LONG-TERM RUNS

Figure 2.14 presents observed and modeled water surface elevation series for three NOAA gages located in the HSC (see Figure 2.4 for NOAA gage locations). As can be seen, the model accurately reflects the tidal elevations for the long-term run. Finally, Figure 2.15 presents modeled flow rate time-series for the 13 calibration locations.

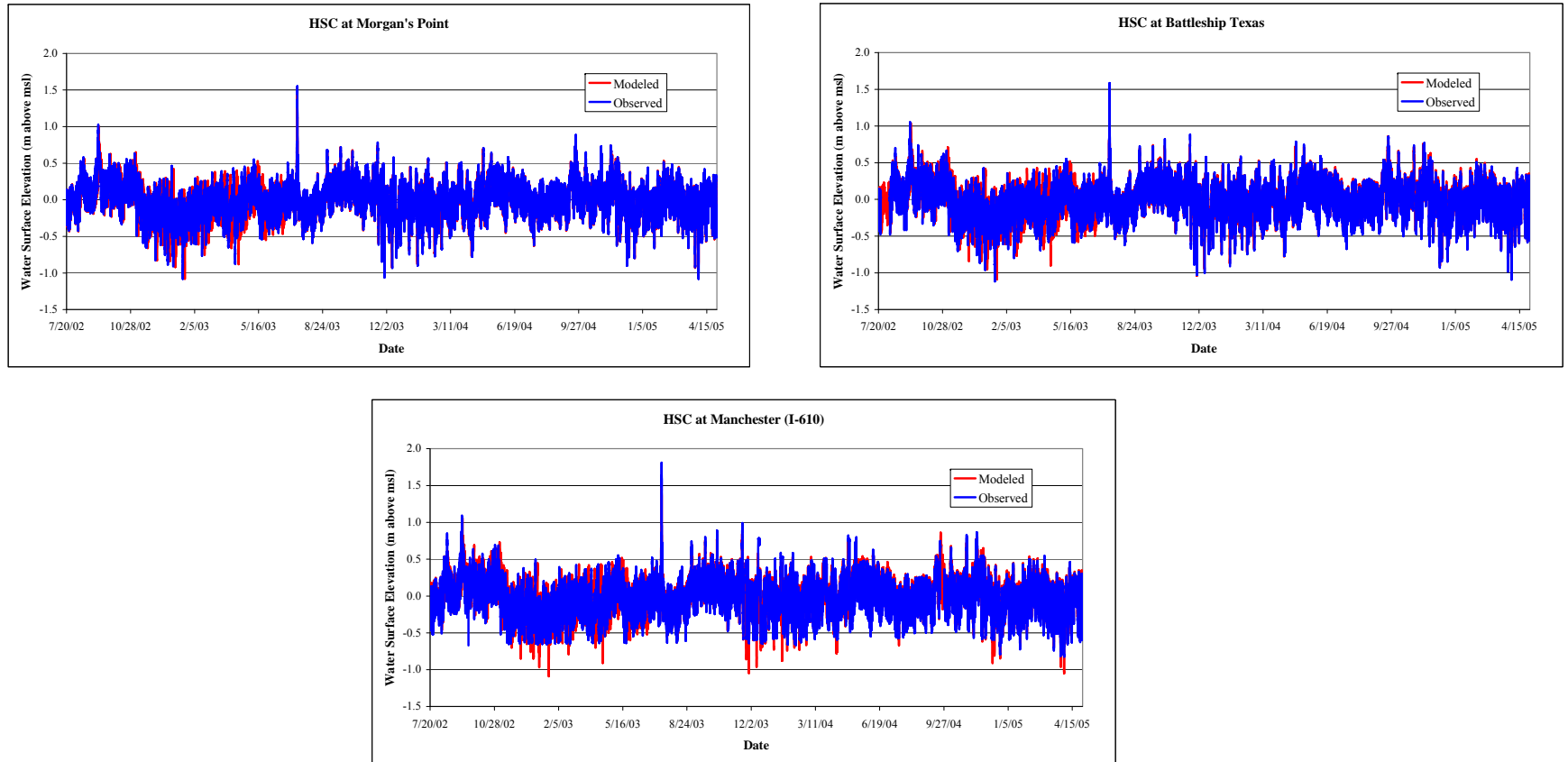


Figure 2.14 Observed and Simulated Water Surface Elevations in the HSC

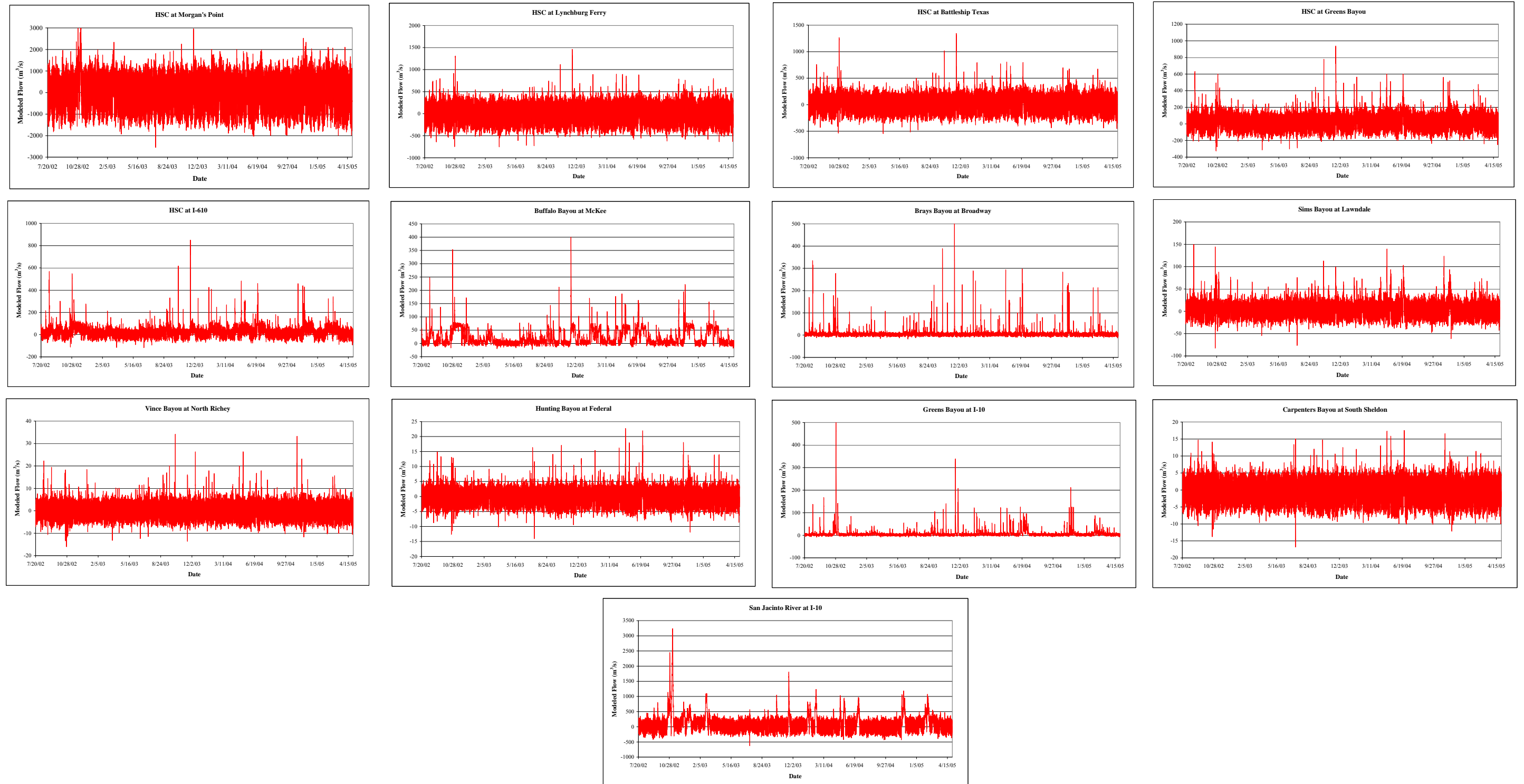


Figure 2.15 Long-term Modeled Flow Rates

2.8 HSCREAD INTERFACE

Once the hydrodynamic model was completed, it was necessary to organize the RMA2 output in a format that could be read by the water quality model (WASP7). In addition, because the model segmentation for WASP7 differed from that of RMA2 (the WASP segments are coarser than the RMA2 elements), it was necessary to “aggregate” the RMA2 results for all the elements that composed a WASP segment. These two operations were accomplished using an interface (HSCREAD) written for this project using Fortran 90. Briefly, HSCREAD reads the output and geometry files from RMA2 and processes 1-D and 2-D segments as follows:

- Reads a “junction file” that includes the segment continuity, pair of segments at each flow interface, and the RMA2 nodes that are part of each WASP segment.
- For 1-D segments (tributaries and main channel up to the confluence with the SJR):
 - Reads from a user supplied file how many and which 1-D RMA2 elements are part of a given 1-D WASP segment;
 - Calculates the average depth of the WASP segment (the depths are weighted by the length of the individual RMA2 elements to obtain a representative average depth);
 - Calculates the volume of the WASP segment by aggregating the volumes of the individual RMA2 elements composing the segment, the volume of each RMA2 element is calculated as the average of the cross-sectional areas upstream and downstream times the length of the element;
 - Calculates the flow into the WASP segment (velocity of the upstream node times the cross-sectional area at the upstream node), and in a similar way the flow out of the segment (using data for the downstream node); and

- Calculates the average velocity of the WASP segment
- For 2-D segments (main channel downstream of Lynchburg Ferry and Galveston Bay):
 - Reads from a user supplied file how many and which 2-D RMA2 elements are part of a given 2-D WASP segment;
 - Computes the surface area of each RMA2 element (on the horizontal plane) using the coordinates for the nodes composing the element;
 - Calculates the average depth of the WASP segment (the depths are weighted by the surface area of the individual RMA2 elements to obtain a representative average depth);
 - Calculates the volume of the WASP segment by aggregating the volumes of the individual RMA2 elements composing the segment. Volume of each RMA2 2-D element is calculated as the average depth times the surface area;
 - Reads from the RMA2 output, the flow crossing all the interfaces of the 2-D segments (continuity lines should be defined at the model interfaces and the segments related to each continuity line are supplied in the “junction file”); and
 - Computes the average velocity for a WASP element by adding the velocity components of the different nodes comprising the segment.
- Because there was a small difference in the volume of WASP elements calculated using the two methods described in equations 2.1 and 2.2, flows were corrected to eliminate any potential errors with the water quality model.
 - For the 1-D elements, HSCREAD adjusts the flows as follows: flows from upstream boundaries are kept unchanged since they correspond to flows measured at USGS gages; for the most upstream segment of each tributary, flow out of the segment is corrected using:

$$Q_{out_t} = Q_{in_t} - \frac{V_t - V_{t-1}}{dt} \quad (2.8)$$

For subsequent segments, the corrected flow out of the previous segment is assumed as the incoming flow and the outgoing flow is calculated using equation 2.8. If a WASP element is downstream of a junction (i.e., after a tributary discharges into the channel), the flow in is the sum of the two corrected outflows.

- For 2-D segments, the flow adjustment was performed using an Excel spreadsheet. In this case, flows out of segments with no inflows (e.g., side bays) are adjusted first and used to correct the flows in the neighboring segments. In both cases, flows are adjusted using equation 2.8. HSCREAD reads the corrected flows from a CSV file supplied by the user.
- When all the calculations are completed, HSCREAD formats a “HYD” file, which is the hydrodynamic file that can be read by WASP. Five records comprise the external hydrodynamic file:

Record 1 - Data Options : includes number of segments connected by flows, number of interfacial flow pairs from the hydrodynamic file, WASP time step (an even multiple of the hydrodynamic time step), beginning time for the hydrodynamic file, ending time for the hydrodynamic file.

Record 2 - Segment Interface Pairs

Record 3 - Initial Segment Properties: volume, average depth, and average velocity of segment "i" at beginning of time step (this record is only input once for each segment). It is noted that WASP uses velocities only to calculate re-aeration rates and, thus, this parameter is not relevant in dioxin simulations.

Record 4 -- Segment Interfacial Flows (repeated for each time step): positive numbers

indicate flows from the “upstream” to the “downstream” segment in the interface (as specified in record 2), while negative numbers indicate flows in the opposite direction.

Record 5 -- Segment Properties: volume, average depth, and average velocity of segment "i"

for each time step. This record is repeated for each time step.

CHAPTER 3

IN-STREAM WATER QUALITY MODEL OF THE HOUSTON SHIP CHANNEL AND UPPER GALVESTON BAY USING WASP7

This chapter summarizes the development and results of dioxin models for the HSC using the Water Quality Analysis Simulation Program (WASP). WASP is a dynamic compartment model that can be used to simulate contaminant fate and transport in surface water and the underlying benthic sediment layer. WASP simulates the time-varying processes of advection, dispersion, point and non-point mass loading, deposition/resuspension, and boundary exchange. For this study WASP version 7.2 (Wool et al, 2004) has been used. The TOXI module was used to simulate both salinity and dioxins. A WASP model for 2378-TCDD in the HSC was developed and calibrated to data collected between 2002 and 2005. Subsequently, additional models were developed for the five additional congeners that contribute more than 1 percent of the toxicity equivalent concentration (TEQ) in tissue (12378-PeCDD, 123678-HxCDD, 2378-TCDF, 23478-PeCDF, and 123678-HxCDF). This was done to aid in determining load reductions.

TOXI can simulate up to six systems and 13 levels of complexity as summarized in Table 3.1.

Table 3.1 TOX15 Systems and Levels of Complexity

System number	Name	Levels of Complexity				
		Solids			Kinetics	
		1,2	3	4	1-3	4
1	Chemical 1	x	x	x	x	x
2	Solid 1		x	x		
3	Solid 2			x		
4	Solid 3			x		
5	Chemical 2					x
6	Chemical 3					x
Complexity Level	Explanation					
Solids 1	Descriptive solids concentration field					
Solids 2	Descriptive solids concentration field with specific solids transport rates					
Solids 3	Simulated total solids					
Solids 4	Three simulated solids types					
Equilibrium 1	Constant partitioning coefficient					
Equilibrium 2	Spatially-variable partitioning coefficients					
Equilibrium 3	Hydrophobic sorption					
Equilibrium 4	Solids-dependent partitioning					
Equilibrium 5	Sorption plus ionic speciation					
Kinetic 1	Constant half-lives or rate constants					
Kinetic 2	Spatially-variable rate constants					
Kinetic 3	Second order rates					
Kinetic 4	Transformation products					

Source: WASP Manual (Ambrose et al., 1993)

For the dioxin model, level three solids (simulated TSS), equilibrium level 3 (hydrophobic sorption), and kinetics 1 or 2 are needed. For this level of complexity, the equations used in the constituent mass balance are (for a 1-D system):

$$\frac{\partial C_w}{\partial t} = \frac{\partial}{\partial x} \left(-U_x A C_w + E_x A \frac{\partial C_w}{\partial x} \right) + A(S_L + S_B + S_K) \quad (3.1a)$$

where C_w = dissolved concentration of the water quality constituent (mg/L)

t = time (days)

A = cross-sectional area (m²)

U_x = longitudinal advective velocity (m/s)

E_x = longitudinal dispersion coefficient (m²/s)

S_L = direct and diffuse loading rate (g/m³-d)

S_B = boundary loading rate (g/m³-d)

S_K = total kinetic transformation rate (g/m³-d)

or

$$\frac{\partial C_s}{\partial t} = -\frac{\partial}{\partial x}(UC_s) + \frac{\partial}{\partial x}\left(E_x \frac{\partial C_s}{\partial x}\right) - \frac{C_s}{S}W_d + \frac{C_{s,b}}{S_b}W_e + S_B + S_K \quad (3.1b)$$

where W_d = rate of sediment deposition (g/m³-s)

W_e = scour rate of sediment (g/m³-s)

C_s = constituent sorbed concentration in the water column (mg/L)

$C_{s,b}$ = constituent sorbed concentration in the bottom sediment (mg/kg)

S = concentration of suspended sediment (mg/L)

S_b = sediment concentration in bottom sediment (mg/kg)

and

$$C_s = K_p SC_w \quad (3.2)$$

where K_p is the linear partitioning coefficient of the constituent (L/kg).

A list of WASP input requirements for the dioxin model is included in Table 3.2.

Table 3.2 Data Requirements for the Dioxin WASP Model for the HSC

Data Group	Description	Source
A	Model Identification and Simulation Control	Basic simulation information including variables to simulate obtained from the statement of the problem
B	Exchange Coefficients Dispersion coefficient-water column Dispersion coefficient-pore water Cross-sectional area Characteristic length	Calibration to salinity values Literature values Channel data Channel data
C	Volumes For water column: number of segments and volumes for each time step For benthic segments: number of segments and volumes	Hydrodynamic file Number of segments equal to water column segments, volumes calculated using site data
D	Flows <i>- Surface Water</i> Flow routing Flow time function <i>- Pore Water</i> Flow routing Flow time function <i>- Sediment Transport</i> Area for settling and resuspension Flow routing Velocity (settling or resuspension)	Hydrodynamic file Hydrodynamic file Conceptual model Literature values Channel data Conceptual model Sediment load study for the HSC, initial settling velocities estimated using Stoke’s equation. Refine initial estimates with channel-specific calibration
E	Boundary Concentrations Concentrations for each system at segments that import, export, or exchange water with locations outside the network	Dioxin dataset collected for this project
F	Waste Loads Point source loadings Non-point source loadings	NPDES permit files, MEGA-TX model for the HSC, Spring 2003 effluent data, and regressions for non-measured outfalls Estimated using GIS and spreadsheets models

Data Group	Description	Source
G	Parameters Spatially variable characteristics of the water body that affect the particular processes being modeled. Dissolved organic carbon concentration Fraction organic carbon of solids Total lumped first-order decay rate	Dataset collected for this project Dataset collected for this project Literature values
H	Constants Organic carbon partitioning coefficient First-order loss rate constant Volatilization rate constant Water column biodegradation rate Benthic biodegradation rate Photolysis rate	Measured effective coefficients using data collected in this project (not needed if DOC and f_{oc} are input in Data Group G) Literature values Literature values Literature values Literature values Literature values
I	Kinetic Time Functions Not used in the dioxin model	
J	Initial Conditions Concentration of each modeled system (dioxin and TSS) for each segment	Dioxin dataset collected for this project

3.1 WASP SEGMENTATION AND TIME STEP

While a large number of small model elements were used in the RMA2 hydrodynamic models to simulate the sinuosity of the main channel and bayous and the change in bottom elevations in the channel and Upper Galveston Bay, there was no need for high spatial resolution simulations in the WASP water quality model, both from a water quality management perspective and because field measurements of water quality for calibration were not of high spatial resolution. The WASP model segmentation was developed by aggregating RMA2 elements to reaches maintaining the minimum segmentation required for water quality management purposes.

The WASP model for the HSC consists of sixty-one 1-D water surface segments, 46 2-D water surface elements, and 107 benthic segments (one underlying each of the surface water

segments). Figure 3.1 illustrates the segmentation of the WASP model for the HSC. Thirty-eight segments correspond to the main channel from Buffalo Bayou to the downstream boundary (as shown in Figure 3.1), twenty to the major tributaries, twenty-one to SJR (including the Old River), and the remaining 28 comprise the side bays, Barbour’s Cut, Bayport Channel, Clear Lake, and Upper Galveston Bay. Table 3.3 summarizes the physical characteristics of the WASP segments. The WASP models were developed using a time step of six minutes.

3.2 MODEL INPUT

3.2.1 Hydrodynamics

As mentioned earlier, the WASP model was linked to the long-term RMA2 hydrodynamic model to obtain data on flows, velocities, and depths. Volumes were calculated by the HSCREAD interface.

3.2.2 Boundary Concentrations

Boundary concentrations include the effect of point sources discharging directly to major tributaries as well as storm water runoff reaching the streams upstream of the WASP model domain. Boundary concentrations were defined at the USGS gages, and input flows to RMA2 were adjusted to account for any point sources discharging between the gage and the beginning of the model domain (see Table 2.5). Because dioxin concentrations were measured at the mouth of the tributaries, they do not represent true boundary conditions as they are influenced by tidal effects. Thus, the following procedure was followed to develop daily boundary time series for each major tributary:

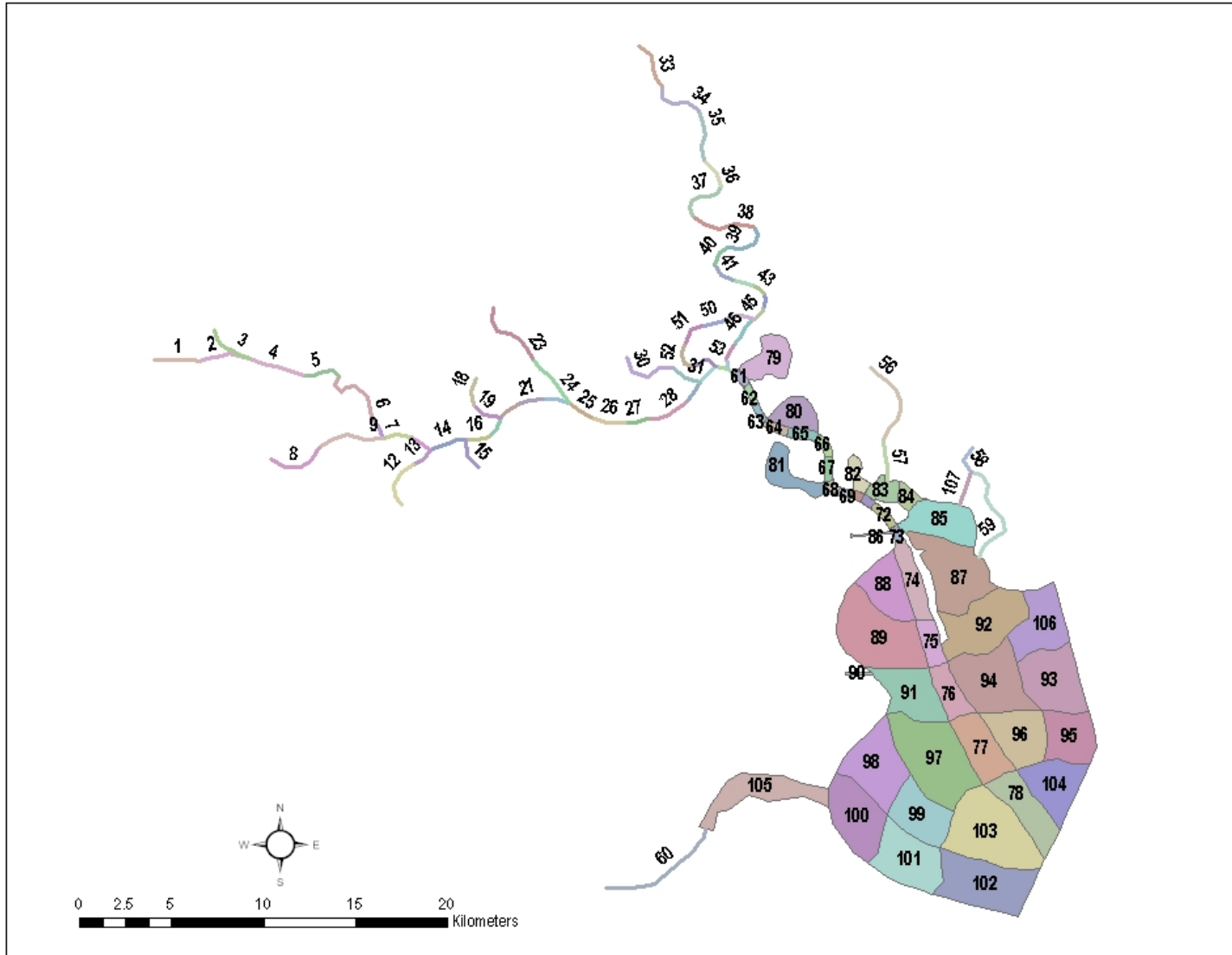


Figure 3.1 WASP Model Segmentation

Table 3.3 Physical Characteristics of WASP Segments

Segment ID	Surface Water Segments					Underlying Benthic Segments	
	Location	Water Quality Segment	Monitoring Station ^a	Average Depth ^b (m)	Average Volume ^b (m ³)	Segment ID	Volume ^c (m ³)
1	Buffalo Bayou	1013		2.3	119,924	108	9,000
2	Buffalo Bayou	1013	11347	4.7	302,696	109	9,900
3	Whiteoak Bayou	1013	11382	2.6	126,105	110	9,500
4	Main Channel	1007_07		5.3	700,026	111	13,700
5	Main Channel	1007	112925	8.3	1,015,854	112	33,300
6	Main Channel	1007		11.8	4,410,797	113	147,000
7	Main Channel	1007		12.3	2,350,245	114	33,800
8	Brays Bayou	1007		4.3	583,325	115	33,600
9	Brays Bayou	1007	11305	6.3	1,051,080	116	38,800
10	Main Channel@I-610	1007		12.3	2,349,566	117	42,500
11	Main Channel	1007	11287	13.3	2,197,958	118	36,900
12	Sims Bayou	1007		5.1	1,405,834	119	12,300
13	Sims Bayou	1007	11302	6.3	228,513	120	5,600
14	Main Channel	1007		13.0	3,985,971	121	69,700
15	Vince Bayou	1007	11300	5.3	766,192	122	13,200
16	Main Channel	1007		12.8	2,615,889	123	49,900
17	Main Channel	1007		12.8	2,265,007	124	35,800
18	Hunting Bayou	1007		3.3	195,916	125	7,400
19	Hunting Bayou	1007	11298	4.3	178,462	126	8,000
20	Main Channel	1007	11280	13.2	2,505,808	127	46,800
21	Main Channel	1007		13.5	3,083,529	128	60,300
22	Main Channel@ Greens	1007	11270	13.8	3,673,840	129	66,600
23	Greens Bayou	1006_03		6.5	1,571,752	130	23,800
24	Greens Bayou	1006_03	11274	9.2	1,142,125	131	18,900
25	Main Channel	1006 upper		14.1	4,711,774	132	85,800
26	Main Channel	1006 upper	15979	14.3	7,724,456	133	139,500
27	Main Channel	1006 upper		14.3	5,223,558	134	83,800
28	Main Channel	1006 lower		14.3	9,093,609	135	153,100
29	Main Channel	1006 lower	11265	15.3	5,445,178	136	91,100
30	Carpenters Bayou	1006 lower	11272	3.3	783,882	137	19,700
31	Carpenters Bayou	1006 lower		5.3	272,034	138	10,200
32	Main Channel@ Battleship	1006 lower	11264	15.3	4,913,496	139	78,500
33	San Jacinto River	1001 upper		4.2	784,156	140	39,800
34	San Jacinto River	1001 upper		4.7	1,231,932	141	43,200
35	San Jacinto River	1001 upper	11200	6.3	3,139,700	142	42,600
36	San Jacinto River	1001 upper		6.3	2,285,792	143	25,500
37	San Jacinto River	1001 upper	16622	6.3	2,853,512	144	41,600
38	San Jacinto River	1001 upper		7.3	3,190,294	145	53,300
39	San Jacinto River	1001 upper		7.3	3,004,694	146	38,700
40	San Jacinto River	1001 upper		7.3	2,148,470	147	37,500
41	San Jacinto River	1001 lower	11197	7.3	2,581,010	148	41,400
42	San Jacinto River	1001 lower		7.8	2,528,354	149	32,700
43	San Jacinto River	1001 lower		8.6	1,348,846	150	27,000
44	San Jacinto River	1001 lower	11193	9.3	1,258,304	151	27,400
45	San Jacinto River@I-10	1001 lower		11.3	1,725,127	152	33,100
46	San Jacinto River	1005 upper		12.8	6,184,997	153	61,500
47	San Jacinto River	1005 upper		14.5	4,864,105	154	37,900
48	San Jacinto River@HSC	1005 upper		15.3	2,635,360	155	38,300
49	Old River	Old River		5.3	2,054,375	156	23,100
50	Old River	Old River		5.3	2,217,326	157	20,000
51	Old River	Old River		5.3	2,451,778	158	22,400
52	Old River	Old River		5.3	2,682,034	159	26,600
53	Old River@HSC	Old River		6.3	2,001,812	160	22,400

Segment ID	Surface Water Segments					Underlying Benthic Segments	
	Location	Water Quality Segment	Monitoring Station ^a	Average Depth ^b (m)	Average Volume ^b (m ³)	Segment ID	Volume ^c (m ³)
54	Main Channel	1005 upper		15.3	2,705,672	161	43,600
55	Main Channel@Lynchburg	1005 upper	11261	14.8	847,312	162	23,500
56	Goose Creek	2426	11092	2.4	975,841	163	10,300
57	Goose Creek	2426		2.4	139,242	164	4,900
58	Cedar Bayou	901	11111	2.8	851,181	165	9,500
59	Cedar Bayou	901		3.0	834,484	166	37,100
60	Clear Creek	Clear Creek		2.8	1,456,428	167	84,800
61	Main Channel	1005 lower		12.5	5,889,177	168	140,900
62	Main Channel	1005 lower		11.8	5,330,508	169	136,000
63	Main Channel	1005 lower		12.1	4,835,774	170	120,300
64	Main Channel	1005 lower		11.4	7,708,792	171	202,500
65	Main Channel	1005 lower	16618	11.4	10,163,636	172	266,400
66	Main Channel	1005 lower		12.3	7,424,858	173	181,100
67	Main Channel	1005 lower		12.1	7,094,695	174	176,000
68	Main Channel	1005 lower		12.7	4,587,032	175	108,500
69	Main Channel	1005 lower		12.2	4,299,394	176	105,800
70	Main Channel	1005 lower		13.0	4,180,399	177	96,600
71	Main Channel	1005 lower		13.3	4,569,366	178	103,000
72	Main Channel	1005 lower		12.6	9,272,426	179	221,400
73	Main Channel@Morgan'sPoint	2421	11252	13.8	5,371,904	180	105,500
74	Main Channel	2421	13309	10.5	43,437,480	181	1,240,900
75	Main Channel	2421		11.2	29,373,580	182	787,100
76	Main Channel	2421	14560	11.0	42,345,480	183	1,154,800
77	Main Channel	2421		10.2	70,040,712	184	2,050,700
78	Main Channel d/s boundary	2421		10.8	77,965,320	185	2,174,100
79	Burnett Bay	2430	13343/13344/16496	1.6	7,126,666	186	1,374,400
80	Scott Bay	2429	13342/17971	1.6	5,762,558	187	1,048,500
81	San Jacinto Bay	2427	16499/13339	2.4	9,254,475	188	1,178,300
82	Black Duck Bay	2428	13340/13341	2.5	3,123,366	189	372,800
83	Tabbs Bay	2426	13337	2.3	4,282,606	190	565,300
84	Tabbs Bay	2426		2.0	2,390,916	191	360,700
85	Tabbs Bay	2421	13336	2.8	19,996,118	192	2,155,300
86	Barbours Cut	2436	13355	15.3	3,428,550	193	78,800
87	Upper Galveston Bay	2421		2.2	25,656,204	194	3,542,600
88	Upper Galveston Bay	2421		2.4	16,179,258	195	2,015,900
89	Upper Galveston Bay	2421	15908	2.5	36,101,172	196	4,279,900
90	Bayport Channel	2438	13589/13363	15.3	2,602,521	197	51,200
91	Upper Galveston Bay	2421		5.6	45,171,780	198	2,406,500
92	Upper Galveston Bay	2421		2.3	26,716,656	199	3,475,400
93	Upper Galveston Bay	2421		2.9	29,733,842	200	3,056,000
94	Upper Galveston Bay	2421		2.8	32,574,628	201	3,530,100
95	Upper Galveston Bay	2421		2.8	19,703,934	202	2,105,900
96	Upper Galveston Bay	2421		2.8	22,547,524	203	2,415,800
97	Upper Galveston Bay	2421		2.9	44,185,788	204	4,588,300
98	Upper Galveston Bay	2421		2.4	25,144,472	205	3,117,500
99	Upper Galveston Bay	2421	16213	2.9	22,310,600	206	2,282,800
100	Upper Galveston Bay	2421	15464	2.7	25,919,706	207	2,864,000
101	Upper Galveston Bay	2421		2.6	25,469,274	208	2,905,300
102	Upper Galveston Bay	2421		2.4	29,443,790	209	3,682,800
103	Upper Galveston Bay	2421		3.0	47,198,236	210	4,660,000
104	Upper Galveston Bay	2421		2.9	22,334,774	211	2,332,600
105	Clear Lake	Clear Lake		3.2	26,044,138	212	2,405,300
106	Upper Galveston Bay	2421		2.6	21,785,156	213	2,494,400
107	Cedar Bayou Cut-off Channel	-		3.3	1,290,541	214	11,500

^a Stations sampled for dioxin as part of this project; ^b Averages for the March 20-April 21, 2005 simulation period; ^c Assuming a layer depth of 0.30 m

- If no rain was recorded at the nearest Harris County Office of Homeland Security and Emergency Management (HCOEM) gage, the load was assumed as the sum of loads from PS discharging upstream of the USGS gage.
- Runoff flow was calculated as the flow at the USGS gage minus the flow from PS discharging upstream of the gage⁸. The estimated runoff flow was then multiplied by the concentration in runoff measured at a given watershed (or the average of runoff concentrations when there were no runoff locations for the watershed) to obtain runoff loads.
- Because runoff was measured in catchments that did not have point sources, both PS and runoff loads upstream of the model domain (i.e., upstream of USGS gages plus the reach between the gage and the beginning of the model domain) were added to estimate the total load at the boundary.
- For SJR, there are no point sources upstream of the boundary or information on dry weather concentrations at Lake Houston. Thus, if no rain was recorded for a given day, the flow from Lake Houston was multiplied by the congener concentration measured at Banana Bend under dry conditions⁹, otherwise the flow was multiplied by the average concentration of a given congener measured in runoff.
- The total load was divided by the flow at the boundary (as included in RMA2) to obtain concentrations.

Tables 3.4a through f present a summary of boundary data for the simulation period. The database developed to obtain daily boundary concentrations is included in Appendix B.

⁸ Runoff flows calculated in this manner compared well with flows obtained from HSPF and GWLF models developed for the individual watersheds. The developed models, however, were not used to generate dioxin time-series because calibration of dioxin proved to be difficult due to the lack of measured data.

Table 3.4a Average 2378-TCDD Loads and Concentrations at Upstream Boundaries

Boundary	Flow at Boundary (m ³ /s) ^a	Point Sources		Storm water Runoff			Total Load (kg/day) ^d	Boundary Concentration (pg/L) ^e
		Flow (m ³ /s) ^b	Load (kg/day)	Flow (m ³ /s)	Concentration (pg/L) ^c	Load (kg/day)		
Buffalo B.	21.5	1.7	3.98E-09	19.9	0.028	4.75E-08	5.15E-08	0.065
Whiteoak B.	6.2	0.9	2.08E-09	5.3	0.022	1.01E-08	1.22E-08	0.024
Brays B.	10.1	3.0	5.90E-09	7.1	0.049	2.99E-08	3.58E-08	0.032
Sims B.	10.1	1.3	2.58E-09	8.8	0.003	2.60E-09	5.18E-09	0.009
Vince B.	0.5	0.0	0	0.5	0.017	7.97E-10	7.97E-10	0.017
Hunting B.	2.0	0.1	4.09E-10	1.9	0.016	2.61E-09	3.02E-09	0.021
Greens B.	8.2	1.0	2.30E-09	7.2	0.024	1.51E-08	1.74E-08	0.025
Carpenters B.	1.0	0.2	4.94E-10	0.8	0.017	1.24E-09	1.73E-09	0.028
San Jacinto R.	163.0	0.0	0	163.0	0.017	2.46E-07	2.46E-07	0.020
Goose C.	1.0	0.0	1.02E-11	1.0	0.018	1.56E-09	1.57E-09	0.018
Cedar B.	1.0	0.4	6.43E-10	0.6	0.017	8.64E-10	1.51E-09	0.017
Clear C.	2	-	-	-	-	-		0.001 ^f

Table 3.4b Average 12378-PeCDD Loads and Concentrations at Upstream Boundaries

Boundary	Flow at Boundary (m ³ /s) ^a	Point Sources		Storm water Runoff			Total Load (kg/day) ^d	Boundary Concentration (pg/L) ^e
		Flow (m ³ /s) ^b	Load (kg/day)	Flow (m ³ /s)	Concentration (pg/L) ^c	Load (kg/day)		
Buffalo B.	21.5	1.7	6.88E-09	19.9	0.081	1.40E-07	1.47E-07	0.134
Whiteoak B.	6.2	0.9	3.38E-09	5.3	0.067	3.06E-08	3.40E-08	0.055
Brays B.	10.1	3.0	7.44E-09	7.1	0.117	7.17E-08	7.91E-08	0.061
Sims B.	10.1	1.3	4.64E-09	8.8	0.008	6.41E-09	1.10E-08	0.018
Vince B.	0.5	0.0	0	0.5	0.079	3.69E-09	3.69E-09	0.079
Hunting B.	2.0	0.1	9.97E-10	1.9	0.099	1.66E-08	1.76E-08	0.099
Greens B.	8.2	1.0	5.15E-09	7.2	0.078	4.86E-08	5.37E-08	0.071
Carpenters B.	1.0	0.2	9.41E-10	0.8	0.079	5.57E-09	6.51E-09	0.068
San Jacinto R.	163.0	0.0	0	163.0	0.079	6.57E-07	6.57E-07	0.040
Goose C.	1.0	0.0	2.29E-11	1.0	0.108	9.27E-09	9.30E-09	0.108
Cedar B.	1.0	0.4	1.13E-09	0.6	0.079	4.00E-09	5.12E-09	0.059
Clear C.	2	-	-	-	-	-		0.001 ^f

Note: these values are averages for the entire simulation period, daily values were input to WASP (see Appendix B)

^a Included in RMA2

^b Average self-reported flow

^c Concentrations in runoff measured in 2003 and 2005

^d PS plus runoff loads

^e Total load divided by flow at boundary

^f Clear Creek is not included in the TMDL and, thus, no dioxin data area available. A 0.001 pg/L concentration was assumed

⁹ The tidal effects at Banana Bend are small.

Table 3.4c Average 123678-HxCDD Loads and Concentrations at Upstream Boundaries

Boundary	Flow at Boundary (m ³ /s) ^a	Point Sources		Storm water Runoff			Total Load (kg/day) ^d	Boundary Concentration (pg/L) ^e
		Flow (m ³ /s) ^b	Load (kg/day)	Flow (m ³ /s)	Concentration (pg/L) ^c	Load (kg/day)		
Buffalo B.	21.5	1.7	3.36E-09	19.9	0.238	4.10E-07	4.14E-07	0.192
Whiteoak B.	6.2	0.9	1.53E-09	5.3	0.353	1.60E-07	1.62E-07	0.188
Brays B.	10.1	3.0	5.25E-09	7.1	0.344	2.10E-07	2.15E-07	0.138
Sims B.	10.1	1.3	2.64E-09	8.8	0.029	2.22E-08	2.49E-08	0.028
Vince B.	0.5	0.0	0	0.5	0.315	1.48E-08	1.48E-08	0.315
Hunting B.	2.0	0.1	7.94E-10	1.9	0.434	7.23E-08	7.31E-08	0.352
Greens B.	8.2	1.0	2.43E-09	7.2	0.326	2.03E-07	2.05E-07	0.212
Carpenters B.	1.0	0.2	3.96E-10	0.8	0.315	2.23E-08	2.27E-08	0.121
San Jacinto R.	163.0	0.0	0	163.0	0.315	2.85E-06	2.85E-06	0.179
Goose C.	1.0	0.0	1.08E-11	1.0	0.553	4.76E-08	4.76E-08	0.551
Cedar B.	1.0	0.4	1.66E-09	0.6	0.315	1.60E-08	1.76E-08	0.204
Clear C.	2	-	-	-	-	-		0.001 ^f

Table 3.4d Average 2378-TCDF Loads and Concentrations at Upstream Boundaries

Boundary	Flow at Boundary (m ³ /s) ^a	Point Sources		Storm water Runoff			Total Load (kg/day) ^d	Boundary Concentration (pg/L) ^e
		Flow (m ³ /s) ^b	Load (kg/day)	Flow (m ³ /s)	Concentration (pg/L) ^c	Load (kg/day)		
Buffalo B.	21.5	1.7	9.84E-09	19.9	0.088	1.51E-07	1.61E-07	0.174
Whiteoak B.	6.2	0.9	4.42E-09	5.3	0.151	6.85E-08	7.30E-08	0.104
Brays B.	10.1	3.0	8.33E-09	7.1	0.145	8.88E-08	9.71E-08	0.073
Sims B.	10.1	1.3	5.19E-09	8.8	0.021	1.57E-08	2.09E-08	0.028
Vince B.	0.5	0.0	0	0.5	0.114	5.37E-09	5.37E-09	0.114
Hunting B.	2.0	0.1	1.19E-09	1.9	0.198	3.29E-08	3.41E-08	0.179
Greens B.	8.2	1.0	7.54E-09	7.2	0.097	6.03E-08	6.78E-08	0.093
Carpenters B.	1.0	0.2	1.05E-09	0.8	0.114	8.11E-09	9.15E-09	0.084
San Jacinto R.	163.0	0.0	0	163.0	0.114	1.37E-06	1.37E-06	0.094
Goose C.	1.0	0.0	3.35E-11	1.0	0.049	4.17E-09	4.21E-09	0.049
Cedar B.	1.0	0.4	4.55E-09	0.6	0.114	5.82E-09	1.04E-08	0.120
Clear C.	2	-	-	-	-	-		0.001 ^f

Note: these values are averages for the entire simulation period, daily values were input to WASP (see Appendix B)

^a Included in RMA2

^b Average self-reported flow

^c Concentrations in runoff measured in 2003 and 2005

^d PS plus runoff loads

^e Total load divided by flow at boundary

^f Clear Creek is not included in the TMDL and, thus, no dioxin data area available. A 0.001 pg/L concentration was assumed

Table 3.4e Average 23478-PeCDF Loads and Concentrations at Upstream Boundaries

Boundary	Flow at Boundary (m ³ /s) ^a	Point Sources		Storm water Runoff			Total Load (kg/day) ^d	Boundary Concentration (pg/L) ^e
		Flow (m ³ /s) ^b	Load (kg/day)	Flow (m ³ /s)	Concentration (pg/L) ^c	Load (kg/day)		
Buffalo B.	21.5	1.7	4.08E-09	19.9	0.040	6.93E-08	7.34E-08	0.108
Whiteoak B.	6.2	0.9	2.15E-09	5.3	0.054	2.45E-08	2.67E-08	0.048
Brays B.	10.1	3.0	4.80E-09	7.1	0.077	4.68E-08	5.16E-08	0.046
Sims B.	10.1	1.3	2.56E-09	8.8	0.011	8.26E-09	1.08E-08	0.019
Vince B.	0.5	0.0	0	0.5	0.061	2.84E-09	2.84E-09	0.061
Hunting B.	2.0	0.1	3.91E-10	1.9	0.124	2.07E-08	2.11E-08	0.118
Greens B.	8.2	1.0	2.83E-09	7.2	0.081	5.06E-08	5.34E-08	0.073
Carpenters B.	1.0	0.2	6.69E-10	0.8	0.061	4.29E-09	4.96E-09	0.062
San Jacinto R.	163.0	0.0	0	163.0	0.061	6.02E-07	6.02E-07	0.039
Goose C.	1.0	0.0	1.26E-11	1.0	0.030	2.55E-09	2.57E-09	0.030
Cedar B.	1.0	0.4	2.24E-09	0.6	0.061	3.08E-09	5.31E-09	0.049
Clear C.	2	-	-	-	-	-		0.001 ^f

Table 3.4f Average 123678-HxCDF Loads and Concentrations at Upstream Boundaries

Boundary	Flow at Boundary (m ³ /s) ^a	Point Sources		Storm water Runoff			Total Load (kg/day) ^d	Boundary Concentration (pg/L) ^e
		Flow (m ³ /s) ^b	Load (kg/day)	Flow (m ³ /s)	Concentration (pg/L) ^c	Load (kg/day)		
Buffalo B.	21.5	1.7	2.26E-09	19.9	0.407	7.01E-07	7.03E-07	0.342
Whiteoak B.	6.2	0.9	1.05E-09	5.3	0.171	7.78E-08	7.89E-08	0.107
Brays B.	10.1	3.0	3.20E-09	7.1	0.186	1.14E-07	1.17E-07	0.086
Sims B.	10.1	1.3	3.51E-09	8.8	0.016	1.23E-08	1.58E-08	0.023
Vince B.	0.5	0.0	0	0.5	0.217	1.02E-08	1.02E-08	0.217
Hunting B.	2.0	0.1	9.62E-10	1.9	0.200	3.33E-08	3.43E-08	0.176
Greens B.	8.2	1.0	1.58E-09	7.2	0.131	8.13E-08	8.28E-08	0.103
Carpenters B.	1.0	0.2	8.64E-10	0.8	0.217	1.54E-08	1.62E-08	0.113
San Jacinto R.	163.0	0.0	0	163.0	0.217	1.69E-06	1.69E-06	0.099
Goose C.	1.0	0.0	6.98E-12	1.0	0.084	7.23E-09	7.24E-09	0.084
Cedar B.	1.0	0.4	3.23E-09	0.6	0.217	1.10E-08	1.43E-08	0.141
Clear C.	2	-	-	-	-	-		0.001 ^f

Note: these values are averages for the entire simulation period, daily values were input to WASP (see Appendix B)

^a Included in RMA2

^b Average self-reported flow

^c Concentrations in runoff measured in 2003 and 2005

^d PS plus runoff loads

^e Total load divided by flow at boundary

^f Clear Creek is not included in the TMDL and, thus, no dioxin data area available. A 0.001 pg/L concentration was assumed

3.2.3 Loads

Total loads of the six dioxin congeners reaching the various WASP segments were calculated as the sum of point sources, storm water runoff, and direct deposition (wet and dry) to the channel surface. The following paragraphs summarize the procedure followed to obtain the datasets and a load database is included in Appendix B.

Point Sources

Input from point sources is simulated in WASP7 by a series of loading versus time values. It is important to note that mass entered as loads is not directly accompanied with inflow. Thus, flows from point sources were input to the RMA2 model. For the WASP model, point sources discharging directly to the main channel were aggregated by segment to determine total loads. Point sources discharging to the major tributaries upstream of the sections simulated in the WASP model were input as part of the boundary concentrations as detailed above. Figure 3.2 shows the distribution of point sources discharging to the main channel. Dioxin data from point sources (PS) gathered in this project during Spring 2003 were used to calculate load inputs. For the point sources that were not sampled for effluent and the SIC was among those identified as potential dioxin dischargers, the concentration of a given congener in effluent was assumed equal to the average concentration of the congener in effluent from facilities with the same SIC code. If the SIC was not among the potential dioxin dischargers, the dioxin concentration was assumed equal to zero. The loads were calculated multiplying the concentrations by the five-year averages of self-reported flows (as included in the TCEQ permittee database dated May 2003). A summary of the point source data for the model is included in Table 3.5. The total loads of dioxins from PS discharging directly to the HSC system calculated in this manner were estimated to be 3.87×10^{-8}

kg/day for 2378-TCDD, 6.16×10^{-8} kg/day for 12378-PeCDD, 7.61×10^{-8} kg/day for 123678-HxCDD, 3.56×10^{-7} kg/day for 2378-TCDF, 1.39×10^{-7} kg/day for 23478-PeCDF, and 1.67×10^{-7} kg/day for 123678-HxCDF.

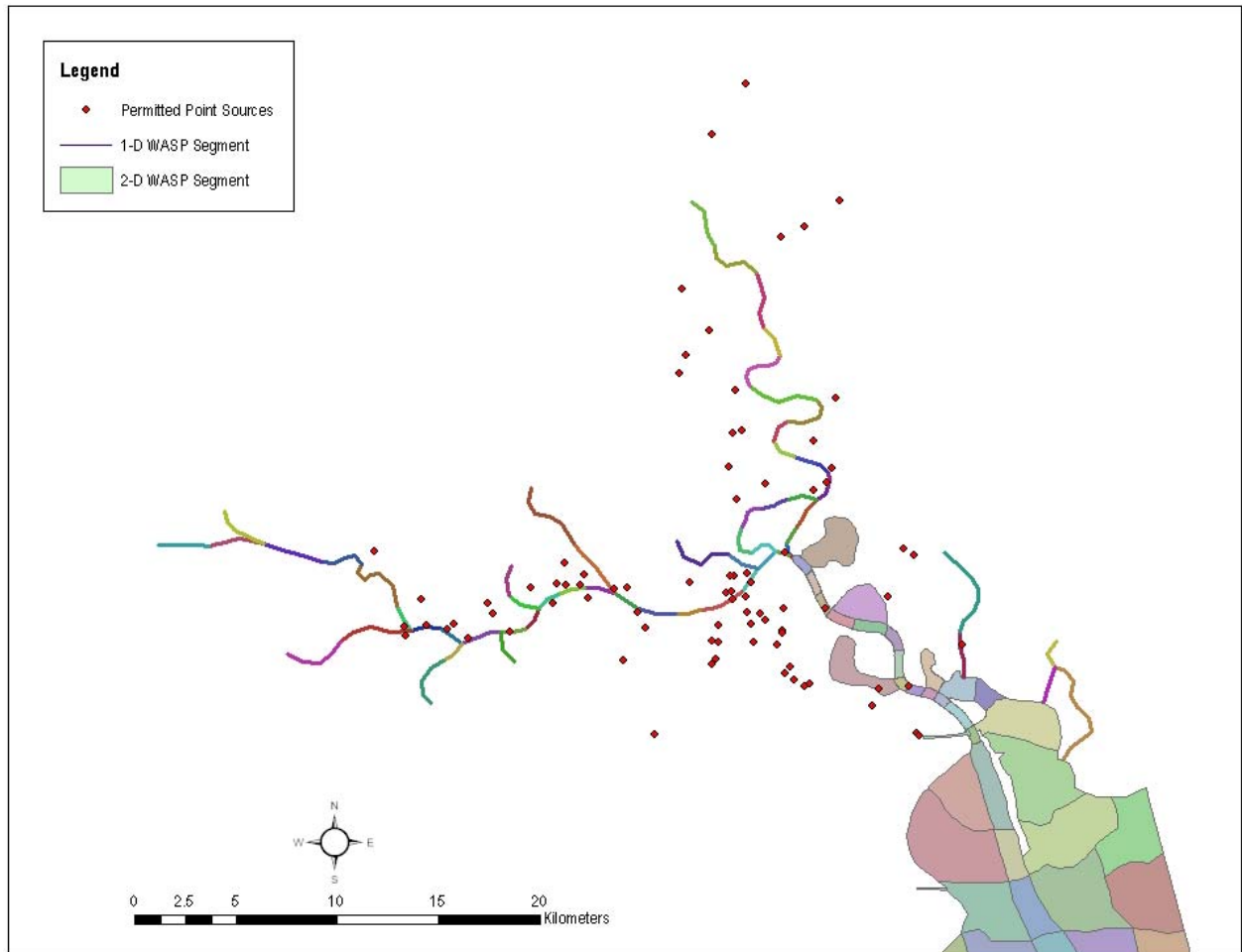


Figure 3.2 Point Sources in WASP

Table 3.5 Summary of Point Source Loads in the WASP Model

WASP Segment	TCEQ Permit #	Self-reported Flow (m ³ /s)	2378-TCDD		12378-PeCDD		123678-HxCDD		2378-TCDF		23478-PeCDF		123678-HxCDF	
			Concentration (pg/L)	Load (kg/day)										
4	02039-000	4.15E-04	0	0	0	0	0	0	0	0	0	0	0	0
5	00635-000	4.11E-03	0	0	0	0	0	0	0	0	0	0	0	0
5	00635-000	5.52E-04	0	0	0	0	0	0	0	0	0	0	0	0
5	00635-000	2.24E-04	0	0	0	0	0	0	0	0	0	0	0	0
6	10495-090	3.88 ^a	0.043	1.39E-08	0.096	3.21E-08	0.102	3.43E-08	0.768	2.57E-07	0.218	7.32E-08	0.054	1.82E-08
6	11773-001	6.37E-05	0.027	1.46E-13	0.059	3.27E-13	0.028	1.54E-13	0.087	4.78E-13	0.033	1.79E-13	0.018	9.96E-14
7	02034-000	5.04E-03	0	0	0	0	0	0	0	0	0	0	0	0
7	10495-010	2.28E-02	0.030	5.95E-11	0.043	8.49E-11	0.015	3.05E-11	0.093	1.84E-10	0.022	4.32E-11	0.006	1.27E-11
9	00542-000	1.72E-02	0	0	0	0	0	0	0	0	0	0	0	0
10	03133-000	1.92E-03	0	0	0	0	0	0	0	0	0	0	0	0
11	00456-000	9.48E-04	0	0	0	0	0	0	0	0	0	0	0	0
11	00535-000	5.71E-02	0.032	1.56E-10	0.027	1.32E-10	0.144	7.10E-10	0.088	4.33E-10	0.042	2.10E-10	0.081	4.02E-10
12	00393-000	3.18E-02	0.045	1.23E-10	0.104	2.86E-10	0.080	2.21E-10	0.129	3.54E-10	0.094	2.58E-10	0.146	4.02E-10
12	00520-000	7.44E-02	0	0	0	0	0	0	0	0	0	0	0	0
12	00587-000	2.03E-02	0	0	0	0	0	0	0	0	0	0	0	0
12	00587-000	2.03E-02	0	0	0	0	0	0	0	0	0	0	0	0
12	10495-002	6.88E-01	0.010	7.53E-10	0.041	1.87E-09	0.056	2.54E-09	0.050	2.27E-09	0.033	1.49E-09	0.015	6.99E-10
12	10495-002	5.30E-01	0.016	5.83E-10	0.023	1.38E-09	0.014	8.26E-10	0.041	2.44E-09	0.038	2.23E-09	0.012	7.37E-10
13	02659-000	3.20E-02	0.000	0.00E+00										
14	00353-000	8.60E-03	0.044	3.30E-11	0.043	3.22E-11	0.105	7.79E-11	0.308	2.29E-10	0.227	1.69E-10	0.470	3.49E-10
15	10053-005	3.32E-01	0.031	8.94E-10	0.054	1.56E-09	0.037	1.05E-09	0.063	1.81E-09	0.046	1.31E-09	0.033	9.51E-10
16	00786-000	5.70E-04	0.045	1.70E-11	0.030	1.15E-11	0.054	2.03E-11	0.100	3.79E-11	0.049	1.86E-11	0.125	4.72E-11
16	01740-000	1.29E+00	0.013	1.47E-09	0.033	3.73E-09	0.045	5.04E-09	0.120	1.35E-08	0.051	5.74E-09	0.126	1.41E-08
19	01745-000	2.06E-04	0	0	0	0	0	0	0	0	0	0	0	0
19	10831-001	3.30E-02	0.027	7.55E-11	0.059	1.69E-10	0.028	7.98E-11	0.087	2.47E-10	0.033	9.28E-11	0.018	5.15E-11
20	00649-000	2.11E-02	0	0	0	0	0	0	0	0	0	0	0	0
20	00649-000	2.45E-02	0	0	0	0	0	0	0	0	0	0	0	0
20	00649-000	1.69E-02	0	0	0	0	0	0	0	0	0	0	0	0
20	00649-000	1.14E-02	0	0	0	0	0	0	0	0	0	0	0	0
21	00509-000	6.43E-03	0	0	0	0	0	0	0	0	0	0	0	0
21	00671-000	2.61E-03	0	0	0	0	0	0	0	0	0	0	0	0
21	03889-000	4.39E-03	0	0	0	0	0	0	0	0	0	0	0	0
22	00815-001	1.39E-01	0	0	0	0	0	0	0	0	0	0	0	0
22	03767-000	2.63E-04	0	0	0	0	0	0	0	0	0	0	0	0

WASP Segment	TCEQ Permit #	Self-reported Flow (m ³ /s)	2378-TCDD		12378-PeCDD		123678-HxCDD		2378-TCDF		23478-PeCDF		123678-HxCDF	
			Concentration (pg/L)	Load (kg/day)										
23	00662-001	2.84E-03	0	0	0	0	0	0	0	0	0	0	0	0
23	10495-077	1.62E-01	0.024	3.38E-10	0.052	7.32E-10	0.016	2.22E-10	0.052	7.32E-10	0.013	1.77E-10	0.009	1.25E-10
23	11727-001	1.97E-02	0.027	4.51E-11	0.059	1.01E-10	0.028	4.76E-11	0.087	1.48E-10	0.033	5.54E-11	0.018	3.08E-11
24	00445-000	3.87E-03	0.045	1.50E-11	0.025	8.39E-12	0.099	3.32E-11	0.346	1.16E-10	0.205	6.87E-11	0.392	1.31E-10
24	00492-000	4.29E-02	0.029	1.09E-10	0.012	4.50E-11	0.020	7.23E-11	0.456	1.69E-09	0.287	1.06E-09	0.127	4.69E-10
24	00749-000	1.95E-02	0.033	5.61E-11	0.019	3.17E-11	0.023	3.96E-11	0.605	1.02E-09	0.108	1.82E-10	0.080	1.35E-10
24	03792-000	1.52E-04	0.000	0.00E+00										
24	03828-000	6.25E-05	0.044	2.39E-13	0.043	2.34E-13	0.105	5.66E-13	0.308	1.66E-12	0.227	1.22E-12	0.470	2.54E-12
24	03828-000	6.25E-05	0.044	1.32E-13	0.043	1.29E-13	0.105	3.12E-13	0.308	9.16E-13	0.227	6.75E-13	0.470	1.40E-12
25	01160-000	5.49E-01	0.049	2.33E-09	0.041	1.92E-09	0.050	2.39E-09	0.104	4.93E-09	0.060	2.84E-09	0.137	6.48E-09
25	02067-000	5.77E-03	0.071	3.52E-11	0.034	1.70E-11	0.042	2.08E-11	0.101	5.05E-11	0.060	2.99E-11	0.127	6.33E-11
26	00002-001	1.37E-01	0.039	4.70E-10	0.042	5.03E-10	0.053	6.32E-10	0.098	1.16E-09	0.068	8.03E-10	0.144	1.71E-09
26	10053-002	1.33E-01	0.027	3.06E-10	0.059	6.85E-10	0.028	3.23E-10	0.087	1.00E-09	0.033	3.76E-10	0.018	2.09E-10
27	00402-000	2.92E-01	0.094	2.37E-09	0.028	6.97E-10	0.175	4.41E-09	0.437	1.10E-08	0.365	9.22E-09	2.516	6.36E-08
27	00403-000	2.79E-01	0.041	1.00E-09	0.108	2.61E-09	0.178	4.30E-09	0.423	1.02E-08	0.512	1.24E-08	0.656	1.58E-08
27	03129-000	4.58E-03	0	0	0	0	0	0	0	0	0	0	0	0
28	00305-001	1.94E-01	0.094	1.57E-09	0.081	1.35E-09	0.077	1.29E-09	0.045	7.55E-10	0.090	1.51E-09	0.184	3.07E-09
28	00305-003	1.82E-01	0.059	9.30E-10	0.049	7.73E-10	0.063	9.99E-10	0.183	2.88E-09	0.194	3.06E-09	0.375	5.90E-09
28	00305-005	3.76E-02	0.059	1.92E-10	0.049	1.60E-10	0.063	2.06E-10	0.183	5.95E-10	0.194	6.32E-10	0.375	1.22E-09
28	00403-000	4.03E-02	0.065	2.26E-10	0.285	9.93E-10	0.377	1.32E-09	1.114	3.88E-09	1.470	5.12E-09	1.872	6.53E-09
28	00458-000	2.29E-01	0.023	4.58E-10	0.035	6.97E-10	0.159	3.14E-09	0.035	6.86E-10	0.019	3.71E-10	0.028	5.47E-10
28	00458-000	5.12E-02	0.045	1.98E-10	0.037	1.62E-10	0.045	2.01E-10	0.093	4.10E-10	0.059	2.60E-10	0.133	5.90E-10
28	00544-001	5.38E-02	0.057	2.63E-10	0.025	1.14E-10	0.080	3.73E-10	0.154	7.14E-10	0.039	1.81E-10	0.054	2.49E-10
28	00639-000	3.92E-02	0.045	4.73E-10	0.030	3.19E-10	0.038	3.98E-10	0.090	9.45E-10	0.049	5.12E-10	0.121	1.28E-09
28	01173-000	2.28E-03	0	0	0	0	0	0	0	0	0	0	0	0
28	01429-000	3.60E-02	0.050	1.56E-10	0.017	5.37E-11	0.042	1.32E-10	0.203	6.32E-10	0.046	1.43E-10	0.061	1.91E-10
28	01984-002	2.57E-03	0	0	0	0	0	0	0	0	0	0	0	0
28	02558-000	2.93E-04	0.045	1.78E-10	0.030	1.18E-10	0.038	1.52E-10	0.094	3.75E-10	0.049	1.96E-10	0.122	4.87E-10
28	03375-000	5.64E-03	0.045	2.19E-11	0.025	1.22E-11	0.099	4.83E-11	0.346	1.68E-10	0.205	1.00E-10	0.392	1.91E-10
28	10519-002	1.44E-01	0.064	7.96E-10	0.020	2.45E-10	0.027	3.39E-10	0.029	3.58E-10	0.034	4.26E-10	0.015	1.87E-10
28	11841-001	1.08E-04	0.000	0.00E+00										
28	12318-001	4.51E-05	0.027	1.03E-13	0.059	2.32E-13	0.028	1.09E-13	0.087	3.39E-13	0.033	1.27E-13	0.018	7.05E-14
28	13203-001	1.25E-05	0.027	2.86E-14	0.059	6.45E-14	0.028	3.04E-14	0.087	9.42E-14	0.033	3.53E-14	0.018	1.96E-14
29	00544-003	2.92E-02	0.040	1.00E-10	0.030	7.64E-11	0.038	9.52E-11	0.090	2.28E-10	0.049	1.24E-10	0.124	3.13E-10
29	01000-000	2.40E-02	0.021	4.40E-11	0.012	2.58E-11	0.039	8.06E-11	0.041	8.41E-11	0.014	2.97E-11	0.028	5.83E-11

WASP Segment	TCEQ Permit #	Self-reported Flow (m ³ /s)	2378-TCDD		12378-PeCDD		123678-HxCDD		2378-TCDF		23478-PeCDF		123678-HxCDF	
			Concentration (pg/L)	Load (kg/day)										
29	01539-000	4.14E-02	0.024	8.53E-11	0.017	6.13E-11	0.050	1.77E-10	0.321	1.15E-09	0.299	1.07E-09	0.566	2.02E-09
29	01731-000	5.99E-03	0.043	2.21E-11	0.020	1.03E-11	0.009	4.71E-12	0.046	2.37E-11	0.015	7.57E-12	0.008	3.89E-12
29	01984-007	8.73E-04	0	0	0	0	0	0	0	0	0	0	0	0
29	02177-000	1.25E-04	0	0	0	0	0	0	0	0	0	0	0	0
29	12406-001	2.71E-03	0.040	9.28E-12	0.020	4.61E-12	0.105	2.45E-11	0.308	7.21E-11	0.227	5.31E-11	0.470	1.10E-10
29	03937-000	4.93E-03	0.046	2.65E-11	0.019	1.06E-11	0.026	1.46E-11	0.124	7.07E-11	0.030	1.72E-11	0.034	1.95E-11
30	01310-001	4.48E-03	0	0	0	0	0	0	0	0	0	0	0	0
30	02419-000	4.63E-03	0.041	1.66E-11	0.108	4.32E-11	0.178	7.12E-11	0.423	1.69E-10	0.512	2.05E-10	0.656	2.62E-10
30	13365-001	7.39E-04	0	0	0	0	0	0	0	0	0	0	0	0
31	02160-000	7.93E-04	0.044	3.04E-12	0.043	2.97E-12	0.105	7.18E-12	0.308	2.11E-11	0.227	1.55E-11	0.470	3.22E-11
31	02458-000	3.90E-03	0	0	0	0	0	0	0	0	0	0	0	0
31	12314-001	2.75E-05	0.027	6.30E-14	0.059	1.41E-13	0.028	6.65E-14	0.087	2.06E-13	0.033	7.73E-14	0.018	4.29E-14
31	12375-001	3.40E-04	0.027	7.80E-13	0.059	1.75E-12	0.028	8.24E-13	0.087	2.56E-12	0.033	9.58E-13	0.018	5.32E-13
31	12874-001	6.68E-05	0.027	1.53E-13	0.059	3.43E-13	0.028	1.62E-13	0.087	5.02E-13	0.033	1.88E-13	0.018	1.04E-13
31	13316-001	4.26E-05	0.027	9.76E-14	0.059	2.19E-13	0.028	1.03E-13	0.087	3.20E-13	0.033	1.20E-13	0.018	6.65E-14
33	10530-001	3.49E-03	0.027	8.00E-12	0.059	1.79E-11	0.028	8.45E-12	0.087	2.62E-11	0.033	9.83E-12	0.018	5.46E-12
33	10668-001	1.17E-02	0.027	2.68E-11	0.059	6.00E-11	0.028	2.83E-11	0.087	8.77E-11	0.033	3.29E-11	0.018	1.83E-11
33	12213-001	4.39E-05	0.027	1.01E-13	0.059	2.26E-13	0.028	1.06E-13	0.087	3.30E-13	0.033	1.24E-13	0.018	6.87E-14
34	12712-000	1.75E-03	0.045	6.79E-12	0.025	3.79E-12	0.054	8.11E-12	0.533	8.07E-11	0.082	1.24E-11	0.128	1.94E-11
34	10541-002	2.68E-03	0.027	6.13E-12	0.059	1.38E-11	0.028	6.48E-12	0.087	2.01E-11	0.033	7.54E-12	0.018	4.19E-12
34	11329-001	2.33E-02	0.027	5.18E-11	0.059	1.08E-09	0.028	8.12E-11	0.087	2.39E-10	0.033	6.13E-11	0.018	2.29E-11
34	11388-001	1.68E-02	0.026	3.85E-11	0.535	4.71E-11	0.040	5.61E-11	0.119	1.35E-10	0.030	7.59E-11	0.011	1.78E-10
36	12386-001	1.06E-04	0.027	2.44E-13	0.032	5.47E-13	0.039	2.57E-13	0.093	7.99E-13	0.052	2.99E-13	0.123	1.66E-13
37	00391-000	1.80E-01	0.027	1.48E-09	0.059	4.37E-10	0.028	1.69E-09	0.087	8.73E-09	0.033	1.64E-09	0.018	4.37E-10
37	03540-000	5.96E-05	0.095	2.28E-13	0.028	2.23E-13	0.108	5.39E-13	0.561	1.59E-12	0.105	1.17E-12	0.028	2.42E-12
37	03540-000	5.96E-05	0.044	2.28E-13	0.043	2.23E-13	0.105	5.39E-13	0.308	1.59E-12	0.227	1.17E-12	0.470	2.42E-12
37	03540-000	5.96E-05	0.044	2.28E-13	0.043	2.23E-13	0.105	5.39E-13	0.308	1.59E-12	0.227	1.17E-12	0.470	2.42E-12
37	03787-001	3.26E-04	0.044	1.25E-12	0.043	1.22E-12	0.105	2.95E-12	0.308	8.67E-12	0.227	6.38E-12	0.470	1.32E-11
37	03787-002	9.31E-04	0.044	2.85E-12	0.043	2.78E-12	0.105	6.73E-12	0.308	1.98E-11	0.227	1.46E-11	0.470	3.02E-11
38	11770-001	2.18E-02	0.088	5.00E-11	0.059	1.12E-10	0.028	5.29E-11	0.087	1.64E-10	0.033	6.15E-11	0.018	3.40E-11
39	01062-000	1.28E-03	0	0	0	0	0	0	0	0	0	0	0	0
39	10104-001	6.21E-02	0.041	2.19E-10	0.045	2.44E-10	0.027	1.44E-10	0.085	4.59E-10	0.027	1.47E-10	0.011	5.67E-11
39	12863-001	4.77E-04	0.027	1.09E-12	0.059	2.45E-12	0.028	1.15E-12	0.087	3.58E-12	0.033	1.34E-12	0.018	7.45E-13
41	02845-000	6.31E-03	0	0	0	0	0	0	0	0	0	0	0	0
41	02927-001	8.61E-02	0.071	5.25E-10	0.033	2.49E-10	0.045	3.35E-10	0.094	6.97E-10	0.050	3.75E-10	0.124	9.19E-10

WASP Segment	TCEQ Permit #	Self-reported Flow (m ³ /s)	2378-TCDD		12378-PeCDD		123678-HxCDD		2378-TCDF		23478-PeCDF		123678-HxCDF	
			Concentration (pg/L)	Load (kg/day)										
42	03445-001	7.93E-04	0	0	0	0	0	0	0	0	0	0	0	0
44	03349-000	9.43E-04	0	0	0	0	0	0	0	0	0	0	0	0
44	10395-008	9.35E-02	0.019	1.56E-10	0.021	1.70E-10	0.023	1.84E-10	0.071	5.77E-10	0.057	4.62E-10	0.035	2.81E-10
49	02605-000	1.54E-03	0	0	0	0	0	0	0	0	0	0	0	0
50	03517-000	2.45E-05	0	0	0	0	0	0	0	0	0	0	0	0
51	10105-001	5.90E-02	0.027	1.35E-10	0.059	3.03E-10	0.028	1.43E-10	0.087	4.43E-10	0.033	1.66E-10	0.018	9.22E-11
51	10558-001	2.51E-02	0.027	5.75E-11	0.033	7.22E-11	0.042	9.20E-11	0.095	2.07E-10	0.054	1.18E-10	0.123	2.67E-10
52	10184-001	7.76E-03	0.027	1.78E-11	0.059	3.99E-11	0.028	1.88E-11	0.087	5.83E-11	0.033	2.19E-11	0.018	1.21E-11
54	13666-001	3.16E-04	0.027	7.25E-13	0.059	1.63E-12	0.028	7.66E-13	0.087	2.38E-12	0.033	8.91E-13	0.018	4.95E-13
55	02097-000	4.85E-02	0.032	1.34E-10	0.025	1.04E-10	0.110	4.62E-10	0.331	1.39E-09	0.409	1.72E-09	1.386	5.81E-09
57	10395-002	1.81E-01	0.022	3.47E-10	0.023	3.56E-10	0.034	5.39E-10	0.136	2.13E-09	0.053	8.29E-10	0.032	5.06E-10
59	01332-000	1.34E-03	0	0	0	0	0	0	0	0	0	0	0	0
66	00592-000	5.21E-02	0.041	1.87E-10	0.108	4.87E-10	0.178	8.01E-10	0.423	1.91E-09	0.512	2.30E-09	0.656	2.95E-09
69	00592-000	7.97E-01	0.028	1.93E-09	0.013	8.94E-10	0.013	8.94E-10	0.068	4.67E-09	0.023	1.59E-09	0.013	8.87E-10
80	02184-000	1.19E-02	0.045	4.61E-11	0.025	2.58E-11	0.099	1.02E-10	0.346	3.55E-10	0.205	2.11E-10	0.392	4.03E-10
81	00474-000	1.02E-01	0.047	4.20E-10	0.022	1.91E-10	0.099	8.75E-10	0.166	1.47E-09	0.021	1.89E-10	0.015	1.29E-10
81	00663-000	2.67E-02	0.041	1.90E-10	0.022	1.02E-10	0.099	4.58E-10	0.200	9.24E-10	0.109	5.04E-10	0.075	3.48E-10
81	01280-000	1.75E-03	0	0	0	0	0	0	0	0	0	0	0	0
81	01785-000	3.45E-03	0	0	0	0	0	0	0	0	0	0	0	0
81	02107-001	1.41E-02	0	0	0	0	0	0	0	0	0	0	0	0
81	02529-000	4.46E-03	0	0	0	0	0	0	0	0	0	0	0	0
81	13949-001	1.08E-04	0	0	0	0	0	0	0	0	0	0	0	0
83	01385-000	3.27E-04	0.045	1.27E-12	0.025	7.08E-13	0.099	2.80E-12	0.346	9.76E-12	0.205	5.79E-12	0.392	1.11E-11
83	01914-000	1.76E-03	0.045	6.83E-12	0.033	5.09E-12	0.718	1.09E-10	0.137	2.08E-11	0.094	1.43E-11	0.383	5.84E-11
86	00440-000	7.66E-03	0.045	2.97E-11	0.032	2.09E-11	0.048	3.20E-11	0.094	6.22E-11	0.052	3.41E-11	0.134	8.89E-11
86	10779-001	3.97E-03	0.027	9.09E-12	0.059	2.04E-11	0.028	9.61E-12	0.087	2.98E-11	0.033	1.12E-11	0.018	6.21E-12
89	10206-001	1.49E-01	0.027	3.41E-10	0.059	7.65E-10	0.028	3.61E-10	0.087	1.12E-09	0.033	4.19E-10	0.018	2.33E-10
90	01054-000	4.69E-01	0.027	1.07E-09	0.031	1.24E-09	0.044	1.78E-09	0.095	3.84E-09	0.051	2.05E-09	0.122	4.96E-09
90	02590-000	6.18E-03	0.000	0.00E+00										
100	10671-001	4.45E-02	0.027	1.02E-10	0.059	2.29E-10	0.028	1.08E-10	0.087	3.34E-10	0.033	1.25E-10	0.018	6.96E-11
100	12039-001	1.90E-02	0.027	4.34E-11	0.059	9.74E-11	0.028	4.59E-11	0.087	1.42E-10	0.033	5.34E-11	0.018	2.96E-11
101	01050-000	6.21E-03	0	0	0	0	0	0	0	0	0	0	0	0
101	10627-001	3.33E-02	0.027	7.64E-11	0.059	1.71E-10	0.028	8.07E-11	0.087	2.50E-10	0.033	9.39E-11	0.018	5.21E-11
102	11546-001	2.95E-02	0.027	6.77E-11	0.059	1.52E-10	0.028	7.15E-11	0.087	2.22E-10	0.033	8.32E-11	0.018	4.62E-11

^a Average values. Daily time series were input to the model

Storm water Runoff

Storm water runoff loads for all the segments (except upstream boundary segments for which runoff was accounted for in the boundary concentration) were input to the model for the days at which a rain event occurred (as indicated by the closest HCOEM gage to each segment). Drainage areas were estimated using TSARP (Tropical Storm Allison Recovery Project) subwatersheds. It is noted that in some cases, the watershed delineated for TSARP covered two WASP segments (e.g., segments 10 and 11, segments 20 and 21). In those cases, the entire load was applied at the downstream segment. Daily dioxin runoff loads were calculated using land cover information (H-GAC 2003), the average of the congener concentrations in runoff measured in this project (0.017 pg/L for 2378-TCDD, 0.079 pg/L for 12378-PeCDD, 0.314 pg/L for 123678-HxCDD, 0.114 pg/L for 2378-TCDF, 0.060 pg/L for 23478-PeCDF, and 0.217 pg/L for 123678-HxCDF), and the amounts of rainfall recorded for the simulation period.

The amount of runoff for each drainage area was calculated using the SCS runoff curve number method (Natural Resource Conservation Service, 1986). The SCS runoff equation is:

$$Q = \frac{(P - I_a)^2}{(P - I_a) + S} \quad (3.3)$$

where Q = runoff (in);

P = rainfall (in);

S = potential maximum retention after runoff begins (in); and

I_a = initial abstraction (in).

Initial abstraction refers to all the losses before runoff begins and includes water intercepted by vegetation, infiltration, evaporation, and water retained in surface depressions.

This parameter is very variable but is correlated to land cover and soil type (NRCS, 1986). The Natural Resource Conservation Service (1986) estimates I_a to be equal to

$$I_a = 0.2S \tag{3.4}$$

thus,

$$Q = \frac{(P - 0.2S)^2}{(P + 0.8S)} \tag{3.5}$$

Finally, S is related to the curve number (CN) by

$$S = \frac{1000}{CN} - 10 \tag{3.6}$$

CN values range from 0 to 100 and are based on land cover and soil group. For this runoff calculation, all subwatersheds were assumed to be in soil group D (silts and clays) that generally has low infiltration rates. Land coverage data developed by the H-GAC in 2002 (H-GAC, 2003) were used. The classification system for the H-GAC dataset and their corresponding runoff curve numbers are included in Table 3.6.

Table 3.6 Runoff Curve Numbers for the HSC Watershed

Land Cover Code	Land Cover Description	CN ^a
1	Developed	98
2	Grass/Agriculture	89
3	Woodland	77
4	Open Water	0
5	Wetlands	30
6	Transitional/Bare	89

^a Obtained from “Urban Hydrology for Small Watersheds.” Natural Resources Conservation Service, Technical Release 55, June 1986.

Average runoff loads by segment are summarized in Table 3.7. Total average daily loads from runoff into the HSC system were estimated to be 3.37×10^{-8} , 1.56×10^{-7} , 6.22×10^{-7} , 2.26×10^{-7} , 1.20×10^{-7} , and 4.29×10^{-7} kg/day for 2378-TCDD, 12378-PeCDD, 123678-HxCDD, 2378-TCDF, 23478-PeCDF, and 123678-PeCDF, respectively.

Table 3.7 Storm Water Runoff Loads to the WASP Model

WASP Segment	Average Flow (m ³ /s)	Average Load (kg/day)					
		2378-TCDD	12378-PeCDD	123678-HxCDD	2378-TCDF	23478-PeCDF	123678-HxCDF
1	4.57E-01	6.71E-10	3.10E-09	1.24E-08	4.52E-09	2.39E-09	8.56E-09
3	4.22E-01	6.20E-10	2.87E-09	1.15E-08	4.17E-09	2.21E-09	7.92E-09
4	7.92E-01	1.16E-09	5.38E-09	2.15E-08	7.83E-09	4.14E-09	1.48E-08
6	1.41E-01	2.07E-10	9.57E-10	3.83E-09	1.39E-09	7.37E-10	2.64E-09
8	9.73E-01	2.78E-09	1.28E-08	5.13E-08	1.87E-08	9.89E-09	3.54E-08
9	1.18E-01	1.74E-10	8.04E-10	3.22E-09	1.17E-09	6.20E-10	2.22E-09
11	3.88E-01	5.71E-10	2.64E-09	1.06E-08	3.84E-09	2.03E-09	7.28E-09
12	3.81E-01	1.20E-09	5.54E-09	2.22E-08	8.07E-09	4.27E-09	1.53E-08
13	1.14E-01	1.68E-10	7.76E-10	3.11E-09	1.13E-09	5.98E-10	2.14E-09
14	2.76E-01	4.05E-10	1.87E-09	7.49E-09	2.72E-09	1.44E-09	5.17E-09
15	4.42E-02	4.18E-10	1.93E-09	7.73E-09	2.81E-09	1.49E-09	5.33E-09
17	6.98E-02	1.03E-10	4.74E-10	1.90E-09	6.90E-10	3.65E-10	1.31E-09
18	2.20E-01	1.24E-09	5.73E-09	2.29E-08	8.34E-09	4.42E-09	1.58E-08
19	7.73E-02	1.14E-10	5.25E-10	2.10E-09	7.64E-10	4.05E-10	1.45E-09
21	2.98E-01	4.37E-10	2.02E-09	8.09E-09	2.94E-09	1.56E-09	5.58E-09
22	1.75E-01	2.57E-10	1.19E-09	4.75E-09	1.73E-09	9.15E-10	3.28E-09
23	1.99E-01	1.67E-09	7.72E-09	3.09E-08	1.12E-08	5.95E-09	2.13E-08
24	3.99E-01	5.86E-10	2.71E-09	1.08E-08	3.94E-09	2.09E-09	7.48E-09
26	3.55E-01	5.21E-10	2.41E-09	9.65E-09	3.51E-09	1.86E-09	6.65E-09
27	4.77E-01	7.00E-10	3.24E-09	1.30E-08	4.71E-09	2.50E-09	8.94E-09
28	3.27E-01	4.81E-10	2.22E-09	8.89E-09	3.24E-09	1.71E-09	6.14E-09
29	2.42E-01	3.55E-10	1.64E-09	6.58E-09	2.39E-09	1.27E-09	4.54E-09
31	2.26E-01	3.32E-10	1.54E-09	6.14E-09	2.24E-09	1.18E-09	4.24E-09
32	2.85E-02	4.18E-11	1.93E-10	7.73E-10	2.81E-10	1.49E-10	5.33E-10
33	3.66E-01	5.38E-10	2.49E-09	9.95E-09	3.62E-09	1.92E-09	6.86E-09
34	1.77E-01	2.61E-10	1.20E-09	4.82E-09	1.75E-09	9.28E-10	3.33E-09
35	6.52E-01	9.58E-10	4.43E-09	1.77E-08	6.45E-09	3.41E-09	1.22E-08
36	3.33E-01	4.89E-10	2.26E-09	9.04E-09	3.29E-09	1.74E-09	6.23E-09
37	4.18E-01	6.13E-10	2.84E-09	1.13E-08	4.13E-09	2.19E-09	7.83E-09
38	4.87E-01	7.15E-10	3.30E-09	1.32E-08	4.81E-09	2.55E-09	9.12E-09
39	1.49E-01	2.19E-10	1.01E-09	4.05E-09	1.47E-09	7.80E-10	2.79E-09
40	4.30E-02	6.31E-11	2.92E-10	1.17E-09	4.25E-10	2.25E-10	8.05E-10

WASP Segment	Average Flow (m ³ /s)	Average Load (kg/day)					
		2378-TCDD	12378-PeCDD	123678-HxCDD	2378-TCDF	23478-PeCDF	123678-HxCDF
50	2.29E-02	3.36E-11	1.55E-10	6.21E-10	2.26E-10	1.20E-10	4.28E-10
51	2.39E-01	3.51E-10	1.62E-09	6.49E-09	2.36E-09	1.25E-09	4.48E-09
53	3.19E-02	4.69E-11	2.17E-10	8.68E-10	3.16E-10	1.67E-10	5.99E-10
56	2.90E-01	4.26E-10	1.97E-09	7.88E-09	2.87E-09	1.52E-09	5.44E-09
57	3.94E-01	5.78E-10	2.67E-09	1.07E-08	3.89E-09	2.06E-09	7.38E-09
58	5.26E-01	1.64E-09	7.56E-09	3.03E-08	1.10E-08	5.83E-09	2.09E-08
59	6.38E-01	9.37E-10	4.33E-09	1.73E-08	6.31E-09	3.34E-09	1.20E-08
60	6.57E-14	5.68E-09	2.63E-08	1.05E-07	3.82E-08	2.02E-08	7.25E-08
61	4.51E-02	6.62E-11	3.06E-10	1.22E-09	4.46E-10	2.36E-10	8.45E-10
62	1.90E-04	2.79E-13	1.29E-12	5.16E-12	1.88E-12	9.94E-13	3.56E-12
63	1.24E-01	1.82E-10	8.41E-10	3.36E-09	1.22E-09	6.48E-10	2.32E-09
65	1.24E-03	1.82E-12	8.42E-12	3.37E-11	1.23E-11	6.49E-12	2.32E-11
66	5.31E-02	7.79E-11	3.60E-10	1.44E-09	5.24E-10	2.78E-10	9.94E-10
67	1.91E-02	2.80E-11	1.30E-10	5.18E-10	1.89E-10	9.98E-11	3.57E-10
68	1.11E-02	1.63E-11	7.54E-11	3.02E-10	1.10E-10	5.81E-11	2.08E-10
69	2.60E-02	3.82E-11	1.77E-10	7.07E-10	2.57E-10	1.36E-10	4.88E-10
70	5.68E-03	8.35E-12	3.86E-11	1.54E-10	5.62E-11	2.97E-11	1.07E-10
71	4.59E-03	6.74E-12	3.12E-11	1.25E-10	4.54E-11	2.40E-11	8.60E-11
72	1.79E-02	2.63E-11	1.22E-10	4.87E-10	1.77E-10	9.37E-11	3.36E-10
73	5.41E-02	7.95E-11	3.67E-10	1.47E-09	5.35E-10	2.83E-10	1.01E-09
79	1.19E-01	1.76E-10	8.11E-10	3.25E-09	1.18E-09	6.25E-10	2.24E-09
80	3.67E-01	5.39E-10	2.49E-09	9.98E-09	3.63E-09	1.92E-09	6.88E-09
81	5.98E-01	8.78E-10	4.06E-09	1.62E-08	5.91E-09	3.13E-09	1.12E-08
82	7.58E-02	1.11E-10	5.15E-10	2.06E-09	7.49E-10	3.97E-10	1.42E-09
83	3.30E-02	4.85E-11	2.24E-10	8.97E-10	3.26E-10	1.73E-10	6.19E-10
84	8.43E-02	1.24E-10	5.72E-10	2.29E-09	8.33E-10	4.41E-10	1.58E-09
85	1.05E-01	1.54E-10	7.12E-10	2.85E-09	1.04E-09	5.49E-10	1.97E-09
86	4.90E-02	7.20E-11	3.33E-10	1.33E-09	4.85E-10	2.57E-10	9.19E-10
87	2.64E-02	3.88E-11	1.79E-10	7.17E-10	2.61E-10	1.38E-10	4.95E-10
88	2.04E-01	3.00E-10	1.39E-09	5.54E-09	2.02E-09	1.07E-09	3.82E-09
89	3.63E-01	5.33E-10	2.46E-09	9.85E-09	3.58E-09	1.90E-09	6.80E-09
90	2.19E-02	3.22E-11	1.49E-10	5.96E-10	2.17E-10	1.15E-10	4.11E-10

WASP Segment	Average Flow (m ³ /s)	Average Load (kg/day)					
		2378-TCDD	12378-PeCDD	123678-HxCDD	2378-TCDF	23478-PeCDF	123678-HxCDF
41	1.11E-01	1.64E-10	7.57E-10	3.03E-09	1.10E-09	5.83E-10	2.09E-09
42	2.75E-02	4.03E-11	1.86E-10	7.46E-10	2.71E-10	1.44E-10	5.15E-10
44	2.35E-02	3.45E-11	1.60E-10	6.38E-10	2.32E-10	1.23E-10	4.40E-10
45	4.02E-03	5.90E-12	2.73E-11	1.09E-10	3.97E-11	2.10E-11	7.53E-11
46	1.24E-02	1.82E-11	8.44E-11	3.38E-10	1.23E-10	6.50E-11	2.33E-10
47	2.95E-02	4.33E-11	2.00E-10	8.01E-10	2.91E-10	1.54E-10	5.52E-10
49	2.19E-02	3.21E-11	1.48E-10	5.94E-10	2.16E-10	1.14E-10	4.10E-10

WASP Segment	Average Flow (m ³ /s)	Average Load (kg/day)					
		2378-TCDD	12378-PeCDD	123678-HxCDD	2378-TCDF	23478-PeCDF	123678-HxCDF
91	2.05E-01	3.02E-10	1.39E-09	5.58E-09	2.03E-09	1.07E-09	3.85E-09
92	2.26E-02	3.32E-11	1.54E-10	6.15E-10	2.24E-10	1.18E-10	4.24E-10
93	4.18E-02	6.14E-11	2.84E-10	1.14E-09	4.13E-10	2.19E-10	7.84E-10
98	1.21E-01	1.78E-10	8.24E-10	3.30E-09	1.20E-09	6.35E-10	2.27E-09
100	6.65E-02	9.77E-11	4.52E-10	1.81E-09	6.58E-10	3.48E-10	1.25E-09
101	1.12E-01	1.64E-10	7.59E-10	3.04E-09	1.10E-09	5.85E-10	2.09E-09
102	1.22E-01	1.79E-10	8.26E-10	3.30E-09	1.20E-09	6.36E-10	2.28E-09

Direct Deposition

Dry and wet direct deposition to the channel was simulated by multiplying the deposition fluxes measured in this study times the surface area of each of the WASP segments. Dry deposition was assumed to occur during days with no rain, while wet deposition was input for days with recorded rain higher than 0.1 inches. Table 3.8 summarizes the average deposition loads input to the model. The average total deposition load was estimated to be 1.1×10^{-7} , 2.6×10^{-7} , 5.0×10^{-7} , 2.1×10^{-7} , 2.5×10^{-7} , and 2.0×10^{-7} kg/day for 2378-TCDD, 12378-PeCDD, 123678-HxCDD, 2378-TCDF, 23478-PeCDF, and 123678-PeCDF, respectively.

3.2.4 Initial Concentrations

For the surface water segments, initial dioxin concentrations were input on a segment-basis using the water concentrations (dissolved + suspended) of the selected congeners for the stations sampled in this project, while initial suspended sediment concentrations were assumed to be equal to the average TSS concentrations also collected in this project (26 mg/L). In addition, for the benthic segments, the average dioxin concentrations in sediment measured in this project were assumed as initial conditions.

In addition to chemical concentrations, the dissolved fractions must be specified for each segment at the beginning of the simulation. For dioxin, the dissolved fraction was set to 0.25. This fraction is internally recalculated by the model at each time step using partition coefficients and suspended sediment concentrations.

Table 3.8 Direct Deposition in the WASP Model

WASP Segment	Surface Area (m ²)	Average Deposition Load (kg/day)						WASP Segment	Surface Area (m ²)	Average Deposition Load (kg/day)					
		2378-TCDD	12378-PeCDD	123678-HxCDD	2378-TCDF	23478-PeCDF	123678-HxCDF			2378-TCDD	12378-PeCDD	123678-HxCDD	2378-TCDF	23478-PeCDF	123678-HxCDF
1	65,000	2.64E-11	6.46E-11	1.25E-10	5.19E-11	6.33E-11	5.01E-11	55	78,000	3.17E-11	7.77E-11	1.53E-10	6.35E-11	7.68E-11	6.17E-11
2	117,000	4.72E-11	1.16E-10	2.24E-10	9.29E-11	1.13E-10	8.98E-11	56	57,000	2.32E-11	5.69E-11	1.11E-10	4.61E-11	5.60E-11	4.47E-11
3	74,000	3.00E-11	7.36E-11	1.43E-10	5.91E-11	7.21E-11	5.71E-11	57	27,000	1.09E-11	2.66E-11	5.20E-11	2.16E-11	2.62E-11	2.09E-11
4	151,000	6.09E-11	1.49E-10	2.89E-10	1.20E-10	1.46E-10	1.16E-10	58	109,000	4.38E-11	1.07E-10	2.10E-10	8.70E-11	1.06E-10	8.43E-11
5	199,000	8.04E-11	1.97E-10	3.80E-10	1.57E-10	1.92E-10	1.51E-10	59	93,000	3.76E-11	9.22E-11	1.80E-10	7.47E-11	9.08E-11	7.24E-11
6	706,000	2.85E-10	6.97E-10	1.35E-09	5.55E-10	6.80E-10	5.35E-10	60	387,000	1.56E-10	3.83E-10	7.51E-10	3.12E-10	3.78E-10	3.03E-10
7	197,000	7.96E-11	1.95E-10	3.76E-10	1.55E-10	1.90E-10	1.50E-10	61	470,000	1.90E-10	4.65E-10	9.14E-10	3.80E-10	4.60E-10	3.69E-10
8	163,000	6.59E-11	1.61E-10	3.11E-10	1.29E-10	1.57E-10	1.24E-10	62	453,000	1.83E-10	4.48E-10	8.76E-10	3.63E-10	4.42E-10	3.52E-10
9	217,000	8.74E-11	2.14E-10	4.13E-10	1.70E-10	2.09E-10	1.64E-10	63	401,000	1.62E-10	3.97E-10	7.75E-10	3.22E-10	3.91E-10	3.12E-10
10	231,000	9.30E-11	2.28E-10	4.39E-10	1.81E-10	2.22E-10	1.75E-10	64	675,000	2.72E-10	6.68E-10	1.30E-09	5.41E-10	6.58E-10	5.24E-10
11	208,000	8.39E-11	2.05E-10	3.96E-10	1.64E-10	2.00E-10	1.58E-10	65	888,000	3.58E-10	8.78E-10	1.72E-09	7.12E-10	8.65E-10	6.90E-10
12	133,000	5.36E-11	1.31E-10	2.56E-10	1.06E-10	1.29E-10	1.03E-10	66	604,000	2.44E-10	5.97E-10	1.17E-09	4.84E-10	5.88E-10	4.69E-10
13	70,000	2.84E-11	6.97E-11	1.36E-10	5.62E-11	6.85E-11	5.44E-11	67	587,000	2.37E-10	5.80E-10	1.13E-09	4.70E-10	5.72E-10	4.56E-10
14	361,000	1.46E-10	3.57E-10	6.96E-10	2.88E-10	3.51E-10	2.79E-10	68	362,000	1.46E-10	3.58E-10	6.99E-10	2.90E-10	3.53E-10	2.81E-10
15	96,000	3.87E-11	9.49E-11	1.85E-10	7.66E-11	9.32E-11	7.41E-11	69	353,000	1.42E-10	3.49E-10	6.81E-10	2.83E-10	3.44E-10	2.74E-10
16	245,000	9.88E-11	2.42E-10	4.71E-10	1.95E-10	2.38E-10	1.89E-10	70	322,000	1.30E-10	3.17E-10	6.07E-10	2.50E-10	3.08E-10	2.40E-10
17	198,000	7.98E-11	1.96E-10	3.81E-10	1.58E-10	1.92E-10	1.53E-10	71	343,000	1.38E-10	3.38E-10	6.47E-10	2.66E-10	3.28E-10	2.56E-10
18	57,000	2.28E-11	5.60E-11	1.09E-10	4.54E-11	5.52E-11	4.40E-11	72	738,000	2.97E-10	7.26E-10	1.39E-09	5.73E-10	7.05E-10	5.50E-10
19	72,000	2.91E-11	7.14E-11	1.39E-10	5.76E-11	7.01E-11	5.57E-11	73	390,000	1.57E-10	3.84E-10	7.35E-10	3.03E-10	3.73E-10	2.91E-10
20	234,000	9.46E-11	2.32E-10	4.53E-10	1.88E-10	2.28E-10	1.82E-10	74	4,136,000	1.67E-09	4.07E-09	7.80E-09	3.21E-09	3.95E-09	3.08E-09
21	288,000	1.16E-10	2.85E-10	5.57E-10	2.31E-10	2.81E-10	2.24E-10	75	2,624,000	1.06E-09	2.58E-09	4.95E-09	2.04E-09	2.51E-09	1.96E-09
22	318,000	1.28E-10	3.14E-10	6.14E-10	2.55E-10	3.10E-10	2.47E-10	76	3,849,000	1.55E-09	3.79E-09	7.26E-09	2.99E-09	3.68E-09	2.87E-09
23	227,000	9.15E-11	2.24E-10	4.38E-10	1.82E-10	2.21E-10	1.76E-10	77	6,836,000	2.76E-09	6.77E-09	1.32E-08	5.51E-09	6.68E-09	5.34E-09
24	231,000	9.33E-11	2.29E-10	4.47E-10	1.85E-10	2.25E-10	1.80E-10	78	7,247,000	2.93E-09	7.17E-09	1.40E-08	5.84E-09	7.08E-09	5.66E-09
25	397,000	1.60E-10	3.93E-10	7.67E-10	3.19E-10	3.87E-10	3.09E-10	79	4,581,000	1.85E-09	4.52E-09	8.78E-09	3.64E-09	4.44E-09	3.51E-09
26	622,000	2.51E-10	6.16E-10	1.21E-09	5.03E-10	6.09E-10	4.89E-10	80	3,495,000	1.41E-09	3.46E-09	6.75E-09	2.80E-09	3.41E-09	2.72E-09
27	384,000	1.55E-10	3.80E-10	7.47E-10	3.11E-10	3.76E-10	3.02E-10	81	3,928,000	1.46E-09	3.88E-09	7.59E-09	3.15E-09	3.83E-09	3.05E-09
28	705,000	2.85E-10	6.98E-10	1.37E-09	5.70E-10	6.91E-10	5.54E-10	82	1,243,000	5.01E-10	1.23E-09	2.40E-09	9.96E-10	1.21E-09	9.65E-10
29	441,000	1.78E-10	4.36E-10	8.57E-10	3.57E-10	4.32E-10	3.47E-10	83	1,884,000	7.60E-10	1.86E-09	3.64E-09	1.51E-09	1.84E-09	1.46E-09
30	134,000	5.41E-11	1.33E-10	2.61E-10	1.08E-10	1.31E-10	1.05E-10	84	1,202,000	4.85E-10	1.19E-09	2.32E-09	9.64E-10	1.17E-09	9.34E-10
31	93,000	3.74E-11	9.18E-11	1.80E-10	7.50E-11	9.08E-11	7.29E-11	85	7,184,000	2.89E-09	7.07E-09	1.36E-08	5.58E-09	6.87E-09	5.35E-09
32	379,000	1.53E-10	3.76E-10	7.38E-10	3.07E-10	3.72E-10	2.98E-10	86	225,000	9.05E-11	2.21E-10	4.24E-10	1.74E-10	2.15E-10	1.67E-10
33	194,000	7.83E-11	1.92E-10	3.77E-10	1.57E-10	1.90E-10	1.53E-10	87	11,808,000	4.75E-09	1.16E-08	2.23E-08	9.17E-09	1.13E-08	8.80E-09

WASP Segment	Surface Area (m ²)	Average Deposition Load (kg/day)					
		2378-TCDD	12378-PeCDD	123678-HxCDD	2378-TCDF	23478-PeCDF	123678-HxCDF
34	219,000	8.85E-11	2.17E-10	4.23E-10	1.76E-10	2.14E-10	1.70E-10
35	244,000	9.85E-11	2.42E-10	4.73E-10	1.97E-10	2.39E-10	1.91E-10
36	146,000	5.91E-11	1.45E-10	2.84E-10	1.18E-10	1.43E-10	1.15E-10
37	238,000	9.60E-11	2.35E-10	4.61E-10	1.92E-10	2.33E-10	1.86E-10
38	326,000	1.32E-10	3.23E-10	6.33E-10	2.63E-10	3.19E-10	2.55E-10
39	236,000	9.54E-11	2.34E-10	4.58E-10	1.90E-10	2.31E-10	1.85E-10
40	178,000	7.18E-11	1.76E-10	3.45E-10	1.43E-10	1.74E-10	1.39E-10
41	195,000	7.86E-11	1.92E-10	3.73E-10	1.55E-10	1.89E-10	1.49E-10
42	144,000	5.81E-11	1.42E-10	2.76E-10	1.14E-10	1.39E-10	1.10E-10
43	116,000	4.67E-11	1.14E-10	2.22E-10	9.19E-11	1.12E-10	8.88E-11
44	132,000	5.31E-11	1.30E-10	2.52E-10	1.04E-10	1.27E-10	1.01E-10
45	171,000	6.88E-11	1.68E-10	3.27E-10	1.35E-10	1.65E-10	1.31E-10
46	312,000	1.26E-10	3.09E-10	5.99E-10	2.48E-10	3.02E-10	2.39E-10
47	192,000	7.73E-11	1.89E-10	3.68E-10	1.52E-10	1.86E-10	1.47E-10
48	167,000	6.74E-11	1.65E-10	3.20E-10	1.33E-10	1.62E-10	1.28E-10
49	153,000	6.17E-11	1.51E-10	2.93E-10	1.21E-10	1.48E-10	1.17E-10
50	132,000	5.34E-11	1.31E-10	2.54E-10	1.05E-10	1.28E-10	1.02E-10
51	148,000	5.96E-11	1.46E-10	2.87E-10	1.19E-10	1.45E-10	1.16E-10
52	176,000	7.11E-11	1.74E-10	3.43E-10	1.43E-10	1.73E-10	1.39E-10
53	163,000	6.58E-11	1.61E-10	3.17E-10	1.32E-10	1.60E-10	1.28E-10
54	205,000	8.27E-11	2.03E-10	3.98E-10	1.66E-10	2.01E-10	1.61E-10

WASP Segment	Surface Area (m ²)	Average Deposition Load (kg/day)					
		2378-TCDD	12378-PeCDD	123678-HxCDD	2378-TCDF	23478-PeCDF	123678-HxCDF
88	6,720,000	2.71E-09	6.61E-09	1.27E-08	5.22E-09	6.42E-09	5.01E-09
89	14,266,000	5.74E-09	1.40E-08	2.69E-08	1.11E-08	1.36E-08	1.06E-08
90	171,000	6.87E-11	1.68E-10	3.22E-10	1.32E-10	1.63E-10	1.27E-10
91	8,022,000	3.23E-09	7.90E-09	1.51E-08	6.23E-09	7.67E-09	5.98E-09
92	11,585,000	4.66E-09	1.14E-08	2.19E-08	9.00E-09	1.11E-08	8.63E-09
93	10,187,000	4.10E-09	1.00E-08	1.92E-08	7.91E-09	9.74E-09	7.59E-09
94	11,767,000	4.74E-09	1.16E-08	2.22E-08	9.14E-09	1.12E-08	8.77E-09
95	7,020,000	2.83E-09	6.95E-09	1.36E-08	5.65E-09	6.86E-09	5.48E-09
96	8,053,000	3.25E-09	7.97E-09	1.56E-08	6.49E-09	7.87E-09	6.29E-09
97	15,294,000	6.17E-09	1.51E-08	2.96E-08	1.23E-08	1.49E-08	1.20E-08
98	10,392,000	4.19E-09	1.03E-08	2.01E-08	8.37E-09	1.02E-08	8.12E-09
99	7,609,000	3.07E-09	7.53E-09	1.47E-08	6.13E-09	7.43E-09	5.95E-09
100	9,546,000	3.85E-09	9.45E-09	1.85E-08	7.69E-09	9.33E-09	7.46E-09
101	9,684,000	3.91E-09	9.58E-09	1.88E-08	7.80E-09	9.46E-09	7.57E-09
102	12,276,000	4.96E-09	1.22E-08	2.38E-08	9.89E-09	1.20E-08	9.59E-09
103	15,533,000	6.27E-09	1.54E-08	3.01E-08	1.25E-08	1.52E-08	1.21E-08
104	7,775,000	3.14E-09	7.70E-09	1.51E-08	6.26E-09	7.60E-09	6.08E-09
105	8,018,000	3.24E-09	7.94E-09	1.55E-08	6.46E-09	7.83E-09	6.26E-09
106	8,315,000	3.35E-09	8.18E-09	1.57E-08	6.46E-09	7.95E-09	6.20E-09
107	51,000	2.07E-11	5.06E-11	9.89E-11	4.11E-11	4.99E-11	3.98E-11

Measured deposition fluxes were as follows:

Congener	Dry deposition flux (pg/m ² /day)	Wet deposition flux (pg/m ² /day)
2378-TCDD	0.62	1.1
12378-PeCDD	0.97	2.15
123678-HxCDD	1.75	13
2378-TCDF	0.7	7
23478-PeCDF	0.9	5.5
123678-HxCDF	0.65	8.5

3.2.5 Solid Transport Parameters

Sediment transport is a very important process in modeling 2378-TCDD because dioxins sorb strongly to sediment and thus undergo settling, scour, and sedimentation. In addition, sorption affects the transformation rates. The suspended sediment was simulated as a single solid class. The major processes affecting sediment distribution are advection and dispersion between the water column segments, and settling to and scour from the benthic segment.⁷

Water Column Transport

Sediment and particulate dioxin in the water column may settle and deposit to the surficial benthic layer. Settling and scour rates in WASP7 are described by velocities and surface areas. Particulate transport velocities are multiplied by cross-sectional areas to obtain flow rates for solids and the particulate fractions of dioxins.

Settling velocities should be set within the Stoke's range of velocities corresponding to the size distribution of suspended particles (Ambrose et al., 1993):

$$V_s = \frac{8.64g}{18\mu}(\rho_p - \rho_w) \cdot d_p^2 \quad (3.7)$$

where V_s = Stokes velocity for particle with diameter d_p and density ρ_p (m/d)

g = acceleration of gravity = 981 cm/s²

μ = absolute viscosity of water = 0.01(g/cm³-s) at 20 °C

ρ_p = density of the solid (g/cm³)

ρ_w = density of water = 1.0 g/cm³

d_p = particle diameter (mm)

Benthic exchange of sediment and particulate chemicals is driven by the net scour and deposition velocities. WASP calculates benthic exchange as:

$$W_{BS} = A_{ij}(w_R S_i - w_D S_j) \quad (3.8)$$

where: W_{BS} = net sediment flux rate (g/d)

S = sediment concentration (g/m³)

w_D = deposition velocity (m/d). The deposition velocity can be calculated as the product of the Stoke's settling velocity and the probability of deposition: $w_D = V_s \alpha_D$ (α_D is probability of deposition upon contact with the bed).

w_R = scour velocity (m/d)

A_{ij} = benthic surface area (m²)

i = benthic segment

j = water segment

Grain size analyses of suspended particles were not completed in this project, so it was assumed that the majority of the particles correspond to the size range for silt (0.0039-0.0625 mm). Thus, settling velocities should be within the range 0.716 and 183.9 m/day. Settling velocities were used as a calibration parameter for the various models.

There are no sediment studies in the HSC that allow determination of scour rates. These rates were initially assumed to be two orders of magnitude lower than the settling rates and adjusted during calibration. It is noted that there are no special process descriptions for solids transport in WASP7. Scour rates, for example, are not programmed as a function of water column shear stress. Consequently, the TOXI sediment model is considered descriptive and must be calibrated to site data (Ambrose et al., 1993). Because WASP does not simulate partitioning between the benthic segments and the water layer, fluxes of dioxins from the sediments

(especially at the hot spots in segments 1006 and 1001) were modeled using scour rates as a calibration parameter.

3.2.6 Pore Water Diffusion

A pore water diffusion velocity of 1×10^{-4} m/s was applied to predict vertical diffusive exchange between the pore water and the water column throughout each segment.

Parameters and Constants

The only constant input to the models corresponds to the logarithm of the dissolved-suspended partitioning coefficients (K_p), which were estimated to be 5.38 for 2378-TCDD, 5.41 for 12378-PeCDD, 5.49 for 123678-HxCDD, 5.31 for 2378-TCDF, 5.32 for 23478-PeCDF, and 5.27 for 123678-HxCDF. Transformation processes (biodegradation, photolysis, and volatilization) were assumed negligible due to the persistent nature of dioxins and the very low rate values reported in the literature.

3.3 SPIN-UP TIME DETERMINATION

The spin-up time of the HSC WASP model was determined by inputting a smooth sinusoidal repetitive salinity condition signal at the downstream boundary together with constant salinity concentrations for the inflows at the upstream boundaries. Figure 3.3 presents the results from the run for the two control locations used to determine the spin-up time for the RMA model. As can be seen, the model requires about 20 days to reach a repetitive salinity concentrations at Morgan's Point. Therefore, a three-week period was added at the beginning of the WASP runs for calibration and long-term simulations.

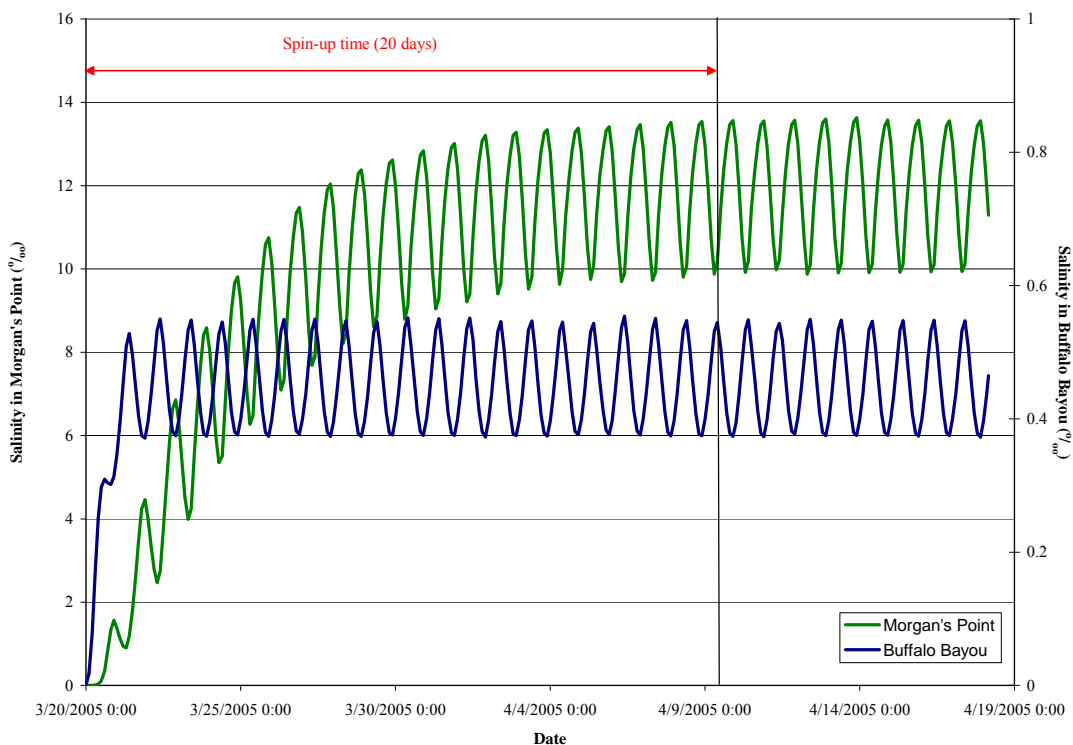


Figure 3.3 Determination of Spin-up Time for the WASP Model

3.4 SALINITY MODEL

Prior to calibrating the dioxin model, a salinity model was run to determine the longitudinal dispersive mixing and exchange coefficients. The WASP longitudinal dispersion formulation is based on the cross-sectional area between adjacent reaches and a characteristic mixing length, taken to be the distance between midpoints of the adjacent reaches. The model was calibrated to the salinity data collected during flow measurement activities in April 2005. The salinity model was run using the TOXI module without benthic segments. It is noted that WASP is a depth- averaged model, however, the salinity concentrations measured in 2005 correspond to a single depth and do not represent the whole depth of each segment. Thus, the goal was to match patterns and ranges rather than absolute values. Salinity series collected by TCOON at Eagle Point were input at the downstream boundaries to simulate the salt exchange

with Galveston Bay. Boundary concentrations for freshwater inflows were assumed equal to 0.2 percent . Initial concentrations for the various WASP segments were calculated as the average salinity concentrations measured in 2005. Figure 3.4 illustrates the locations at which salinity was calibrated. Calibrated longitudinal dispersion coefficients for surface waters ranged from 10 to 250 m²/s. Figure 3.5 shows time-series of observed and modeled salinity concentrations and Table 3.9 summarizes two statistical error measures calculated for salinity runs. It can be seen that the modeled values simulate the salinity patterns observed at most locations with the exception of Vince Bayou. Field data at Brays Bayou show a sudden increase in salinity that could not be reproduced by the model; that peak may have been the result of the passing of a large ship that moved a significant amount of saltwater into the bayou or could be the result of a problem with the field probe. Another comment relates to the model results at the SJE. The modeled values reproduce the peaks but not the low concentrations measured in the field.

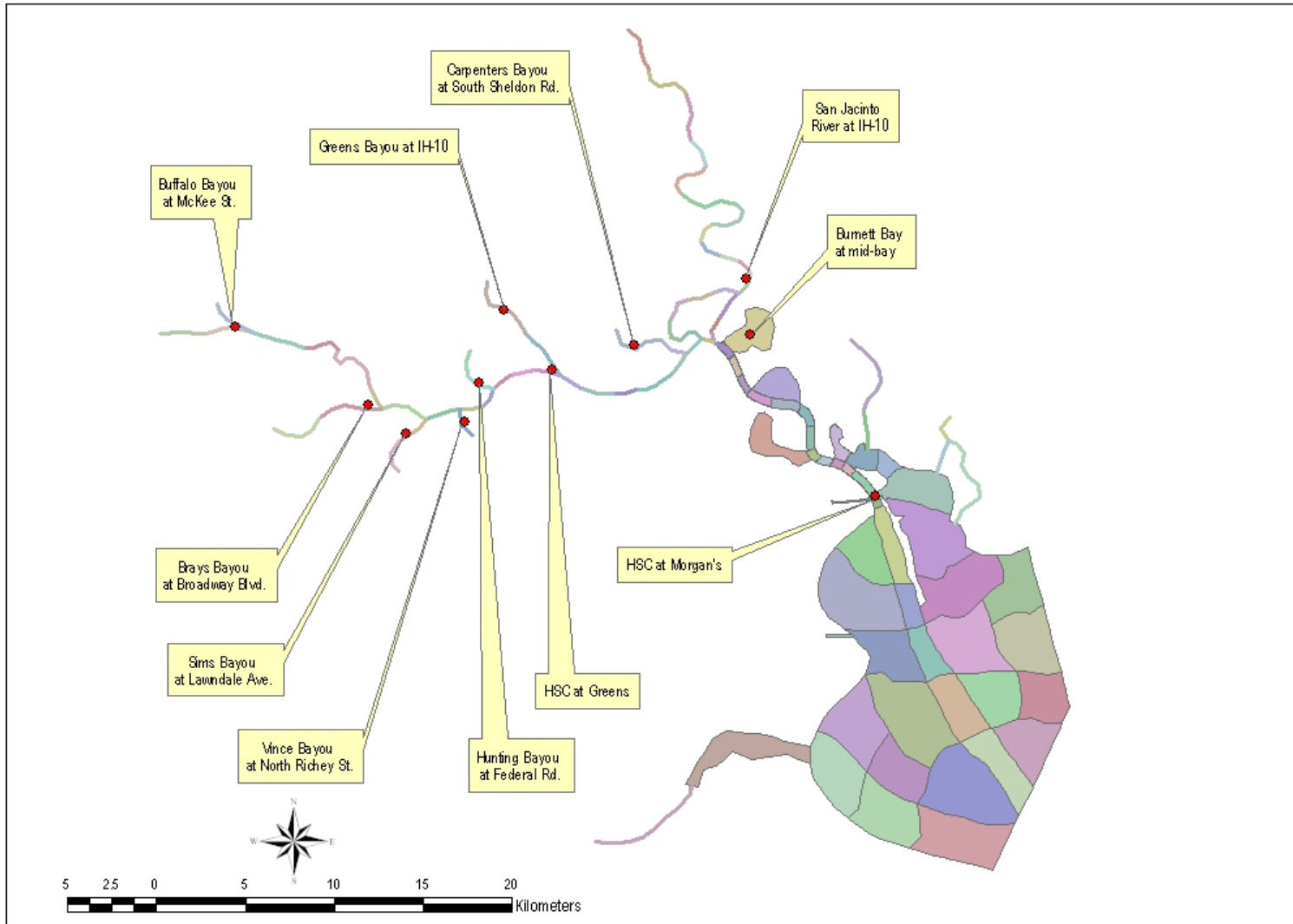


Figure 3.4 Salinity Calibration Locations

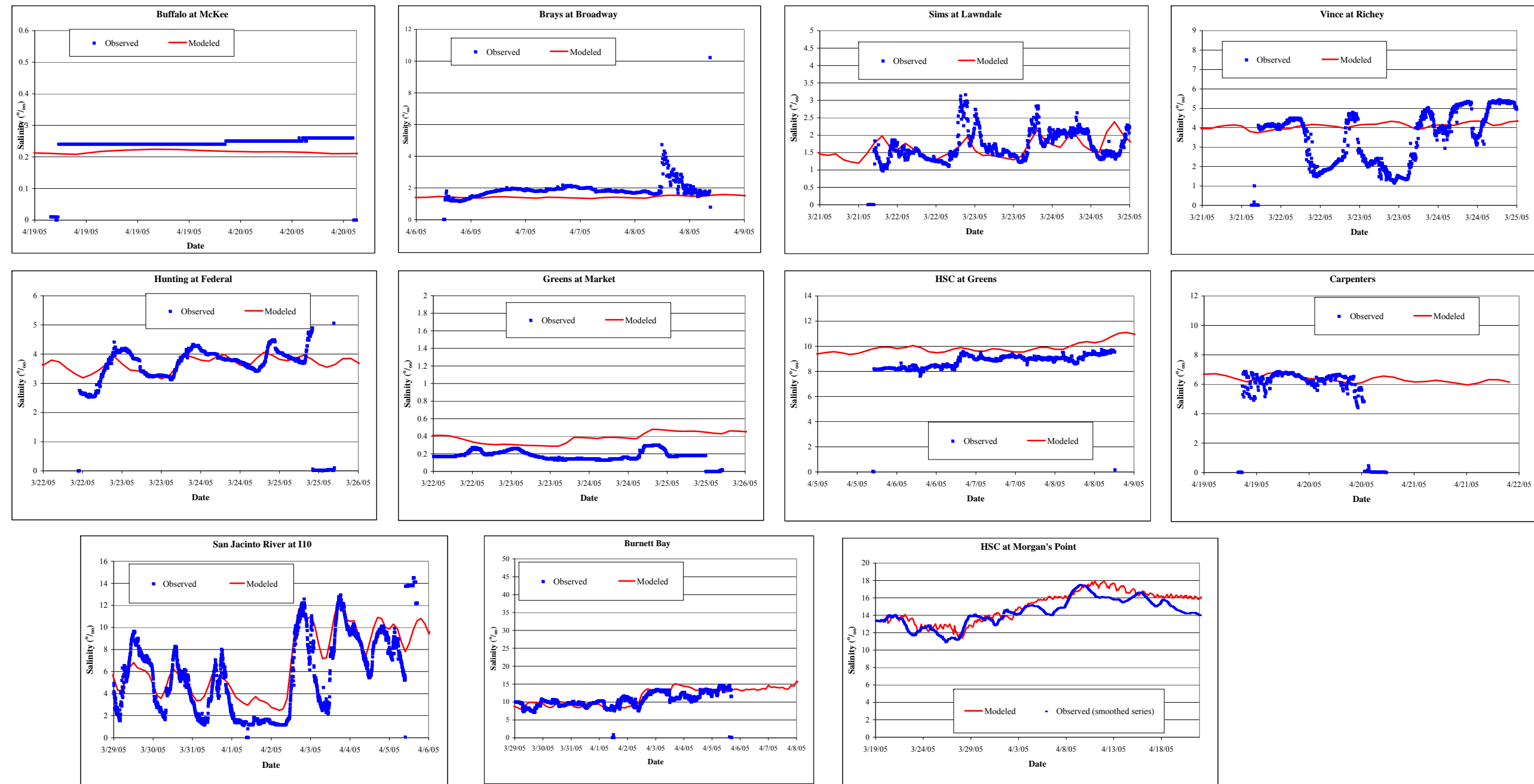


Figure 3.5 Modeled and Measured Salinity Concentrations

Table 3.9 Model Summary Statistics for Salinity

Observation Point	RMSE(‰) ^a	Average Abs. Error^b
Buffalo Bayou	0.01	15%
Brays Bayou	0.09	23%
Sims Bayou	0.03	16%
Vince Bayou	0.10	49%
Hunting Bayou	0.03	7%
Greens Bayou	0.02	40%
HSC@Greens	0.10	13%
Carpenters Bayou	0.06	5%
San Jacinto River	0.11	98%
Burnett Bay	0.09	15%
HSC@Morgan's	0.04	11%

$$^a \text{RMSE} = \frac{\sqrt{\sum_{i=1}^n (P_i - O_i)^2}}{n}$$

$$^b \text{Abserror} = \frac{1}{n} \sum_{i=1}^n \frac{\text{abs}(P_i - O_i)}{O_i}$$

3.5 DIOXIN MODEL CALIBRATION

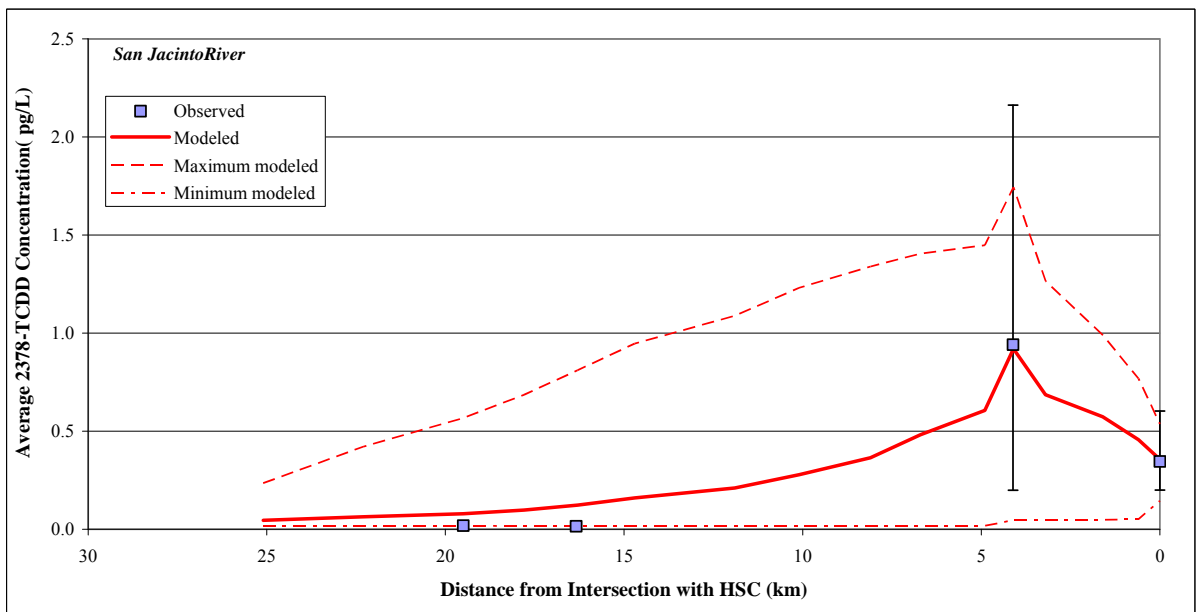
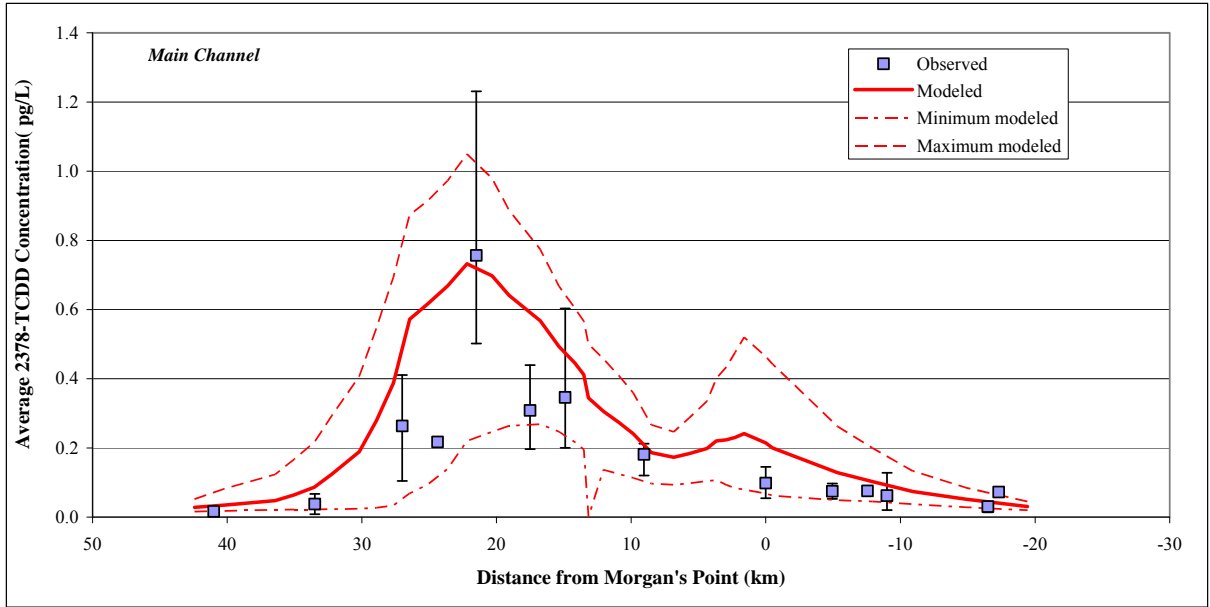
The dioxin models were run using the loads described in section 3.2.3, the pore water dispersion coefficient described in section 3.2.5 (Solid Transport Parameters) and the longitudinal dispersion coefficients calibrated in the salinity model. The goal of the dioxin model calibration was to match the average concentrations for the simulation period to the average concentrations measured in the channel as part of this project. The calibration parameters were those related to the exchange of contaminants between the benthic and the surface water layers (i.e., scour/settling velocities).

An initial calibrated WASP model was presented to the stakeholders during the April 7, 2007 meeting, and it was noted that the modeled 2378-TCDD profile in the main

channel was too “broad” and over-predicted concentrations down stream from the peak in Segment 1006 to the mouth. One possible remedy that was suggested included the use of a higher settling rate to account for the exchange of contaminants between the water column and the benthic segments in locations other than the “hot spots”. Another suggestion was to exclude wet weather concentrations when comparing modeled and measured concentrations because all measured concentrations were dry weather data. A third suggestion included looking at median values from the model as opposed to average concentrations for the modeling period. Therefore, the WASP model for 2378-TCDD was re-calibrated and models for the remaining congeners were developed and calibrated using higher settling rates to account for the exchange of contaminants between the water column and the benthic segments.

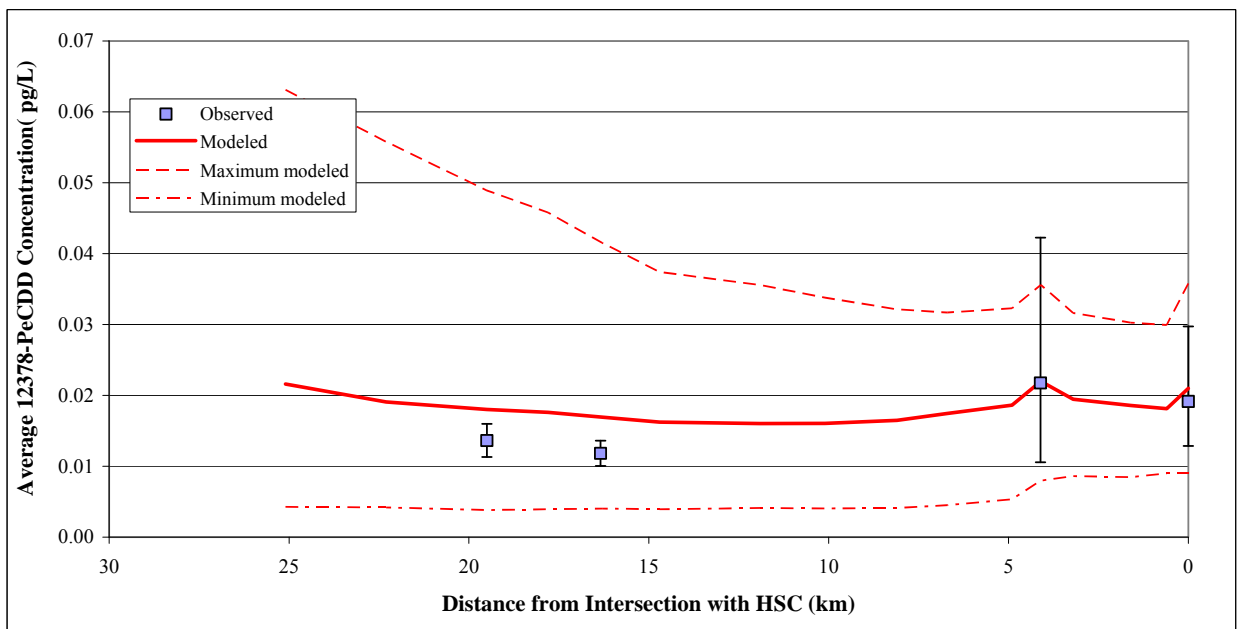
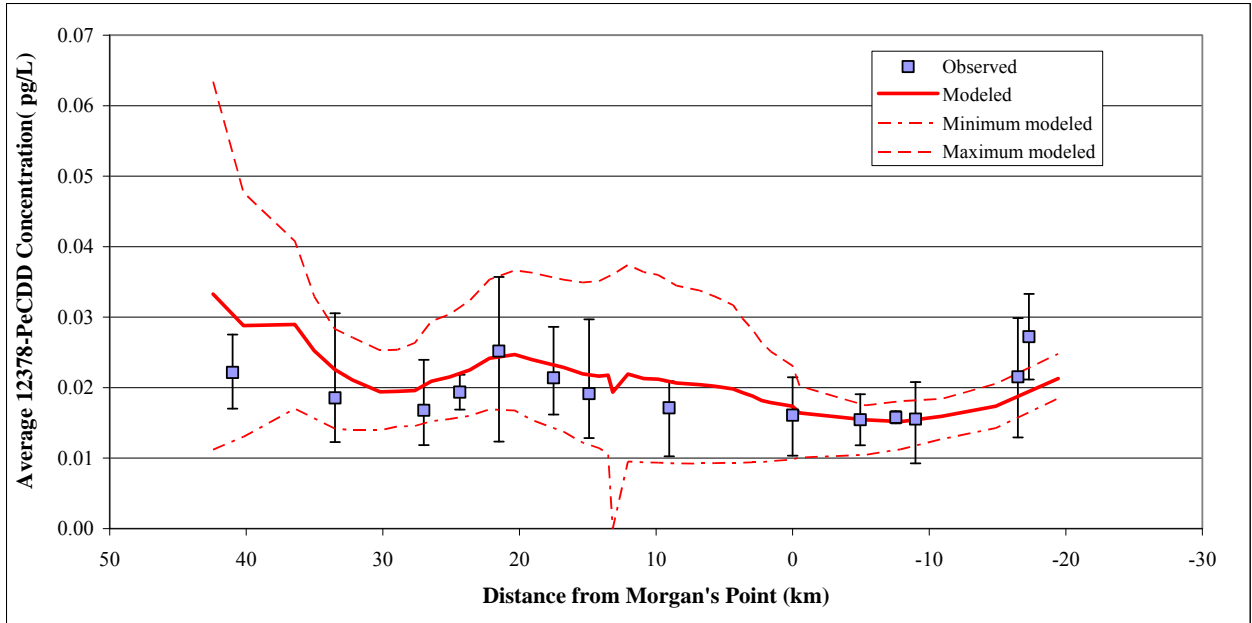
Average measured concentrations were compared to the average concentrations predicted by the model for dry weather only. To separate dry from wet data, rainfall data from HCOEM (used as input to RMA2) were used. If the total rainfall for a given day was greater or equal than 0.1 inches, the day was considered a wet day, otherwise it was considered a dry day. The datasets were also divided based on flow instead of rainfall but the results were similar.

Longitudinal plots of the measured and modeled concentrations for dry days for the calibrated models are shown in Figures 3.6a-f and 3.7a-f. The data shown in Figures 3.6 are all averages, whereas the data shown in Figures 3.7 are median



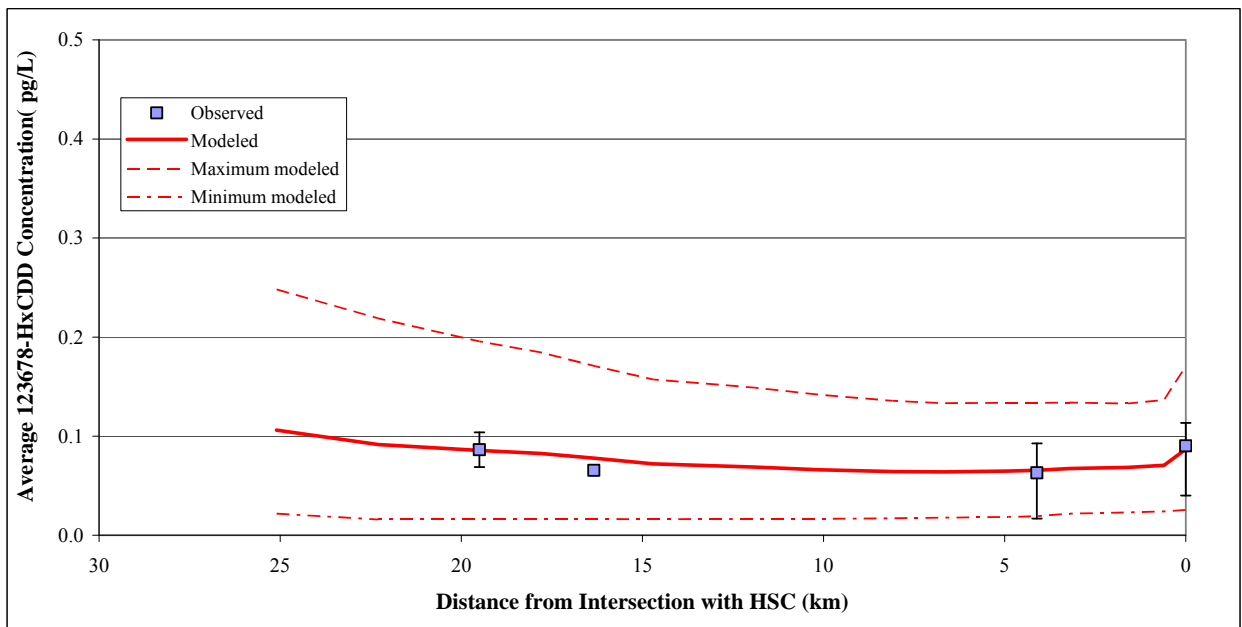
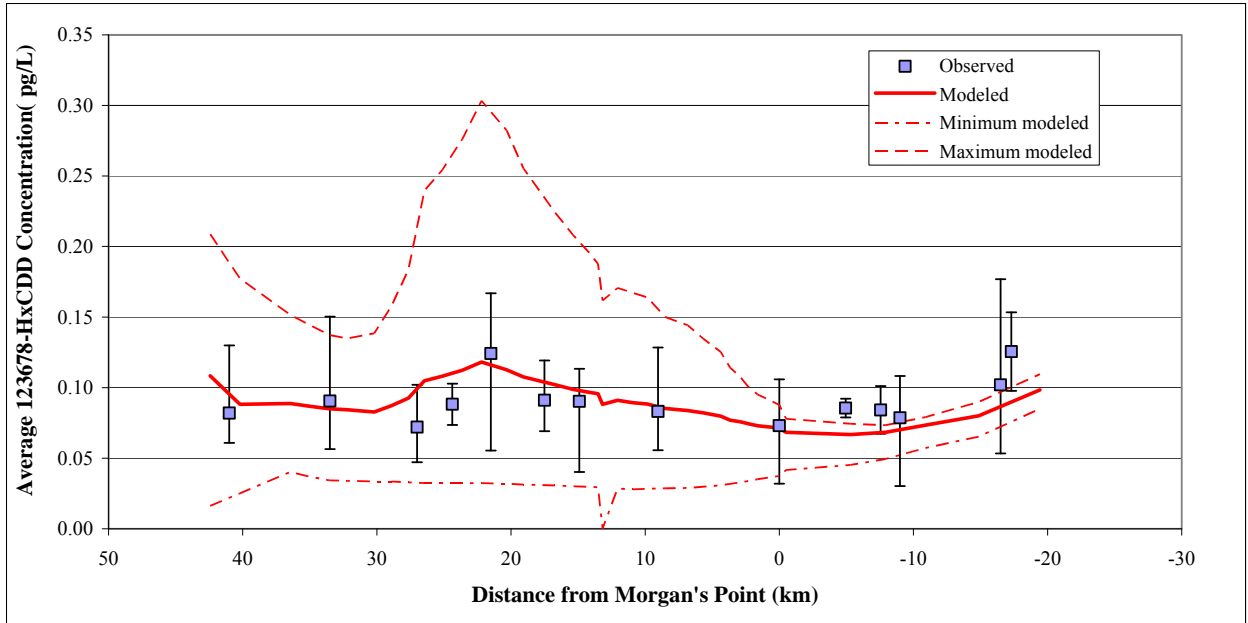
Error bars denote the range of measured concentrations
 Maximum and minimum lines represent the single time-step max and min concentrations during dry days at each model segment

Figure 3.6a Modeled and Observed 2378-TCDD Concentrations (Averages)



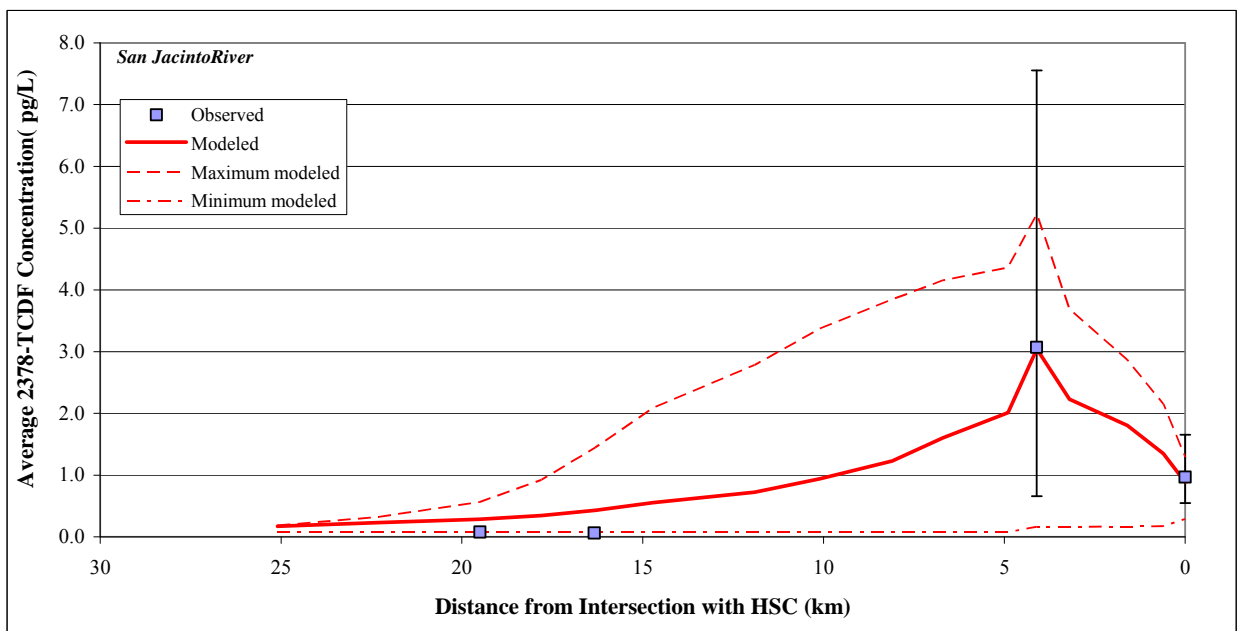
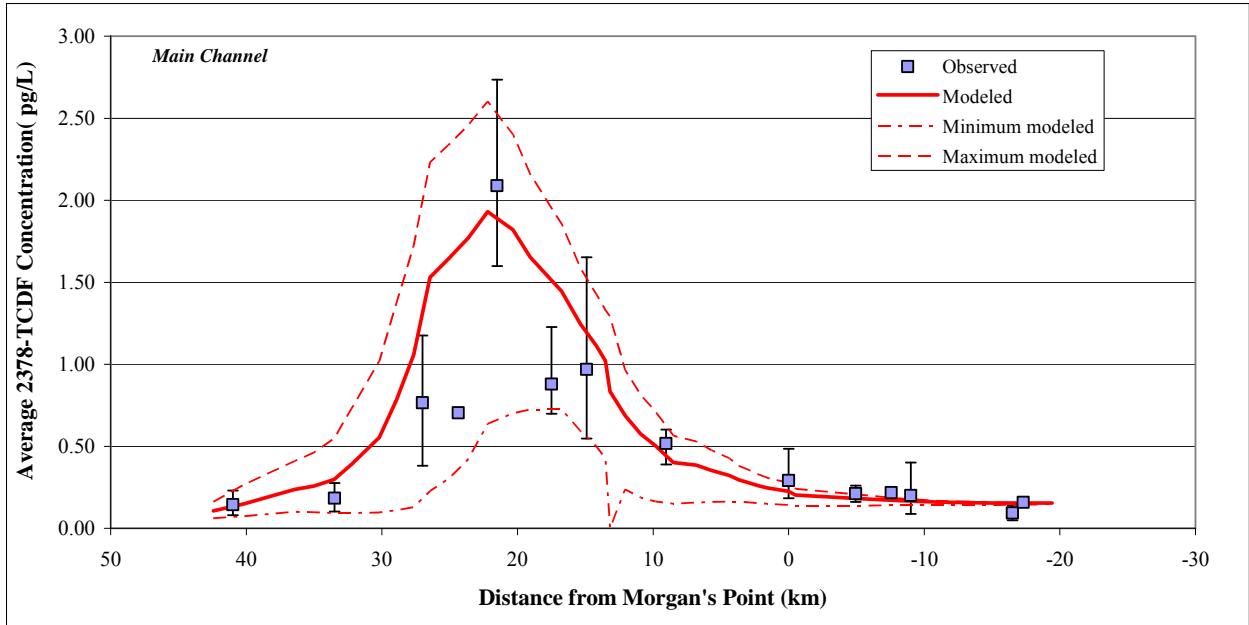
Error bars denote the range of measured concentrations
 Maximum and minimum lines represent the single time-step max and min concentrations during dry days at each model segment

Figure 3.6b Modeled and Observed 12378-PeCDD Concentrations (Averages)



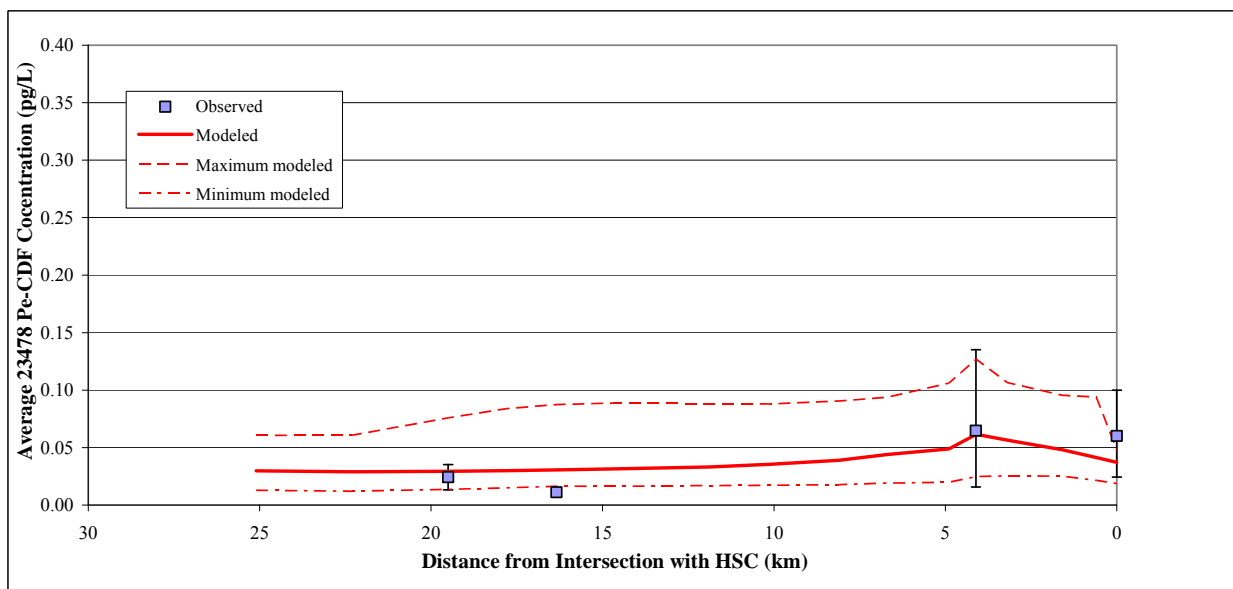
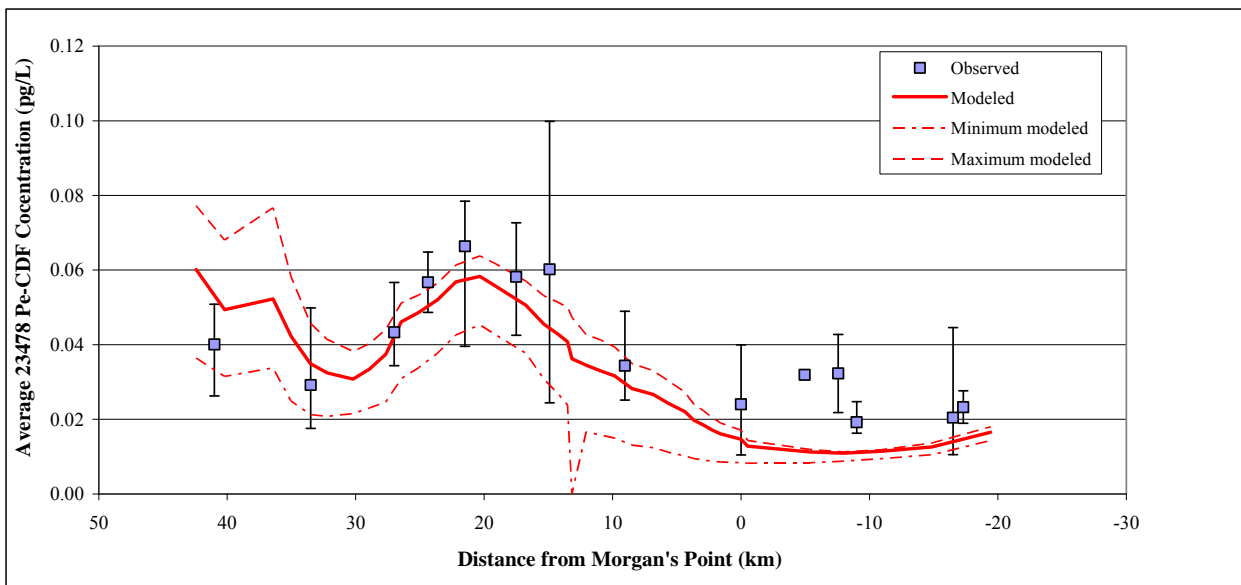
Error bars denote the range of measured concentrations
 Maximum and minimum lines represent the single time-step max and min concentrations during dry days at each model segment

Figure 3.6c Modeled and Observed 123678-HxCDD Concentrations (Averages)



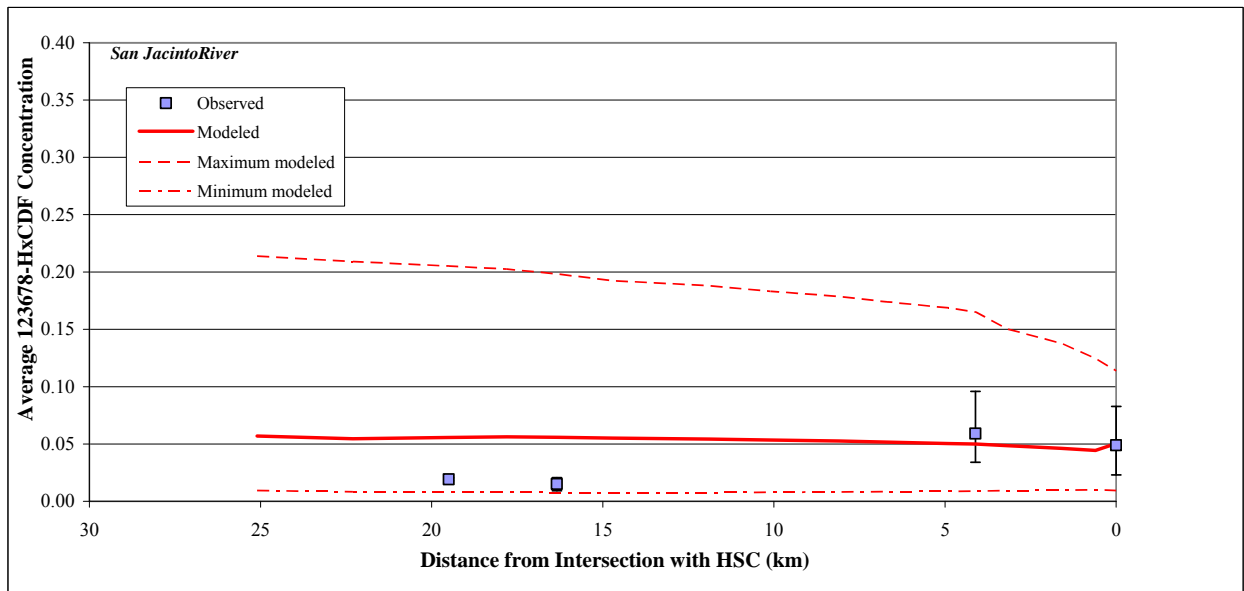
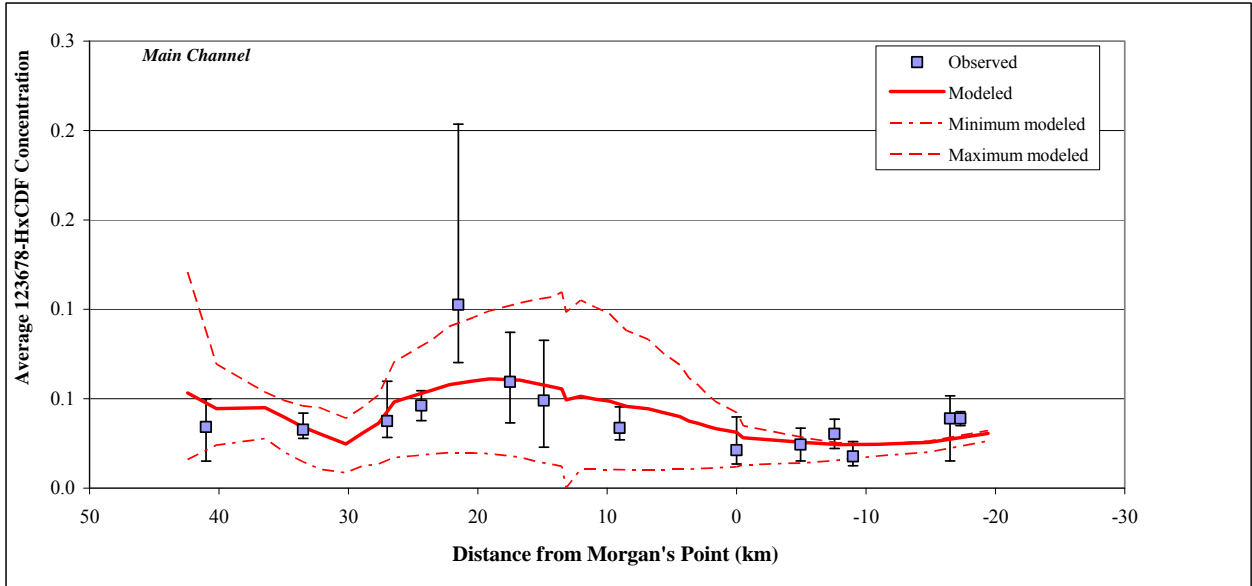
Error bars denote the range of measured concentrations
 Maximum and minimum lines represent the single time-step max and min concentrations during dry days at each model segment

Figure 3.6d Modeled and Observed 2378-TCDF Concentrations (Averages)



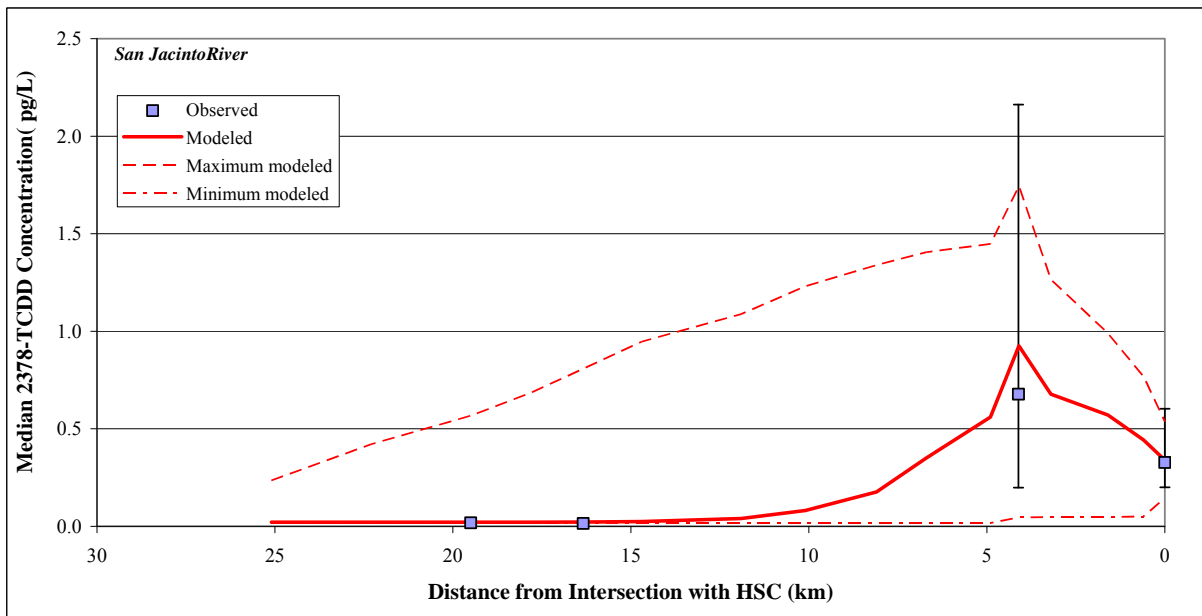
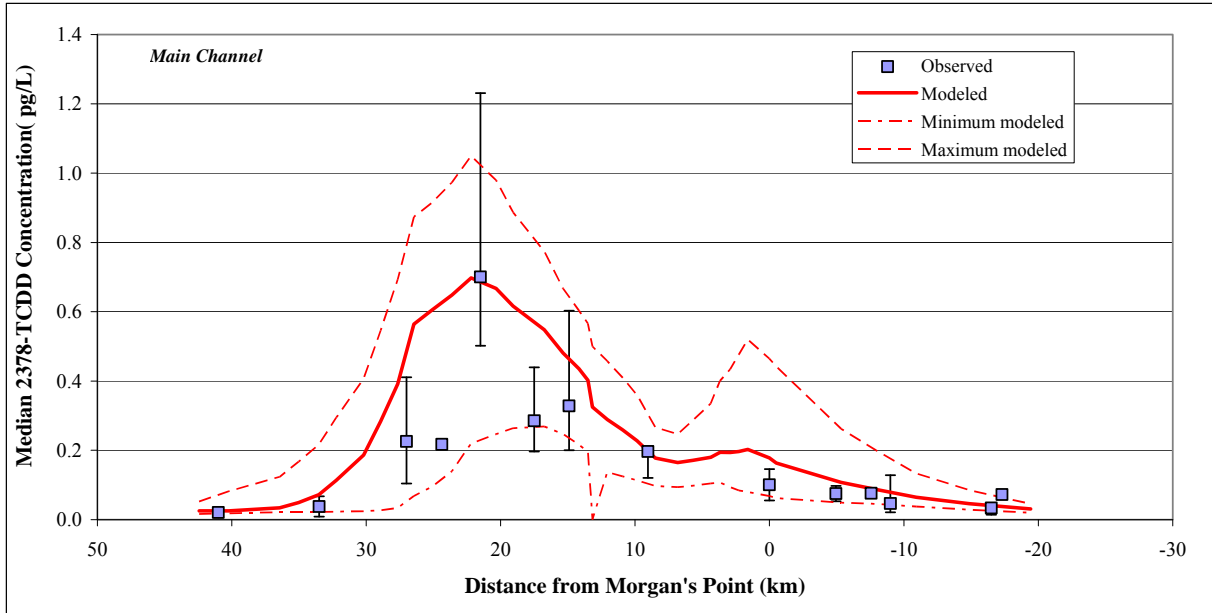
Error bars denote the range of measured concentrations
 Maximum and minimum lines represent the single time-step max and min concentrations during dry days at each model segment

Figure 3.6e Modeled and Observed 23478-PeCDF Concentrations (Averages)



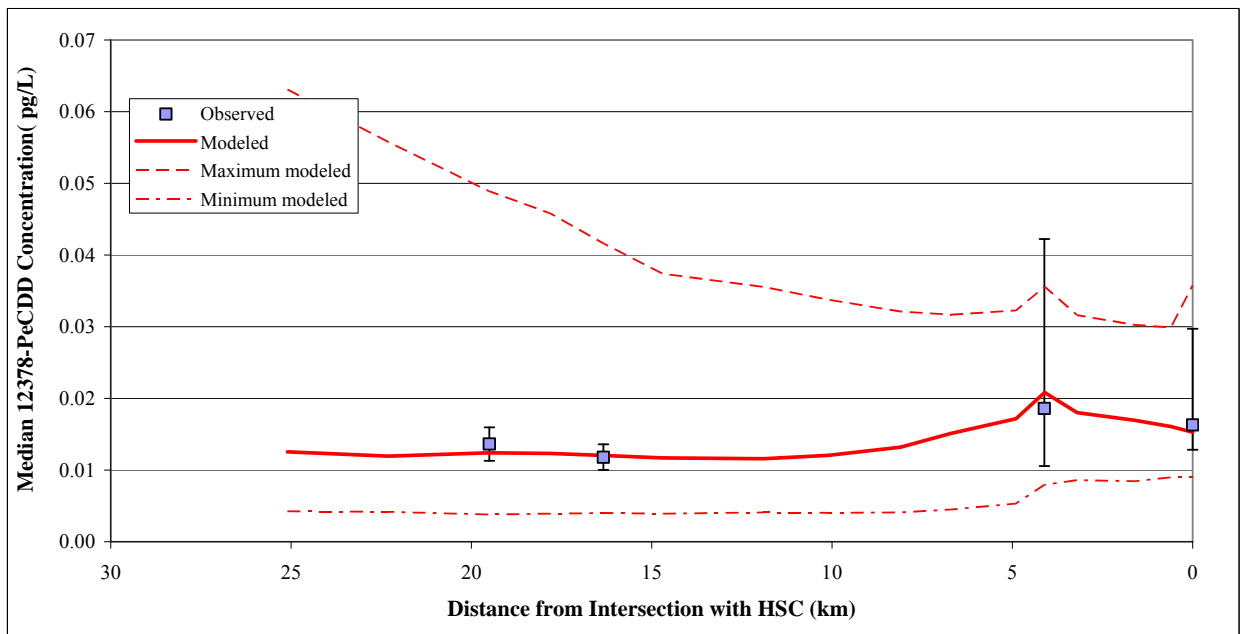
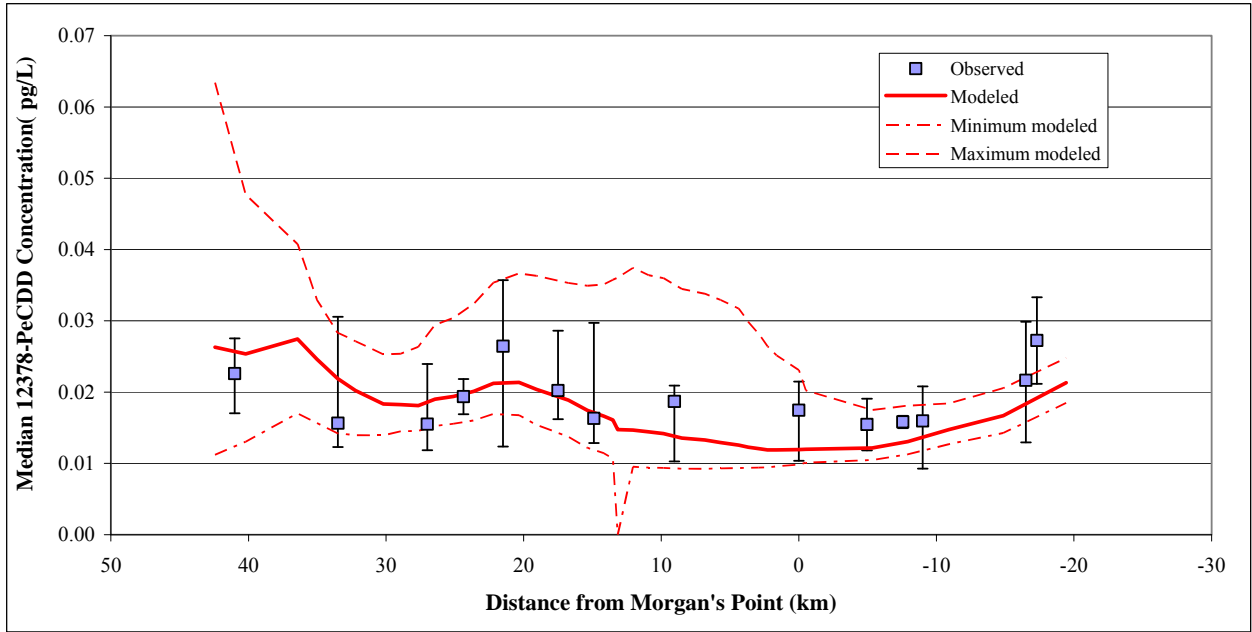
Error bars denote the range of measured concentrations
 Maximum and minimum lines represent the single time-step max and min concentrations during dry days at each model segment

Figure 3.6f Modeled and Observed 123678-HxCDF Concentrations (Averages)



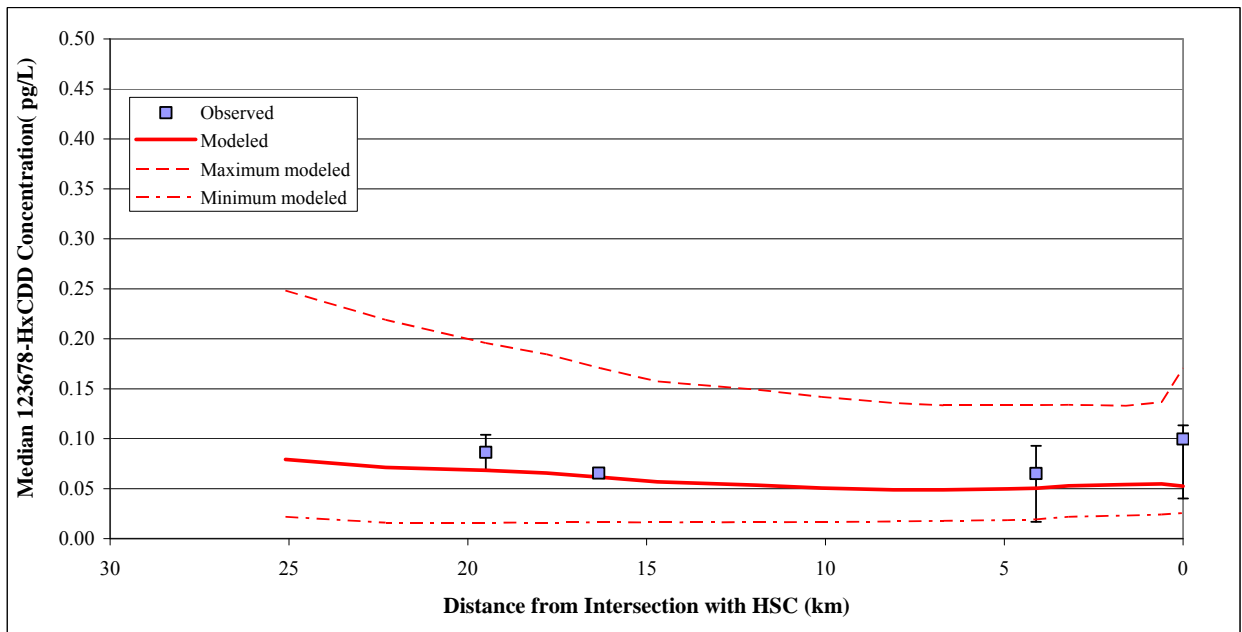
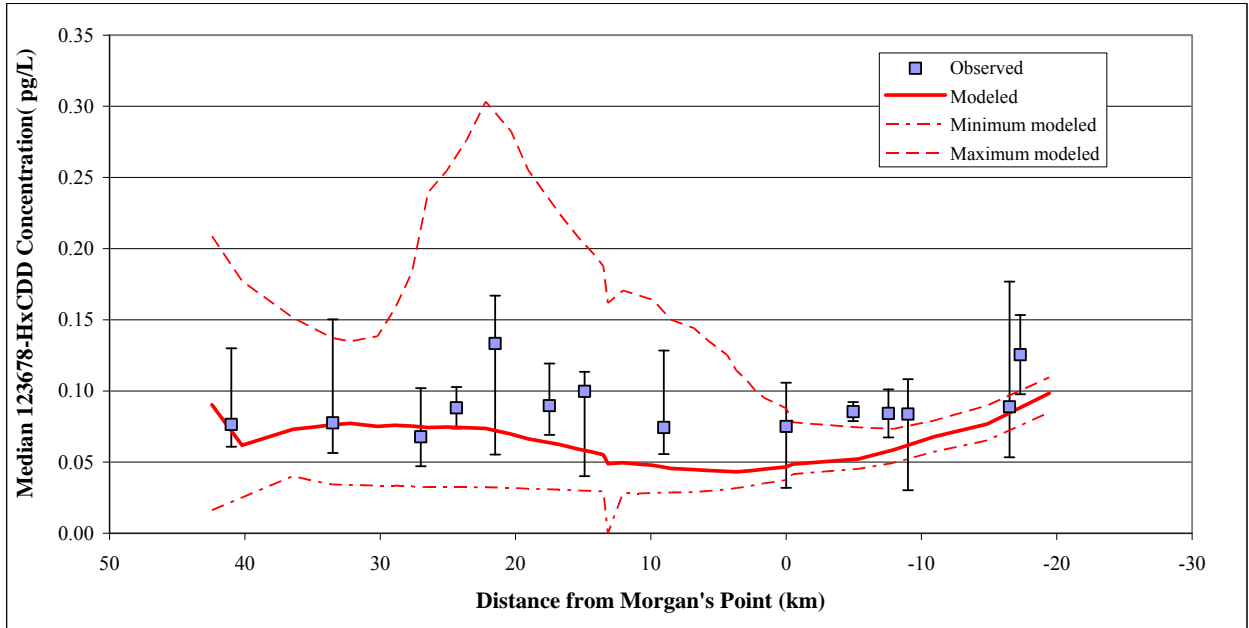
Error bars denote the range of measured concentrations
 Maximum and minimum lines represent the single time-step max and min concentrations during dry days at each model segment

Figure 3.7a Modeled and Observed 2378-TCDD Concentrations (Medians)



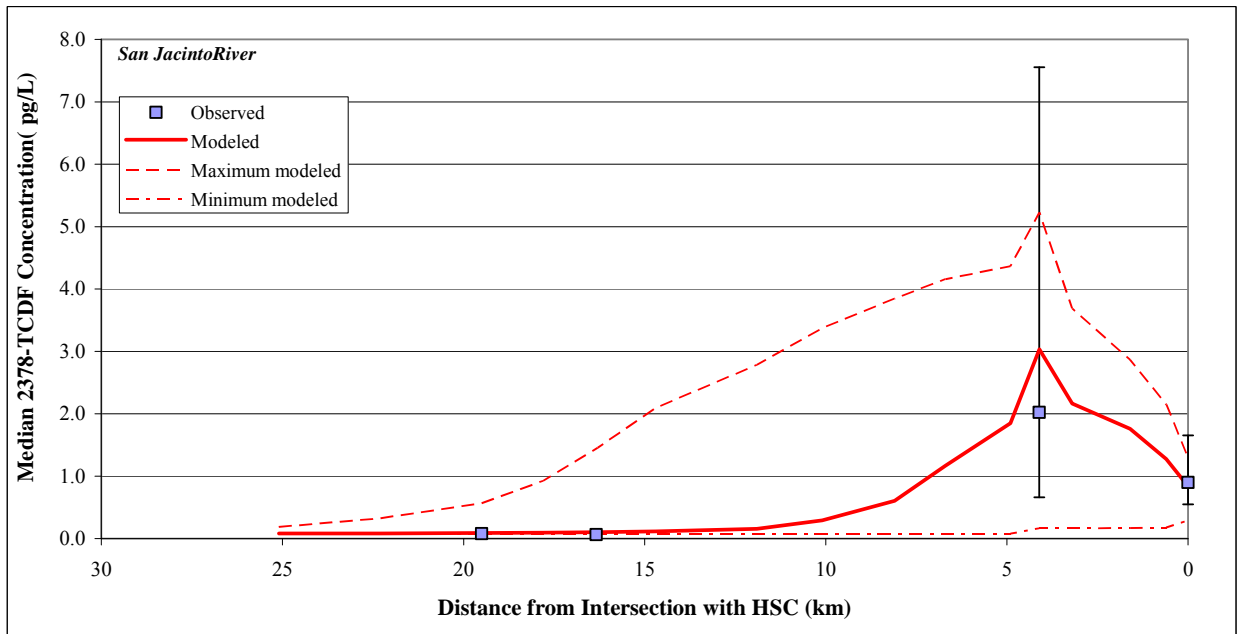
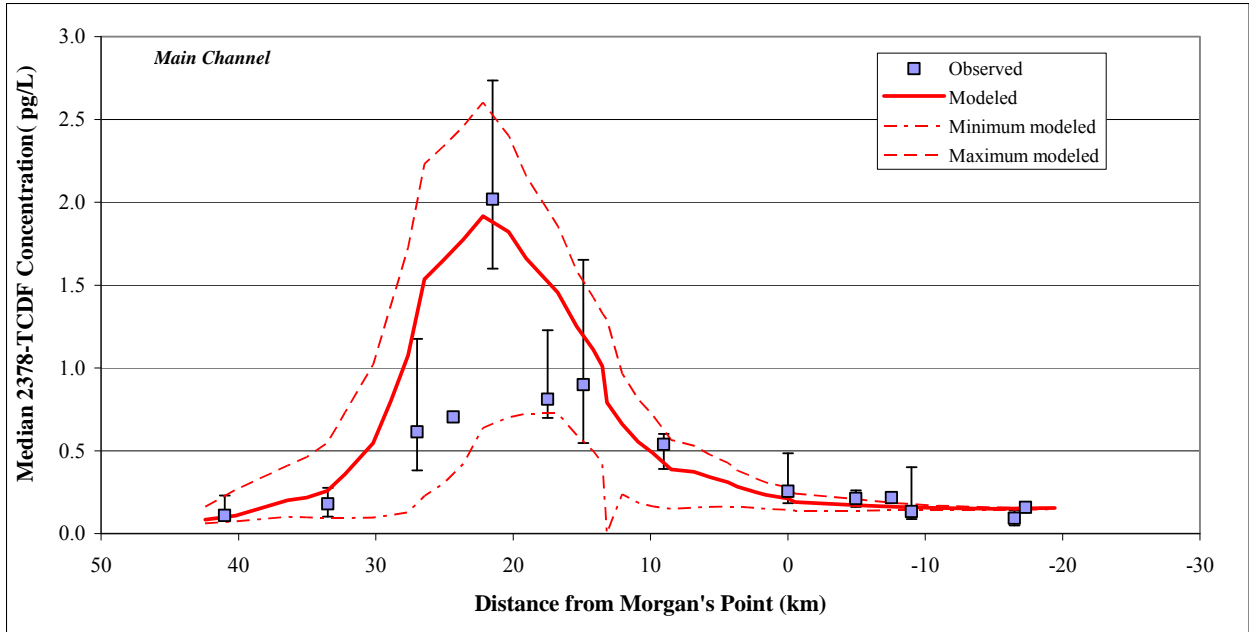
Error bars denote the range of measured concentrations
 Maximum and minimum lines represent the single time-step max and min concentrations during dry days at each model segment

Figure 3.7b Modeled and Observed 12378-PeCDD Concentrations (Medians)



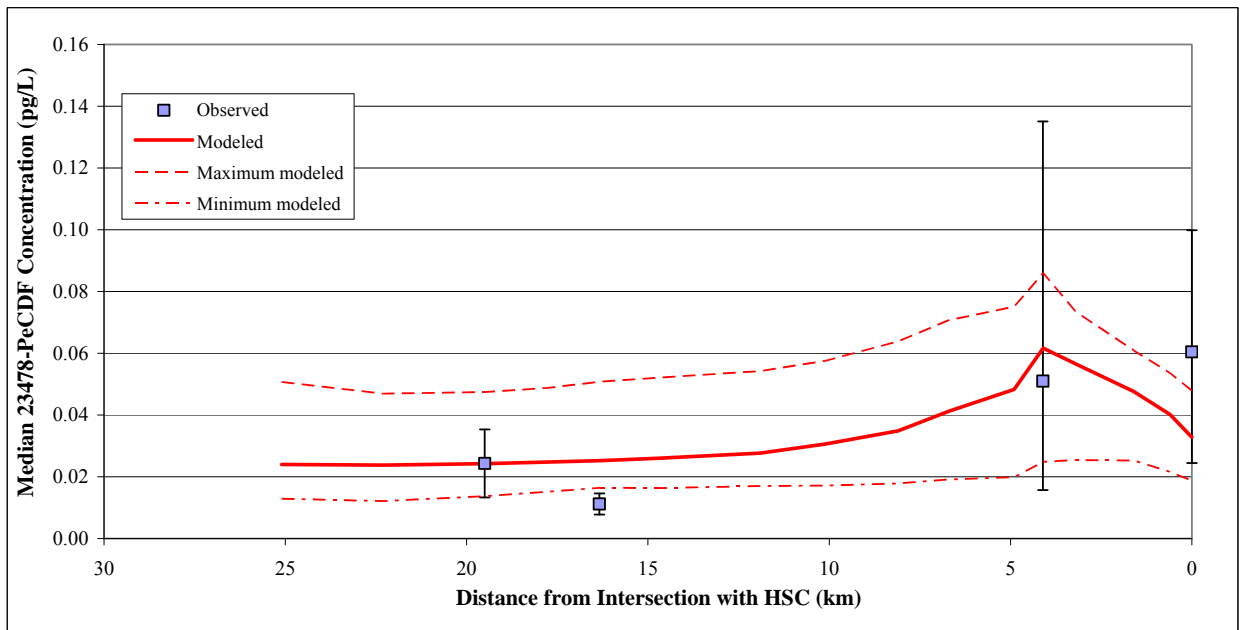
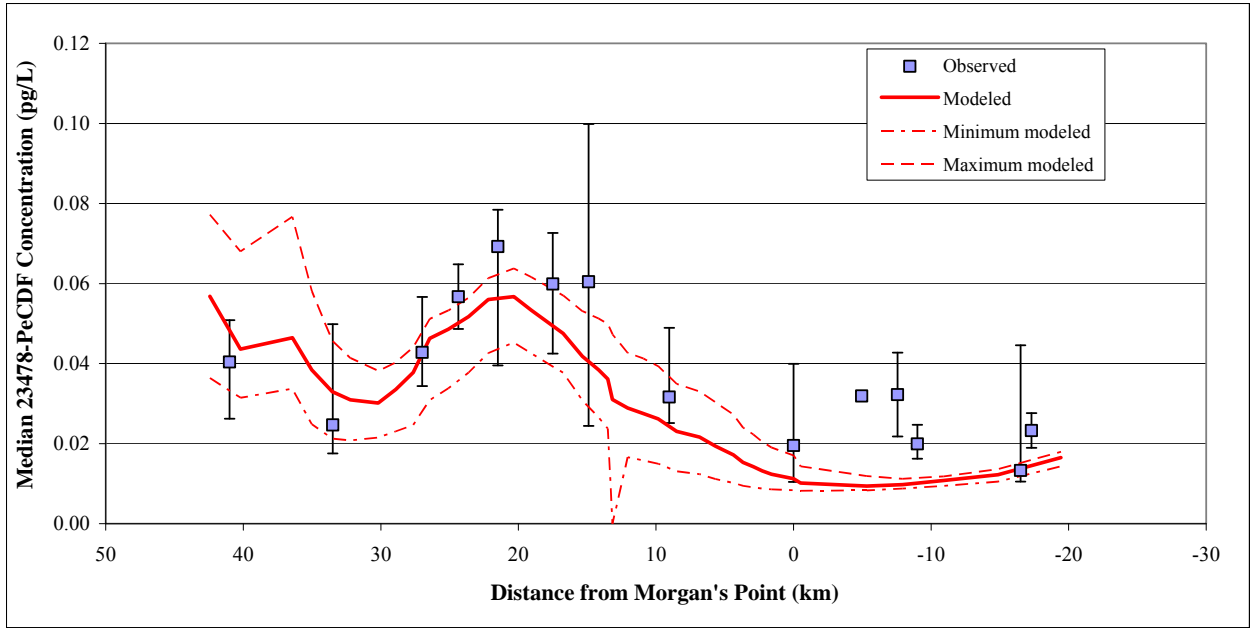
Error bars denote the range of measured concentrations
 Maximum and minimum lines represent the single time-step max and min concentrations during dry days at each model segment

Figure 3.7c Modeled and Observed 123678-HxCDD Concentrations (Medians)



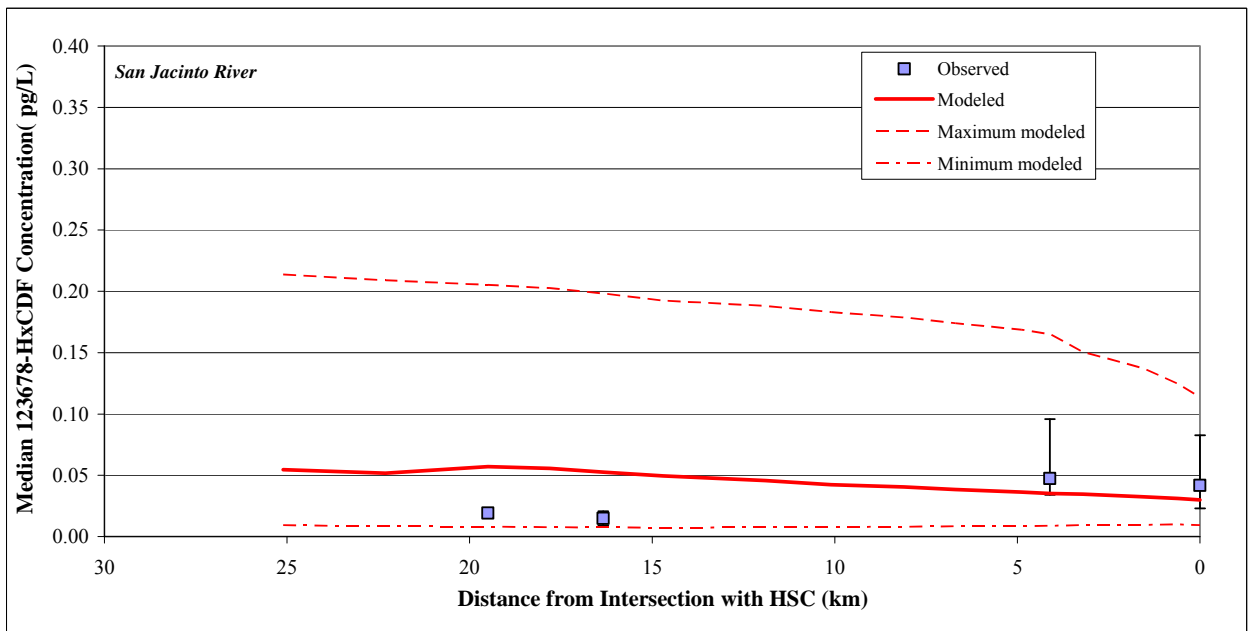
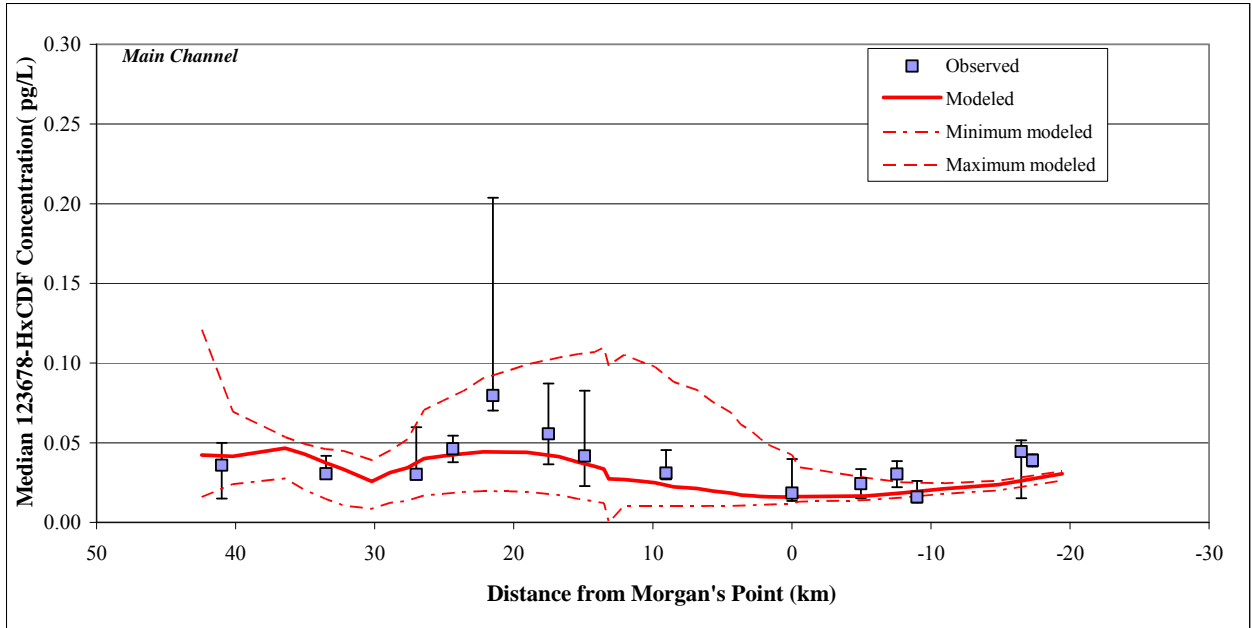
Error bars denote the range of measured concentrations
 Maximum and minimum lines represent the single time-step max and min concentrations during dry days at each model segment

Figure 3.7d Modeled and Observed 2378-TCDF Concentrations (Medians)



Error bars denote the range of measured concentrations
 Maximum and minimum lines represent the single time-step max and min concentrations during dry days at each model segment

Figure 3.7e Modeled and Observed 23478-PeCDF Concentrations (Medians)



Error bars denote the range of measured concentrations

Maximum and minimum lines represent the single time-step max and min concentrations during dry days at each model segment

Figure 3.7f Modeled and Observed 123678-HxCDF Concentrations (Medians)

values. In general, the maximum concentrations predicted by the model for the 3-year period were reduced when eliminating data from wet days, while the average concentrations did not change significantly.

To measure model performance, scatterplots of modeled versus observed data were prepared and compared to 1:1 lines for all the observation locations (Figures 3.8a to f). When one-to-one comparisons are made, the model performance is relatively good. However, the modeled concentrations are generally higher than the measured values for 2378-TCDD and 23478-PeCDF, whereas they are lower than their observed counterparts for the remaining congeners. Finally, the statistics described in equations 2.4 through 2.7 were computed to quantify model performance and compare the goodness-of-fit for the main channel and SJR. The summary statistics are presented in Table 3.10 and confirm a reasonable model performance with regards to average concentrations.

Table 3.10 Model Summary Statistics for WASP Models

	Congener	r^a	MEF^b	d^c	$RMSE$ (pg/L)	% $RMSE^d$
Main Channel	2378-TCDD	0.850	0.362	0.868	0.038	18%
	12378-PeCDD	0.680	0.339	0.813	0.001	4%
	123678-HxCDD	0.648	0.416	0.779	0.003	3%
	2378-TCDF	0.863	0.657	0.918	0.084	13%
	23478-PeCDF	0.926	0.547	0.904	0.003	6%
	123678-HxCDF	0.862	0.635	0.841	0.004	8%
San Jacinto River	2378-TCDD	0.952	0.820	0.952	0.080	24%
	12378-PeCDD	0.888	-0.063	0.732	0.002	12%
	123678-HxCDD	0.857	-0.486	0.789	0.007	10%
	2378-TCDF	0.980	0.892	0.971	0.202	19%
	23478-PeCDF	0.998	0.962	0.989	0.037	11%
	123678-HxCDF	0.998	0.962	0.989	0.037	11%

^a A value close to 1 indicates a good match

^b A value near 1 indicates a close match, a value near zero indicates that the model predicts individual observations no better than the average of observations, a negative value indicates that the observation average would be a better predictor than the model results (Stow *et al.*, 2003)

- c Higher values indicate higher agreement between the model and observations
- d Relative to the measured average concentration

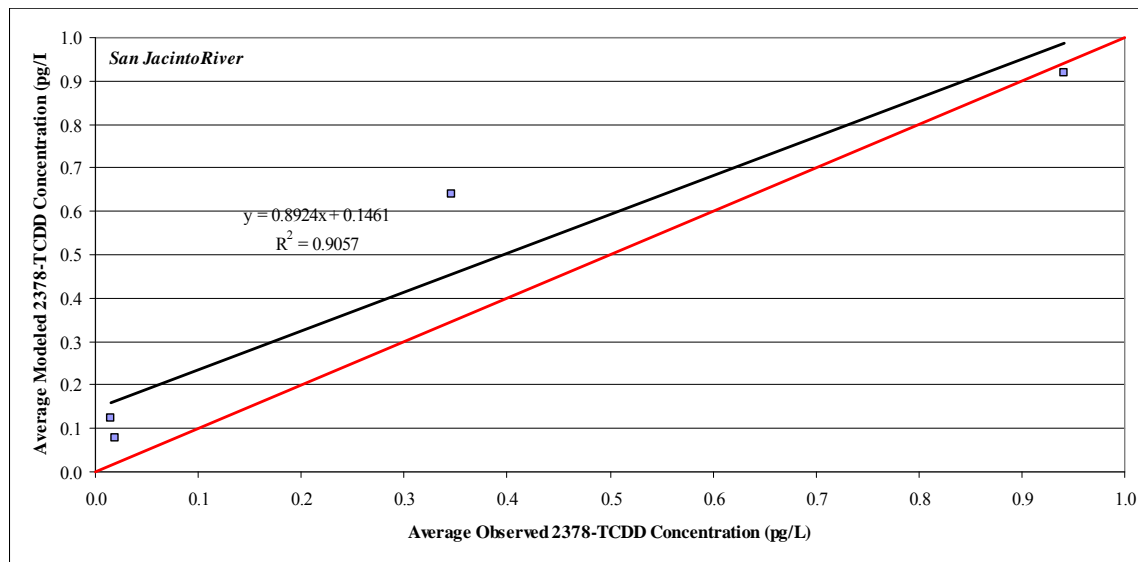
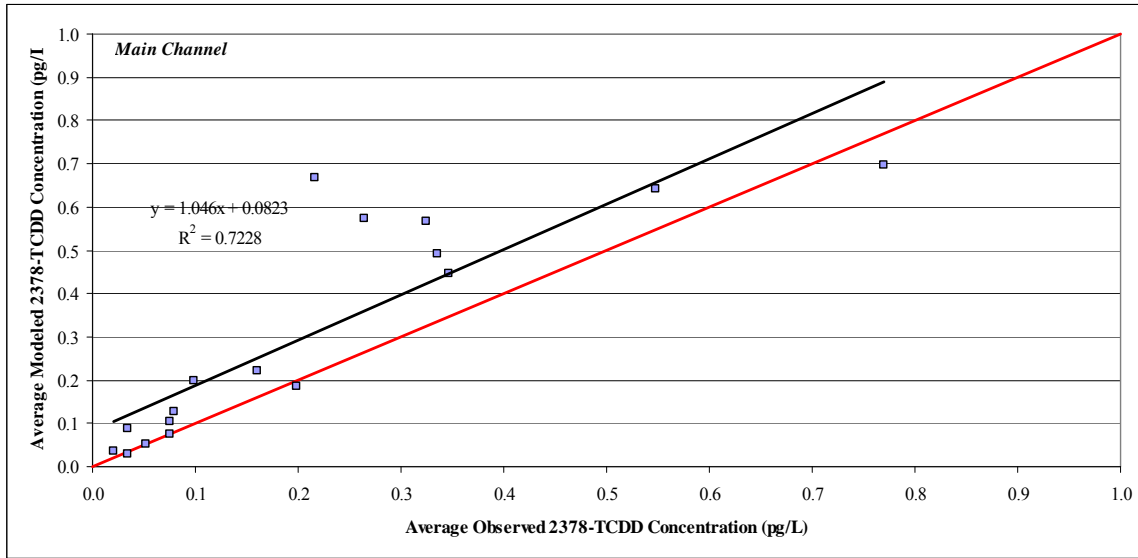


Figure 3.8a Observed versus Modeled Average 2378-TCDD Concentrations

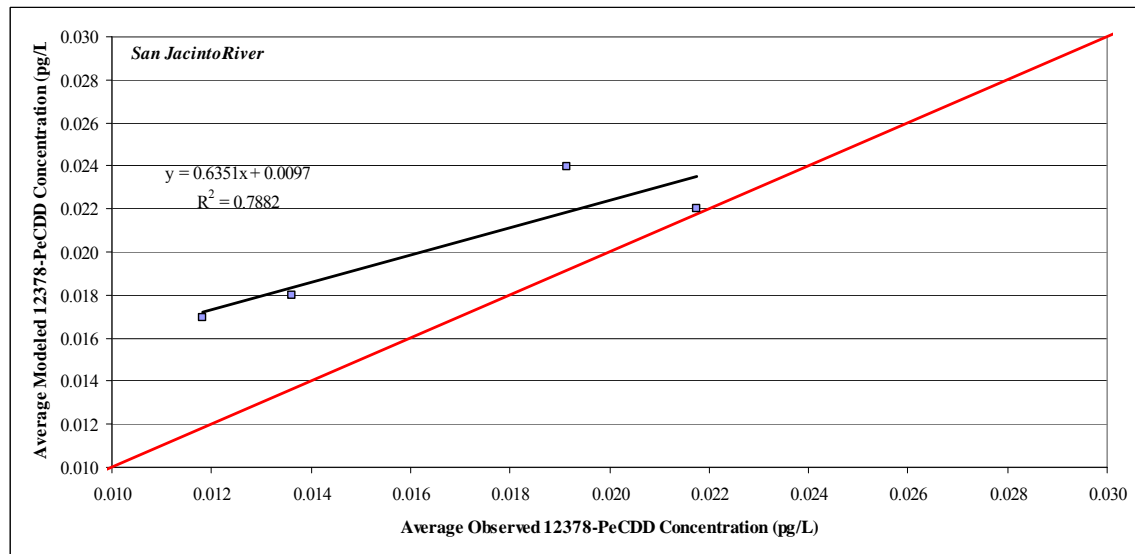
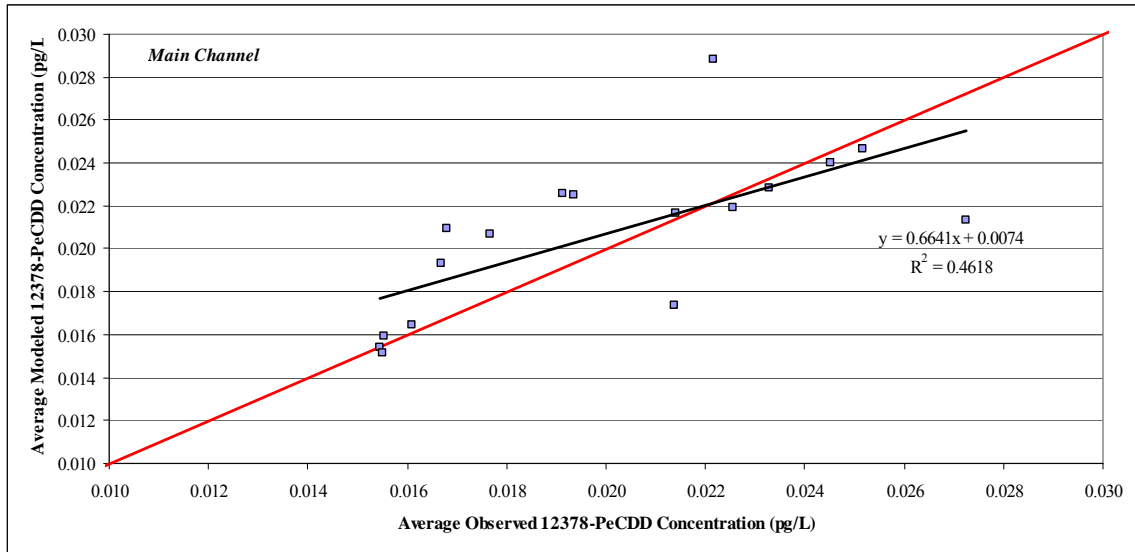


Figure 3.8b Observed versus Modeled Average 12378-PeCDD Concentrations

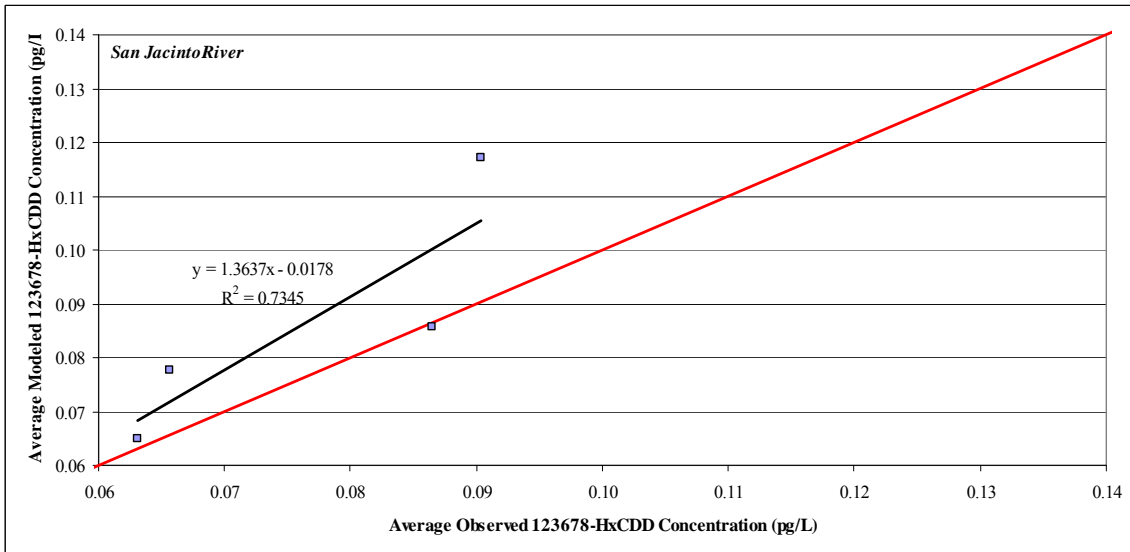
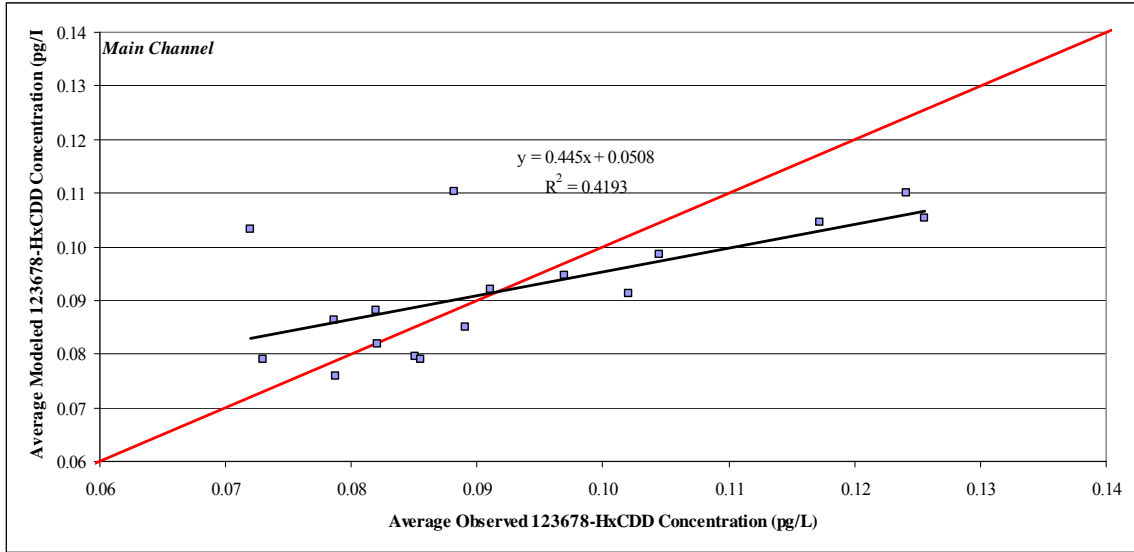


Figure 3.8c Observed versus Modeled Average 123678-HxCDD Concentrations

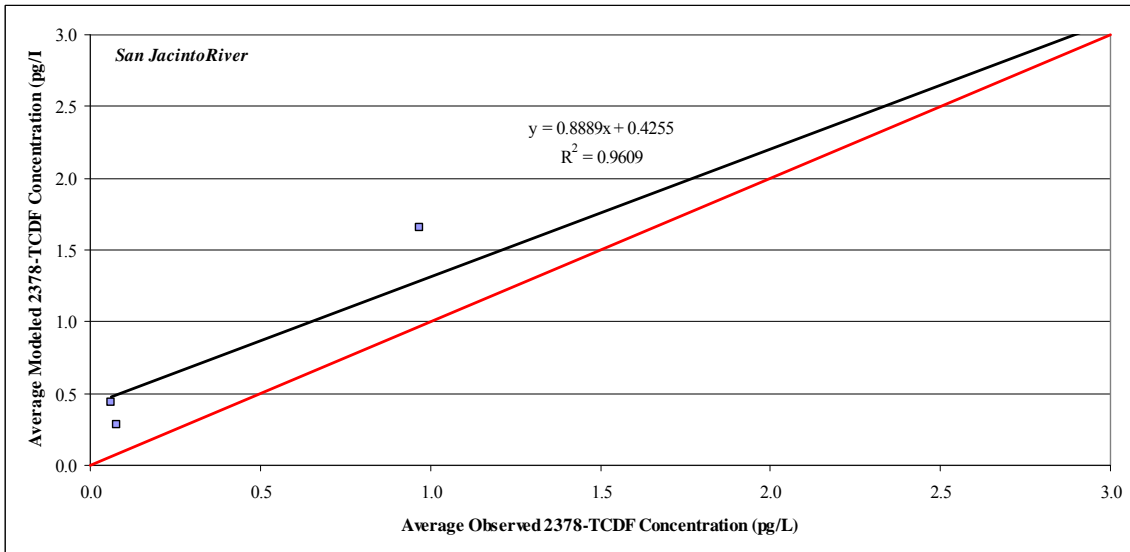
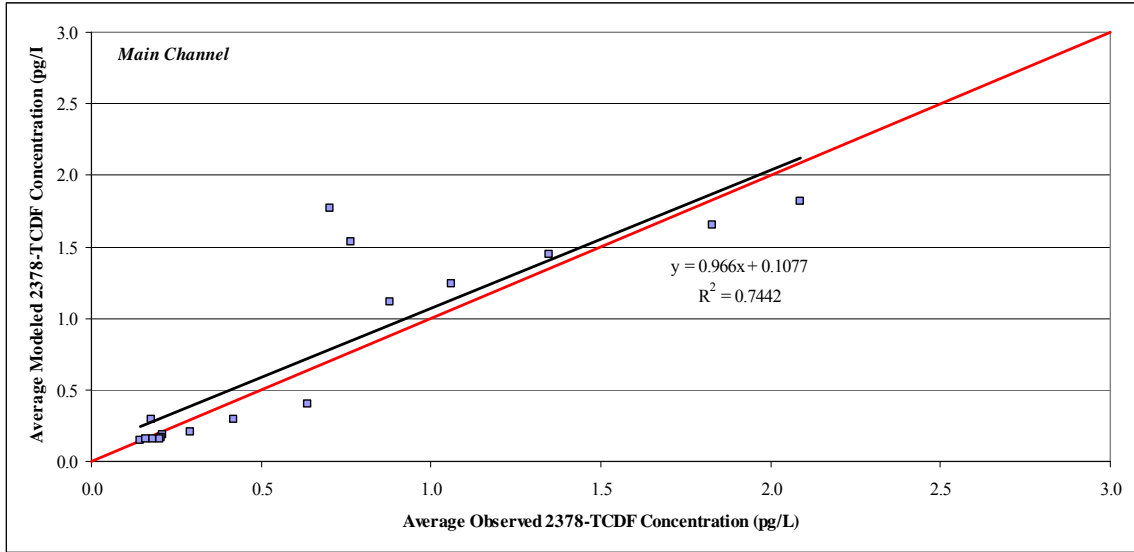


Figure 3.8d Observed versus Modeled Average 2378-TCDF Concentrations

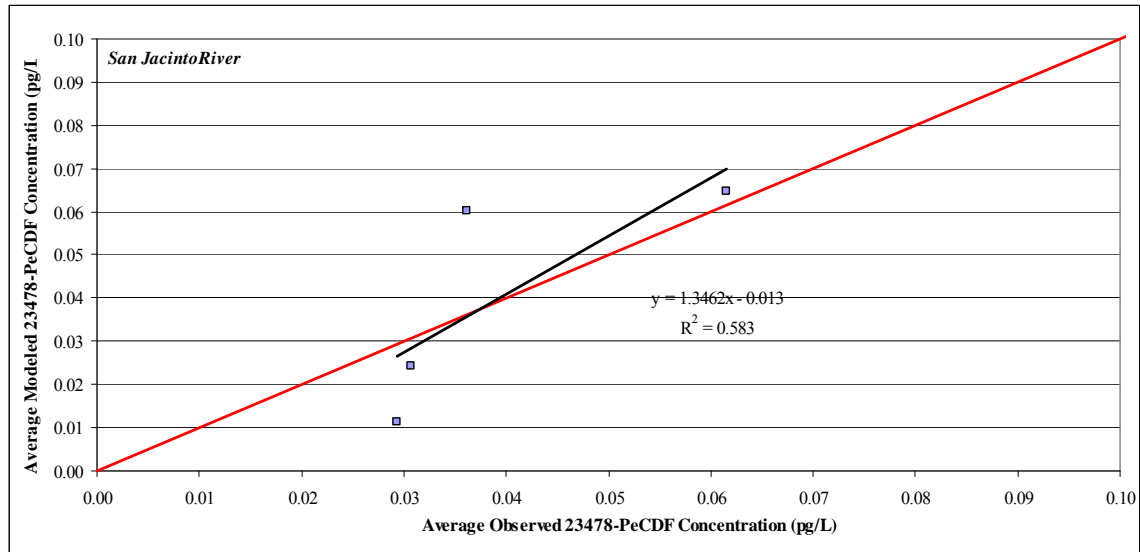
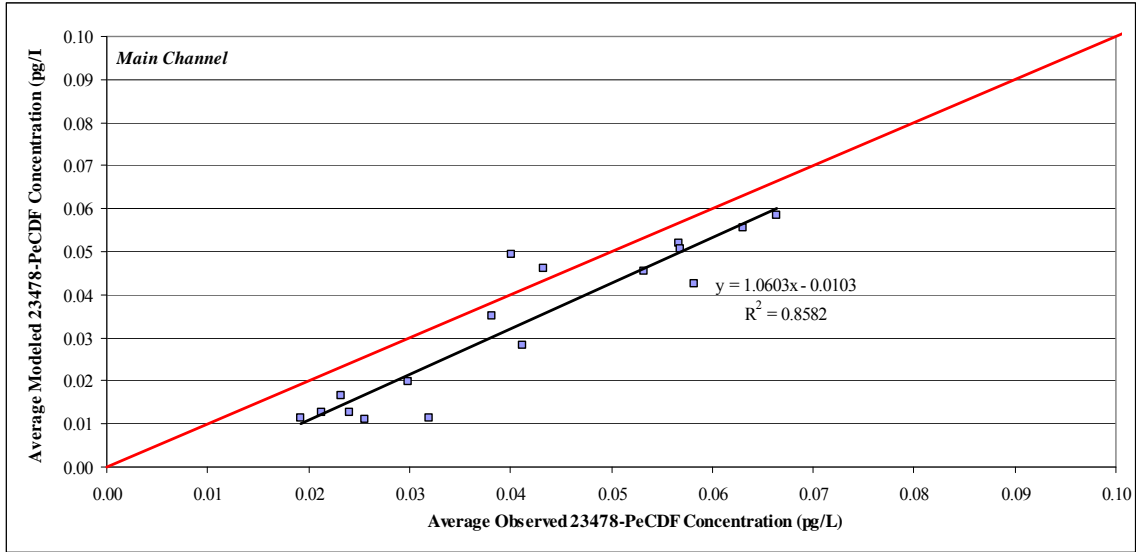


Figure 3.8e Observed versus Modeled Average 23478-PeCDF Concentrations

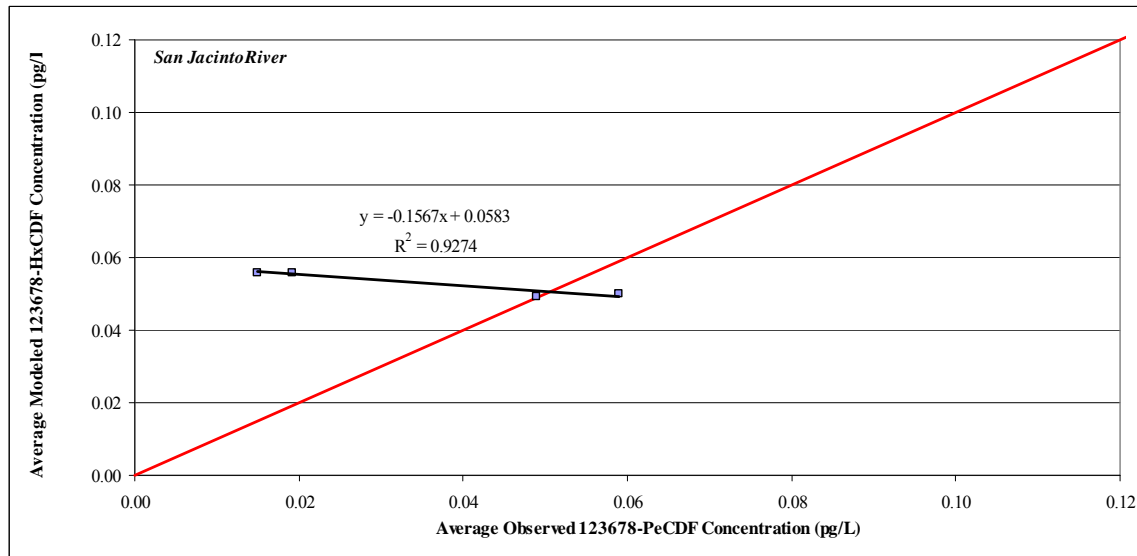
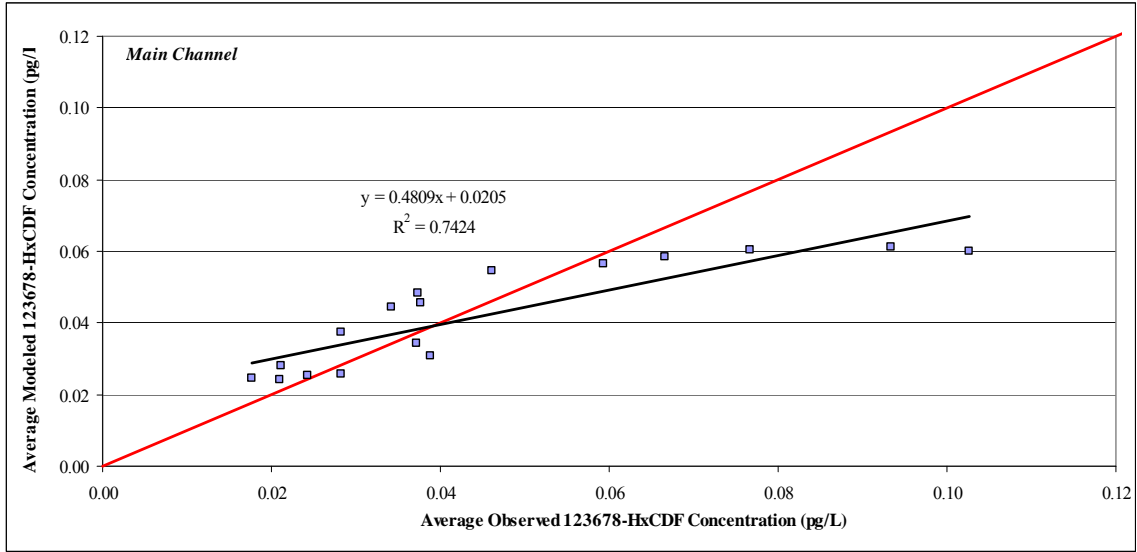


Figure 3.8f Observed versus Modeled Average 123678-HxCDF Concentrations

3.6 SENSITIVITY ANALYSIS

Sensitivity analysis helps in understanding the underestimation or overestimation of concentration profiles due to the errors associated with the calibration parameters. Sensitivity analysis also helps in understanding the importance of parameters and loads influencing the concentration profile. So the sensitivity analyses were conducted to examine the effect of the following on the concentration profile

- changes in settling velocity,
- changes in scour rates,
- changes in source loadings (point source, runoff, deposition),
- changes in dispersion,
- changes in diffusion coefficient,
- changes in benthic layer concentration,
- changes in benthic layer depth, and
- changes in partition coefficient.

Sensitivity analysis scenarios are summarized in Table 3.11. The loadings and model parameters were varied individually by factors equal to 0.1, 0.2, 0.5, 2, 5, and 10 from the calibration scenario (hereafter referred to as base case). Results from the sensitivity analysis are presented in Figures 3.9 through 3.18 for the Main Channel and SJR. In general, variations in 2378-TCDD and 2378-TCDF behaved alike in comparison to other congeners. Due to model instability, the sensitivity analysis for the 123678-HxCDF model was completed for a reduced set of parameters.

Table 3.11 Summary of Sensitivity Analysis Scenarios

Case No.	Description
Base Case	Calibrated model
Case 1	Base case/2 (Parameter of consideration/2)
Case 2	Base case/5 (Parameter of consideration/5)
Case 3	Base case/10 (Parameter of consideration/10)
Case 4	Base case×2 (Parameter of consideration×2)
Case 5	Base case×5 (Parameter of consideration×5)
Case 6	Base case×10 (Parameter of consideration×10)

3.6.1 Effect of Diffusion Coefficient

Sensitivity analysis was carried out with decrease/increase in diffusion coefficients for each congener and the changes in concentration profiles in comparison to the base case are shown in Figure 3.9. Due to model instability, it was not possible to run the diffusion coefficient scenarios for 123678-HxCDF. Overall diffusion coefficient had an insignificant effect on the average concentration profiles. The specific inferences from the sensitivity analysis are:

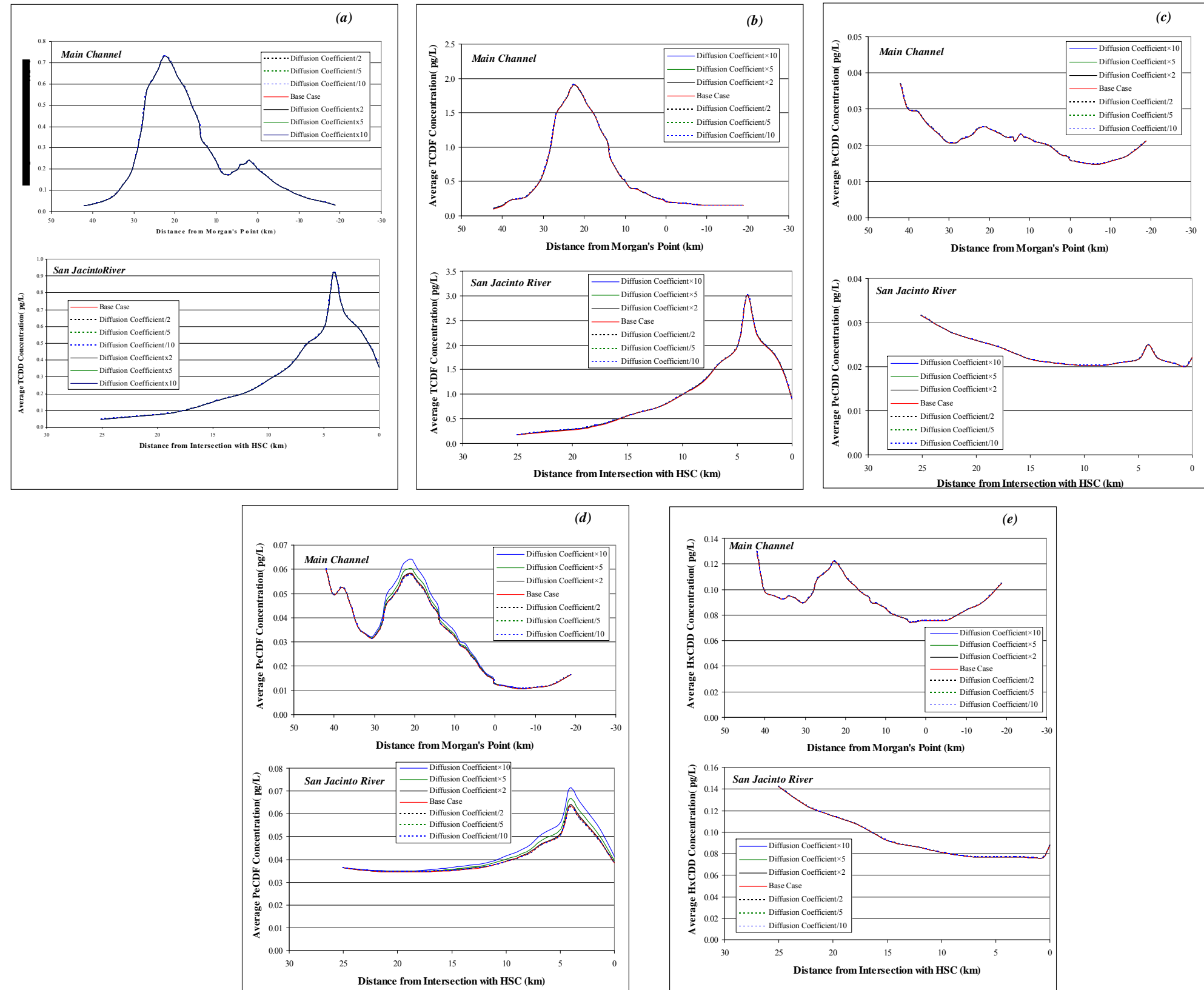
- The diffusion coefficient did not have a significant effect on the concentration profile except in the case of 2378-TCDD and 23478-PeCDF.
- In the case of 23478-PeCDF, an increase in diffusion coefficient resulted in a small increase in concentration, both in the Main Channel and in SJR.
- In the case of 2378-TCDD, a decrease in diffusion coefficient resulted in a small decrease in concentration, both in the Main Channel and in SJR.

3.6.2 Effect of Dispersion

Sensitivity analysis was carried out with decrease in dispersion and the changes in concentration profiles in comparison to base case are shown in Figure 3.10. The 123678-HxCDF model could not be sensitized for dispersion due to model instability. Overall,

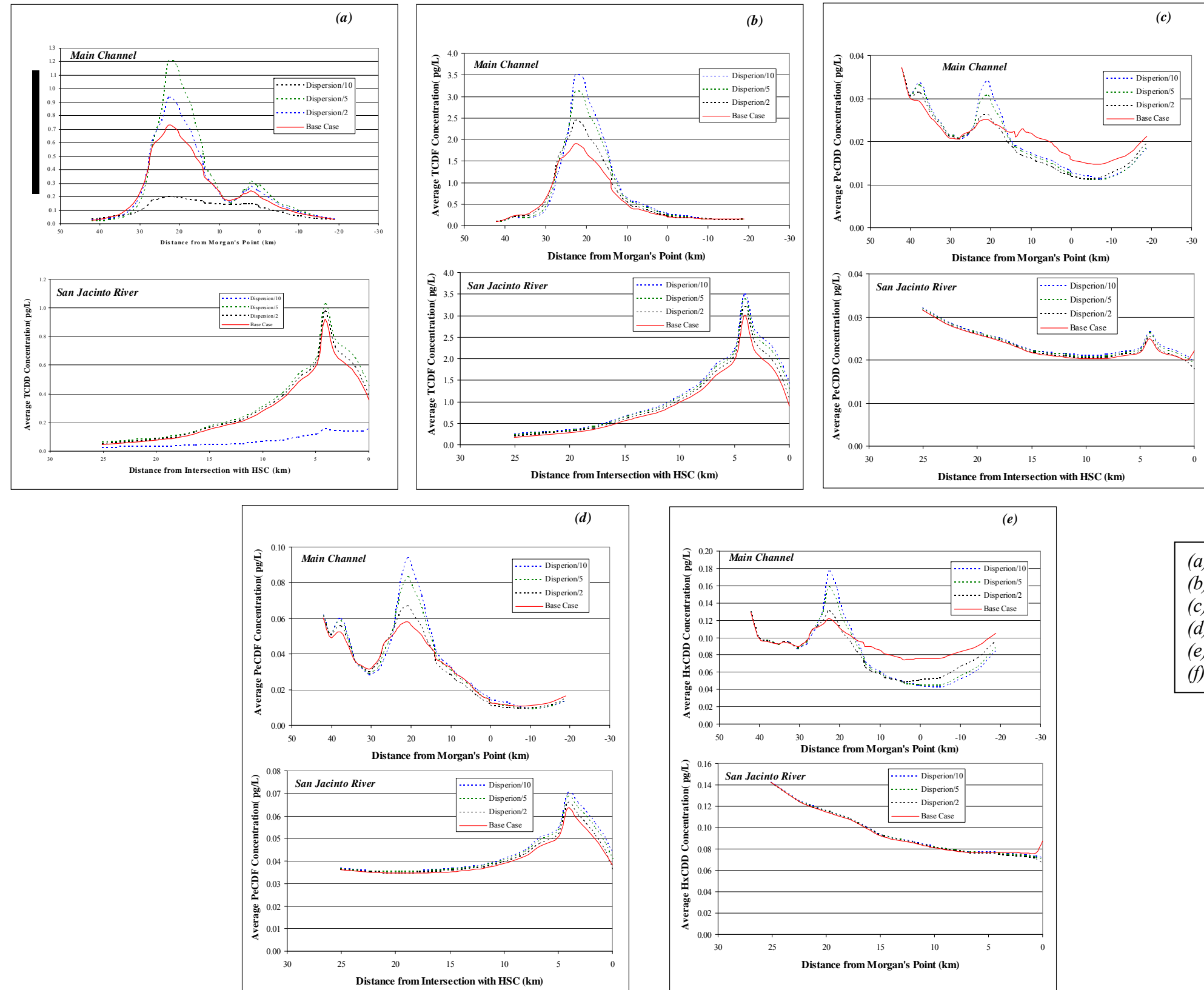
dispersion rates showed some effect on the average concentration profiles, mainly for the Main Channel. The specific inferences from the sensitivity analysis are:

- A decrease in dispersion resulted in an increase in water concentration.
- Dispersion had significant effect at peak concentrations both at Main Channel and SJR.
- The effect of dispersion was significant in the Main Channel compared to SJR.
- There was a reversal in trend or cross over (change in concentration from increase to decrease from base case and vice versa) in concentration profiles in the Main Channel with all congeners tested. A cross over was observed around 25-30 km from Morgan's Point and another one at around 10-20 km with some congeners.



- | | |
|-----|--------------|
| (a) | 2378-TCDD |
| (b) | 2378-TCDF |
| (c) | 12378-PeCDD |
| (d) | 23478-PeCDF |
| (e) | 123678-HxCDD |
| (f) | 123678-HxCDF |

Figure 3.9 Diffusion Coefficient Scenarios



- (a) 2378-TCDD
- (b) 2378-TCDF
- (c) 12378-PeCDD
- (d) 23478-PeCDF
- (e) 123678-HxCDD
- (f) 123678-HxCDF

Figure 3.10 Dispersion Scenarios

3.6.3 Effect of Partition Coefficient

Sensitivity analysis was carried out with decrease/increase in partition coefficients for each congener. The change in concentration profiles are shown in Figure 3.11. Overall, partition coefficients had a significant effect on the average concentration profiles. The specific inferences from the sensitivity analysis are:

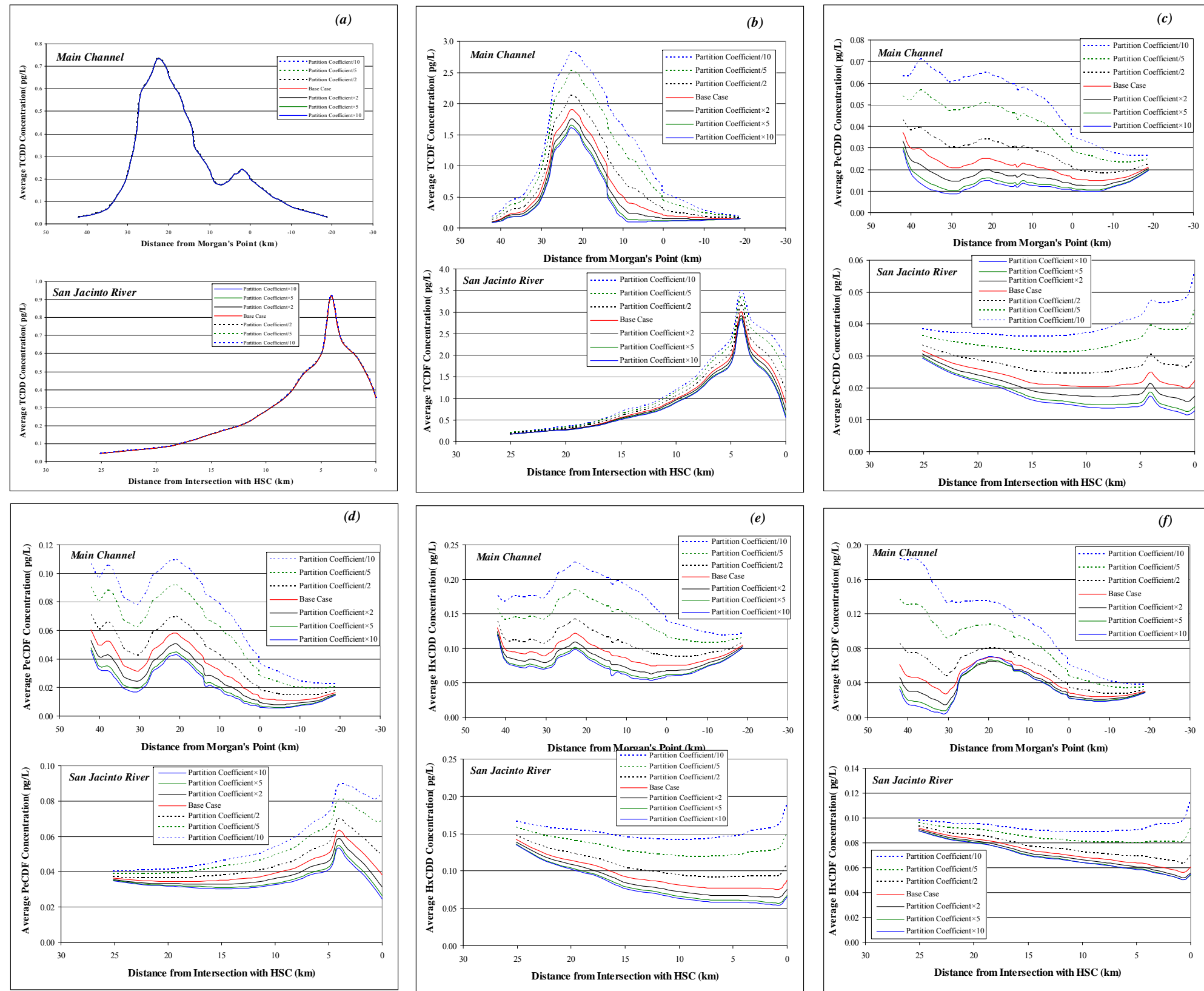
- There 2378-TCDD model appeared to be insensitive to changes in the partition coefficient.
- Except for 2378-TCDD, a decrease in partition coefficient resulted in an increase in concentration, while an increase in partition coefficient resulted in concentration decrease.
- The effect of partition coefficient was more pronounced upstream compared to downstream segments in the Main Channel. This may be the result of having a fixed lower boundary.
- The effect of partition coefficient on the concentration profile was more significant with a decrease in partition coefficient rather than an increase in partition coefficient.
- For the 12378-PeCDD, 23478-PeCDF, 123678-HxCDD, and 123678-HxCDF models, there was a sharp increase at the confluence of SJR, which seems like a model effect. The increase at the confluence was probably due to matching of the concentration at the SJR confluence with the concentration in the Main Channel, 15 km from the Morgan's point.

- In all cases there was a change in concentration profile in the Main Channel at Morgan's point (0 km) possibly due to bay effect and at 15 km from Morgan's point possibly due to the SJR confluence.

3.6.4 Effect of Settling

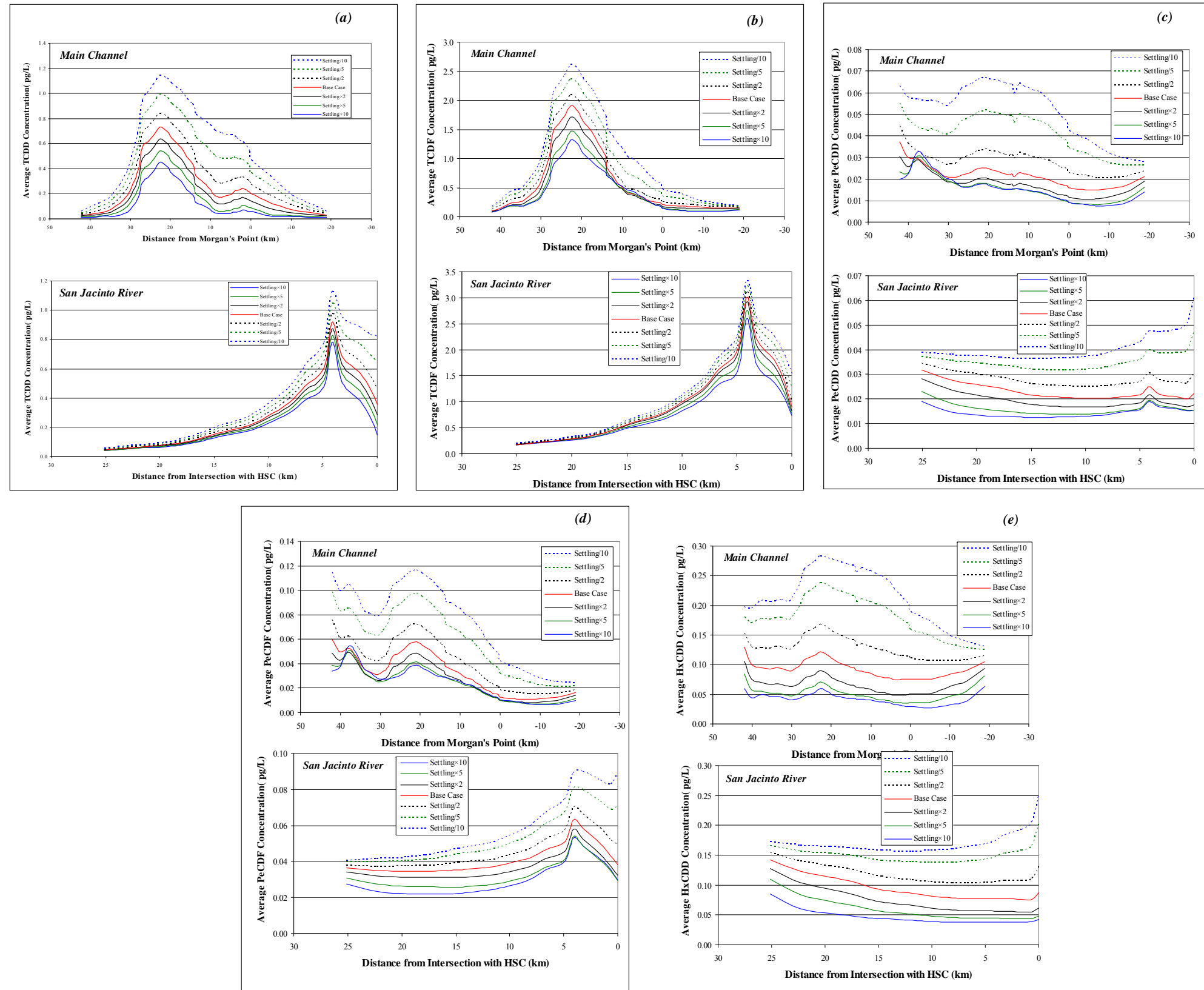
Sensitivity to settling rates was evaluated for all the models except 123678-HxCDF. The change in concentration profiles are shown in Figure 3.12. Overall, settling had a significant effect on the average concentration profiles, except for that of 2378-TCDD. The specific inferences from the sensitivity analysis are:

- There was no significant effect on the 2378-TCDD concentration profile as a result of changes in settling rates both in the Main Channel and SJR. The reason for insignificant effect is probably due to 2378-TCDD being mainly in the dissolved phase.
- Except for 2378-TCDD, a decrease in settling rates resulted in an increase in the concentration, while an increase in settling rates resulted in concentration decreases.
- The effect of settling rates was pronounced all along the channel and SJR except in the case of 2378-TCDF, where the effect was insignificant at the boundaries.
- A cross over in concentration profiles was observed with increase in settling rates in the case of 12378-PeCDD and 23478-PeCDF at about 37 km from Morgan's Point.
- In the case of 12378-PeCDD, 23478-PeCDF, and 123678-HxCDD, there was a sharp increase at the confluence of SJR, which was probably due to matching of the congener concentration at the SJR confluence with the concentration in the Main Channel, 15 km from the Morgan's point.



- (a) 2378-TCDD
- (b) 2378-TCDF
- (c) 12378-PeCDD
- (d) 23478-PeCDF
- (e) 123678-HxCDD
- (f) 123678-HxCDF

Figure 3.11 Partition Coefficient Scenarios



- | | |
|-----|--------------|
| (a) | 2378-TCDD |
| (b) | 2378-TCDF |
| (c) | 12378-PeCDD |
| (d) | 23478-PeCDF |
| (e) | 123678-HxCDD |
| (f) | 123678-HxCDF |

Figure 3.12 Settling Scenarios

3.6.5 Effect of Scour

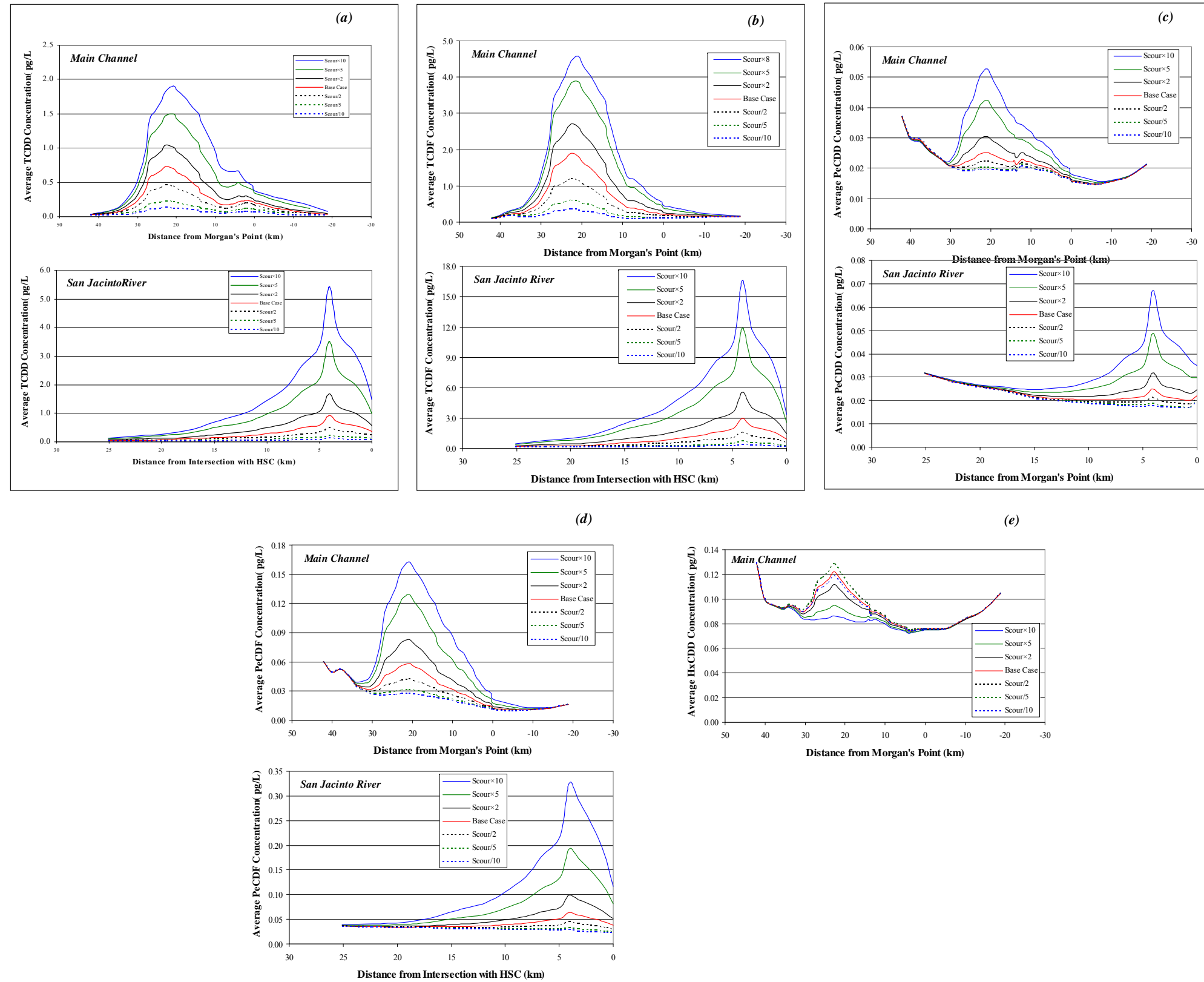
The change in concentration profiles as a result of changes in scour velocities is shown in Figure 3.13. Overall, concentrations were very sensitive to changes in scour velocity, with model concentrations increasing with increasing scour rates. The specific inferences from the sensitivity analysis are:

- There was a significant effect of scour velocity on concentration profiles in the 2378-TCDD, 2378-TCDF, 12378-PeCDD, and 23478-PeCDF models.
- An increase in scour velocity resulted in a significant increase in concentration, while a decrease in scour velocity resulted in decrease in concentration.
- The effect was significant both in the Main Channel and SJR, with the most significant effects at the peak concentrations. This indirectly indicates that the spikes are due to the sediment sourcing.
- Low scour rates resulted in significant decrease in concentrations and the concentration profiles being flat with no peaks, both in the Main channel and SJR. This flat profile resulted in masking the effects of sediment sourcing at low scour velocity. For example, spikes in the Main Channel and waste pits in SJR (at 5 km) were not visible at low scour rates.

3.6.6 Effect of Benthic Concentration

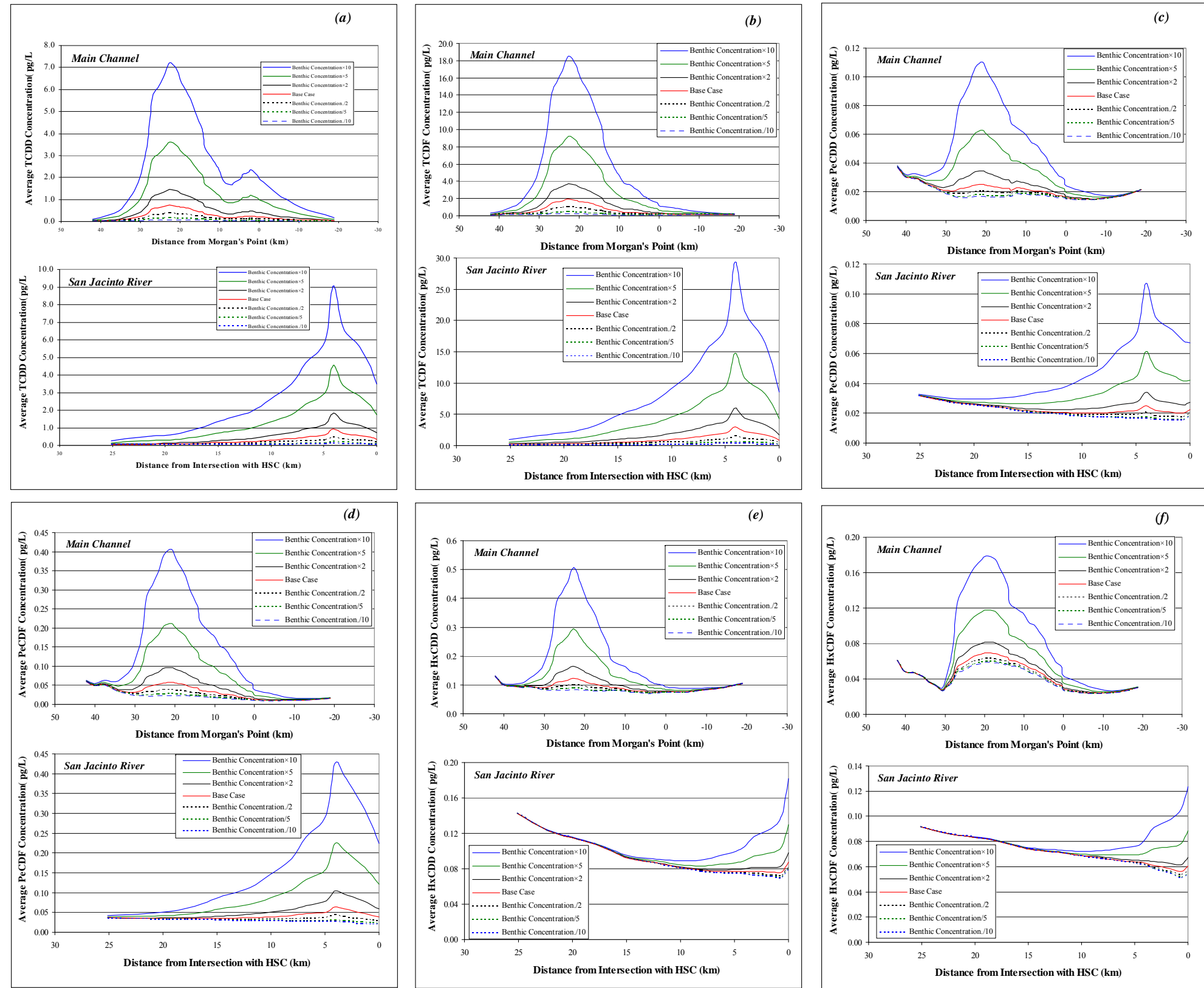
Results of the sensitivity analysis for dioxin concentrations in the benthic layers are shown in Figure 3.14. Of all the parameters tested benthic concentrations was found to be the one the models are most sensitive to. The specific inferences from the sensitivity analysis are:

- An increase in benthic concentration resulted in an increase in water concentration profile, while a decrease in benthic concentration resulted in decrease in concentration.
- The effect was significant both at the Main Channel and SJR, with the most significant effects at the peak concentrations.
- An increase in benthic concentration resulted in as much as a ten fold increase in water concentration.
- A decrease in benthic concentration resulted in significant decrease in concentrations and the concentration profiles were flat both at Main Channel and SJR.
- The effect of benthic concentration was greater for the 2378-TCDD, 2378-TCDF, 12378-PeCDD, and 23478-PeCDF models in comparison to the 123678-HxCDD and 123678-HxCDF models.
- For the 123678-HxCDD and 123678-HxCDF models, there was a sharp increase at the confluence of SJR.



- | | |
|-----|--------------|
| (a) | 2378-TCDD |
| (b) | 2378-TCDF |
| (c) | 12378-PeCDD |
| (d) | 23478-PeCDF |
| (e) | 123678-HxCDD |
| (f) | 123678-HxCDF |

Figure 3.13 Scour Scenarios



- (a) 2378-TCDD
- (b) 2378-TCDF
- (c) 12378-PeCDD
- (d) 23478-PeCDF
- (e) 123678-HxCDD
- (f) 123678-HxCDF

Figure 3.14 Benthic Concentration Scenarios

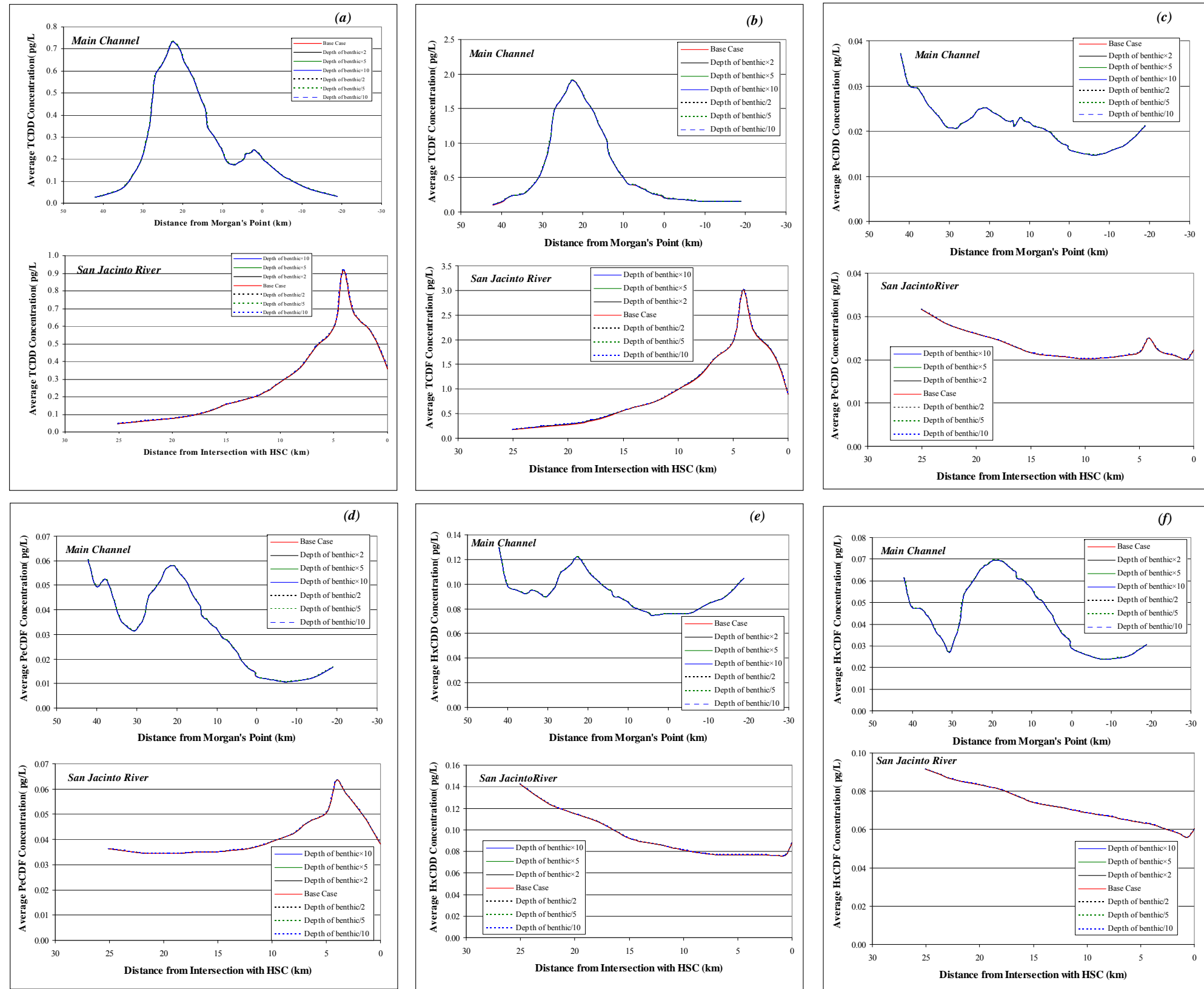
3.6.7 Effect of Benthic Layer Depth

Sensitivity analysis was carried out with decrease/increase in benthic layer depth in segments 108 to 214 (benthic segments) and the changes in concentration profiles are shown in Figure 3.15. Overall, concentrations were not sensitive to benthic layer depths, both in the Main Channel and SJR for all congeners.

3.6.8 Effect of Runoff Load

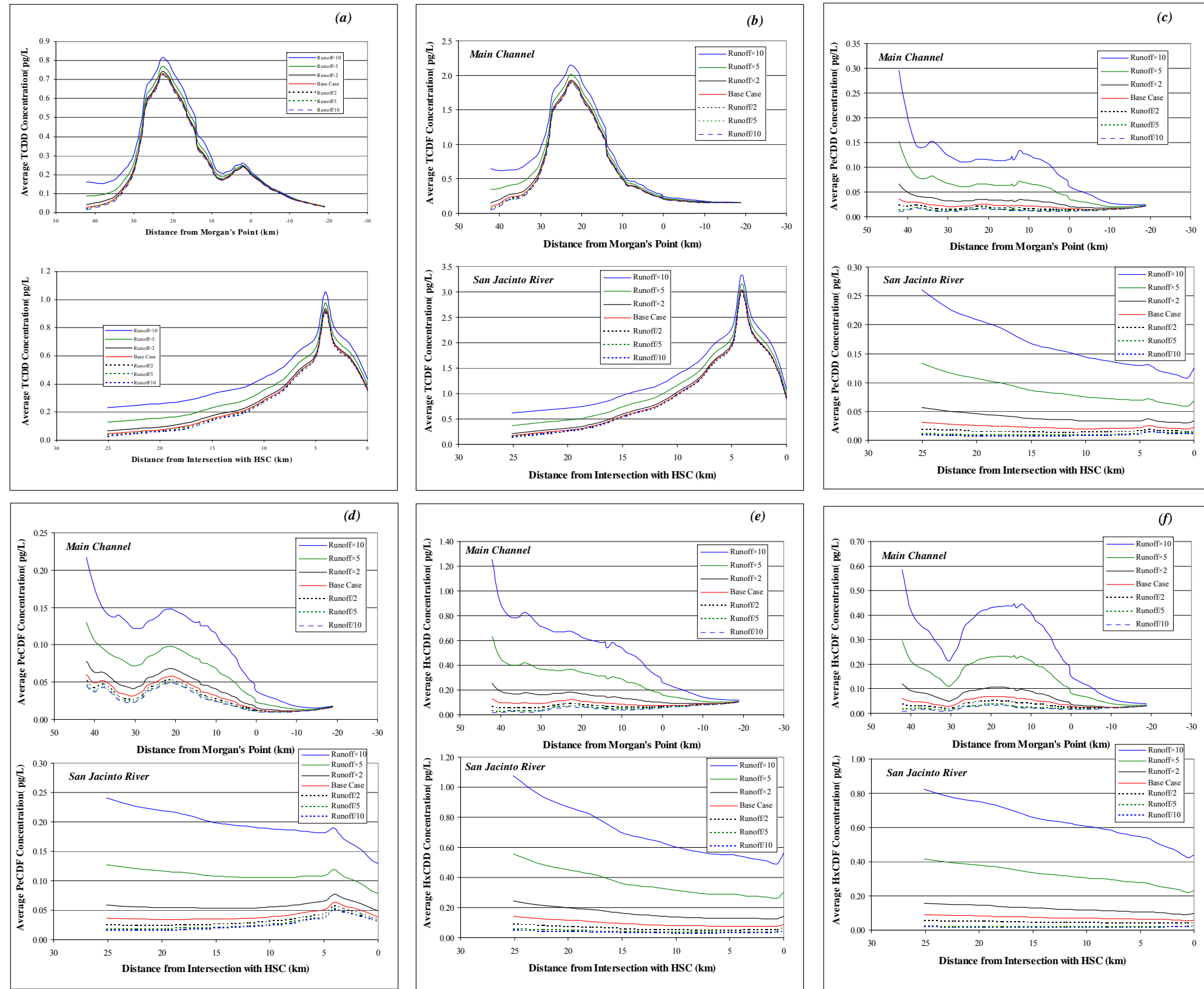
Results of the sensitivity analysis for runoff loads are shown in Figure 3.16. Overall, runoff loads were found to have some effect on the concentration profiles. The specific inferences from the sensitivity analysis are:

- The effect of runoff loads on 2378-TCDD and 2378-TCDF was smaller than that for the remaining congeners. The effect was minor at the boundaries and at peaks in the case of 2378-TCDD and 2378-TCDF.
- An increase in runoff load resulted in increases in concentration profiles in the 12378-PeCDD, 23478-PeCDF, 123678-HxCDD and 123678-HxCDF models, particularly at the upstream boundaries both in the Main Channel and SJR.
- A decrease in runoff did not have a significant effect on the concentration profiles, which indirectly indicates that the base case had insignificant runoff compared to the total load.
- The runoff load did not have any impact on the downstream concentration in the Main Channel probably due to large dilution. This also may reflect the effect of a fixed lower boundary.



- (a) 2378-TCDD
- (b) 2378-TCDF
- (c) 12378-PeCDD
- (d) 23478-PeCDF
- (e) 123678-HxCDD
- (f) 123678-HxCDF

Figure 3.15 Benthic Layer Depth Scenarios



- (a) 2378-TCDD
- (b) 2378-TCDF
- (c) 12378-PeCDD
- (d) 23478-PeCDF
- (e) 123678-HxCDD
- (f) 123678-HxCDF

Figure 3.16 Runoff Load Scenarios

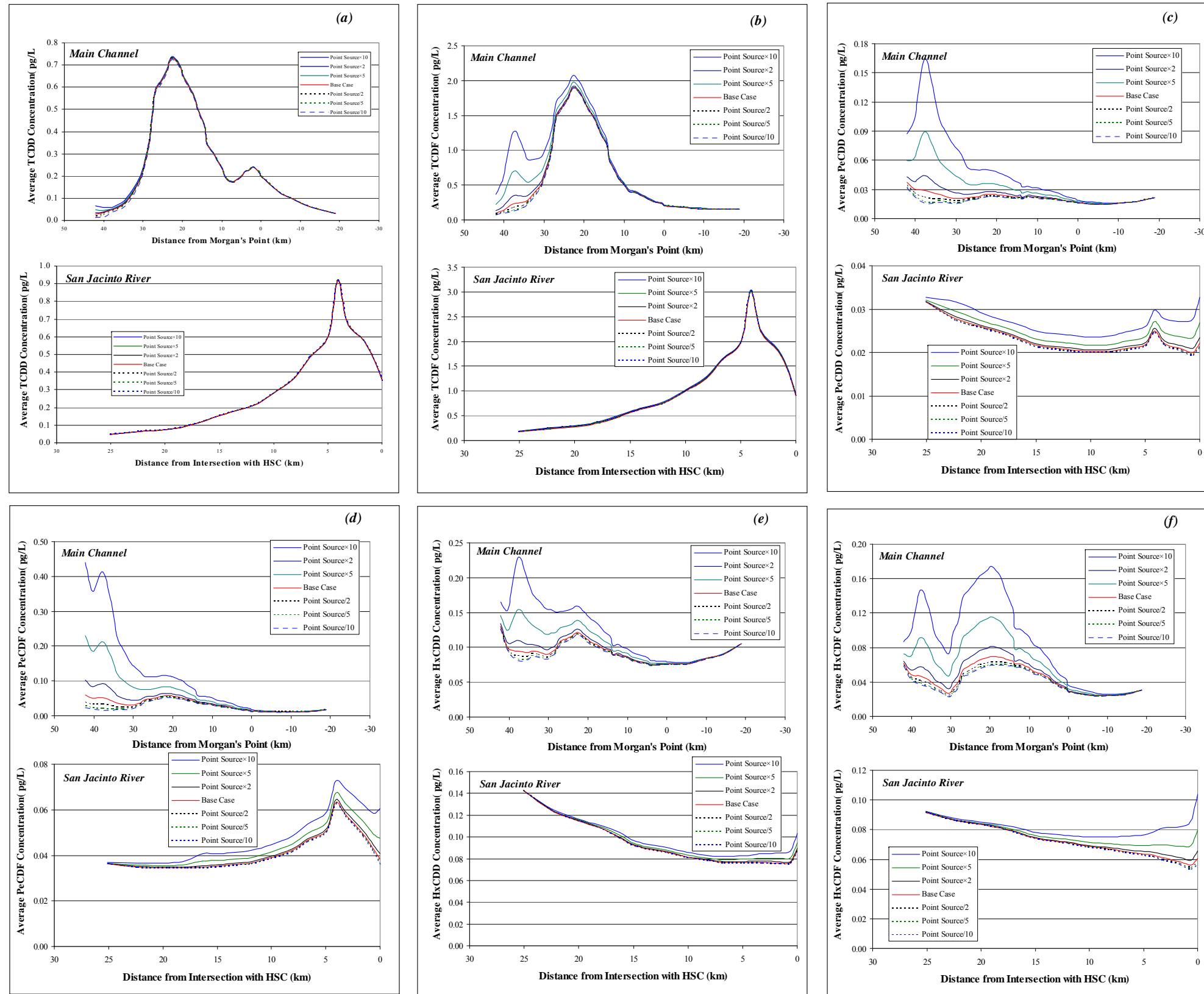
3.6.9 Effect of Point Source Load

Model responses to changes in point source loads are shown in Figure 3.17. Overall, concentration profiles were slightly affected by changes in point source loads. The specific inferences from the sensitivity analysis are:

- A minor effect was observed in general with increase in point source loads.
- The increase in point source load had a noticeable effect on the concentration profile at about 37 km from Morgan’s point in the Main Channel with all congeners. However with a decrease in PS load, the point source effect was not observable.
- The effect of point source loads on the 2378-TCDD and 2378-TCDF models was smaller than that for the other congeners.

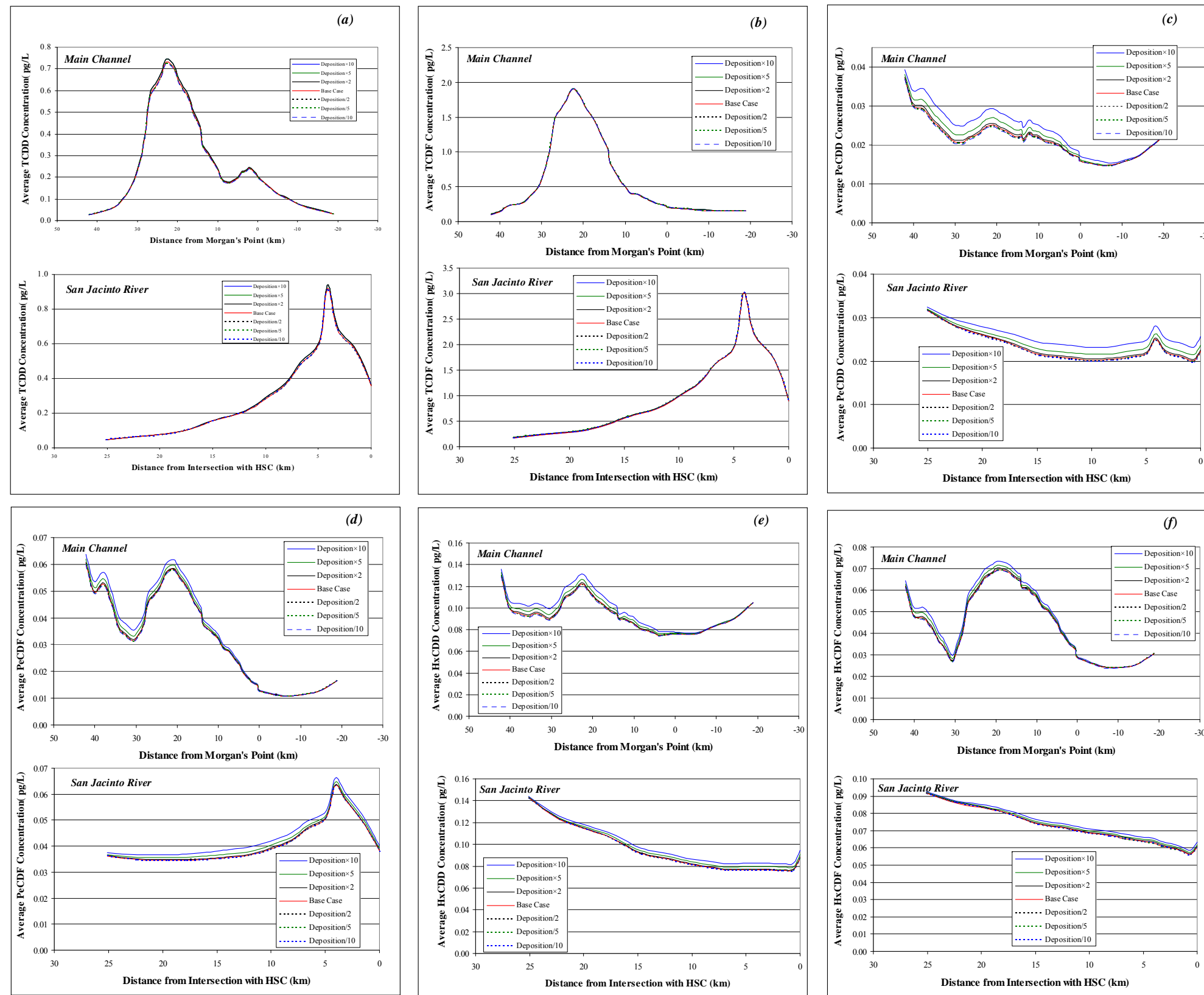
3.6.10 Effect of Deposition Load

Changes in concentration profiles as a result of changes in deposition loads are shown in Figure 3.18. The change in deposition load did not affect the concentration profiles, which indicated that deposition was not a significant contributor to total load.



- (a) 2378-TCDD
- (b) 2378-TCDF
- (c) 12378-PeCDD
- (d) 23478-PeCDF
- (e) 123678-HxCDD
- (f) 123678-HxCDF

Figure 3.17 Point Source Load Scenarios



- (a) 2378-TCDD
- (b) 2378-TCDF
- (c) 12378-PeCDD
- (d) 23478-PeCDF
- (e) 123678-HxCDD
- (f) 123678-HxCDF

Figure 3.18 Deposition Load Scenarios

3.6.11 Summary of Sensitivity Analysis

To better determine the parameter with the highest impact on model input on a congener-basis, spider plots were developed using the results discussed in sections 3.6.1 to 3.6.10. Spider plots depict the change in parameter magnitude in the x-axis and the resulting change in model results in the y-axis. These plots help in “normalizing” the effect of the different input variables, eliminating the effect of scale. Changes in both input parameter and model output were calculated as

$$\%change = \frac{Value - Value_{base\ case}}{Value_{base\ case}} \quad (3.9)$$

The output variable of interest is the concentration at a given WASP reach. For each input variable, two cases were analyzed: (i) percent change in concentration at the peak (i.e., reach 25 in main channel and reach 44 in the SJR), and (ii) greatest percent change across the main channel and SJR. Figures 3.19 to 3.24 present spider plots for the various modeled congeners. As can be seen, initial sediment concentrations have a very significant impact on water concentrations for all six congeners, causing increases in modeled output between 300 and 900% of the base case. Similarly, increases in scour rates yielded increases in model output between 200% and 500%. Runoff concentrations also have a great impact on model output, but it is limited to reaches near freshwater inflows and/or with relatively low water concentrations. Runoff loads do not appear to have a major effect at the highest contaminated areas.

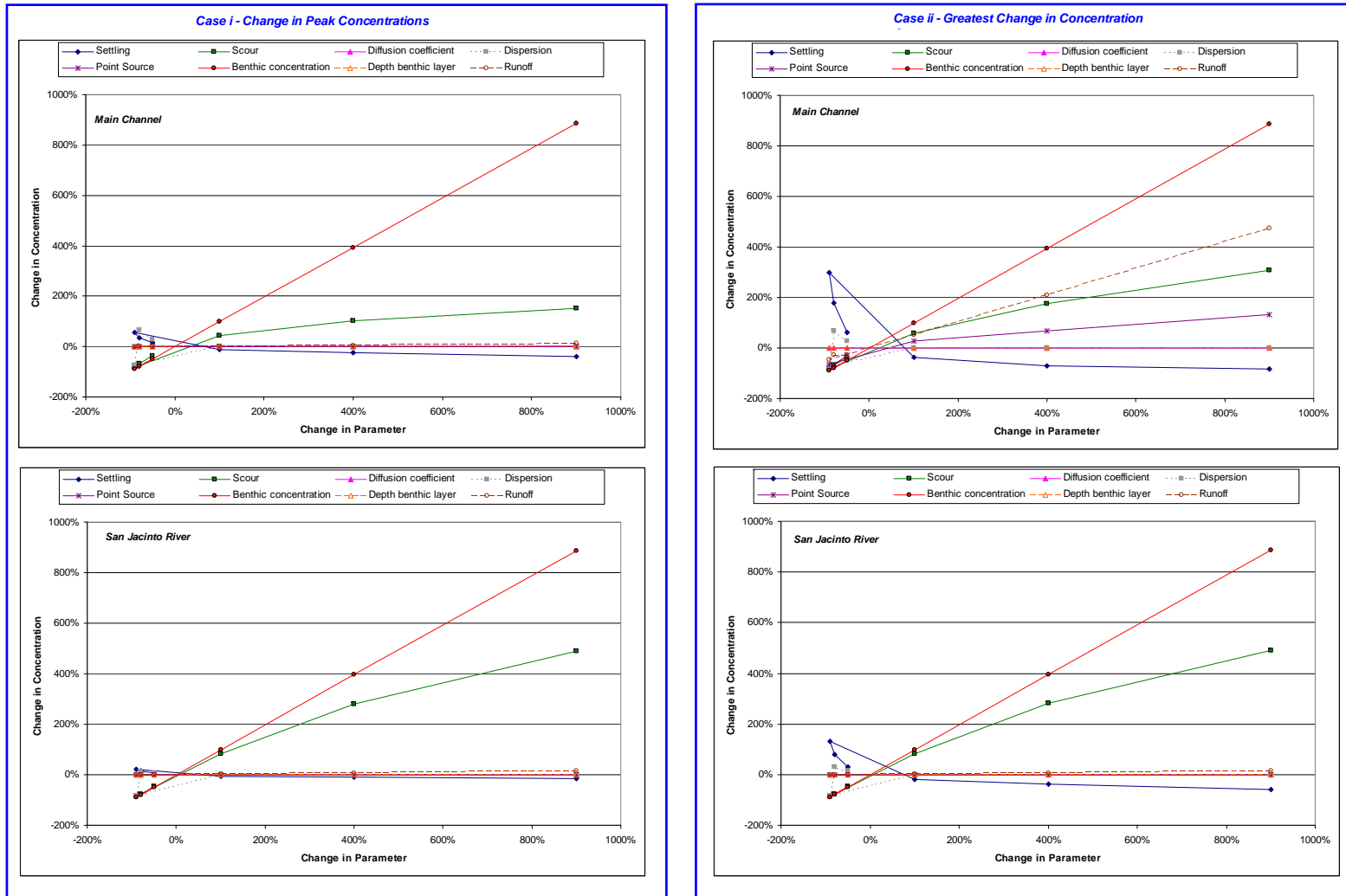


Figure 3.19 Sensitivity Summary for 2378-TCDD

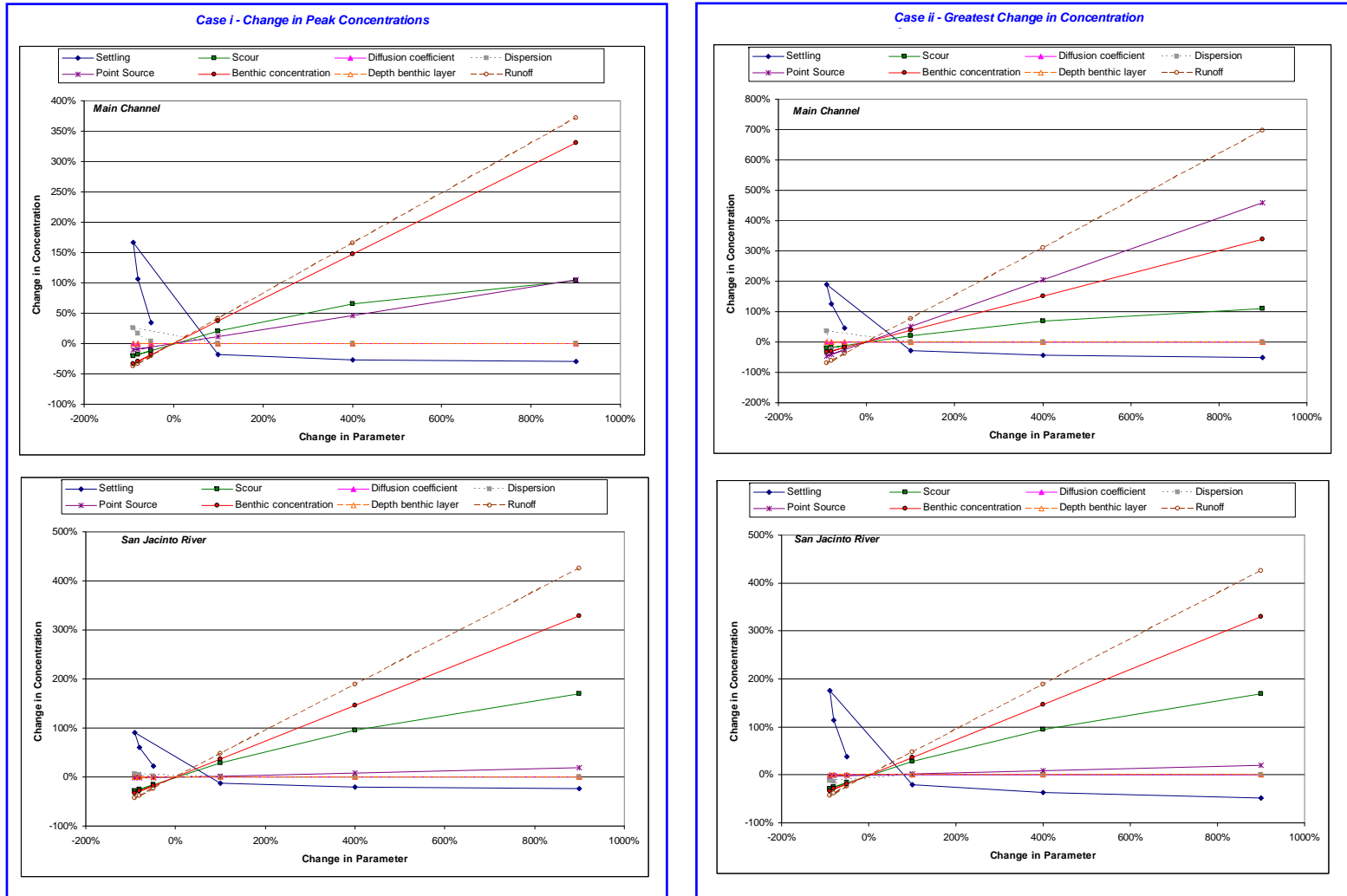


Figure 3.20 Sensitivity Summary for 12378-PeCDD

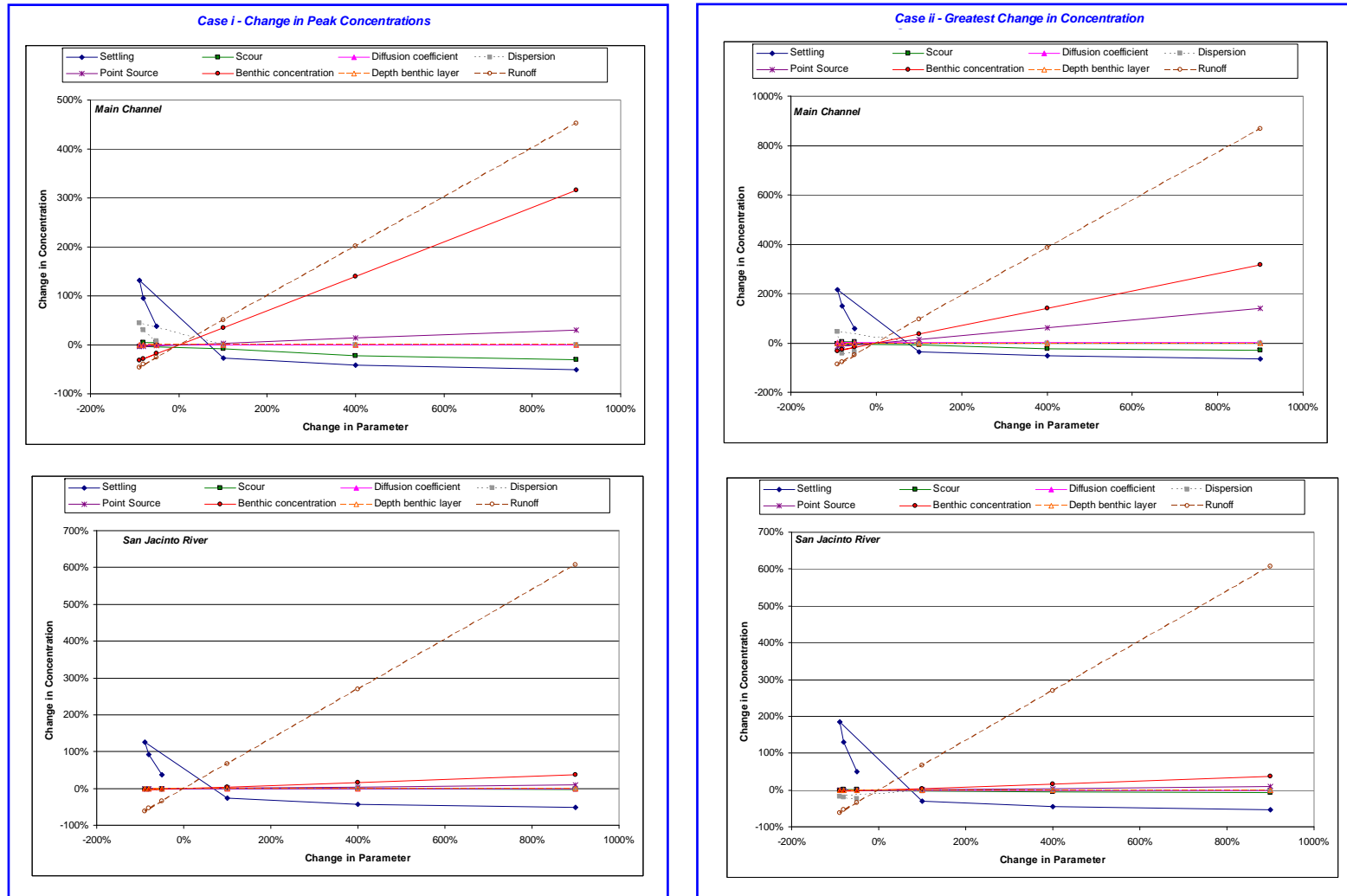


Figure 3.21 Sensitivity Summary for 123678-HxCDD

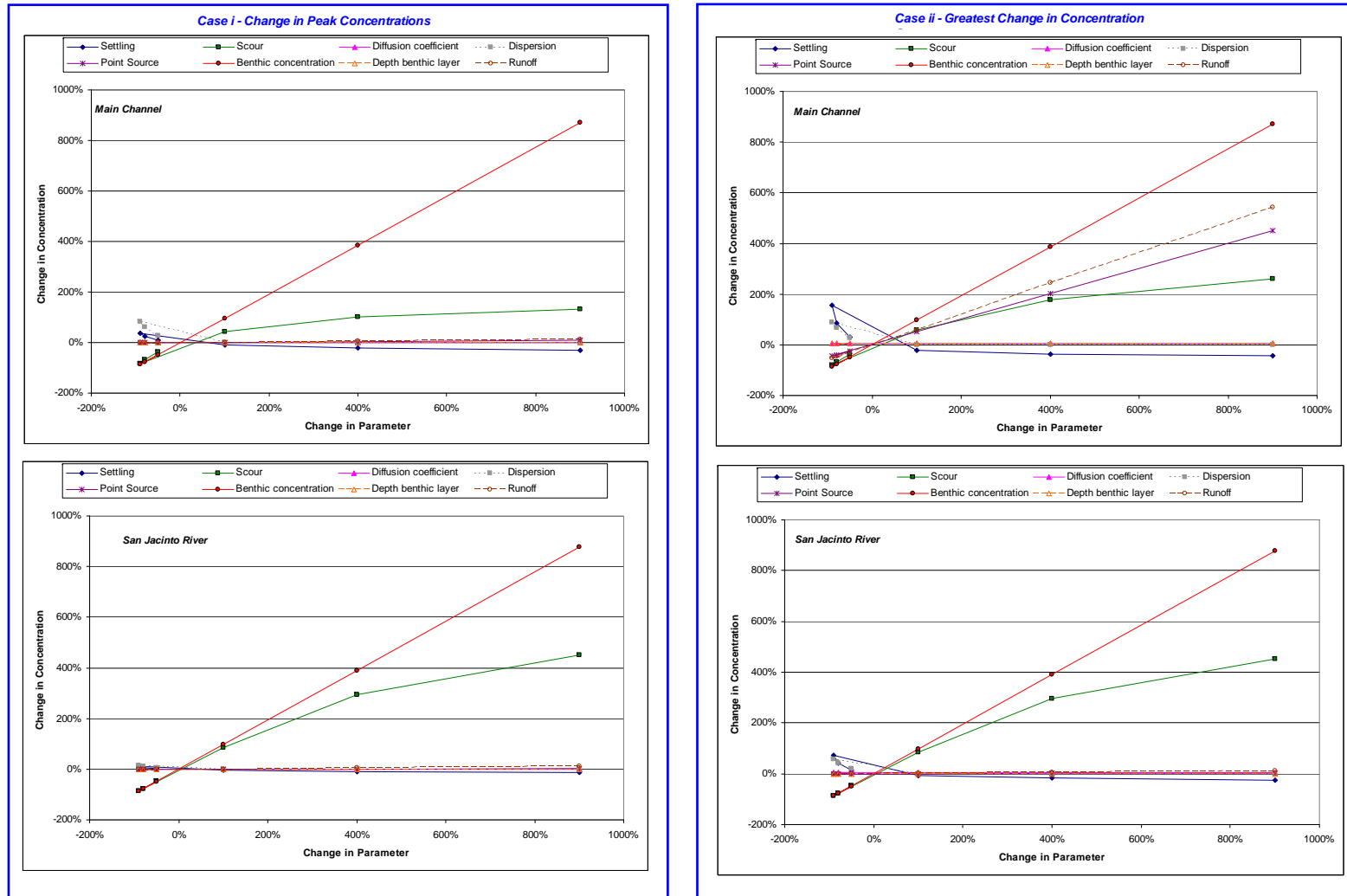


Figure 3.22 Sensitivity Summary for 2378-TCDF

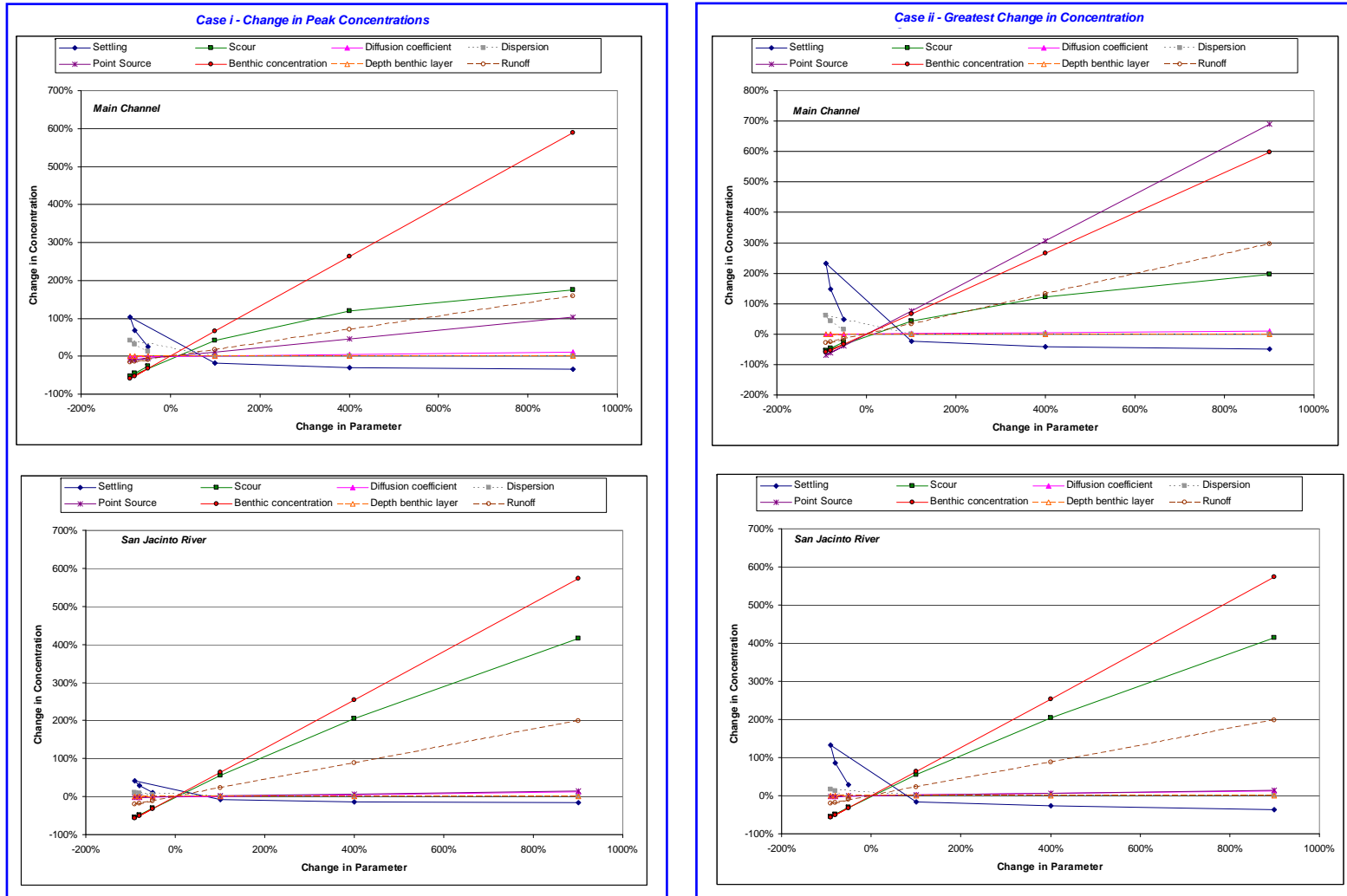


Figure 3.23 Sensitivity Summary for 23478-PeCDF

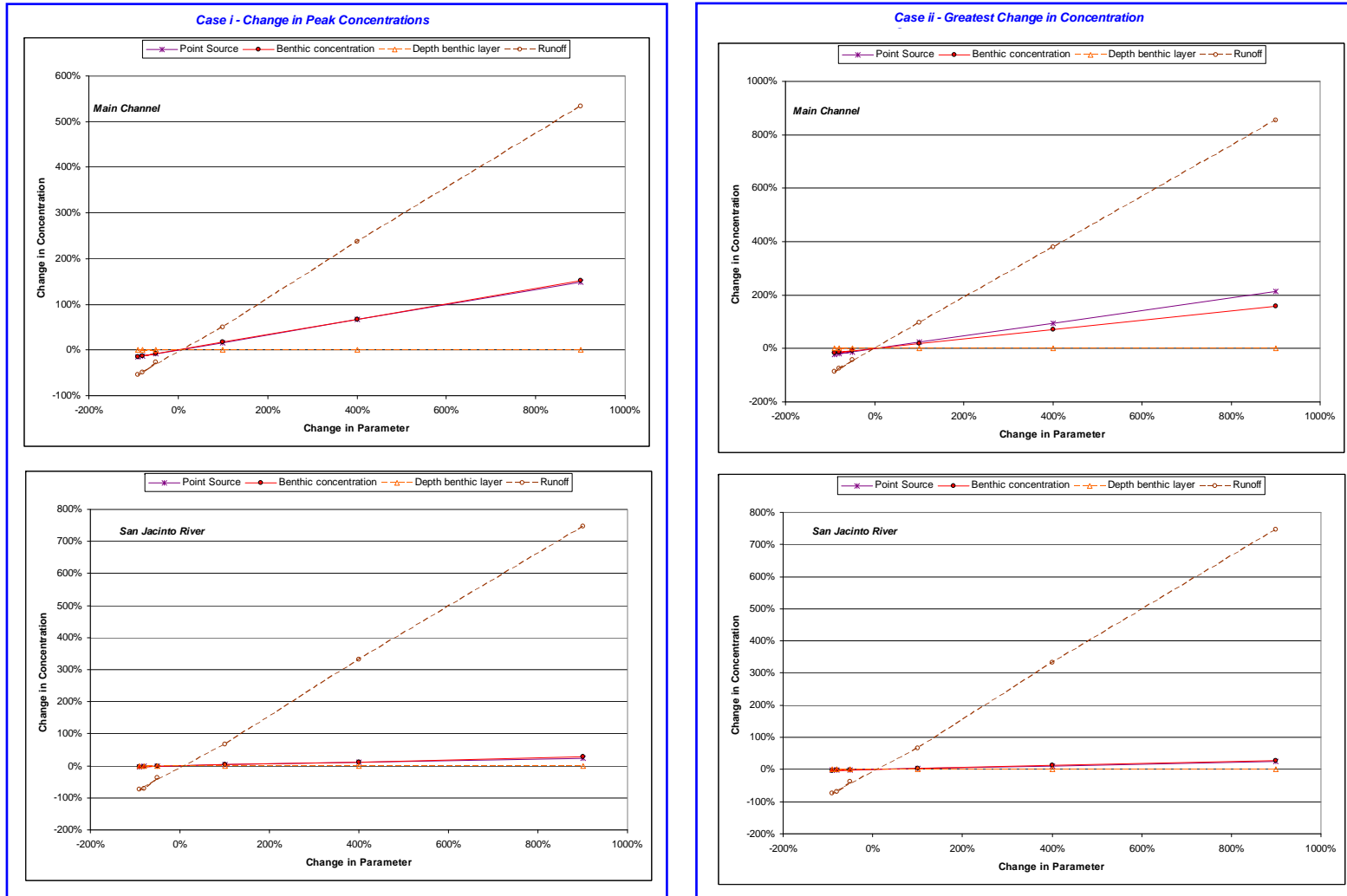


Figure 3.24 Sensitivity Summary for 123678-HxCDF

3.7 LOAD SCENARIOS

The calibrated models were used to evaluate various loading scenarios, including scenarios with one source only at a time for each congener. A summary of results is shown in Figures 3.25a through f. It is noted that when the sediment loads are eliminated (point sources, runoff, and direct deposition are the only sources of dioxin to the HSC), the concentration profiles for 2378-TCDD, 2378-TCDF, and 23478-PeCDF changed substantially. The concentration profiles for 12378-PeCDD and 123678-HxCDD, on the other hand, were dominated by boundary conditions; while the profile for 123678-HxCDF showed the greatest change when all the external loads were removed (only sediment loads were kept).

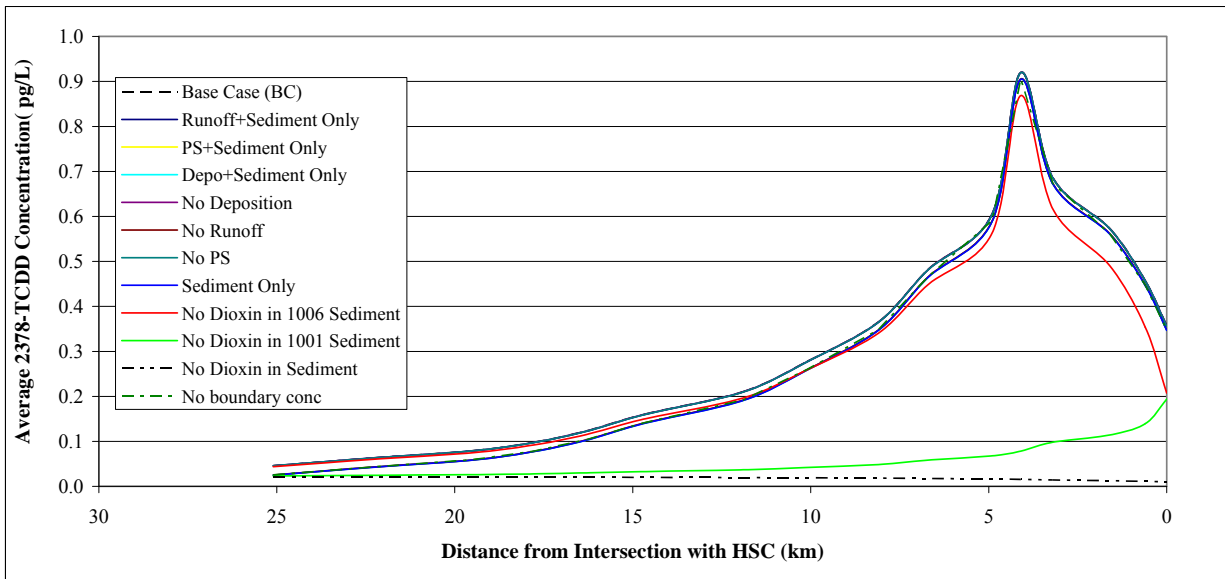
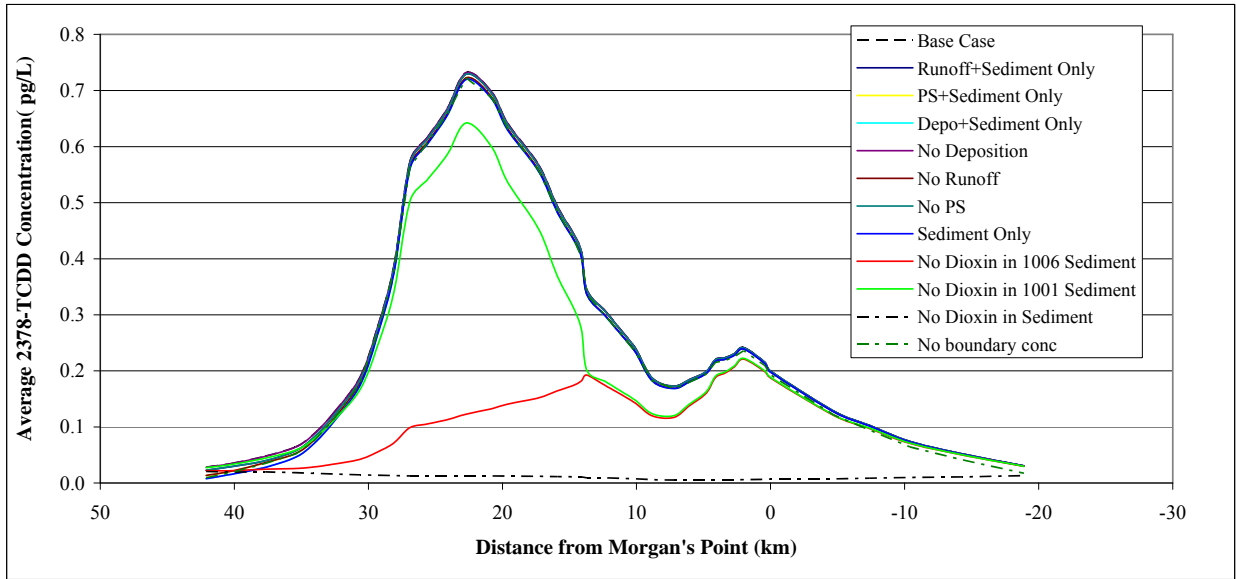


Figure 3.25a 2378-TCDD Load Scenarios

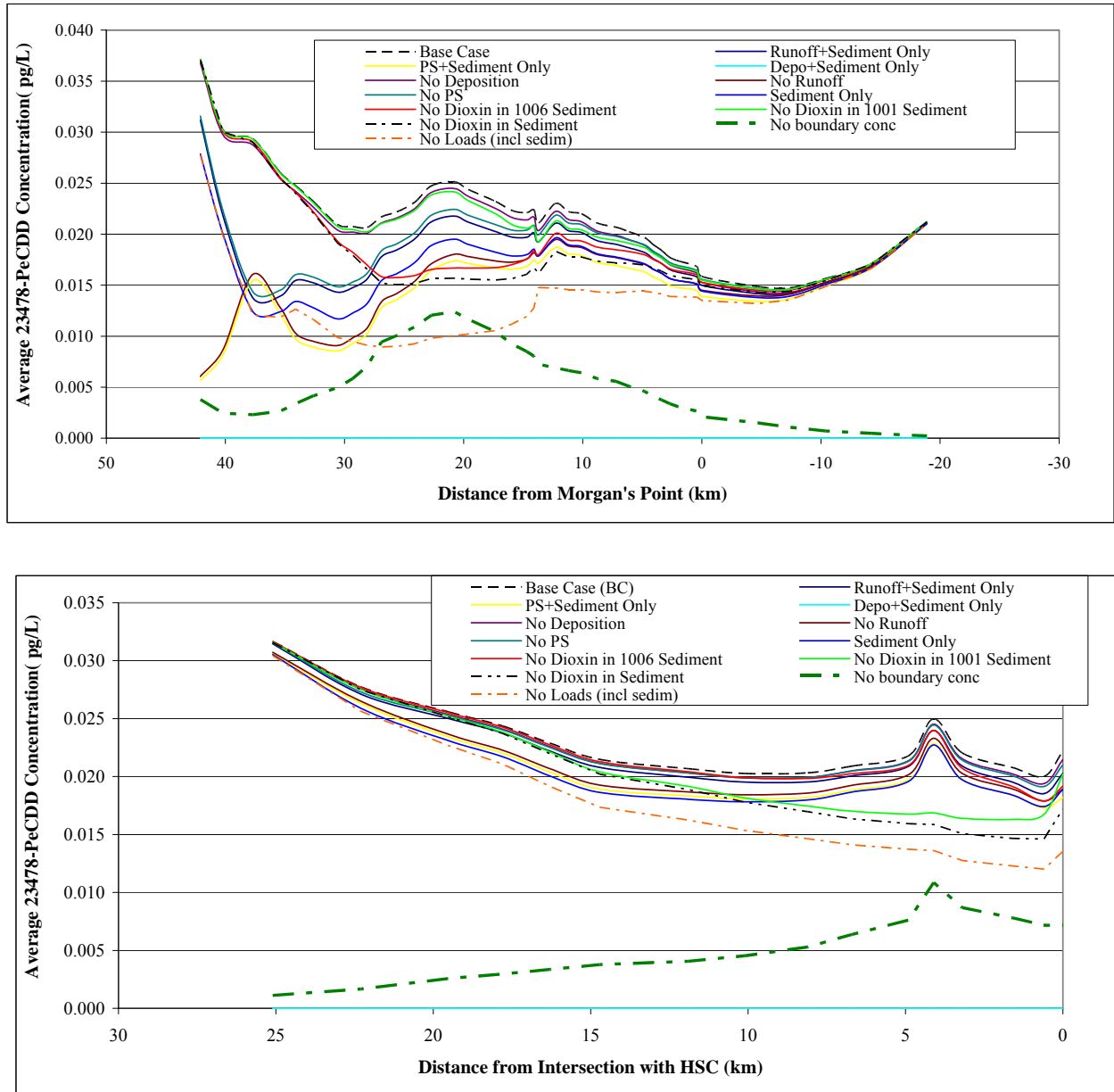


Figure 3.25b 12378-PeCDD Load Scenarios

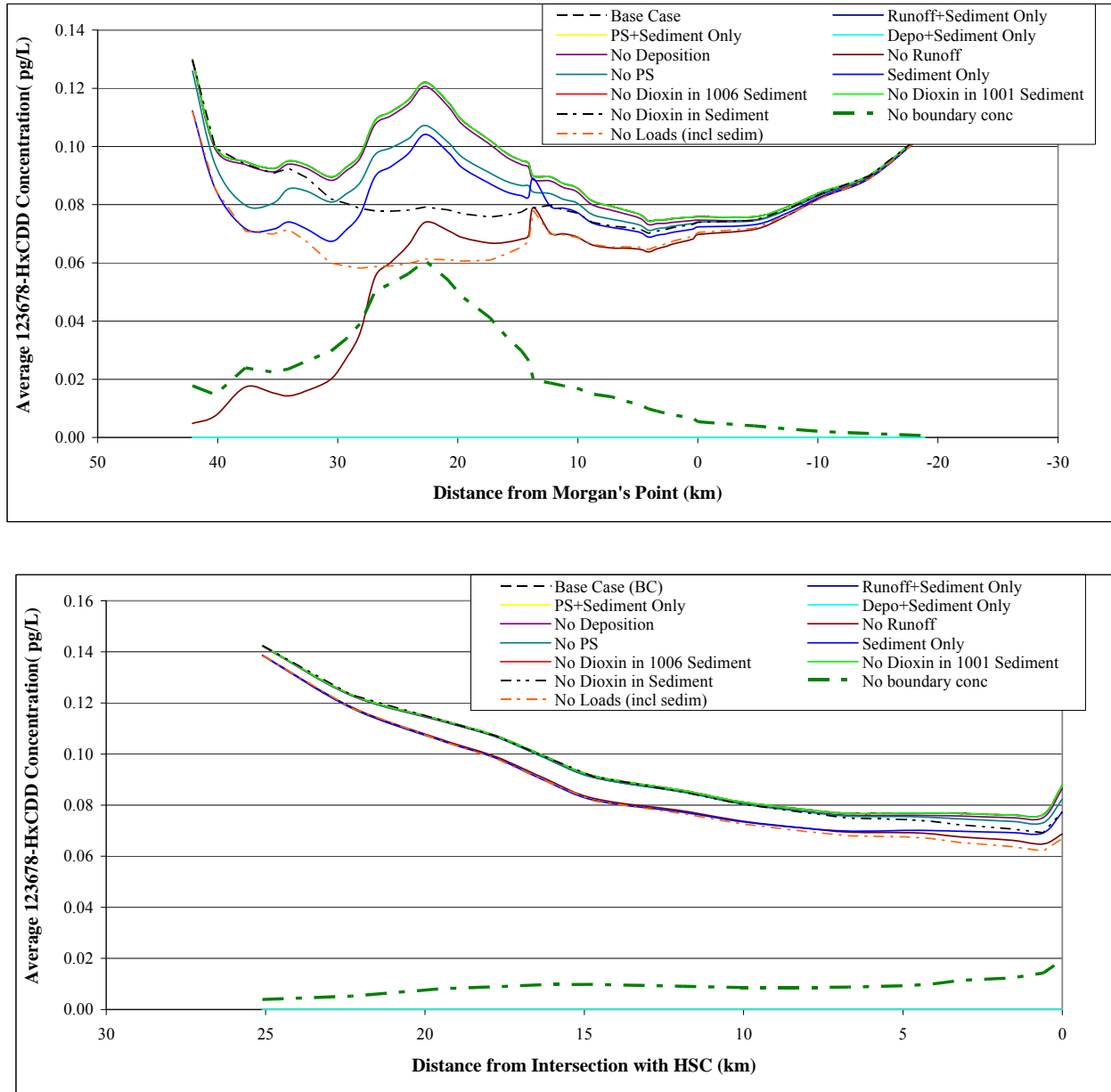


Figure 3.25c 123678-HxCDD Load Scenarios

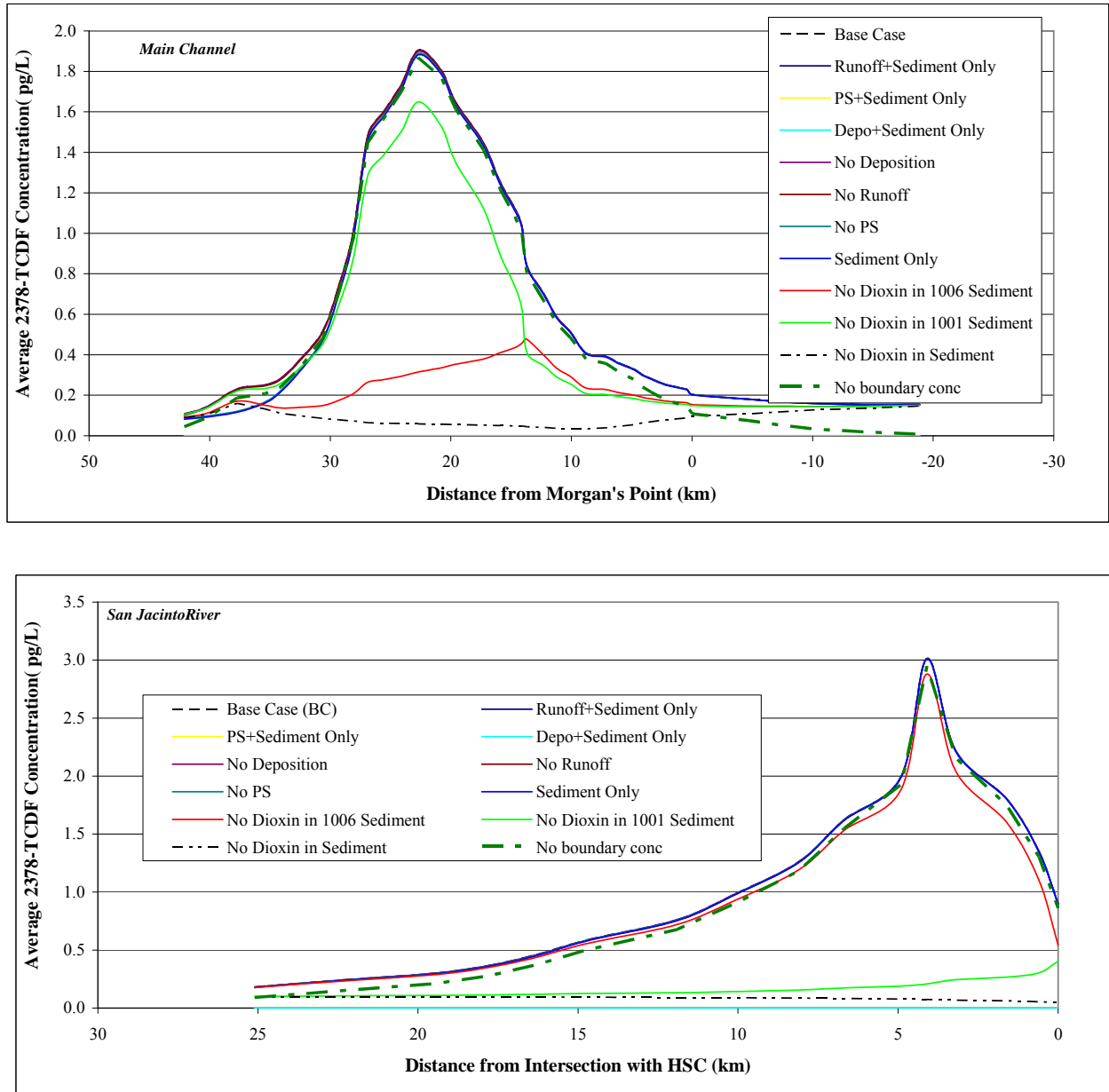


Figure 3.25d 2378-TCDF Load Scenarios

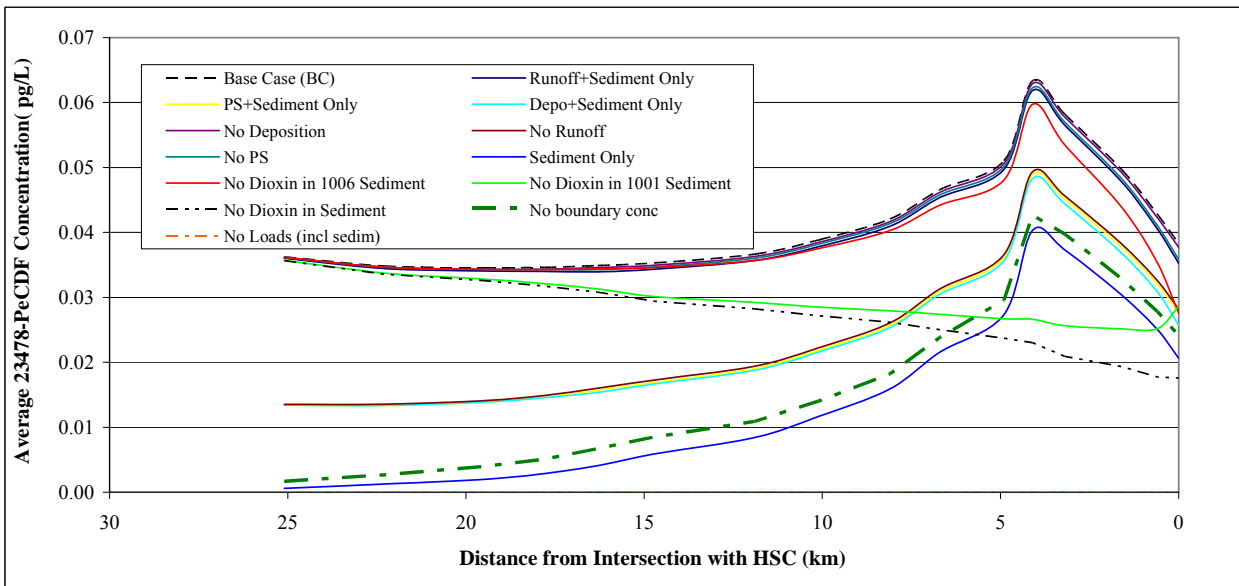
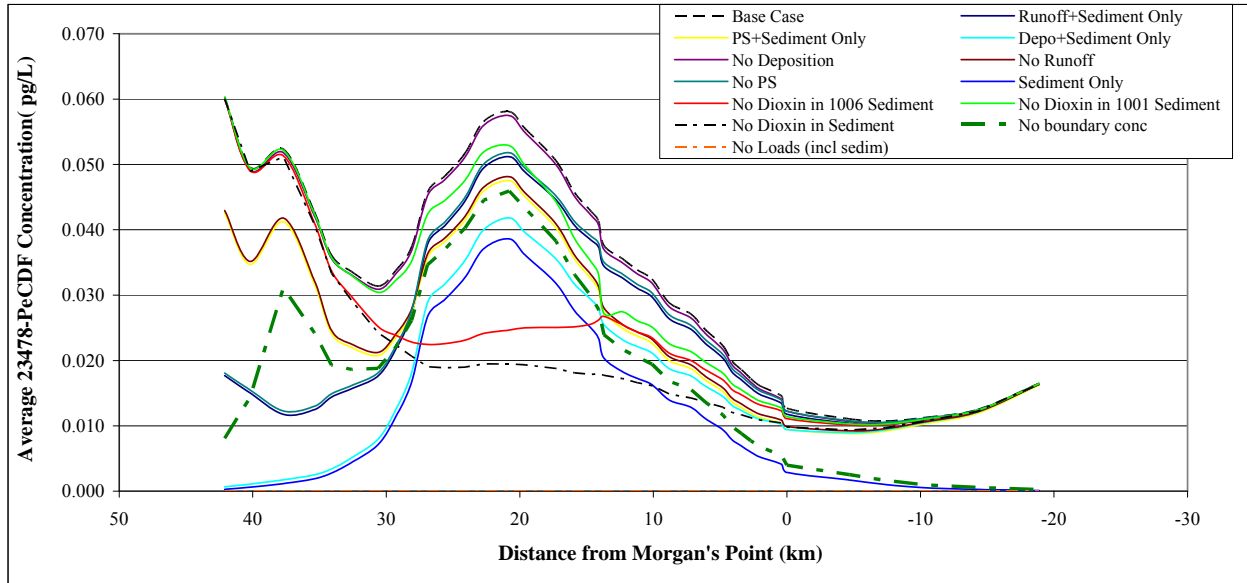


Figure 3.25e 23478-PeCDF Load Scenarios

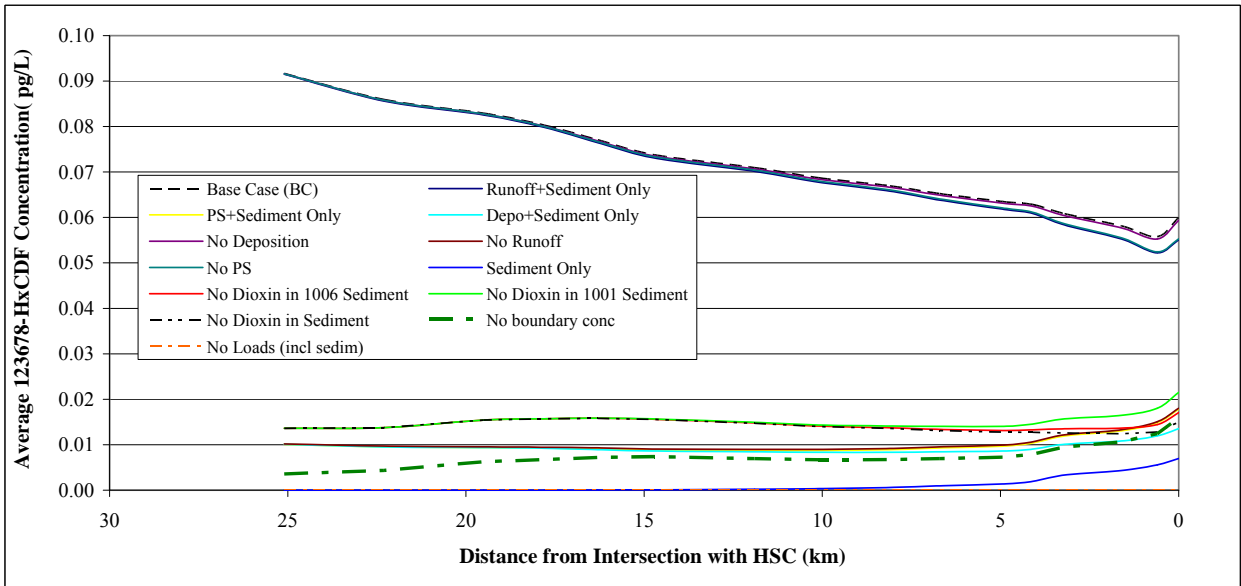
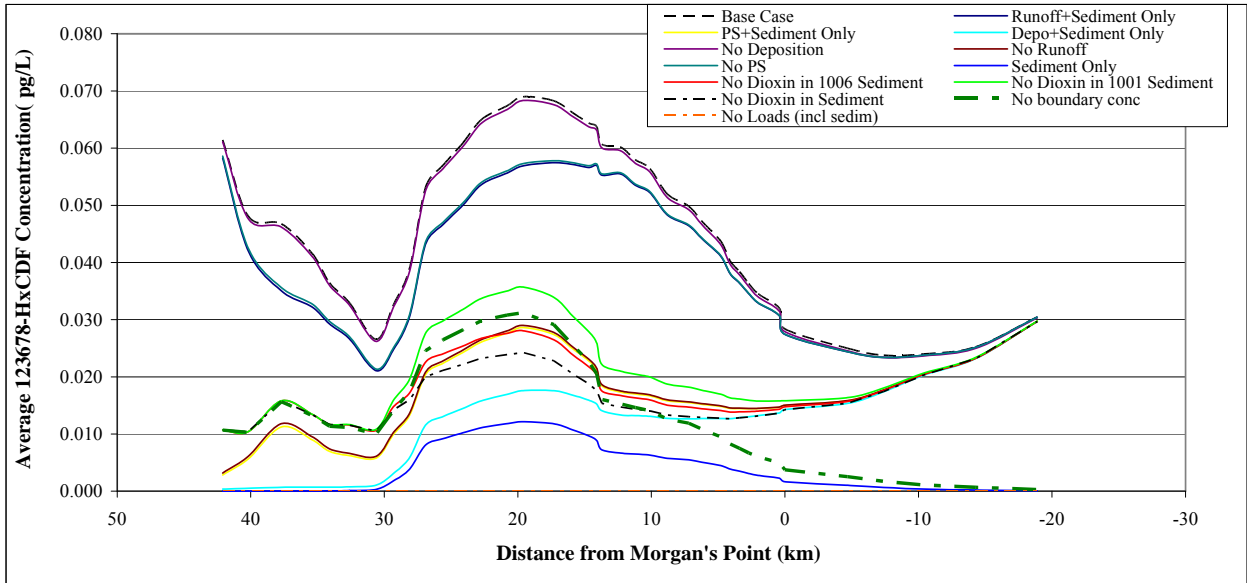


Figure 3.25f 123678-HxCDF Load Scenarios

CHAPTER 4

SPREADSHEET APPROACH TO SUMMARIZE WASP RESULTS AND OBTAIN LOADS ACROSS WATER QUALITY SEGMENTS

This section presents a mass-balance spreadsheet tool developed for this project. The dioxin load spreadsheet can be used to provide insight into the relative magnitude of the different sources of dioxins to the HSC as well as a means to summarize long data sets obtained from the dioxin models described in the previous chapter. The spreadsheet provides estimates of sources of the six selected congeners to the HSC by segment and compares them to estimated (modeled) in-stream loads.

The model system (RMA2 + WASP) used for the HSC dioxin project integrates the basic dioxin conceptual equation across time and space, while incorporating transport and other physical phenomena that affect water quality. The summary spreadsheet organizes the model results into long-term averages amenable to use in the TMDL equation. Stated as an illustrative “equation”, the model predicts

Water quality = function of (*flow, physical processes, point source, runoff, direct deposition, upstream loads, sediment loads*)
or, in shorter form,

$$WQ = f(Q, PhysProc, PS, RO, DD, U/S, Sed)$$

It should be noted that in the equation above, *Sed* represents the effect of sediment-source loading on predicted water column concentrations. Running the model does require that initial bed sediment concentrations be specified and those were established based on field data and through the model calibration process (Figure 4.1).

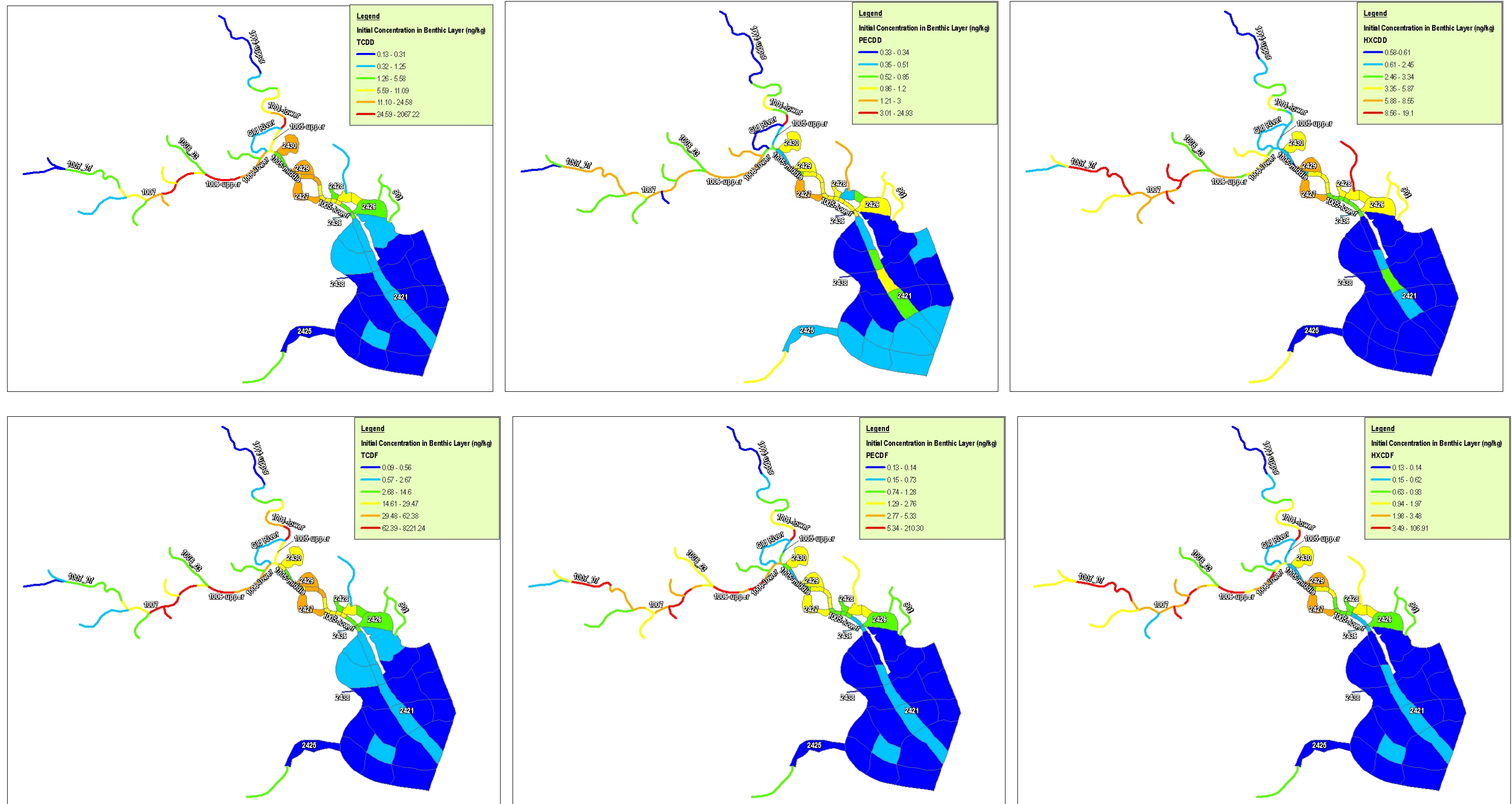


Figure 4.1 Distribution of Initial Dioxin Concentrations in Sediment in the WASP Models

4.1 SPREADSHEET CONCEPTUAL MODEL

An initial version of the spreadsheet calculated the load leaving a given water quality (WQ) segment as the product of the average flow at the most downstream WASP reach within the WQ segment and the average concentration of the same WASP reach (University of Houston and Parsons 2007). The averages were calculated using WASP output for the entire simulation period (07/20/2002 to 04/30/2005). This approach was found to be inappropriate because the product of average flow and average concentration is not equal to the average flux (or load) leaving the WQ segment. Consequently, the spreadsheet was modified to calculate loads for every time-step, which were subsequently used to calculate average loads. Calculations were completed using the same time-step used for the hydrodynamic RMA2 model (30 minutes).

In addition, to solve any flow/mass balance issues, the spreadsheet was extensively restructured to account for fluxes of dioxin across each interface for a given WQ segment. Figure 4.2 shows the conceptual model for a generic WQ segment.

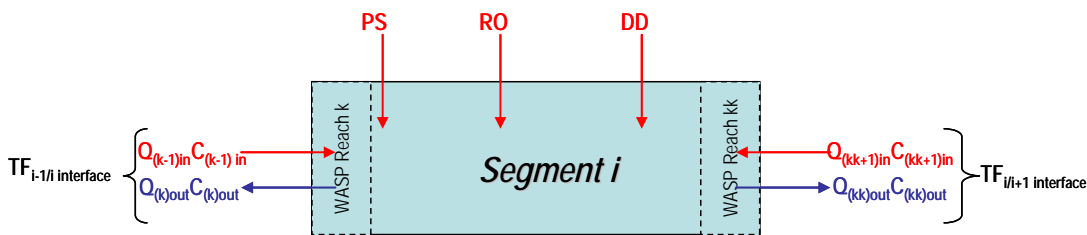


Figure 4.2 Conceptual Model for Mass-Balance Spreadsheet

The conceptual basic equation for the spreadsheet summary of model results is:

$$PS + RO + DD + U/S + \Sigma(Q_{ini} * C_i) \pm dS = net\ load = \Sigma(Q_{outi} * C_{average})$$

The model predicts water quality as a function of loads, flows, transport, settling/

resuspension, etc. Using the calibrated model, water quality in the form of “net load” is predefined by the observed conditions within the channel. Loading from point sources, runoff, and direct deposition, plus flows, transport, and settling/resuspension, were also predetermined based on calibration. In the spreadsheet, the HSC system was divided into 21 intercommunicated segments as shown in Figure 4.3.

Figure 4.4 presents schematics of all the WQ segments in the HSC to aid in understanding how the spreadsheet was built. In Figure 4.4 and subsequent calculations, “Gross Load” refers to the loadings that enters the segment from any external source, before any loss or assimilation; thus, gross load is calculated as the sum of PS, RO, DD, U/S, and incoming tidal flux [$\Sigma(Q_{in} * C_{in})$]. “Net Load” refers to the load that exits the segment in any direction (similar concept to the “In-stream Load” column in the previous version of the spreadsheet). The net load is compared to water quality standards to determine if attainment is reached or if loads need to be reduced to attain it.

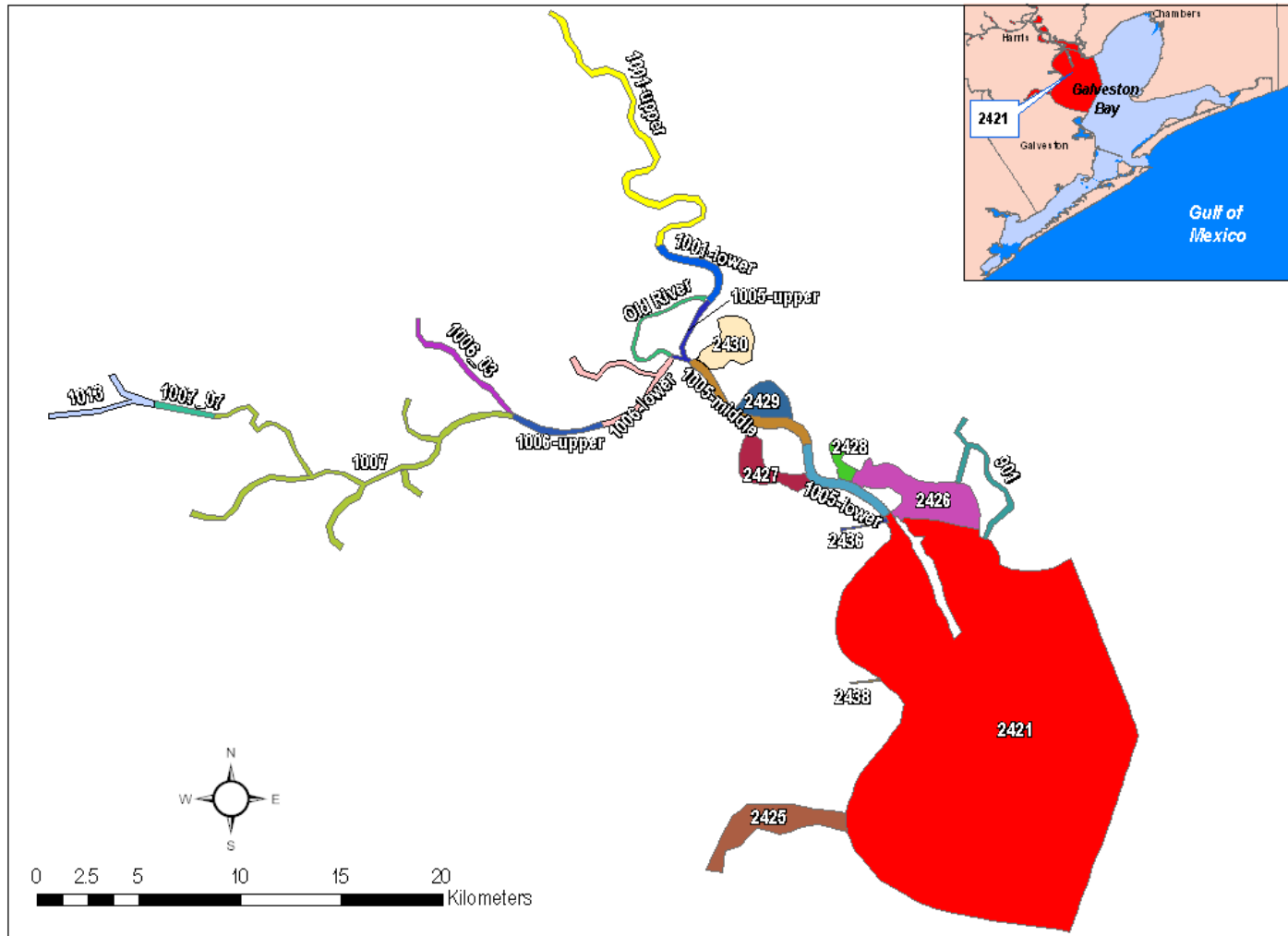


Figure 4.3 Spreadsheet Segmentation

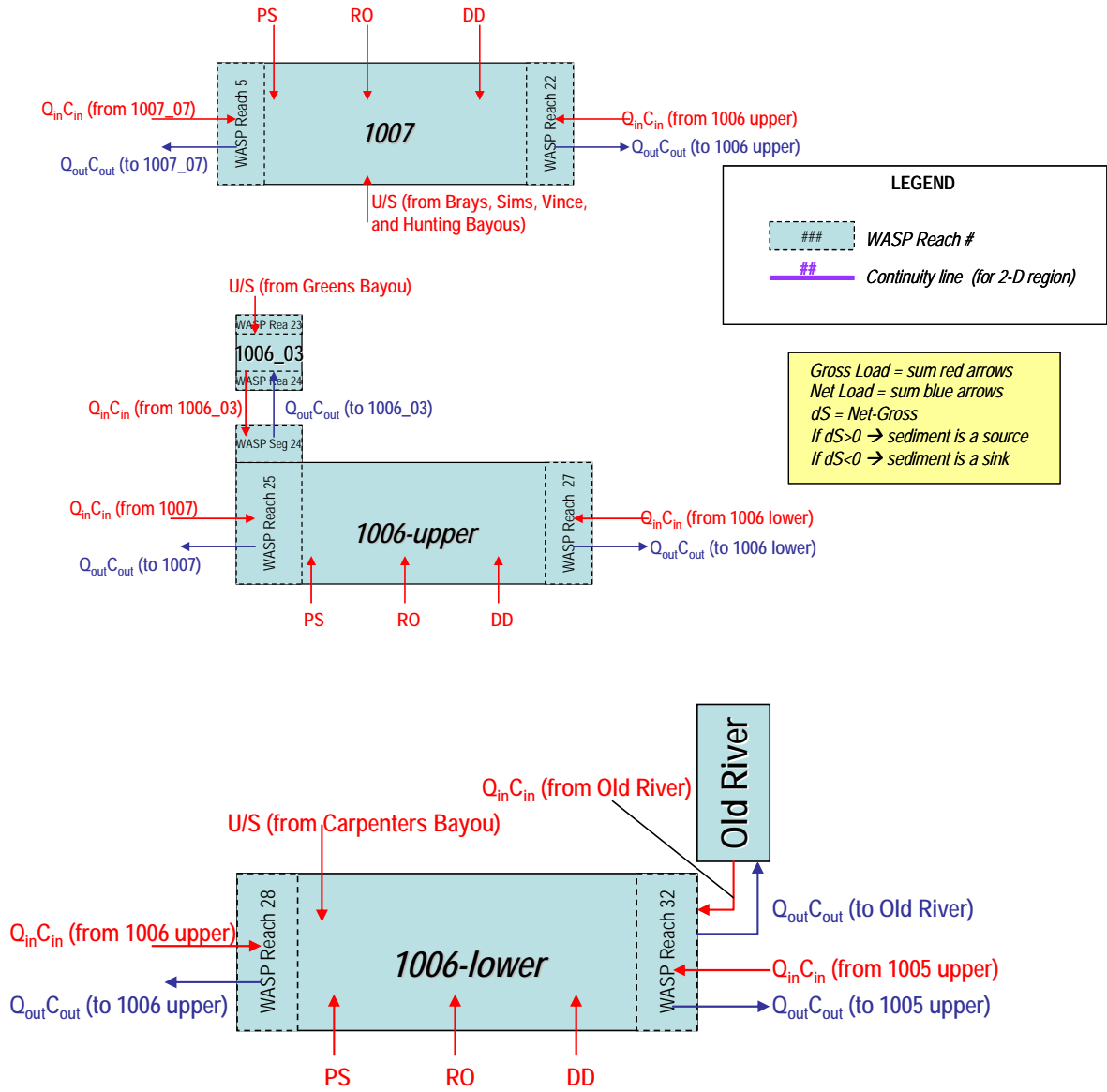


Figure 4.4 Schematic of Mass-balance Spreadsheet for the Houston Ship Channel

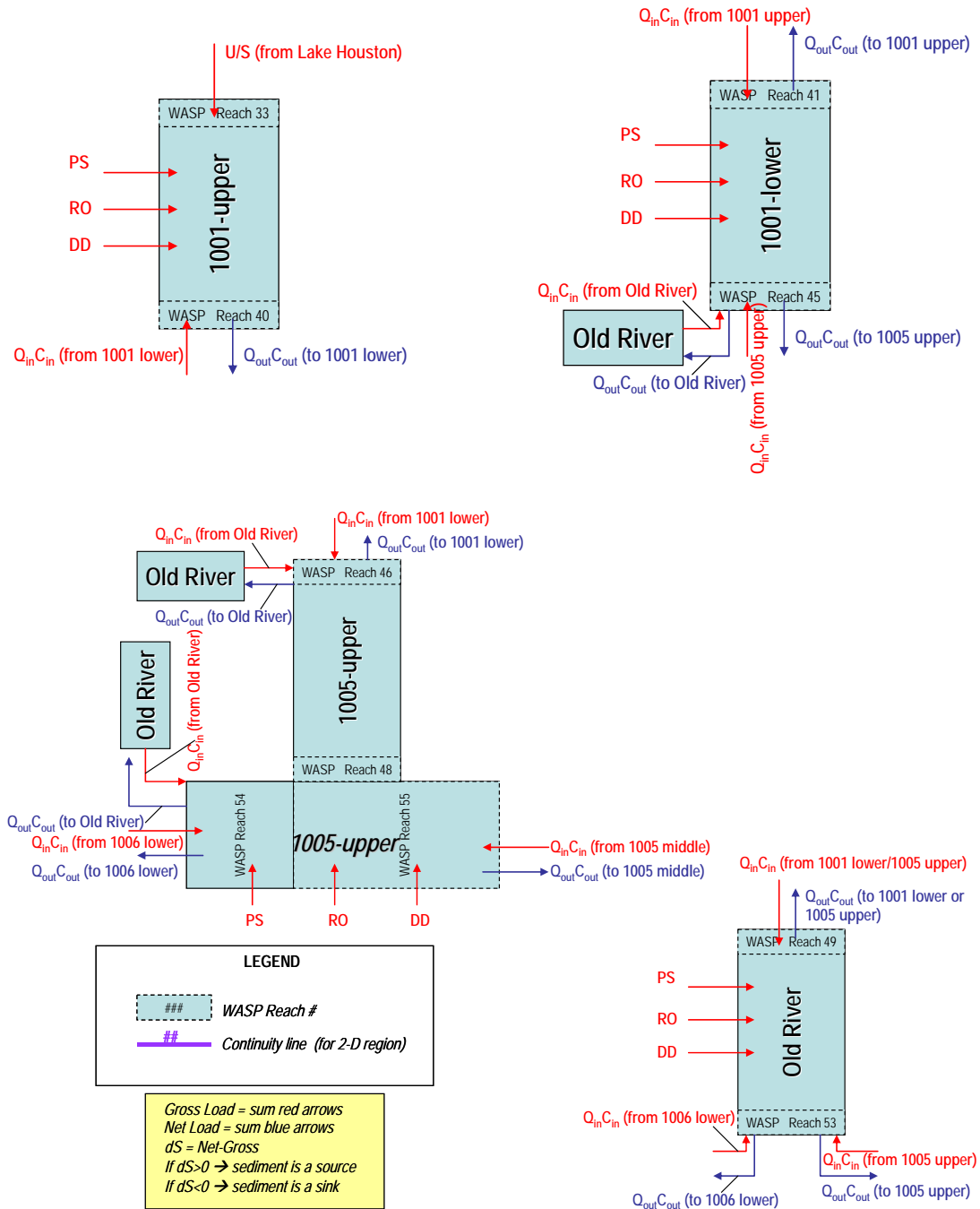


Figure 4.4 Schematic of Mass-balance Spreadsheet for the Houston Ship Channel-Cont'd

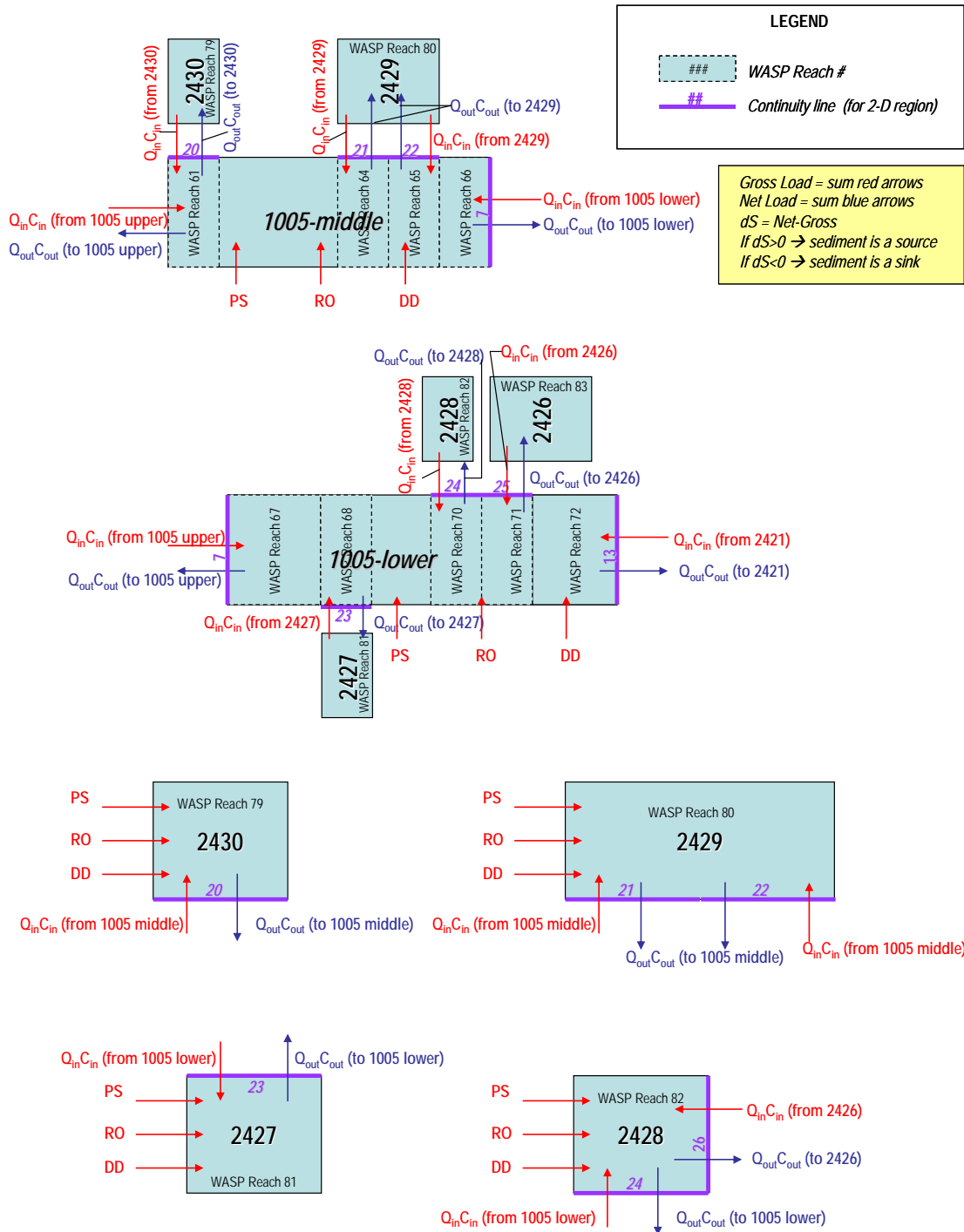


Figure 4.4 Schematic of Mass-balance Spreadsheet for the Houston Ship Channel-Cont'd

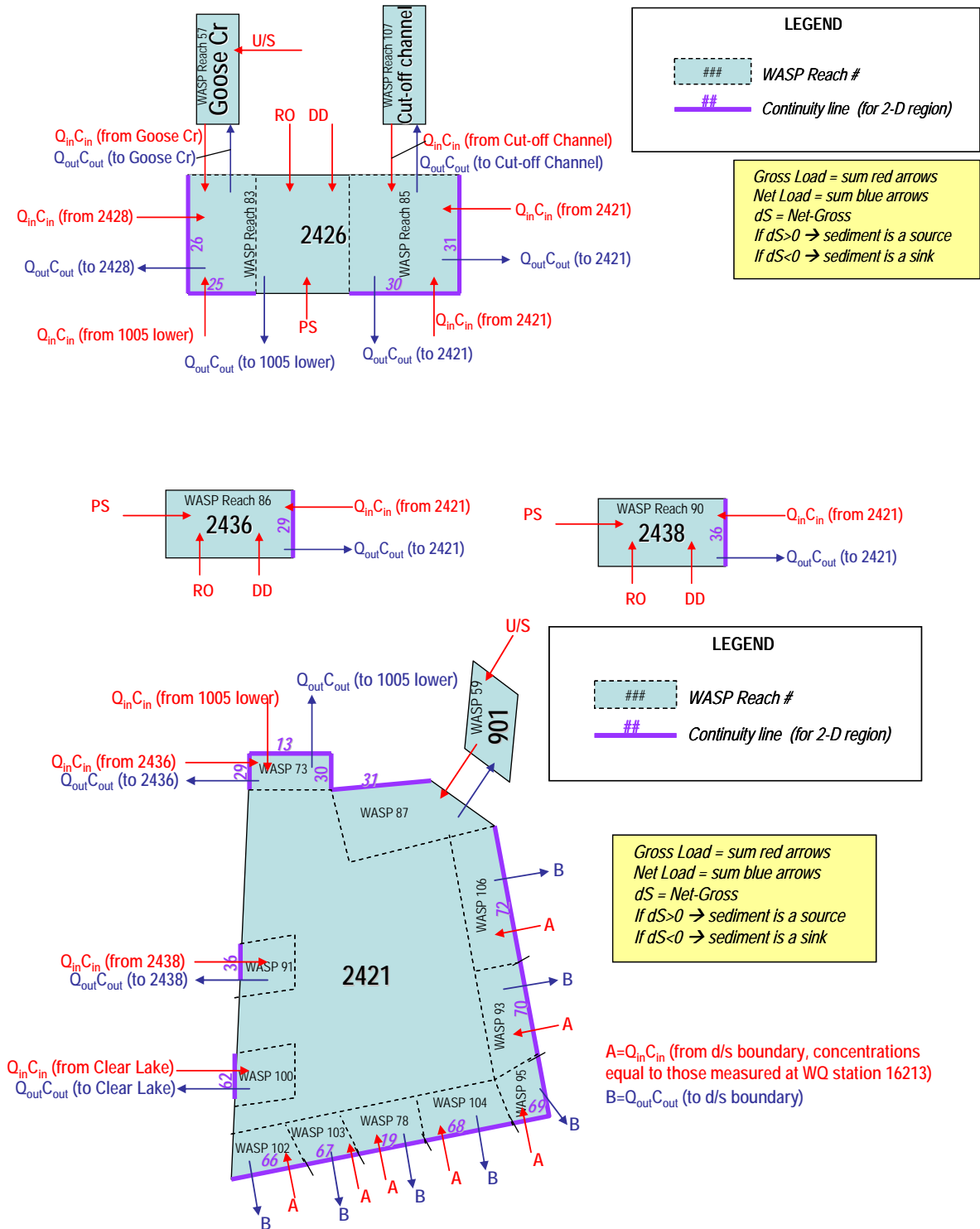


Figure 4.4 Schematic of Mass-balance Spreadsheet for the Houston Ship Channel-Cont'd

4.2 SOURCE LOADS BY WATER QUALITY SEGMENT

Point and non-point source loadings discharging to each of the segments defined in the spreadsheet were calculated. Four main sources were considered in this assessment: (i) point sources; (ii) wet weather (runoff) loadings, (iii) upstream loads (outside model domain), and (iv) direct wet/dry deposition to the HSC surface area. These loads were input to the WASP models either as boundary concentrations (associated with a flow) or as direct loads (see Chapter 3).

4.2.1 Point Source Loads

The procedure followed to determine the point source loads into the HSC System was described in Section 3.2.3. For the spreadsheet tool, PS loads were summarized by segment as shown in Table 4.1. Note that these loads include those discharged directly to the WASP reaches only, not the ones at the upstream boundaries. Estimated PS daily loads were 38,702 ng for 2378-TCDD, 61,624 ng for 12378-PeCDD, 76,078 ng for 123678-HxCDD, 356,033 ng for 2378-TCDF, 139,429 ng for 23478-PeCDF, and 166,912 ng for 123678-HxCDF.

Table 4.1 Estimated Loads from Point Sources

SEGMENT	REPORTED FLOW (m ³ /s) ^a	LOAD (ng/day)						ΣTEQ _{major congeners}
		2378-TCDD	12378-PeCDD	123678-HxCDD	2378-TCDF	23478-PeCDF	123678-HxCDF	
<i>TEF</i>		<i>1</i>	<i>0.5</i>	<i>0.1</i>	<i>0.1</i>	<i>0.5</i>	<i>0.1</i>	
1013	0	0	0	0	0	0	0	0
1007_07	0.0004	0	0	0	0	0	0	0
1007	7.6	18,066	41,316	44,917	278,916	84,727	35,910	117,060
1006_03	0.3	564	918	416	3,709	1,545	895	2,297
1006-upper	1.4	6,511	6,432	12,076	28,340	25,669	87,860	35,389
1006-lower	1.3	5,775	5,238	9,076	14,224	14,037	23,260	20,068

SEGMENT	REPORTED FLOW (m ³ /s) ^a	LOAD (ng/day)						ΣTEQ _{major congeners}
		2378-TCDD	12378-PeCDD	123678-HxCDD	2378-TCDF	23478-PeCDF	123678-HxCDF	
1001-upper	0.3	1,893	2,023	2,088	9,980	2,075	828	5,232
1001-lower	0.2	681	419	519	1,274	837	1,200	1,608
Old River	0.1	210	415	254	708	306	371	704
1005-upper	0.05	135	106	463	1,392	1,721	5,810	1,815
1005-middle	0.1	187	487	801	1,910	2,300	2,950	2,147
1005-lower	0.8	1,930	894	894	4,670	1,590	887	3,817
2430	0	-	-	-	-	-	-	0
2429	0.01	46	26	102	355	211	403	251
2427	0.2	610	293	1,333	2,394	693	477	1,523
2428	0	-	-	-	-	-	-	0
2426	0.2	355	362	651	2,161	849	576	1,299
2436	0.01	39	41	42	92	45	95	105
2438	0.5	1,070	1,240	1,780	3,840	2,050	4,960	3,773
901	0.001	0	0	0	0	0	0	0
2421	0.3	631	1,414	667	2,068	775	431	2,042
TOTAL	13.1	38,702	61,624	76,078	356,033	139,429	166,912	199,132

^a From self-reporting database as of 2003

^b Σ TEQ from six selected congeners

Non-detects assumed as 1/2 MDL

Segments 2430 and 2428 do not have point sources. Segments 1007_07 and 901 have point sources with SIC codes that were not identified as potential dioxin sources, thus, the estimated loads are zero.

4.2.2 Runoff Loads

As stated in Section 3.2.3, runoff flows were determined via the SCS runoff curve number method (Natural Resource Conservation Service, 1986). Wet weather loadings were then computed using the dioxin concentrations in runoff measured in 2003 and 2005 as part of this project. The resulting daily loads by segment are summarized in Table 4.2. The estimated loads for individual congeners ranged from 32 to 149,220 ng/day. The total TEQ from the main congeners discharged to the system is about 299 thousand ng/day.

Table 4.2 Estimated Dioxin Runoff Loads by Subwatershed

SEGMENT	AVERAGE FLOW (m ³ /s)	LOAD (ng/day)						
		2378-TCDD	12378-PeCDD	123678-HxCDD	2378-TCDF	23478-PeCDF	123678-HxCDF	ΣTEQ _{major congeners} ^a
<i>TEF</i>		<i>1</i>	<i>0.5</i>	<i>0.1</i>	<i>0.1</i>	<i>0.5</i>	<i>0.1</i>	
1013	0.6	1,291	5,970	23,900	8,690	4,600	16,480	11,483
1007_07	0.8	1,160	5,380	21,500	7,830	4,140	14,800	10,333
1007	3.3	8,074	37,256	149,220	54,294	28,740	102,900	71,713
1006_03	0.6	2,256	10,430	41,700	15,140	8,040	28,780	20,053
1006-upper	0.8	1,221	5,650	22,650	8,220	4,360	15,590	10,872
1006-lower	0.8	1,210	5,593	22,383	8,151	4,309	15,453	10,760
1001-upper	2.6	3,856	17,822	71,230	25,945	13,743	49,165	34,273
1001-lower	0.2	245	1,130	4,523	1,643	871	3,120	2,174
Old River	0.3	464	2,140	8,573	3,118	1,651	5,917	4,120
1005-upper	0.04	62	284	1,139	414	219	785	547
1005-middle	0.2	328	1,517	6,059	2,204	1,169	4,186	2,916
1005-lower	0.1	124	574	2,293	835	441	1,582	1,103
2430	0.1	176	811	3,250	1,180	625	2,240	1,561
2429	0.4	539	2,490	9,980	3,630	1,920	6,880	4,793
2427	0.6	878	4,060	16,200	5,910	3,130	11,200	7,804
2428	0.1	111	515	2,060	749	397	1,420	990
2426	0.9	1,331	6,148	24,617	8,959	4,743	16,989	11,833
2436	0.05	72	333	1,330	485	257	919	640
2438	0.02	32	149	596	217	115	411	287
901	1.2	2,577	11,890	47,600	17,310	9,170	32,900	22,888
2421	1.3	1,967	9,085	36,362	13,221	7,002	25,073	17,476
2425	0.01	5,680	26,300	105,000	38,200	20,200	72,500	50,500
TOTAL	15.3	33,652	155,528	622,165	226,344	119,843	429,290	299,117

^a Σ TEQ from six selected congeners
Non-detects assumed as 1/2 MDL

4.2.3 Upstream Loads

This group of loads corresponds to PS and runoff loads discharged to the major freshwater tributaries to the HSC, outside the model domain. These loads were entered into the WASP models as boundary concentrations associated with fresh water inflows (see Section 3.2.2). Table 4.3 summarizes the upstream loads by segment.

Table 4.3 Estimated Dioxin Loads from Upstream Tributaries

SEGMENT	TRIBUTARY	LOAD (ng/day)						Σ TEQ _{major congeners} ^a
		2378-TCDD	12378-PeCDD	123678-HxCDD	2378-TCDF	23478-PeCDF	123678-HxCDF	
TEF		1	0.5	0.1	0.1	0.5	0.1	
1013	Buffalo Bayou	51,504	146,697	413,540	161,323	73,373	703,333	289,358
	Whiteoak Bayou	12,219	34,016	161,873	72,966	26,680	78,852	73,936
1007	Brays Bayou	35,839	79,145	215,329	97,127	51,556	116,796	144,115
	Sims Bayou	5,177	11,050	24,885	20,921	10,822	15,837	22,277
	Vince Bayou	797	3,688	14,754	5,368	2,841	10,177	7,092
	Hunting Bayou	3,019	17,565	73,106	34,136	21,141	34,258	36,522
1006_03	Greens Bayou	17,384	53,720	205,274	67,838	53,418	82,847	106,549
1006-lower	Carpenters Bayou	1,731	6,511	22,681	9,153	4,960	16,236	12,273
1001-upper	Lake Houston discharge	245,924	656,825	2,849,210	1,373,063	601,729	1,685,239	1,465,952
2426	Goose Creek	1,567	9,297	47,565	4,208	2,567	7,241	13,401
901	Cedar Bayou	1,507	5,124	17,645	10,366	5,314	14,262	10,954
TOTAL		376,669	1,023,637	4,045,863	1,856,467	854,401	2,765,078	2,182,429

^a Σ TEQ from six selected congeners
Non-detects assumed as 1/2 MDL

4.2.4 Direct Deposition Loads

Deposition loads were estimated using the dry/wet deposition fluxes measured in this project¹⁰ multiplied by the area of the different water quality segments (see Section 3.2.3). Only direct deposition to the channel was included since deposition to the watershed is ultimately carried to the channel via runoff and, thus, was included in the wet weather load calculation. Table 4.4 presents a summary of deposition loads by segment. Deposition loads from the six major congeners varied from 69 to 419,345 ng/day. The total TEQ load discharged to the system (from the six major congeners) is 452,897 ng/day.

¹⁰ Measured dry deposition fluxes were 0.62, 0.97, 1.75, 0.7, 0.9, and 0.65 pg/m²/day, for TCDD, PeCDD,

Table 4.4 Dioxin Loads from Direct Deposition

Segment	Area (m ²)	Average Load (ng/day) ^a						Σ TEQ _{major} ^b congeners
		2378-TCDD	12378-PeCDD	123678-HxCDD	2378-TCDF	23478-PeCDF	123678-HxCDF	
<i>TEF</i>		<i>1</i>	<i>0.5</i>	<i>0.1</i>	<i>0.1</i>	<i>0.5</i>	<i>0.1</i>	
1013	256,000	104	254	492	204	248	197	444
1007_07	151,000	61	149	289	120	146	116	261
1007	3,993,000	1,611	3,946	7,662	3,168	3,866	3,062	6,906
1006_03	458,000	185	453	885	367	446	356	795
1006-upper	1,403,000	566	1,389	2,724	1,133	1,372	1,100	2,442
1006-lower	1,752,000	708	1,735	3,406	1,417	1,717	1,377	3,053
1001-upper	1,781,000	720	1,764	3,454	1,436	1,743	1,394	3,102
1001-lower	758,000	305	746	1,450	600	732	580	1,307
Old River	772,000	312	763	1,494	620	754	602	1,342
1005-upper	954,000	385	944	1,838	763	928	737	1,655
1005-middle	3,491,000	1,409	3,453	6,755	2,802	3,404	2,716	6,065
1005-lower	2,705,000	1,090	2,668	5,154	2,132	2,610	2,057	4,663
2430	4,581,000	1,850	4,520	8,780	3,640	4,440	3,510	7,923
2429	3,495,000	1,410	3,460	6,750	2,800	3,410	2,720	6,072
2427	3,928,000	1,460	3,880	7,590	3,150	3,830	3,050	6,694
2428	1,243,000	501	1,230	2,400	996	1,210	965	2,157
2426	10,354,000	4,169	10,204	19,723	8,122	9,962	7,810	17,817
2436	225,000	91	221	424	174	215	167	385
2438	171,000	69	168	322	132	163	127	292
901	253,000	102	250	489	203	247	197	439
2421	218,952,000	88,287	216,174	419,345	173,663	211,933	167,681	378,409
2425	387,000	156	383	751	312	378	303	673
TOTAL	262,063,000	105,549	258,753	502,177	207,953	253,754	200,823	452,897

^a Calculated as measured flux times surface area^b Σ TEQ from six selected congeners

Non-detects assumed as 1/2 MDL

4.3 LOADS ACROSS SEGMENT BOUNDARIES

The steps followed to build spreadsheets for the various WQ segments by congener are described below:

HxCDD, TCDF, PeCDF, and HxCDF, respectively. Wet deposition fluxes were 1.1, 2.15, 13, 7, 5.5, and 8.5 pg/m²/day, for the six congeners respectively.

1. Find flows in and out of the WASP reaches at each end of the WQ segment. These are the flows obtained using the RMA2 output and the HSCREAD interface.
2. Copy dioxin concentrations for the WASP reaches next to all interfaces of a WQ segment. This includes the WASP reaches within the WQ segment and their adjacent counterparts outside the WQ segment. For example, in the generic case depicted in Figure 4.2, not only are the concentrations for WASP reaches k and kk (within the WQ segment) needed, but also those for reaches $k-1$ and $kk+1$.
3. Calculate the time-step-based individual $(Q_{in} * C_{in})\Delta t$ and $(Q_{out} * C_{out})\Delta t$ terms appropriate for each WQ segment, based on how it is connected to others within the system.
4. Sum the $(Q_{in} * C_{in})\Delta t$ and $(Q_{out} * C_{out})\Delta t$ terms for each segment by time-step. These calculations correspond respectively to the mass in and out of the segment during a given time-step.
5. Add the sums obtained in the previous step for the entire simulation period and divide by the number of days in the simulation (1015 days). This results in average daily loads in and out of the WQ segment.
6. Derive the dS term for each segment using a mass-balance equation (units of each term are $[MT^{-1}]$):

$$PS + RO + DD + U/S + \Sigma(Q_{in} * C_{in}) - \Sigma(Q_{out} * C_{out}) \pm dS = 0 \quad (4.1)$$

where PS is sum of point source loads to the WQ segment, RO is the sum of runoff loads to the segment, DD is the deposition load to the segment, and dS is “delta

Summary daily load calculations for the six dioxin congeners are presented in Tables 4.5 through 4.10. Overall, sediment is an internal source of contamination for 2378-TCDD and 2378-TCDF, whereas sediment acts as a sink for 12378-PeCDD, 123678-HxCDD, 23478-PeCDF, and 123678-HxCDF. Figure 4.6 includes the distribution of dS values for the six modeled congeners.

The six individuals spreadsheets were combined into a single TEQ spreadsheet. This was accomplished by adding the columns from the various spreadsheets weighted by the respective toxicity equivalent factor (TEF). Table 4.11 presents the summary of the TEQ_{major congeners} calibration spreadsheet. The total sediment-source dioxin load into the system (sum of positive dS values) was calculated to be 19,517,672 ng/day, which corresponds to 86 percent of the TEQ load into the system. On the other hand, 12,315,933 ng TEQ/day (sum of negative dS values) redeposit within the model extent during the simulation period. Therefore, 7,201,739 ng TEQ/day (the total net sediment load) are transported between model segments as sediment, as a daily average over the model period. So sediment transports about 69.7 percent of the average daily dioxin flux among the model segments.

Table 4.5 Mass-balance Spreadsheet for 2378-TCDD

Segment	Description	Average Downstream Net Flow ^a (m ³ /s)	Loads (ng/day)								% total load from sediment ^d
			PS	RO	DD	U/S ^b	ΣCinQin	ΣCoutQout	dS ^c	dS action	
1013	Buffalo Bayou	23.5	0	1,291	104	63,723	1,266	54,644	-11,740	SINK	
1007_07	Buffalo Bayou Tidal/HSC	23.6	0	1,160	61		58,995	58,863	-1,353	SINK	
1007	1007	41.0	18,066	8,074	1,611	44,832	1,705,784	3,405,502	1,627,135	SOURCE	95.7%
1006_03	Greens Bayou	9.1	564	2,256	185	17,384	157,297	148,268	-29,418	SINK	
1006-upper	1006-upper	50.1	6,511	1,221	566		5,554,995	6,567,047	1,003,754	SOURCE	99.2%
1006-lower	1006-lower	50.4	5,775	1,210	708	1,731	6,650,733	6,033,466	-626,691	SINK	
1001-upper	San Jacinto River	138.1	1,893	3,856	720	245,924	1,119,999	2,203,061	830,669	SOURCE	76.7%
1001-lower	San Jacinto River	137.9	681	245	305		4,722,838	8,490,536	3,766,467	SOURCE	100.0%
Old River	Old River	-0.5	210	464	312		1,819,200	2,119,314	299,129	SOURCE	99.7%
1005-upper	1005-upper	188.3	135	62	385		13,314,965	18,466,875	5,151,329	SOURCE	100.0%
2430	Burnett Bay	-0.012		176	1,850		688,651	713,323	22,647	SOURCE	91.8%
2429	Scott Bay	-0.009	46	539	1,410		580,176	569,089	-13,083	SINK	
1005-middle	1005-middle	188.2	187	328	1,409		17,779,450	12,333,686	-5,447,689	SINK	
2427	San Jacinto Bay	-0.009	610	878	1,460		431,922	468,722	33,852	SOURCE	92.0%
2428	Black Duck Bay	-0.002		111	501		230,925	190,020	-41,517	SINK	
2426	Tabbs Bay	1.7	355	1,331	4,169	1,567	1,844,547	2,443,112	591,143	SOURCE	98.8%
2436	Barbours Cut	-0.0005	39	72	91		19,685	21,840	1,953	SOURCE	90.7%
1005-lower	1005-lower	186.9	1,930	124	1,090		11,482,660	13,807,108	2,321,304	SOURCE	99.9%
2438	Bayport Channel	0.0001	1,070	32	69		6,343	6,892	-622	SINK	
2421	Upper Galveston Bay	209.1	631	1,967	88,287		12,035,856	10,659,027	-1,467,714	SINK	
901	Cedar Bayou	2.7	0	2,577	102	1,507	72,212	67,049	-9,349	SINK	
2425	Clear Lake	2.0		5,680	156		265,393	281,795	10,566	SOURCE	64.4%
OVERALL			38,702	33,652	105,549	376,669	80,543,891	89,109,237	8,010,774	SOURCE	93.5%

^a Average of flows across downstream boundary of segment (includes both positive and negative flows). Averaging was completed on a time-step basis.

^b Load from upstream freshwater streams outside the HSC System (Table 4.3)

^c ΣQoutCout - (PS+RO+DD+ΣQinCin) = dS. Values for PS, RO, and DD were obtained from Tables 4.1, 4.2, and 4.4, respectively.

^d dS/(PS+RO+DD+U/S+dS)

Table 4.6 Mass-balance Spreadsheet for 12378-PeCDD

Segment	Description	Average Downstream Net Flow ^a (m ³ /s)	Loads (ng/day)								% total load from sediment ^d
			PS	RO	DD	U/S ^b	ΣCinQin	ΣCoutQout	dS ^c	dS action	
1013	Buffalo Bayou	23.5	0	5,970	254	180,713	1,055	135,270	-52,722	SINK	
1007_07	Buffalo Bayou Tidal/HSC	23.6	0	5,380	149		137,702	120,600	-22,631	SINK	
1007	1007	41.0	41,316	37,256	3,946	111,448	172,943	285,937	-80,971	SINK	
1006_03	Greens Bayou	9.1	918	10,430	453	53,720	4,899	41,926	-28,495	SINK	
1006-upper	1006-upper	50.1	6,432	5,650	1,389		266,012	269,822	-9,661	SINK	
1006-lower	1006-lower	50.4	5,238	5,593	1,735	6,511	309,268	302,946	-25,399	SINK	
1001-upper	San Jacinto River	138.1	2,023	17,822	1,764	656,825	36,205	417,979	-296,660	SINK	
1001-lower	San Jacinto River	137.9	419	1,130	746		487,515	494,359	4,549	SOURCE	66.5%
Old River	Old River	-0.5	415	2,140	763		85,752	85,824	-3,246	SINK	
1005-upper	1005-upper	188.3	106	284	944		755,494	1,566,958	810,130	SOURCE	99.8%
2430	Burnett Bay	-0.012		811	4,520		51,884	52,275	-4,939	SINK	
2429	Scott Bay	-0.009	26	2,490	3,460		71,541	69,665	-7,852	SINK	
1005-middle	1005-middle	188.2	487	1,517	3,453		1,740,306	1,561,517	-184,246	SINK	
2427	San Jacinto Bay	-0.009	293	4,060	3,880		36,581	36,142	-8,672	SINK	
2428	Black Duck Bay	-0.002		515	1,230		15,301	14,990	-2,056	SINK	
2426	Tabbs Bay	1.7	362	6,148	10,204	9,297	150,077	140,882	-35,204	SINK	
2436	Barbours Cut	-0.0005	41	333	221		1,671	1,699	-567	SINK	
1005-lower	1005-lower	186.9	894	574	2,668		1,538,808	1,336,585	-206,359	SINK	
2438	Bayport Channel	0.0001	1,240	149	168		1,139	1,144	-1,552	SINK	
2421	Upper Galveston Bay	209.1	1,414	9,085	216,174		4,752,804	3,531,533	-1,447,944	SINK	
901	Cedar Bayou	2.7	0	11,890	250	5,124	5,463	19,977	-2,750	SINK	
2425	Clear Lake	2.0		26,300	383		50,681	39,865	-37,499	SINK	
OVERALL			61,624	155,528	258,753	1,023,637	10,673,100	10,527,896	-1,644,747	SINK	

^a Average of flows across downstream boundary of segment (includes both positive and negative flows). Averaging was completed on a time-step basis.

^b Load from upstream freshwater streams outside the HSC System (Table 4.3)

^c ΣQoutCout - (PS+RO+DD+ΣQinCin) = dS. Values for PS, RO, and DD were obtained from Tables 4.1, 4.2, and 4.4, respectively.

^d dS/(PS+RO+DD+U/S+dS)

Table 4.7 Mass-balance Spreadsheet for 123678-HxCDD

Segment	Description	Average Downstream Net Flow ^a (m ³ /s)	Loads (ng/day)								% total load from sediment ^d
			PS	RO	DD	U/S ^b	ΣCinQin	ΣCoutQout	dS ^c	dS action	
1013	Buffalo Bayou	23.5	0	23,900	492	575,414	3,012	454,447	-148,370	SINK	
1007_07	Buffalo Bayou Tidal/HSC	23.6	0	21,500	289		459,325	429,859	-51,255	SINK	
1007	1007	41.0	44,917	149,220	7,662	328,075	670,373	1,216,234	15,987	SOURCE	2.9%
1006_03	Greens Bayou	9.1	416	41,700	885	205,274	23,352	210,076	-61,551	SINK	
1006-upper	1006-upper	50.1	12,076	22,650	2,724		1,286,156	1,239,377	-84,229	SINK	
1006-lower	1006-lower	50.4	9,076	22,383	3,406	22,681	1,365,702	1,333,244	-90,003	SINK	
1001-upper	San Jacinto River	138.1	2,088	71,230	3,454	2,849,210	118,970	1,807,020	-1,237,931	SINK	
1001-lower	San Jacinto River	137.9	519	4,523	1,450		2,030,420	1,961,597	-75,315	SINK	
Old River	Old River	-0.5	254	8,573	1,494		341,533	344,598	-7,255	SINK	
1005-upper	1005-upper	188.3	463	1,139	1,838		3,134,314	6,677,073	3,539,319	SOURCE	99.9%
2430	Burnett Bay	-0.012		3,250	8,780		202,073	192,307	-21,795	SINK	
2429	Scott Bay	-0.009	102	9,980	6,750		280,993	272,531	-25,294	SINK	
1005-middle	1005-middle	188.2	801	6,059	6,755		7,361,066	6,256,222	-1,118,459	SINK	
2427	San Jacinto Bay	-0.009	1,333	16,200	7,590		145,263	132,216	-38,170	SINK	
2428	Black Duck Bay	-0.002		2,060	2,400		66,731	64,808	-6,383	SINK	
2426	Tabbs Bay	1.7	651	24,617	19,723	47,565	753,842	694,063	-152,335	SINK	
2436	Barbours Cut	-0.0005	42	1,330	424		8,100	8,093	-1,802	SINK	
1005-lower	1005-lower	186.9	894	2,293	5,154		6,558,848	5,709,915	-857,274	SINK	
2438	Bayport Channel	0.0001	1,780	596	322		6,364	6,321	-2,742	SINK	
2421	Upper Galveston Bay	209.1	667	36,362	419,345		21,797,352	18,090,144	-4,163,583	SINK	
901	Cedar Bayou	2.7	0	47,600	489	17,645	27,750	87,255	-6,230	SINK	
2425	Clear Lake	2.0		105,000	751		328,778	271,555	-162,974	SINK	
OVERALL			76,078	622,165	502,177	4,045,863	46,970,317	47,458,955	-4,757,644	SINK	

^a Average of flows across downstream boundary of segment (includes both positive and negative flows). Averaging was completed on a time-step basis.

^b Load from upstream freshwater streams outside the HSC System (Table 4.3)

^c ΣQoutCout - (PS+RO+DD+ΣQinCin) = dS. Values for PS, RO, and DD were obtained from Tables 4.1, 4.2, and 4.4, respectively.

^d dS/(PS+RO+DD+U/S+dS)

Table 4.8 Mass-balance Spreadsheet for 2378-TCDF

Segment	Description	Average Downstream Net Flow ^a (m ³ /s)	Loads (ng/day)								% total load from sediment ^d
			PS	RO	DD	U/S ^b	ΣCinQin	ΣCoutQout	dS ^c	dS action	
1013	Buffalo Bayou	23.5	0	8,690	204	234,289	5,167	186,710	-61,640	SINK	
1007_07	Buffalo Bayou Tidal/HSC	23.6	0	7,830	120		206,827	211,526	-3,250	SINK	
1007	1007	41.0	278,916	54,294	3,168	157,551	4,571,004	9,225,392	4,160,459	SOURCE	89.4%
1006_03	Greens Bayou	9.1	3,709	15,140	367	67,838	414,734	422,717	-79,071	SINK	
1006-upper	1006-upper	50.1	28,340	8,220	1,133		14,586,873	17,058,722	2,434,156	SOURCE	98.5%
1006-lower	1006-lower	50.4	14,224	8,151	1,417	9,153	16,925,127	15,244,589	-1,713,484	SINK	
1001-upper	San Jacinto River	138.1	9,980	25,945	1,436	1,373,063	3,766,742	7,695,771	2,518,606	SOURCE	64.1%
1001-lower	San Jacinto River	137.9	1,274	1,643	600		15,588,239	28,102,162	12,510,406	SOURCE	100.0%
Old River	Old River	-0.5	708	3,118	620		5,032,239	6,233,069	1,196,384	SOURCE	99.6%
1005-upper	1005-upper	188.3	1,392	414	763		40,037,557	47,006,226	6,966,100	SOURCE	100.0%
2430	Burnett Bay	-0.012		1,180	3,640		1,502,758	1,628,501	120,923	SOURCE	96.2%
2429	Scott Bay	-0.009	355	3,630	2,800		1,255,771	1,229,058	-33,497	SINK	
1005-middle	1005-middle	188.2	1,910	2,204	2,802		39,191,791	25,289,837	-13,908,871	SINK	
2427	San Jacinto Bay	-0.009	2,394	5,910	3,150		566,583	551,625	-26,412	SINK	
2428	Black Duck Bay	-0.002		749	996		208,082	216,222	6,395	SOURCE	78.6%
2426	Tabbs Bay	1.7	2,161	8,959	8,122	4,208	1,730,980	1,783,365	28,935	SOURCE	55.2%
2436	Barbours Cut	-0.0005	92	485	174		20,806	21,410	-148	SINK	
1005-lower	1005-lower	186.9	4,670	835	2,132		18,057,584	16,793,504	-1,271,717	SINK	
2438	Bayport Channel	0.0001	3,840	217	132		12,345	12,339	-4,195	SINK	
2421	Upper Galveston Bay	209.1	2,068	13,221	173,663		32,197,332	29,461,773	-2,924,511	SINK	
901	Cedar Bayou	2.7	0	17,310	203	10,366	52,556	83,213	2,778	SOURCE	9.1%
2425	Clear Lake	2.0		38,200	312		640,443	641,315	-37,641	SINK	
OVERALL			356,033	226,344	207,953	1,856,467	196,571,542	209,099,045	9,880,706	SOURCE	78.9%

^a Average of flows across downstream boundary of segment (includes both positive and negative flows). Averaging was completed on a time-step basis.

^b Load from upstream freshwater streams outside the HSC System (Table 4.3)

^c ΣQoutCout - (PS+RO+DD+ΣQinCin) = dS. Values for PS, RO, and DD were obtained from Tables 4.1, 4.2, and 4.4, respectively.

^d dS/(PS+RO+DD+U/S+dS)

Table 4.9 Mass-balance Spreadsheet for 23478-PeCDF

Segment	Description	Average Downstream Net Flow ^a (m ³ /s)	Loads (ng/day)								% total load from sediment ^d
			PS	RO	DD	U/S ^b	ΣCinQin	ΣCoutQout	dS ^c	dS action	
1013	Buffalo Bayou	23.5	0	4,600	248	100,053	2,649	696,605	589,055	SOURCE	84.9%
1007_07	Buffalo Bayou Tidal/HSC	23.6	0	4,140	146		702,209	115,327	-591,168	SINK	
1007	1007	41.0	84,727	28,740	3,866	86,360	240,999	999,939	555,247	SOURCE	73.2%
1006_03	Greens Bayou	9.1	1,545	8,040	446	53,418	11,918	50,517	-24,851	SINK	
1006-upper	1006-upper	50.1	25,669	4,360	1,372		521,194	583,468	30,873	SOURCE	49.6%
1006-lower	1006-lower	50.4	14,037	4,309	1,717	4,960	630,187	586,744	-68,465	SINK	
1001-upper	San Jacinto River	138.1	2,075	13,743	1,743	601,729	93,815	578,597	-134,507	SINK	
1001-lower	San Jacinto River	137.9	837	871	732		770,434	946,865	173,991	SOURCE	98.6%
Old River	Old River	-0.5	306	1,651	754		174,043	190,061	13,307	SOURCE	83.1%
1005-upper	1005-upper	188.3	1,721	219	928		1,429,957	2,330,589	897,764	SOURCE	99.7%
2430	Burnett Bay	-0.012		625	4,440		80,516	76,490	-9,090	SINK	
2429	Scott Bay	-0.009	211	1,920	3,410		92,360	90,121	-7,780	SINK	
1005-middle	1005-middle	188.2	2,300	1,169	3,404		2,322,450	1,905,563	-423,760	SINK	
2427	San Jacinto Bay	-0.009	693	3,130	3,830		37,652	35,616	-9,689	SINK	
2428	Black Duck Bay	-0.002		397	1,210		13,930	14,633	-905	SINK	
2426	Tabbs Bay	1.7	849	4,743	9,962	2,567	121,044	106,915	-32,250	SINK	
2436	Barbours Cut	-0.0005	45	257	215		1,313	1,352	-479	SINK	
1005-lower	1005-lower	186.9	1,590	441	2,610		1,585,642	1,242,340	-347,943	SINK	
2438	Bayport Channel	0.0001	2,050	115	163		819	828	-2,319	SINK	
2421	Upper Galveston Bay	209.1	775	7,002	211,933		4,048,632	2,755,826	-1,512,515	SINK	
901	Cedar Bayou	2.7	0	9,170	247	5,314	4,532	19,896	633	SOURCE	4.1%
2425	Clear Lake	2.0		20,200	378		39,462	31,456	-28,584	SINK	
OVERALL			139,429	119,843	253,754	854,401	12,925,756	13,359,749	-933,434	SINK	

^a Average of flows across downstream boundary of segment (includes both positive and negative flows). Averaging was completed on a time-step basis.

^b Load from upstream freshwater streams outside the HSC System (Table 4.3)

^c ΣQoutCout - (PS+RO+DD+ΣQinCin) = dS. Values for PS, RO, and DD were obtained from Tables 4.1, 4.2, and 4.4, respectively.

^d dS/(PS+RO+DD+U/S+dS)

Table 4.10 Mass-balance Spreadsheet for 123678-HxCDF

Segment	Description	Average Downstream Net Flow ^a (m ³ /s)	Loads (ng/day)								% total load from sediment ^d
			PS	RO	DD	U/S ^b	ΣCinQin	ΣCoutQout	dS ^c	dS action	
1013	Buffalo Bayou	23.5	0	16,480	197	782,185	1,714	299,617	-500,960	SINK	
1007_07	Buffalo Bayou Tidal/HSC	23.6	0	14,800	116		303,489	220,051	-98,354	SINK	
1007	1007	41.0	35,910	102,900	3,062	177,068	339,075	656,850	-1,165	SINK	
1006_03	Greens Bayou	9.1	895	28,780	356	82,847	11,346	130,604	6,381	SOURCE	5.4%
1006-upper	1006-upper	50.1	87,860	15,590	1,100		678,093	671,707	-110,936	SINK	
1006-lower	1006-lower	50.4	23,260	15,453	1,377	16,236	780,872	809,240	-27,956	SINK	
1001-upper	San Jacinto River	138.1	828	49,165	1,394	1,685,239	107,610	1,338,030	-506,206	SINK	
1001-lower	San Jacinto River	137.9	1,200	3,120	580		1,491,123	1,445,010	-51,014	SINK	
Old River	Old River	-0.5	371	5,917	602		223,521	227,843	-2,569	SINK	
1005-upper	1005-upper	188.3	5,810	785	737		2,133,999	4,242,749	2,101,418	SOURCE	99.7%
2430	Burnett Bay	-0.012		2,240	3,510		125,498	120,905	-10,343	SINK	
2429	Scott Bay	-0.009	403	6,880	2,720		163,567	158,745	-14,826	SINK	
1005-middle	1005-middle	188.2	2,950	4,186	2,716		4,461,128	3,732,153	-738,827	SINK	
2427	San Jacinto Bay	-0.009	477	11,200	3,050		72,870	68,414	-19,183	SINK	
2428	Black Duck Bay	-0.002		1,420	965		29,480	30,172	-1,693	SINK	
2426	Tabbs Bay	1.7	576	16,989	7,810	7,241	284,694	239,829	-77,480	SINK	
2436	Barbours Cut	-0.0005	95	919	167		2,903	2,956	-1,128	SINK	
1005-lower	1005-lower	186.9	887	1,582	2,057		3,477,831	2,745,554	-736,803	SINK	
2438	Bayport Channel	0.0001	4,960	411	127		1,788	1,810	-5,476	SINK	
2421	Upper Galveston Bay	209.1	431	25,073	167,681		4,486,929	5,254,917	574,803	SOURCE	74.8%
901	Cedar Bayou	2.7	0	32,900	197	14,262	12,309	58,021	-1,647	SINK	
2425	Clear Lake	2.0		72,500	303		92,733	66,985	-98,550	SINK	
OVERALL			166,912	429,290	200,823	2,765,078	19,282,571	22,522,161	-322,513	SINK	

^a Average of flows across downstream boundary of segment (includes both positive and negative flows). Averaging was completed on a time-step basis.

^b Load from upstream freshwater streams outside the HSC System (Table 4.3)

^c ΣQoutCout - (PS+RO+DD+ΣQinCin) = dS. Values for PS, RO, and DD were obtained from Tables 4.1, 4.2, and 4.4, respectively.

^d dS/(PS+RO+DD+U/S+dS)

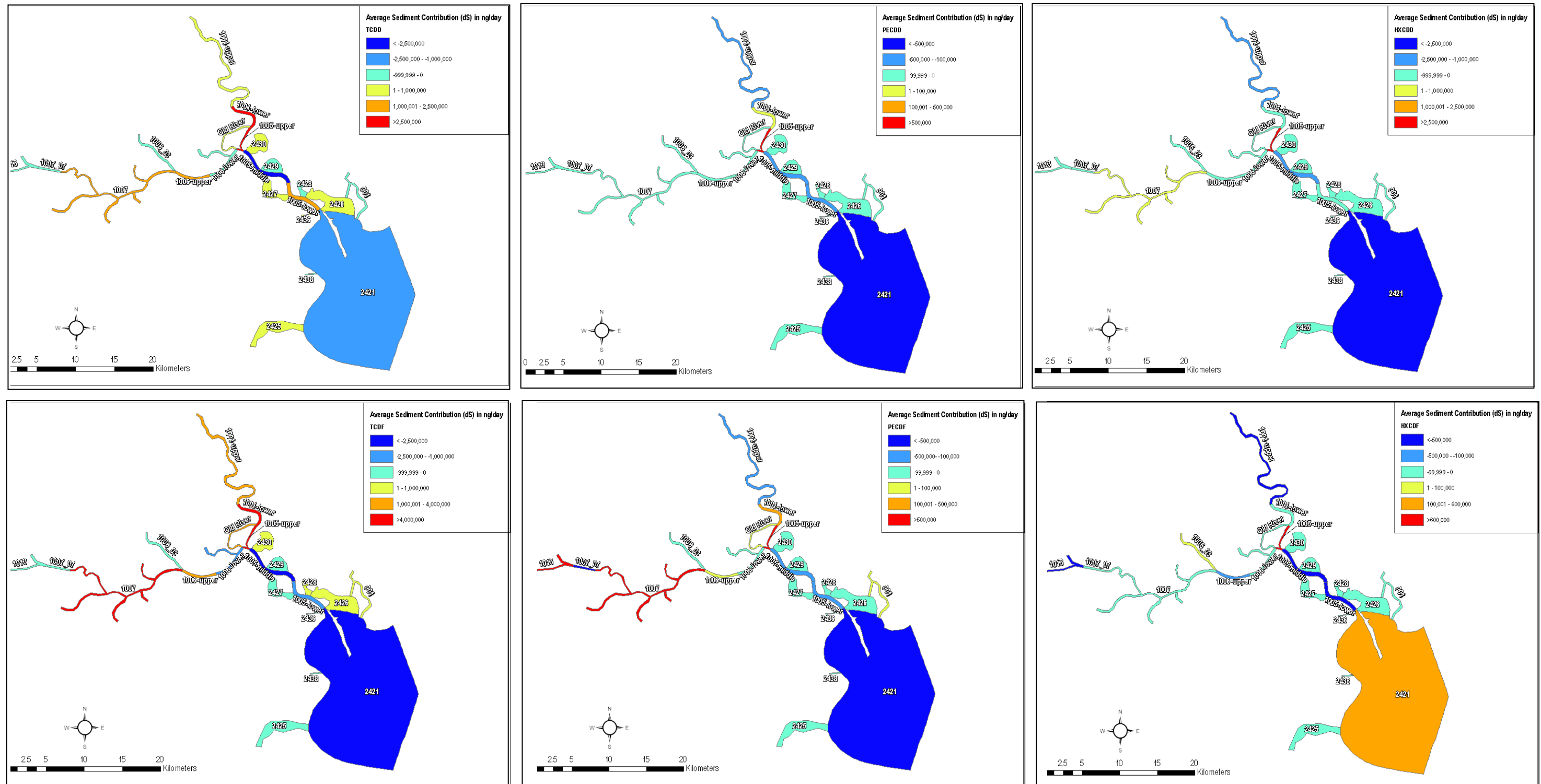


Figure 4.6 Average Sediment Contribution (dS) by Segment

Table 4.11 Mass-balance Spreadsheet for Σ TEQ_{major congeners}

Segment	Description	Average Downstream Net Flow ^a (m ³ /s)	Loads (ng/day)								% total load from sediment ^d
			PS	RO	DD	U/S ^b	Σ CinQin	Σ CoutQout	dS ^c	dS action	
1013	Buffalo Bayou	23.5	0	11,483	444	363,294	4,108	564,659	185,330	SOURCE	33.1%
1007_07	Buffalo Bayou Tidal/HSC	23.6	0	10,333	261	0	575,915	262,970	-323,538	SINK	
1007	1007	41.0	117,062	71,713	6,906	210,005	2,470,800	5,158,288	2,281,801	SOURCE	84.9%
1006_03	Greens Bayou	9.1	2,297	20,053	795	106,549	210,649	270,828	-69,515	SINK	
1006-upper	1006-upper	50.1	35,389	10,872	2,442	0	7,603,710	8,890,673	1,238,259	SOURCE	96.2%
1006-lower	1006-lower	50.4	20,068	10,760	3,053	12,273	9,027,631	8,217,018	-856,767	SINK	
1001-upper	San Jacinto River	138.1	5,232	34,273	3,102	1,465,952	1,584,340	3,785,431	692,533	SOURCE	31.5%
1001-lower	San Jacinto River	137.9	1,608	2,174	1,307	0	7,262,791	12,362,025	5,094,145	SOURCE	99.9%
Old River	Old River	-0.5	704	4,120	1,342	0	2,508,826	2,937,807	422,815	SOURCE	98.6%
1005-upper	1005-upper	188.3	1,815	547	1,655	0	18,938,278	26,208,253	7,265,959	SOURCE	99.9%
2430	Burnett Bay	-0.012	0	1,561	7,923	0	937,883	971,878	24,510	SOURCE	72.1%
2429	Scott Bay	-0.009	251	4,793	6,072	0	832,160	815,015	-28,261	SINK	
1005-middle	1005-middle	188.2	2,147	2,916	6,065	0	24,912,227	17,595,047	-7,328,308	SINK	
2427	San Jacinto Bay	-0.009	1,523	7,804	6,694	0	547,510	579,827	16,295	SOURCE	50.4%
2428	Black Duck Bay	-0.002	0	990	2,157	0	275,970	235,952	-43,165	SINK	
2426	Tabbs Bay	1.7	1,299	11,833	17,817	13,401	2,257,058	2,838,736	537,328	SOURCE	92.4%
2436	Barbours Cut	-0.0005	105	640	385	0	24,358	26,612	1,123	SOURCE	49.8%
1005-lower	1005-lower	186.9	3,817	1,103	4,663	0	15,854,312	17,621,468	1,757,573	SOURCE	99.5%
2438	Bayport Channel	0.0001	3,773	287	292	0	9,372	9,925	-3,798	SINK	
2421	Upper Galveston Bay	209.1	2,042	17,476	378,409	0	22,284,736	19,083,390	-3,599,272	SINK	
901	Cedar Bayou	2.7	0	22,888	439	10,954	86,470	109,835	-10,916	SINK	
2425	Clear Lake	2.0	0	50,500	673	0	416,659	415,441	-52,392	SINK	
OVERALL			199,132	299,117	452,897	2,182,429	118,625,762	128,961,075	7,201,739	SOURCE	69.7% ^e

^a Average of flows across downstream boundary of segment (includes both positive and negative flows). Averaging was completed on a time-step basis.

^b Load from upstream freshwater streams outside the HSC System (Table 4.3)

^c Σ QoutCout - (PS+RO+DD+ Σ QinCin) = dS. Values for PS, RO, and DD were obtained from Tables 4.1, 4.2, and 4.4, respectively.

^d dS/(PS+RO+DD+U/S+dS)

^e Average daily dioxin flux among the modeled segments transported by sediment

Using the TEQ mass-balance spreadsheet, the fluxes out of the lower boundary of Upper Galveston Bay as well as the flux from the bay to Clear Creek were also estimated. This was done by adding fluxes out of the bay across continuity lines 66, 67, 19, 68, 69, 70, and 72 for lower boundary and continuity line 62 for Clear Lake (see Figure 4.4). Table 4.12 summarizes the estimated fluxes.

Table 4.12 Daily Fluxes from Galveston Bay to Lower Bay System and Clear Lake

Continuity Line	Average Net Flow ^a (m ³ /s)	Average Flow Out ^b (m ³ /s)	Average Daily Flux Out ^c (ng/day)
Line 66	37.8	306.2	978,954
Line 67	-24.1	174.8	515,663
Line 19	100.2	1365.2	4,644,814
Line 68	6.7	314.3	1,045,256
Line 69	60.2	243.1	904,126
Line 70	38.9	457.4	1,622,271
Line 72	-10.7	326.1	1,108,331
Total flux out of lower boundary			10,819,415
Line 62 (to Clear Lake)	2.0	88.8	251,903

^a Average flow across continuity line (includes negative and positive flows).

^b Average of flows out of the model domain (includes only positive flows).

^c Average for the 1,015.9 days simulated in WASP.

4.4 CONVERTING DIOXIN FLUXES INTO LOAD ALLOCATION EQUATIONS

In the basic “allowable TMDL equation” of $LA + WLA + MOS = TMDL$, “TMDL” is the Gross Load from the model scenario that predicted water quality target attainment based on the value of the predicted Net Load. In other words, $TMDL = \text{allowable Gross Load}$.

The approach to develop load allocations is described in a separate allocation document for this project.

REFERENCES

- Ambrose, R.B., T.A. Wool, and J.L. Martin. 1993. The Water Quality Analysis Simulation Program, WASP5. Environmental Research Laboratory, US Environmental Protection Agency, Athens, Georgia.
- US Army, Engineer Research and Development Center (ERDC). 2005. Users Guide to RMA2 WES Version 4.5. Waterways Experiment Station, Coastal and Hydraulics Laboratory, April 22, 2005.
- Legates, D. and G. McCabe Jr. (1999). Evaluating the Use of “Goodness-of-fit” Measures in Hydrologic and Hydroclimatic Model Validation. *Water Resources Research*, 35(1): 233-241.
- Natural Resource Conservation Service. 1986. Urban Hydrology for Small Watersheds – TR55. United States Department of Agriculture, June 1986.
- Stow, C., C. Roessler, M. Borsuk, J. Bowen, and K. Reckhow (2003). Comparison of Estuarine Water Quality Model for Total Maximum Daily Load Development in Neuse River Estuary. *Journal of Water Resources Planning and Management*, 129(4): 307-314.
- University of Houston (2005a). Final Report for the Total Maximum Daily Loads for Fecal Pathogens in Buffalo Bayou and Whiteoak Bayou – Work Order No. 582-0-80121-06. Prepared for the Texas Commission on Environmental Quality. January, 2005.
- University of Houston (2005b). Final Report for the Total Maximum Daily Loads for Dioxins in the Houston Ship Channel – Work Order No. 582-0-80121-07. Prepared for the Texas Commission on Environmental Quality. November, 2005.
- University of Houston and Parsons, 2007
- U.S. Environmental Protection Agency (2000a). “Dioxin: Scientific Highlights from Draft Reassessment.” *Information Sheet 2*, National Center for Environmental Assessment, Office of Research and Development, Washington, DC.
- Wool, T.A., R.B. Ambrose, J.L. Martin, and E.A. Comer. 2004. The water quality analysis simulation program (WASP) version 6.0: Draft User’s Manual. Distributed by USEPA Region 4, Atlanta, GA.

APPENDIX A

**CROSS-SECTIONS FROM BEAMS USED TO SET UP THE 1-D
PORTION OF THE MAIN CHANNEL**

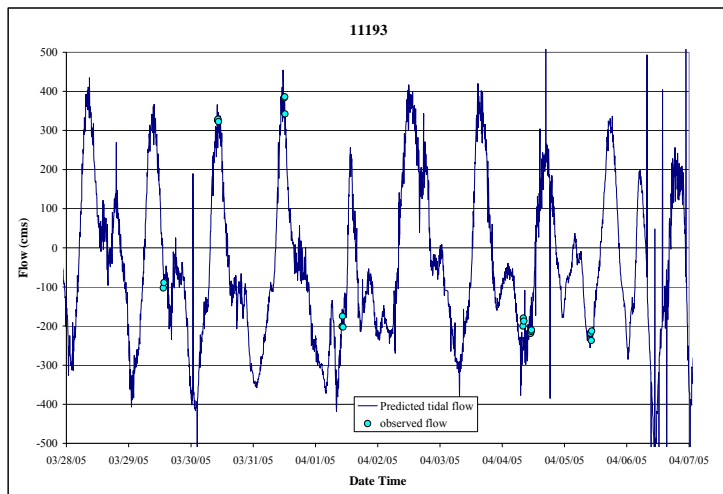
APPENDIX B
INPUT TIME SERIES

Appendix B1 – Tide and Inflow Database (Electronic)

**Appendix B2 – Rating Curve used to Estimate Hourly Discharges from the Lake Houston
to the San Jacinto River (Electronic)**

Appendix B3 – Flow Regression for the San Jacinto River

All the measured flows were used for the regression rather than the averages for the various events. It was considered that the freshwater inflow from Lake Houston was significant when compared to the measured flows at I-10. Thus, the freshwater flows were subtracted from the measured flows (assuming a 6-hour lag) and a regression between the resulting flows and the change in tide height was completed. To obtain predicted flows, the freshwater inflows were added to the flows obtained using the regression equation.



Site	Date	Time	Measured Q	Predicted Q
11193	03/29/05	13:11	-184.38	8.76
11193	03/29/05	13:24	-171.19	-65.72
11193	03/30/05	10:06	268.50	364.22
11193	03/30/05	10:16	271.64	332.62
11193	03/30/05	10:27	265.37	321.34
11193	03/31/05	11:48	326.25	357.21
11193	03/31/05	11:58	325.99	332.38
11193	03/31/05	12:05	282.02	382.04
11193	04/01/05	10:06	-232.58	-181.91
11193	04/01/05	10:15	-206.42	-206.73
11193	04/01/05	10:27	-234.21	-188.68
11193	04/04/05	7:50	-244.55	-270.00
11193	04/04/05	8:00	-229.19	-260.97
11193	04/04/05	8:12	-236.72	-242.91
11193	04/04/05	10:47	-273.19	-180.42
11193	04/04/05	10:57	-271.37	-148.82
11193	04/04/05	11:06	-267.47	-212.02
11193	04/05/05	9:51	-237.62	-230.44
11193	04/05/05	10:08	-256.22	-232.70
11193	04/05/05	10:18	-232.01	-232.70

SUMMARY OUTPUT

Regression Statistics

Multiple R	0.989
R Square	0.978
Adjusted R	0.977
Standard Err	39.19
Observation	20

ANOVA

	df	SS	MS	F	Significance F
Regression	1	1244977.792	1244978	810.7377618	2.01493E-16
Residual	18	27640.99726	1535.61		
Total	19	1272618.789			

	Coefficien	Standard Error	t Stat	P-value	Lower 95%	Upper 95%	Lower 95.0%	Upper 95.0%
Intercept	12.89	8.890232746	1.44966	0.164353865	-5.78987252	31.56549926	-5.78987252	31.56549926
96	-2257	79.25570332	-28.473	2.01493E-16	-2423.193926	-2090.173818	-2423.193926	-2090.173818

Appendix B4 – Daily Flows for City of Houston 69th Street WWTP (Electronic)

Appendix B5 – Wind, Rainfall and Evaporation Data (Electronic)

Appendix B6 – Boundary Database for WASP (Electronic)

Appendix B7 – Load Database for WASP (Electronic)

APPENDIX C

MODEL INPUT AND OUTPUT FILES

(Electronic)

Appendix C-1 RMA2 Model Input Files (Electronic)

Appendix C-2 WASP Model Input and Output Files (Electronic)

APPENDIX D

MASS-BALANCE SPREADSHEETS

(Electronic)